frontiers | Research Topics

Cyanobacterial biology in 21st century

Edited by
Prashant Kumar Singh, Ajay Kumar, Michel Passarini and Vijay Pratap Singh

Published in
Frontiers in Microbiology

ISSN 1664-8714
ISBN 978-2-83252-160-1
DOI 10.3389/978-2-83252-160-1

About Frontiers

Frontiers is more than just an open access publisher of scholarly articles: it is a pioneering approach to the world of academia, radically improving the way scholarly research is managed. The grand vision of Frontiers is a world where all people have an equal opportunity to seek, share and generate knowledge. Frontiers provides immediate and permanent online open access to all its publications, but this alone is not enough to realize our grand goals.

Frontiers journal series

The Frontiers journal series is a multi-tier and interdisciplinary set of open-access, online journals, promising a paradigm shift from the current review, selection and dissemination processes in academic publishing. All Frontiers journals are driven by researchers for researchers; therefore, they constitute a service to the scholarly community. At the same time, the *Frontiers journal series* operates on a revolutionary invention, the tiered publishing system, initially addressing specific communities of scholars, and gradually climbing up to broader public understanding, thus serving the interests of the lay society, too.

Dedication to quality

Each Frontiers article is a landmark of the highest quality, thanks to genuinely collaborative interactions between authors and review editors, who include some of the world's best academicians. Research must be certified by peers before entering a stream of knowledge that may eventually reach the public - and shape society; therefore, Frontiers only applies the most rigorous and unbiased reviews. Frontiers revolutionizes research publishing by freely delivering the most outstanding research, evaluated with no bias from both the academic and social point of view. By applying the most advanced information technologies, Frontiers is catapulting scholarly publishing into a new generation.

What are Frontiers Research Topics?

Frontiers Research Topics are very popular trademarks of the *Frontiers journals series*: they are collections of at least ten articles, all centered on a particular subject. With their unique mix of varied contributions from Original Research to Review Articles, Frontiers Research Topics unify the most influential researchers, the latest key findings and historical advances in a hot research area.

Find out more on how to host your own Frontiers Research Topic or contribute to one as an author by contacting the Frontiers editorial office: frontiersin.org/about/contact

Cyanobacterial biology in 21st century

Topic editors

Prashant Kumar Singh — Mizoram University, India

Ajay Kumar — Department of Postharvest Science of Fresh Produce, Agricultural Research Organization (ARO), Israel

Michel Passarini — Universidade Federal da Integração Latino-Americana, Brazil

Vijay Pratap Singh — University of Allahabad, India

Citation

Singh, P. K., Kumar, A., Passarini, M., Singh, V. P., eds. (2023). *Cyanobacterial biology in 21st century*. Lausanne: Frontiers Media SA. doi: 10.3389/978-2-83252-160-1

Table of contents

frontiers | Frontiers in Microbiology

TYPE Editorial
PUBLISHED 29 March 2023
DOI 10.3389/fmicb.2023.1184669

OPEN ACCESS

EDITED AND REVIEWED BY
William James Hickey,
University of Wisconsin-Madison, United States

*CORRESPONDENCE
Prashant Kumar Singh
✉ prashantbotbhu@gmail.com
Vijay Pratap Singh
✉ vijaypratap.au@gmail.com
Michel Rodrigo Zambrano Passarini
✉ michel.passarini@unila.edu.br
Ajay Kumar
✉ ajaykumar_bhu@yahoo.com;
✉ ajayk@volcani.agri.gov.il

SPECIALTY SECTION
This article was submitted to Microbiotechnology, a section of the journal Frontiers in Microbiology

RECEIVED 12 March 2023
ACCEPTED 20 March 2023
PUBLISHED 29 March 2023

CITATION
Singh PK, Singh VP, Passarini MRZ and Kumar A (2023) Editorial: Cyanobacterial biology in twenty-first century.
Front. Microbiol. 14:1184669.
doi: 10.3389/fmicb.2023.1184669

Editorial: Cyanobacterial biology in twenty-first century

Prashant Kumar Singh[1]*, Vijay Pratap Singh[2]*, Michel Rodrigo Zambrano Passarini[3]* and Ajay Kumar[4]*

[1]Department of Biotechnology, Mizoram University, Pacchunga University College, Aizawl, India, [2]Department of Botany, CMP Post Graduate College, University of Allahabad, Allahabad, India, [3]Latin American Institute of Life and Nature Sciences (ILACVN), Environmental Biotechnology Laboratory, Federal University of Latin American Integration (UNILA), Foz do Iguaçu, Paraná, Brazil, [4]Department of Post-Harvest, Agriculture Research Organization, The Volcani Centre, Rishon LeZion, Israel

KEYWORDS

cyanobacteria, bioremediation, microcystin (MC), stress, CRISPR

Editorial on the Research Topic
Cyanobacterial biology in twenty-first century

Cyanobacterial Biology in the twenty-first century Research Topic gathers different contributions high- lighting the cyanobacterial basic to advanced research going worldwide. Cyanobacteria are ancient photosynthetic prokaryotes and sustained during evolution. This sustainability is because of their fitness (stress adaptations) to the extreme environment and ability to fix atmospheric carbon dioxide and nitrogen. These tiny creatures have recently gained popularity due to their ability to produce biodegradable plastics (PHAs; polyhydroxyalkanoates) and biofuel; carbon sequestration ability, and they are a natural reservoir of various metabolites (alkaloids, ribosomal peptides, non-ribosomal peptides, cyanotoxins, and polyketides), food additives and drug designing. Furthermore, their universal presence, rapid growth, survivability under extreme conditions and minimum growth requirements make them a popular resource for sustainable agriculture. The cyanobacterial photosynthetic lamellae (thylakoid membranes) possess substantial amounts of lipids and offer greater photosynthesis efficiency; hence these attributes could be exploited to produce biofuel and bioplastic. The production of bioplastics uses the carbon sink concept and cyanobacteria's role in PHAs (polyhydroxyalkanoates) production as a source of intracellular energy. It is warranted to mention that cyanobacteria are a great source of biologically active compounds with anticancer, antifungal, antibacterial and antiviral properties. However, the knowledge behind the mode of action associated with these active compounds is still limited, even with advancements in the latest omics and technologies. Henceforth, this Research Topic mainly aims to assemble the most recent global cyanobacterial research to comprehend cyanobacteria's metabolism and physiology for better utilization for human welfare. In the current issue, nine articles have been published, which empowers our understanding of cyanobacteria's role in managing abiotic and biotic stress, biostimulants, biofuel production, and molecular aspects associated with cyanobacterial physiology.

Agarwal et al. emphasize different cyanobacterial species' ability to produce biodegradable plastics and their significance as green and clean energy sources. Future generations can rely on cyanobacteria to reach sustainable environmental goals due to their role in producing (PHAs) polyhydroxyalkanoates as a better alternative to conventional plastics. Compared to other energy sources, such as green plants, Cyanobacteria shows a more effective photosynthetic mechanism, which provides maximum output with limited

affordable land resources. An unconventional solution for a sustainable future is the synthesis of biodiesel from cyanobacteria, which reduces the emission of hazardous sulfur and prevents the addition of aromatic hydrocarbons with a high oxygen content and excellent combustion potential.

Ding et al. investigated the molecular aspect of cyanobacterial physiology—two accessory CARF-domain proteins from cyanobacterium *Synechocystis* sp. PCC III-D type CRISPR systems have been isolated and characterized. They found a model organism, *Synechocystis* sp. PCC 6803 contains ring nuclease proteins and a functional CARF-domain effector. SyCsx1, a cyclic tetraadenylate (cA4)-dependent RNase with strong specificity for cytosine nucleotides, is the homolog of Csx1. SyCsm6, a second CARF-domain protein that shares similarities with Csm6 effectors, broke down cOAs while attenuating SyCsx1 RNase activity. Their findings imply that *Synechocystis* CRISPR systems provide a multilayered cA4-mediated defense mechanism.

He et al. demonstrate *Prochlorococcus* global gene expression changes due to low salinity stress and their expanding salinity range. In this investigation, researchers discovered that *Prochlorococcus* strain NATL1A, which is low-light adapted, and strain MED4, which is high-light adapted, could acclimate in the lowest salinities of 25 and 28 psu. While both strains were grown in salinity more bass than 34 psu, the effective quantum yield of PSII photochemistry (Fv/Fm) showed that both the strains were stressed. To adapt to low salinity, the transcript of genes involved in translation, biogenesis, ribosomal structure and ATP generation was downregulated by NATL1A, whereas MED4 upregulated genes linked to photosynthesis. Moreover, the iron ABC transporter gene idiA was upregulated in both strains, indicating that low salinity acclimated cells may be iron deficient.

Kar et al. reviewed the characteristics, potential uses, and critical analysis of cyanobacterial metabolites and the mechanisms of action associated with contributing to the hunt for novel antimicrobials. Singh K.B. et al. addressed the limitations of using tetrapyrrole rings and natural nutrient supplements as therapeutic agents. Also, they demonstrated the various aspects of tetrapyrrole rings in the food and pharmaceutical industries. Singh R.P. et al. isolated several microalgae species from the wastewater environment, and their lipid accumulation and maximum growth rates were assessed. All isolated microalgae can adapt to a carbon source evaluated by adding sodium bicarbonate to BG-11N+ media. Further best Microalgal strains were chosen for biofuel feedstock based on growth parameters and sodium bicarbonate uptake rates among all the selected strains *Scenedesmus* sp. BHU1 strain was found to be highly efficient for biofuel production.

Srivastava et al. perform research to understand the information gaps about how pretreatment affects cyanobacteria. It is analyzed that the detrimental effects of salt can be reduced in filamentous cyanobacteria after pretreatment with heat, hence providing a basis for increased cyanobacterial tolerance to salt stress. Yalcin et al. examined the effects of kanamycin, ampicillin, cefotaxime and tetracycline on photosynthetic capacity and pigment fluorescence in *Fremyella diplosiphon* strains. Studies on the hormetic effect of antibiotics on *F. diplosiphon* show that excessive antibiotic concentrations significantly damage cellular functionality, and appropriate antibiotic doses stimulate cellular growth. Finally, Guo et al. identified a new microcystinase (MlrC) enzyme that degrades microcystin toxins produced by cyanobacteria.

It can be concluded that cyanobacteria show wide adaptability to biotechnological uses. They have been employed in drug development, bioremediation and medical diagnostics. In addition, they are potent sources of bioplastics, bioactive substances, food supplements, biofertilizers and energy. To enable their use, the additional study must concentrate on the thriving axenic culture of these microorganisms. In addition, new techniques must be developed to allow the cultivation of previously "uncultivable" strains.

We hope that the reader will find in this Research Topic a valuable reference for the state-of-the-art in the emerging field of tools rooted in information theory and applied to neuroscience.

Author contributions

All authors listed have made a substantial, direct, and intellectual contribution to the work and approved it for publication.

Acknowledgments

PS is thankful to University Grant Commission (UGC), New Delhi, for a start-up research grant 30/555/2021/UGC (BSR).

Conflict of interest

The authors declare that the research was conducted in the absence of any commercial or financial relationships that could be construed as a potential conflict of interest.

Publisher's note

frontiers in Microbiology

ORIGINAL RESEARCH
published: 29 March 2022
doi: 10.3389/fmicb.2022.839800

Physiological and Biochemical Responses of Bicarbonate Supplementation on Biomass and Lipid Content of Green Algae *Scenedesmus* sp. BHU1 Isolated From Wastewater for Renewable Biofuel Feedstock

*Rahul Prasad Singh[1], Priya Yadav[1], Ajay Kumar[1], Abeer Hashem[2], Al-Bandari Fahad Al-Arjani[2], Elsayed Fathi Abd_Allah[3], Angélica Rodríguez Dorantes[4] and Rajan Kumar Gupta[1]**

[1]Laboratory of Algal Research, Centre of Advanced Study in Botany, Institute of Science, Banaras Hindu University, Varanasi, India, [2]Botany and Microbiology Department, College of Science, King Saud University, Riyadh, Saudi Arabia, [3]Plant Production Department, College of Food and Agricultural Sciences, King Saud University, Riyadh, Saudi Arabia, [4]Escuela Nacional de Ciencias Biológicas, Instituto Politécnico Nacional, Mexico City, México

OPEN ACCESS

Edited by:
Hiroyuki Yamada,
Japan Anti-tuberculosis Association, Japan

Reviewed by:
Xianhua Liu,
Tianjin University, China
Pau Loke Show,
University of Nottingham Malaysia Campus, Malaysia

***Correspondence:**
Rajan Kumar Gupta
rajang.bot@bhu.ac.in

Specialty section:
This article was submitted to Microbial Physiology and Metabolism, a section of the journal Frontiers in Microbiology

Received: 20 December 2021
Accepted: 15 February 2022
Published: 29 March 2022

Citation:
Singh RP, Yadav P, Kumar A, Hashem A, Al-Arjani A-BF, Abd_Allah EF, Rodríguez Dorantes A and Gupta RK (2022) Physiological and Biochemical Responses of Bicarbonate Supplementation on Biomass and Lipid Content of Green Algae Scenedesmus sp. BHU1 Isolated From Wastewater for Renewable Biofuel Feedstock. Front. Microbiol. 13:839800. doi: 10.3389/fmicb.2022.839800

In the present study, different microalgae were isolated from wastewater environment and evaluated for higher growth and lipid accumulation. The growth adaptability of all the isolated microalgae were tested for carbon source with supplementation of sodium bicarbonate in BG-11 N^+ medium. Further based on the uptake rate of sodium bicarbonate and growth behavior, microalgal strains were selected for biofuel feedstock. During the study, growth parameters of all the isolates were screened after supplementation with various carbon sources, in which strain *Scenedesmus* sp. BHU1 was found highly effective among all. The efficacy of *Scenedesmus* sp. BHU1 strain under different sodium bicarbonate (4–20 mM) concentration, in which higher growth 1.4 times greater than control was observed at the concentration 12 mM sodium bicarbonate. In addition, total chlorophyll content (Chl-a + Chl-b), chlorophyll fluorescence (Fv/Fm, Y(II), ETR max, and NPQmax), and biomass productivity were found to be 11.514 μg/ml, 0.673, 0.675, and 31.167 μmol electrons $m^{-2} s^{-1}$, 1.399, 59.167 mg/L/day, respectively, at the 12 mM sodium bicarbonate. However, under optimum sodium bicarbonate supplementation, 56.920% carbohydrate and 34.693% lipid content were accumulated, which showed potential of sodium bicarbonate supplementation in renewable biofuel feedstock by using *Scenedesmus* sp. BHU1 strain.

Keywords: *Scenedesmus* sp., sodium bicarbonate, chlorophyll fluorescence, molecular analysis, scanning electron microscopy, biofuel

HIGHLIGHTS

- The physiological and biochemical composition of microalgae affected by sodium bicarbonate supplementation.
- Photosynthetic efficiency and microalgal biomass of isolate was found to be maximum at the 12 mM bicarbonate concentration.
- At 12 mM sodium bicarbonate, the maximum total chlorophyll content and biomass productivity were reported to be 11.514 g/ml and 59.167 mg/L/day, respectively.
- 56.92% carbohydrate and 34.69% lipid accumulated under optimum sodium bicarbonate supplementation.
- Strain *Scenedesmus* sp. BHU1 can be used as a potent renewable biofuel feedstock.

INTRODUCTION

In recent years, search of an alternative renewable energy resource is of great concern worldwide. The rapid industrialization and the needs of a burgeoning human population put extra pressure on energy resources. However, the limited stock of fossil fuels, regular price hiking of conventional energy resources, and release of toxic effluents after utilization need an immediate search of an alternative that must be economic, ecofriendly, and renewable in nature. In this regard, biofuel appears as a suitable alternative in terms of sustainability, reducing greenhouse gas emissions, and controlling changing climatic conditions. Generally, biofuels are classified into first, second, third, and fourth generations and objectives of all these are to meet the needs of global energy requirements in sustainable ways (Khoo et al., 2020; Mat Aron et al., 2020).

In the recent past, different microalgal strains have been frequently utilized as renewable energy feedstock with potential to replace traditional fuels (Behera et al., 2015; Cheah et al., 2018). Microalgae are photosynthetic organisms that use CO_2 and sunlight to develop and produce various value-added products such as carotenoids, fatty acids, and natural antioxidants, which are directly or indirectly utilized for human welfare (Borowitzka, 1992). However, for biofuel production, various higher plants have been reported to date, but high photosynthetic rate, greater nutrient uptake ability, short generation time, easy growth conditions, higher biomass, and lipid content make microalgae preferred over the higher plants (Karemore et al., 2013; Rawat et al., 2013; Arenas et al., 2017). The biomass, carbohydrate, and lipid productivity are crucial factors to optimize or enhance the economic viability of microalgae-based biofuels. Changes in medium ingredients or growing conditions can easily increase the biomass content of microalgae resulting in a greater yield of value-added products (Vijay et al., 2021; Siddiki et al., 2022).

Biofuel production from microalgal biomass is still in the initial stages and the industrial growth is largely dependent on the viability of large-scale microalgal cultivation. To ensure the economic feasibility of microalgal cultivation and biofuel production, selection of suitable strain, cultivation methods, nutrient supply, and feasible source of water (Borowitzka and Vonshak, 2017). Even though microalgae have high oil content in their biomass, their ability to synthesize substantial amounts of lipid is often strain-specific and varies with surrounding environmental conditions. In a study, Parichehreh et al. (2021) evaluated several factors including light intensity, temperature, salinity, $NaHCO_3$, CO_2, and other nitrogen sources on the growth, biomass, and lipid production of *Chlorella* sp. Authors reported light intensity and temperature have significant effects on algal growth. However, bicarbonate as carbon and ammonium as nitrogen source play significant roles in biomass and lipid production compared to CO_2 and nitrate, respectively.

Wastewater microalgal strains are referred to as a promising option for biofuel generation, due to their tolerance to climatic and environmental changes (Priyadharshini et al., 2021; Renuka et al., 2021). Several strains of freshwater microalgae *Scenedesmus* and *Chlorella* have been documented as potential candidates for the large-scale production of biofuel owing to its high biomass productivity and favorable biochemical composition. In addition, the ability to modulate their metabolic productivity under varying nutritional conditions, which showed significant morphological variability and phenotypic plasticity in response to changing environmental factors (Chung et al., 2018; Yun et al., 2019; Vijay et al., 2021). Microalgal biomass production on a large-scale is difficult as is microalgal strains that can develop robustly under stress conditions. Although under ideal stress conditions, various microalgal species have been examined and reported to produce 30%–50% lipid of dry cell weight (Maheshwari et al., 2020; Han et al., 2021). About 60 microalgal species have been thoroughly studied to produce enormous amounts of biomass and high biofuel yield (Tripathi et al., 2015).

The *Scenedesmus* sp. is a microscopic unicellular microalga that can be found in both fresh and effluent streams. The microalga *Scenedesmus* sp. is a significant biofuel feedstock because of its capacity to grow in a variety of carbon-rich habitat with high biomass yield and lipid content (Mata et al., 2012). Previously, several species of *Tetradesmus/Acutodesmus* which belong to the Scenedesmaceae family have been reported as promising candidates for biofuel production due to their high lipid content and suitable fatty acid profile (Ferrigo et al., 2015; Ismagulova et al., 2018; Umetani et al., 2021). However, limited information is available for *Scenedesmus* sp. Therefore, we are selecting *Scenedesmus* sp. to evaluate its physiological and biochemical responses to bicarbonate supplementation and to use it for various biotechnological applications.

Therefore, the current research has been designed to isolate different microalgal strains from wastewater environment. Furthermore, screening of different microalgal strains have been carried out under supplementation of different ranges of sodium bicarbonate as a carbon source and determine the physiological and biochemical responses in terms of biomass and lipid content to bicarbonate supplementation from microalgae as a biofuel feedstock.

Abbreviations: Chl-a, Chlorophyll-a; Chl-b, Chlorophyll-b; Fv, Variable chlorophyll fluorescence; Fm, Maximum chlorophyll fluorescence; Fo, Minimum chlorophyll fluorescence; Fv/Fm, Maximum photochemical quantum efficiency; YII, Effective photochemical quantum yield; ETRmax, Maximum electron transport rate; NPQmax, Maximum non-photochemical quenching; PSII, Photosystem II.

MATERIALS AND METHODS

Isolation and Cultivation of Microalgae

The samples of microalgae were collected aseptically from the wastewater environment of Banaras Hindu University (BHU) campus, Varanasi, India. A total of 10 ml of microalgal culture was inoculated in 250 ml Erlenmeyer conical flasks with 100 ml BG-11 N^+ broth medium at pH 7.4 (Rippka et al., 1979). The cultured samples were disseminated on BG-11 N^+ agar plate and incubated in an artificial photoperiod of 14 h light and 10 h dark, illuminated by white fluorescent tube light (55 μ mol $m^{-2} s^{-1}$) at 28 ± 2°C and each flask was shaken at 50 rpm continuously. The separate colonies that appeared on agar plate were picked and transferred to a similar medium for purification using BG-11 N^+ broth and agar plates in a sequential culture. The procedure was repeated until axenic microalgal cultures were achieved.

Screening of Potential Microalgal Isolates

The microalgal isolates capable of using high inorganic carbon as sodium bicarbonate from the aquatic environment were screened. The selection of isolates was performed in BG-11 N^+ medium with 12 mM sodium bicarbonate and the growth was analyzed in terms of optical density (OD) every alternate day until the 16 days at 680 nm wavelength by UV-2600 UV–VIS Spectrophotometer, SHIMADZU (Japan). The microalgal isolates that respond better at 12 mM sodium bicarbonate were transferred to a 250-ml flask with a 100-ml working volume for further study.

Morphological Identification of Microalga by Scanning Electron Microscopy

On the center of a coverslip (22 mm × 22 mm Blue Star) a drop of exponentially growing microalgal suspension (0.7 OD) was placed and dried in air. It was then chemically fixed with 3% (w/v) glutaraldehyde and left overnight before being rinsed thrice in distilled water and dehydrated with a graded series of ethanol (30%, 50%, 80%, 90%, 95%, and 100%) and air dried. In a quorum Sc 7620 sputter coater air dried sample was coated with a 30 Å thick gold palladium coating for 9 min. Scanning electron microscopy, EVO18 Research ZEISS (Germany) was used to examine coated materials at 15 and 5 kV (Sadiq et al., 2011).

Molecular Identification of the Potential Microalgal Isolate

Based on a microscopic study the microalgal strain was initially recognized morphologically. After that 18S rDNA sequencing was used to confirm the identity of the microalgal isolate. The manual DNA isolation technique was used to isolate genomic DNA from a microalgal strain (Aboul-Maaty and Oraby, 2019). The 18S rDNA was amplified using PCR with forward 5′-GCTTAATTTGACTCAACACGGGA-3′ and reverse 3′-AGCTATCAATCTGTCAATCCTGTC-5′ primers (Gargas and DePriest, 1996). A reaction mixture containing 0.2 mM deoxynucleoside triphosphates, 1.5 mM $MgCl_2$, 0.5 mM of each primer and 1.25 units of *Taq* DNA polymerase were used for amplification. The following polymerase chain reaction procedure was used: 94°C for 3 min, 35 cycles of 1 min at 94°C, 1 min at 59°C, and 1 min at 72°C (Valiente Moro et al., 2009). The 400–900 bp amplicon was gel eluted and the amplicon was sequenced using the Sanger technique of DNA sequencing (Sanger et al., 1977). The outcomes of the sequencing were combined and compared with existing National Center for Biotechnology Information (NCBI) data base of gene bank.

Phylogenetic Analysis

The 18S rDNA sequence of isolated microalga was matched with previously reported sequences of other intimately related microalgal species to determine its phylogeny. Using the nucleotide BLAST tool, the 18S rDNA gene sequence obtained in our study and NCBI reference sequences were downloaded and aligned using Clustal-W multiple sequence alignment. The Neighbor-Joining approach was used to create a phylogenetic tree and the Maximum Composite Likelihood technique was used to calculate the evolutionary distances (Saitou and Nei, 1987; Tamura et al., 2004). Bootstrap analysis based on 1,000 replications was used to determine the tree resilience. The MEGA 11 software was used to conduct evolutionary analyses (Tamura et al., 2021).

Growth Characterization

The growth was measured at 680 nm OD and the pigment content (chl-a, chl-b, and carotenoid), chlorophyll fluorescence, and biomass of each culture growing in different concentrations of sodium bicarbonate ranges from 4 to 20 mM were measured in terms of their growth.

Determination of Photosynthetic Pigments

To assess pigment content, 2 ml microalgal culture was centrifuged for 5 min at 10,000 rpm, the pellet was dissolved in 99.9% methanol and kept at 4°C overnight in the dark. The absorbance of the supernatant was taken at 470, 652.4, and 665.2 nm using a UV-2600 UV–VIS Spectrophotometer, SHIMADZU (Japan) and the pigment content was calculated using the following formulas (Lichtenthaler, 1987).

$$\text{Chlorophyll a; Chl-a}\left(\mu g / \text{ml}\right) = 16.72\, A_{665.2} - 9.16\, A_{652.4}$$

$$\text{Chlorophyll b; Chl-b}\left(\mu g / \text{ml}\right) = 34.09\, A_{652.4} - 15.28\, A_{665.2}$$

$$\text{Carotenoid}\left(\mu g / \text{ml}\right) = \left(1000\, A_{470} - 1.63\, \text{Chl-a} - 104.9\, \text{Chl-b}\right) / 221$$

Chlorophyll Fluorescence Analysis

Chlorophyll fluorescence (ChlF) used as a non-destructive marker of photosynthetic performance and various photosynthetic parameters like the maximum photochemical quantum efficiency (Fv/Fm), effective photochemical quantum yield [Y(II)], the maximum electron transport rate (ETRmax), and maximum non-photochemical quenching (NPQmax) of photosystem II

(PSII). These parameters were measured using a KS-2500 pulse-amplitude modulation (PAM) device (Heinz Walz GmbH D-91090 Effeltrich, Germany) and computed using PAM software (PamWin-3). The 0.5 ml aliquot of dark-adapted (20 min) culture was poured into a glass cuvette attached to a PAM fluorometer with a micromagnetic stirrer. Maximum chlorophyll fluorescence (Fm) was measured using high intensity saturating pulses of more than 3,000 mol m^{-2} s^{-1}, while minimal chlorophyll fluorescence (Fo) was measured using a light-emitting diode providing 0.001 mol m^{-2} s^{-1}. A range of photosynthetic active radiation (PAR) (0–2,973 mol m^{-2} s^{-1}) was used for light curve analysis of samples. The maximum electron transport rate (ETR) was determined to be 984 mol m^{-2} s^{-1}.

Biomass Productivity

At the 14th day, dry cell weight of each culture treated with different concentrations of sodium bicarbonate (4–20 mM) was measured to estimate biomass. To achieve constant weight, 2 ml of each microalgal culture was centrifuged and transferred to pre-weighted Eppendorf tube for drying in the oven at 70°C. The biomass content (c) was calculated using formula $c = m/0.02\,\text{L}$ (Chen et al., 2021), where m is the weight of the dry cell pellet.

Determination of Protein, Carbohydrate, and Lipid Content

The Lowry method was used to estimate the protein content of the microalgal biomass (Lowry et al., 1951) and the anthrone method was used to determine total carbohydrate content (Loewus, 1952). The anthrone reagent was prepared by dissolving 0.2 g anthrone in 100 ml chilled 95% H_2SO_4. There was 1 ml stationary phase microalgal culture pelleted and treated with 1 ml 1 N NaOH. The total carbohydrate was determined using 100 µl of supernatant, 900 µl of deionized water, and 4 ml anthrone reagent and incubated at room temperature for 10 min in the dark, a greenish-blue color appeared, and absorbance was measured at 625 nm. For the standard, glucose stock was used.

The Bligh and Dyer method was used to extract total lipids content from microalgae (Bligh and Dyer, 1959). For lipid extraction, stationary phage grown microalgal cells were collected, after centrifugation for 6 min at 8,000 rpm. The extraction solvent chloroform:methanol:water (2:1:1 v/v/v) was added in the microalgal cells and disrupted with a Sonics vibra cell sonicator for 10 min. The mixture sample was centrifuged and the chloroform layer containing lipid fraction was isolated and evaporated using a speed vacuum centrifuge evaporator and the total lipid content was determined gravimetrically using formula $c\ (\%) = (m_c - m_e)/m_a \times 100\%$, where m_c is the weight of the tube containing the dry total lipids, m_e is the weight of the empty collection tube, and m_a is the weight of the dry cell pellet used for extraction.

Qualitative Analysis of Lipid by BODIPY 505/515 and Nile Red Dyes

Two lipophylic dyes BODIPY 505/515 and Nile Red (NR-47353) powder (0.250 µg) were dissolved in 1 ml of acetone, which was used as the stock solution to detect the presence of neutral lipid in microalgal cells (Singh et al., 2019). Stationary phase microalgal cells (2 ml) were collected by centrifugation and washed three times with 1x Phosphate Buffer Saline (PBS). There was 5 µl microalgal suspensions taken on the center of slide and 2 µl stock solution was added and incubated for 5 min in the dark. The stained microalgal cells were observed by fluorescent microscopy (Nikon ECLIPSE 90i, United States) using 20x objective lens with a common exposure period for all images, having NIS-Elements AR 4.0 microscope imaging software (Nikon Instech Co. Ltd., Japan) at 465–495 and 590–650 nm for green and red channel excitation emission wavelengths, respectively.

Statistical Analysis

The consequences were presented as three replicate averages with standard errors. Using SPSS software version 21, the significance of differences between treatment was examined using the Tukey's-b *post hoc* test at a $p < 0.05$ probability threshold.

RESULTS AND DISCUSSION

Isolation and Screening of Microalgal Strains

Using standard microbiological procedures, five axenic microalgal isolated strains namely BHU1, BHU2, BHU3, BHU4, and BHU5 capable of thriving in inorganic enriched environments were identified from wastewater habitat. Among the five isolates, the strain BHU1 grew vigorously after supplementation of 12 mM sodium bicarbonate than BHU2, BHU3, BHU4, and BHU5 (**Figure 1**), which indicates that it can effectively absorb excess inorganic carbon given as bicarbonate and sequester it into increased biomass. *Scenedesmus* sp. along with other microalgae is commonly found in wastewater environment (Apandi et al., 2017; López-Pacheco et al., 2021). At such ecological niche, carbonate and bicarbonate ions are the primary sources of inorganic carbon, hence microalgal group inhabitant

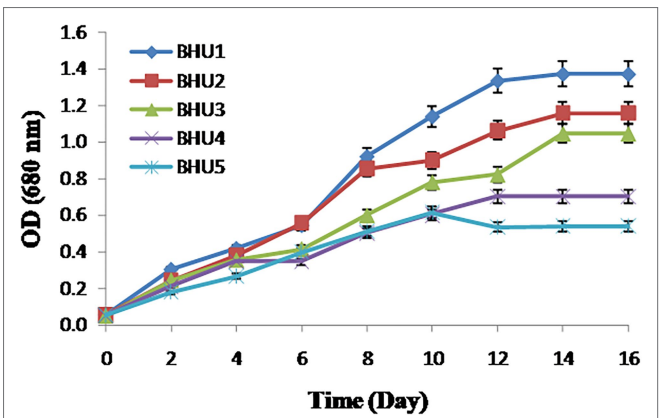

FIGURE 1 | Growth measurement in terms of optical density of different algal strains grown in BG – 11 N^+ medium supplemented with 12 mM $NaHCO_3$. The data represents mean ± SE ($n = 3$).

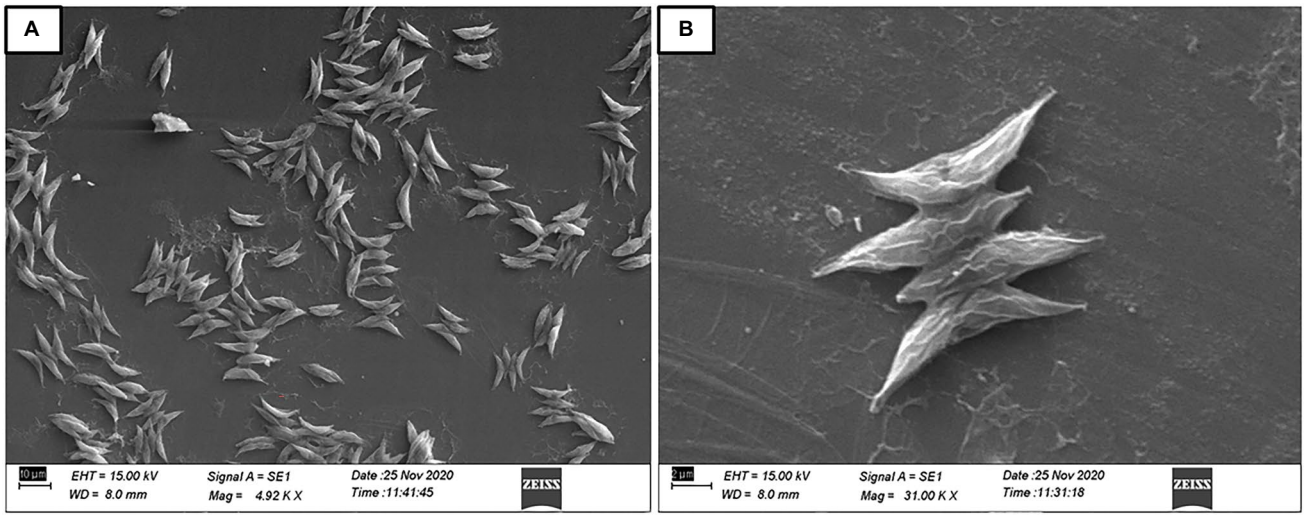

FIGURE 2 | Scanning electron micrograph of isolated strain *Scenedesmus* sp. BHU1 from aquatic habitat of Banaras Hindu University. **(A)** 4.92 KX and **(B)** 31.00 KX magnifications were used to capture the image by scanning electron microscopy (EVO18 Research ZEISS).

of wastewater, naturally adopted to survive under high inorganic carbon concentrations and possibly improve inorganic carbon uptake as well as enhancement in biomass and lipid productivity (Lee et al., 2014; Pandey et al., 2019).

Identification of Isolated Microalga Using Microscopic and Molecular Techniques

The purity and shape of prospective microalgal strains were revealed by scanning electron microscopy. The morphological features of the isolate have confirmed its close relationship with the genus *Scenedesmus*. The microalgal strain BHU1 showed green, cylindrical cells with pointed ends that are joined laterally into 2–4 cell colonies (**Figure 2**), pair-wise alignments and pointed end gave the closest match with *Scenedesmus* sp. (Guiry and Guiry, 2021), which was later confirmed by 18S rDNA sequence analysis (Gene Bank Accession Number MZ788699) by confirming 99.77% phylogenetic identity with *Scenedesmus* sp. as described in **Figure 3**. *Scenedesmus* belongs to Scenedesmaceae family, which are already reported as a probable source for biofuel production in recent years with limited information (Pancha et al., 2015; Tripathi et al., 2015; Kumar et al., 2021).

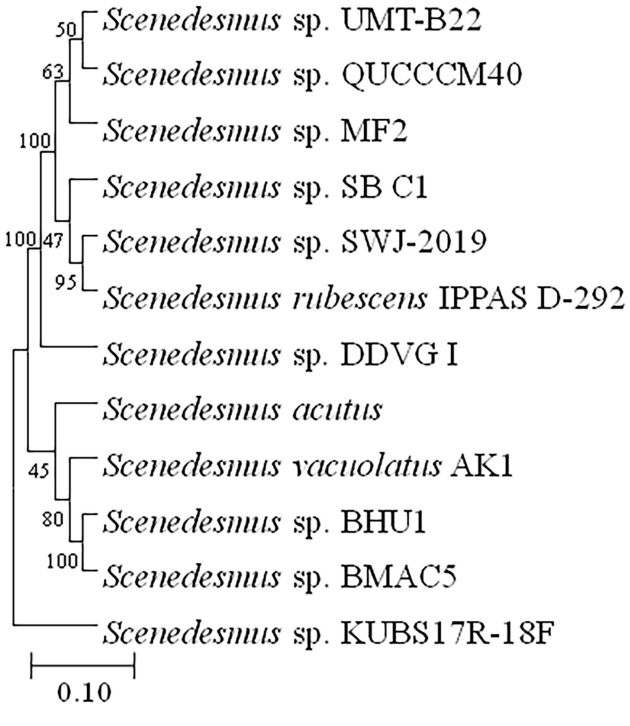

FIGURE 3 | Phylogenetic tree and evolutionary relationships of microalga *Scenedesmus* sp. BHU1 based on 18S rDNA gene sequence. The boot strap consensus tree was created using the MEGA 11 software and multiple sequence alignment with the neighbor-joining method.

Effect of Sodium Bicarbonate Supplementation on Growth of Microalgae

The supplementation of sodium bicarbonate in the range of 4–12 mM, significantly enhances the growth of *Scenedesmus* sp. BHU1 as compared to control, while a higher concentration (16–20 mM) of sodium bicarbonate significantly reduced growth due to enhanced concentration of sodium ions in the growth culture with increasing sodium bicarbonate supplementation has been shown (**Figure 4**). The highest significant growth was observed in the case of 12 mM sodium bicarbonate (2.331 ± 0.179), which was almost 1.3 times higher than the control grown culture (1.714 ± 0.037). The previous research with *Chlorella vulgaris* reported that adding sodium bicarbonate (1 g/L) in growing culture media increased the optical density to 0.5 (Borowitzka, 2005).

The growth of algae was inhibited after higher supplementation of sodium bicarbonate (16–20 mM) and this may be because

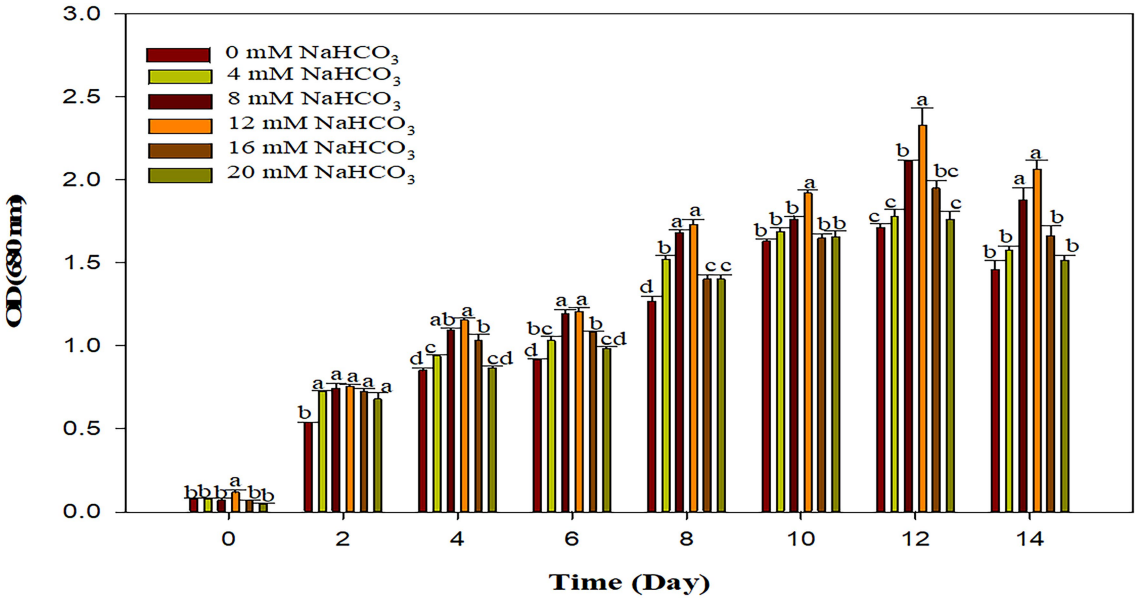

FIGURE 4 | Effect of different sodium bicarbonate concentrations with time (day) on growth pattern of microalga *Scenedesmus* sp. BHU1. Bars are mean ± SE of three replicates. Bars adhered with different alphabets (a, b, c, and d) are statistically significant at $p < 0.05$ (Tukey's-b *post hoc* test).

TABLE 1 | Effect of different concentration of sodium bicarbonate on photosynthetic pigment content of *Scenedesmus* sp. BHU1.

$NaHCO_3$ (mM)	Chl-a* (μg/ml)	Chl-b** (μg/ml)	Caro*** (μg/ml)	Chl a + b (μg/ml)	Chl a/b	Caro/Chl a + b
0	5.416 ± 0.127^{c}	1.307 ± 0.134^{b}	2.478 ± 0.024^{c}	6.723 ± 0.198^{e}	4.265 ± 0.588^{a,b}	0.369 ± 0.003^{a}
4	7.047 ± 0.105^{a,b}	1.424 ± 0.115^{b}	2.520 ± 0.036^{c}	8.471 ± 0.010^{d}	5.033 ± 0.523^{a}	0.297 ± 0.004^{b}
8	7.533 ± 0.183^{a}	2.729 ± 0.248^{a,b}	2.940 ± 0.058^{b}	10.263 ± 0.068^{b}	2.821 ± 0.336^{a,b}	0.286 ± 0.007^{b,c}
12	8.321 ± 0.828^{a}	3.192 ± 0.904^{a}	2.981 ± 0.072^{a,b}	11.514 ± 0.778^{a}	3.500 ± 1.609^{a,b}	0.259 ± 0.004^{c}
16	7.149 ± 0.132^{a,b}	4.539 ± 0.123^{a}	2.986 ± 0.091^{a,b}	11.687 ± 0.043^{a}	1.579 ± 0.072^{a,b}	0.255 ± 0.007^{c}
20	5.648 ± 0.054^{b,c}	3.961 ± 0.311^{a}	3.236 ± 0.057^{a}	9.609 ± 0.286^{c}	1.444 ± 0.116^{b}	0.337 ± 0.015^{a}

Values are mean ± SE, n = 3. Values adhered with different alphabets (a, b, c, d, and e) are statistically significant at $p < 0.05$.

**Chl-a: chlorophyll-a.*

***Chl-b: chlorophyll-b.*

****Caro: carotenoids.*

introducing sodium bicarbonate in such quantities causes a rapid increase in pH, resulting in a slightly alkaline solution, which is unfavorable for microalgal growth. Previous studies have found that at the 75 ppm bicarbonate the *Chlorella* sp. grows at its fastest and has the highest lipid content suggesting it could be used as a biodiesel feedstock (Devgoswami et al., 2011). The result in terms of optical density revealed that elevated concentration of carbon as bicarbonate to the microalgal photosynthetic activity can boost the rate of microalgal reproduction and ultimately growth. The maximum specific growth rate was greater when 1 g L^{-1} bicarbonate was supplemented to green microalgae *C. vulgaris* and *Dunaliella salina* grown culture (Mokashi et al., 2016; Srinivasan et al., 2018). The photosynthetic rate, biomass yield, and fatty acid production of a green microalga *Tetradesmus wisconsinensis* were also improved by an inorganic carbon regime (Umetani et al., 2021). Our research findings also suggest the supplementation of optimum concentration of bicarbonate can boost microalgal growth and biofuel production.

Effect of Sodium Bicarbonate Supplementation on Photosynthetic Pigment

Based on pigment content, the microalga *Scenedesmus* sp. BHU1 was examined for its growth response after different concentrations of sodium bicarbonate supplementation. The addition of sodium bicarbonate in the growth culture significantly enhanced the photosynthetic pigments including Chl-a, Chl-b, and carotenoid in the microalga *Scenedesmus* sp. BHU1 (**Table 1**). The Chl-a, Chl-b, and carotenoid content was significantly ($p < 0.05$) increased, when the sodium bicarbonate concentration was increased from 4 to 12 mM, except with 20 mM sodium bicarbonate supplementation, where the Chl-a and Chl-b content was low and carotenoid was high. The highest amount of Chl-a (8.321 ± 0.828 μg/ml) was found in 12 mM sodium bicarbonate supplied culture, which was almost 1.5 times higher than the control grown culture 5.416 ± 0.127 μg/ml (Pancha et al., 2015). Similar to our result, *Scenedesmus* sp. CCNM 1077 had a higher level of Chl-a (6.11 ± 1.14 μg/ml) in a 0.9 g/L sodium bicarbonate

enriched culture, which was almost 1.1 times higher than the control grown culture. 5.18 ± 0.32 µg/ml (Pancha et al., 2015). In another study, *Nannochloropsis salina* and *Tetraselmis suecica* were cultivated with 1 g/L bicarbonate supplementation, their Chl-a concentration increased 1.9 and 2.2 times as compared to control grown culture (White et al., 2013). The enhancement in carotenoid was dose dependent with addition of sodium bicarbonate. The highest amount of carotenoid (3.236 ± 0.057 µg/ml) was found in 20 mM sodium bicarbonate supplemented grown culture followed by 16 mM (2.986 ± 0.091 µg/ml) and 12 mM (2.981 ± 0.072 µg/ml) sodium bicarbonate supplemented cultures. Further, sodium bicarbonate addition (up to 12 mM) to the growing culture increased the total chlorophyll (a + b) content (11.514 ± 0.778 µg/ml). In our study, addition of 20 mM sodium bicarbonate to the growing culture lowered the ratio of Chl a/b (0.3-fold) and carotenoid/total Chl (0.9-fold) as compared to the control for microalga *Scenedesmus* sp. BHU1. The decreased pigment ratio can be explained by the fact that adding sodium bicarbonate to such amounts causes a rapid increase in pH, resulting in an alkaline environment, which is unfavorable for microalgal growth. In similar research, there was no discernible difference in pigment ratio when *T. suecica* was cultured with sodium bicarbonate supplementation, whereas *N. salina*, carotenoid/Chl-a ratio increased when sodium bicarbonate in the growth culture was increased (White et al., 2013). Because of this, alga could have CO_2 concentrating mechanism, and contribute a role in the pH balance. Previous research has found that at 75 ppm bicarbonate, the *Chlorella* strain grows at its fastest and has the highest lipid content, suggesting that it could be used as a biodiesel feedstock (Devgoswami et al., 2011). In our study, *Scenedesmus* sp. BHU1 grew optimally at 12 mM sodium bicarbonate supplementation, and it belongs to the same group of previously investigated green microalgae.

Effect of Sodium Bicarbonate Supplementation on Chlorophyll Fluorescence and Photosynthetic Performance

Pulse amplitude modulated (PAM) fluorometry is one of the frequently used, non-invasive, and quick procedures that measure the chlorophyll fluorescence variability and photosynthetic activity in microalgae (Baker, 2008; White et al., 2011). The physiological condition of the *Scenedesmus* sp. BHU1 with varied concentrations of sodium bicarbonate was recorded significantly over the full course of the studies using the PAM Flourometer with various parameters such as Fv/Fm, Y(II), ETRmax, and NPQmax (**Figures 5A-D**). Microalgal cells treated with varied concentrations of sodium bicarbonate ranging from 4 to 12 mM showed a gradually significant ($p < 0.05$) raise in Fv/Fm and Y(II) as compared to the control, showing a good photosynthetic performance in these sodium bicarbonate concentration ranges. The highest Fv/Fm and Y(II) were found in culture grown with 12 mM sodium bicarbonate at 10 days (0.673 ± 0.006, 0.675 ± 0.008) which was 1.2- and 1.2-fold higher than the 12 mM sodium bicarbonate at 0 day of growth culture (0.558 ± 0.010, 0.558 ± 0.010), respectively, and no discernible change ($p < 0.05$) in Fv/Fm and Y(II) was observed beyond 12 mM sodium bicarbonate. In a

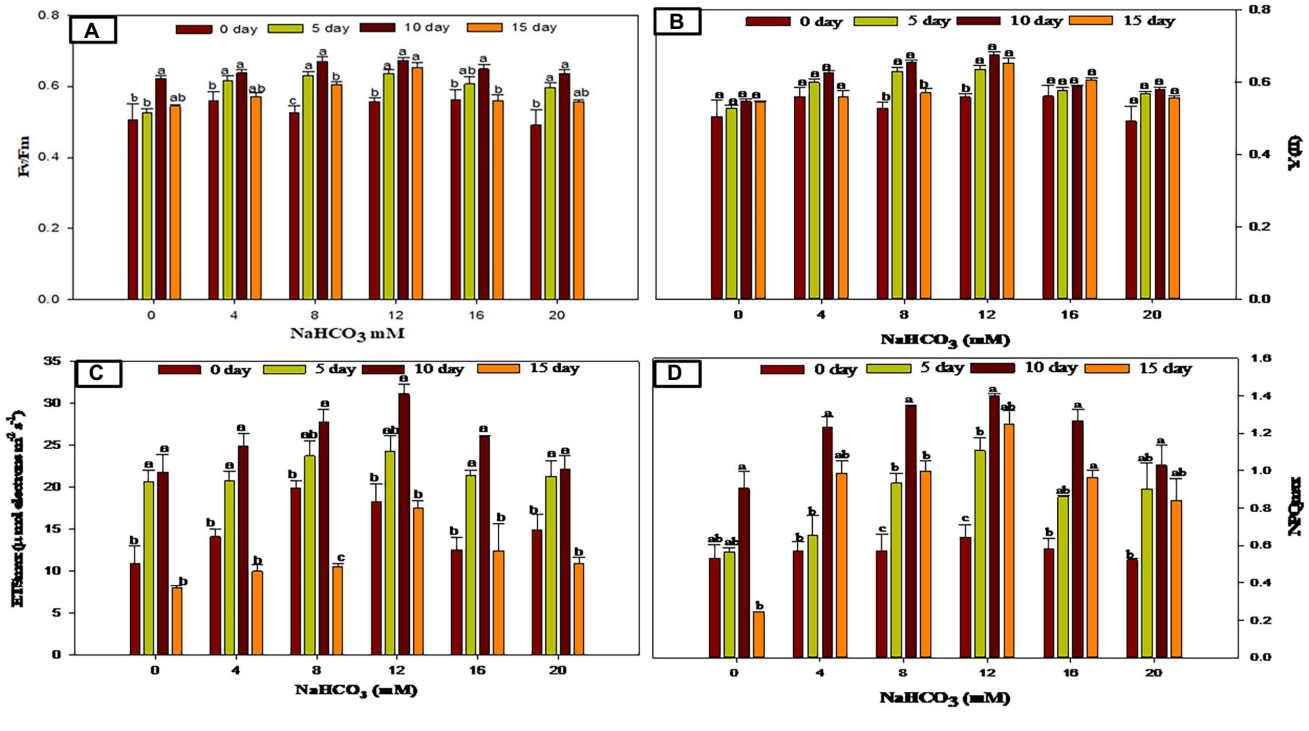

FIGURE 5 | Chlorophyll fluorescence and photosynthetic performance in *Scenedesmus* sp. BHU1 with various $NaHCO_3$ concentrations at different days. Bars are mean ± SE of three replicates. Bars adhered with different alphabets (a, b, and c) are statistically significant at $p < 0.05$ (Tukey's-b *post hoc* test).

similar study, the presence of sodium bicarbonate enhanced Fv/Fm and Y(II) in the green alga *Chlorella sorokiniana* (Salbitani et al., 2020). The Fv/Fm and Y(II) rising could suggest increased photosynthetic carbon fixation and metabolic activity. The ETRmax followed the same patterns as Fv/Fm and Y(II). Bicarbonate (4–12 mM) considerably enhanced the photosynthetic efficiency of *Scenedesmus* sp. BHU1 culture in exponential phase, but elevated levels (beyond 12 mM sodium bicarbonate) had little effect. Several studies have been published describing the effects of salinity on photosynthetic activity, which decreased after increasing salinity (Salbitani et al., 2020), which led to the conclusion that salinity induced suppression of Photosystem II (PSII) activity is thought to be produced by impaired PSII repair and lower D1 protein turnover (Allakhverdiev et al., 2002).

The maximum non-photochemical quenching (NPQmax) is caused by excess excitation energy dissipation of the PSII reaction center as heat (Ware et al., 2015). The present NPQmax data show an initial increase in NPQmax with increasing sodium bicarbonate supplementations up to 12 mM followed by a descending order in the range of 16–20 mM sodium bicarbonate. The highest NPQmax was found in culture grown with 12 mM sodium bicarbonate at 10 days (1.399 ± 0.014), which was 2.1-fold higher than the 12 mM sodium bicarbonate at 0 days grown culture (0.643 ± 0.070). Salinity induced PSII reaction center inactivation could explain a decrease in the NPQmax at higher concentrations of sodium bicarbonate (Szabó et al., 2005). Overall, the results suggest that *Scenedesmus* sp. BHU1 with optimum bicarbonate dose results in a significant and quick increase in cell proliferation. These beneficial and dose-dependent positive effects on growth, photosynthetic efficiency, and pigment content suggest that this salt could be a good as inorganic carbon source for lipid accumulation.

Effect of Sodium Bicarbonate Supplementation on Dry Cell Weight and Biomass Productivity

Next to sunlight and water, the most prerequisite resource for photoautotrophic cell growth and lipid synthesis is inorganic carbon. In the present study, addition of sodium bicarbonate to the growth medium significantly increased the dry cell weight (DCW) and biomass productivity (BP) of the microalgae *Scenedesmus* sp. BHU1. The dry cell weight and biomass productivity of the microalga *Scenedesmus* sp. BHU1 has been demonstrated in **Figure 6**. In general, photoautotrophic microalgae use ambient CO_2 as a source of inorganic carbon. However, CO_2 has an exceptionally low solubility rate in water, hence sodium bicarbonate supplementation is used for microalga *Scenedesmus* sp. BHU1 which provide the inorganic carbon required to develop higher biomass. It has been reported that adding sodium bicarbonate as a carbon source to the microalgae growing in culture medium enhances the DCW and biomass of microalgae (White et al., 2013; Pancha et al., 2015). The sodium bicarbonate increased biomass of the *Scenedesmus* sp. BHU1, substantially in this investigation (**Figure 6**) suggests that supplementing microalgae with sodium bicarbonate improves cell division and metabolism.

Addition of sodium bicarbonate (4–12 mM) enhanced biomass yields dose-dependently, with no considerable difference in

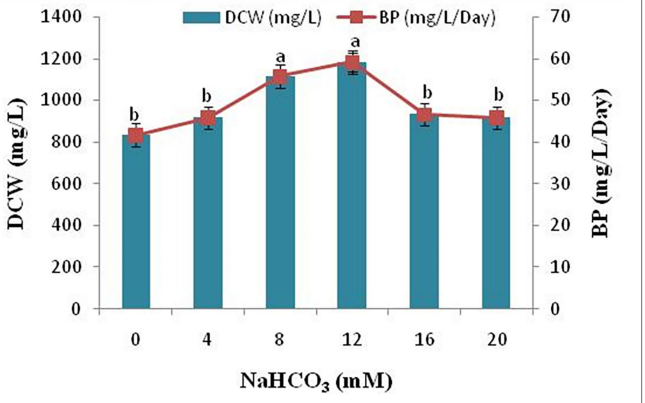

FIGURE 6 | Effect of different sodium bicarbonate concentrations on biomass yield and lipid content of microalga *Scenedesmus* sp. BHU1. Bars are mean ± SE of three replicates. Bars adhered with different alphabets (a and b) are statistically significant at $p < 0.05$ (Tukey's-b *post hoc* test).

DCW and biomass content ($p < 0.05$) detected beyond 12 mM, sodium bicarbonate supplementation because above which it becomes intolerable to the microalgal cells. The DCW and biomass productivity of the microalga *Scenedesmus* sp. BHU1 was significantly reduced in the range of 16–20 mM sodium bicarbonate growing culture. The decline in DCW and biomass of microalgae can be due to the fact that addition of sodium bicarbonate to growing culture leads to a sharp increase in the pH, making the solution alkaline, which is not suitable for growth of microalgae. The highest DCW and biomass content was found with 12 mM sodium bicarbonate (1183.333 ± 44.096 mg/L and 59.167 ± 2.205 mg/L/day) which was 1.4- and 1.4-fold higher than the control grown culture (833.333 ± 33.333 mg/L and 41.667 ± 1.667 mg/L/day). In a similar investigation, the presence of sodium bicarbonate increased biomass yield and lipid content in the green microalga *Scenedesmus* sp. CCNM 1077, *C. vulgaris*, and the diatom *Phaeodactylum tricornutum* (Peng et al., 2014; Pancha et al., 2015; Tu et al., 2018). When *Scenedesmus* sp. CCNM 1077 were treated with 0.6 g/L supplemented sodium bicarbonate the biomass yield was 28.32 mg/L/day (Pancha et al., 2015). In our study, the biomass yield of isolated microalga *Scenedesmus* sp. BHU1 is higher than that of earlier reported isolated strains that have been proposed as greater possible biofuel feedstock. The biomass productivity showed that adding an optimum amount of carbon as sodium bicarbonate can boost the microalgal photosynthetic performance and increasing the rate of reproduction. This study shows that using bicarbonate at the right concentration can boost microalgal development for CO_2 reduction and biofuel generation.

Effect of Sodium Bicarbonate Supplementation on Biochemical Composition

In microalgal cells, a reliable supply of inorganic carbon is required for regular photosynthesis, carbon fixation, and the production of biochemical components such as protein, carbohydrate, and

lipid. This can be accomplished by supplying CO_2 gas into the media or adding salts such as sodium bicarbonate. Bicarbonate has a higher solubility than CO_2 and, hence, has the potential to be employed commercially. The effect of sodium bicarbonate addition on the protein, carbohydrate, and lipid contents of the microalgae *Scenedesmus* sp. BHU1 is shown in **Figure 7**. Protein content of microalgae *Scenedesmus* sp. BHU1 increased in a dose-dependent manner. In the present study, microalgal cells cultured with 16 mM sodium bicarbonate has the highest protein content (33.782 ± 0.900%), followed by 20 mM (29.752 ± 1.658%). Changing protein content with different sodium bicarbonate supplemented microalgal culture can be advantageous because these proteins can also be utilized to produce biofuels, such as biomethane.

Carbon availability and supply is a critical metabolic regulator in microalgae, governing carbohydrate and lipid synthesis (Fan et al., 2012). The addition of 16 mM sodium bicarbonate to the growth medium increased the carbohydrate content from (25.787 ± 2.366 to 56.920 ± 6.390%), as shown in **Figure 7**. In the microalgae *Scenedesmus* sp. BHU1, the results show a positive relationship between sodium bicarbonate supplementation and cellular carbohydrate content. It is already reported that high inorganic carbon availability has been linked to increased activity of Ribulose-1, 5-bisphosphate carboxylase/oxygenase (RuBisCO), a crucial enzyme in the conversion of 3-phosphoglycerate, a substrate for carbohydrate and fatty acid production in microalgae (Peng et al., 2014). There was no significant difference ($p < 0.05$) found in carbohydrate content in cells cultivated with 8 mM (54.111 ± 4.355%) and 20 mM (55.047 ± 2.844%) sodium bicarbonate supplemented culture. Because of the high starch content, which can be quickly turned into hexose sugar, several recent studies demonstrate that microalgal carbohydrates are superior to plant-derived carbohydrates. In the present study, the carbohydrate content of leftover de-oiled microalgal biomass was investigated, which was then utilized in biodiesel coproduction, lowering the cost of value-added product generation. In our study, *Scenedesmus* sp. BHU1 has carbohydrate content (56.920 ± 6.390%) with 16 mM sodium bicarbonate, indicating that this microalga could be a possible source of carbohydrate for biofuel synthesis such as biomethane or other value-added products.

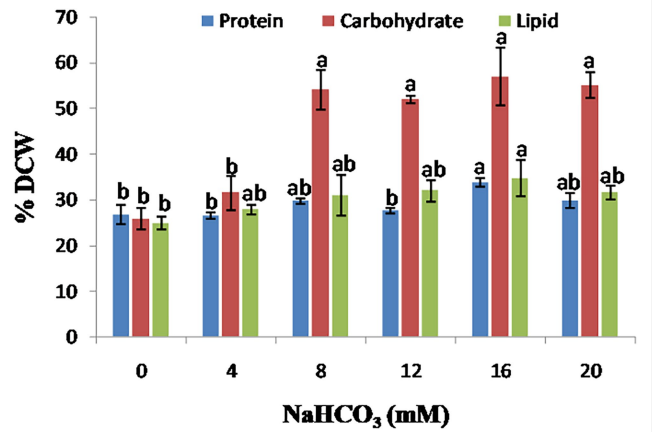

FIGURE 7 | Effect of different sodium bicarbonate concentrations on biochemical composition of microalga *Scenedesmus* sp. BHU1. Bars are mean ± SE of three replicates. Bars adhered with different alphabets (a and b) are statistically significant at $p < 0.05$ (Tukey's-b *post hoc* test).

In microalgae *Scenedesmus* sp. BHU1, sodium bicarbonate addition also enhanced the total lipid content along with carbohydrate as shown in **Figure 7**. There was no significant difference ($p < 0.05$) in total lipid content of microalgal cells cultivated with 8 mM (30.971 ± 4.548%) and 12 mM (31.973 ± 2.336%) sodium bicarbonate supplementation. In the present study, the microalgal cultures treated with 16 mM (34.693 ± 4.001%) sodium bicarbonate have the highest lipid content. When bicarbonate is added to the culture medium, the pH rises, and microalgae modify their membrane composition to cope with the alkaline stress. The biochemical content of green microalgae *Scenedesmus* sp. BHU1 has been compared to previously reported microalgae as shown in **Table 2**

TABLE 2 | The biochemical content of green microalgae *Scenedesmus* sp.

Microalgae strain	Protein (%)	Carbohydrates (%)	Total lipid content (%)
Ankistrodesmus sp.	16.24–18.66	4.48–5.97	11.48–31
Chlamydomonas sp.	58.8	18.5	22.7
Chlorella minutissima	47.89	8.06	14–57
Chlorella sorokiana	40.5	26.8	22–24
Chlorella vulgaris	51–58	12–17	41–58
Dunaliella salina	57	32	6–25
Dunaliella tertiolecta	20–29	12.2–14	11–16
Nannochloropsis oculata	10–27	17–27	22–29
Scenedesmus dimorphos	8–18	21–52	16–40
Scenedesmus falcatus	3.37–7.83	2.73–6.83	6.41–9.6
Scenedesmus protuberans	25.4–45.05	20.95–29.21	17.53–29.30
Scenedesmus sp. CCNM 1077	50.12	25.56	20.91
Scenedesmus sp.	29–37	32.7–41	17–24
Scenedesmus obliquus	10–45	20–40	30–50
Scenedesmus sp. BHU1	33.782	56.920	34.69

BHU1 has been compared to previously reported microalgae (modified from Sajjadi et al., 2018).

(Sajjadi et al., 2018). The results suggest that the microalgae *Scenedesmus* sp. BHU1 is a potential strain for biofuel feedstock because of their high carbohydrate and lipid contents.

Lipid Analysis by BODIPY 505/515 and Nile Red Staining at 16 mM Sodium Bicarbonate Supplementation

BODIPY 505/515 and Nile Red are fluorescent dyes that preferentially stain microalgal cellular lipids (Govender et al., 2012; Sitepu et al., 2012; Katayama et al., 2019). For many years, BODIPY and Nile Red have been used as microalgal lipid probes and their mechanisms are beginning to be understood. The use of BODIPY and Nile Red fluorescence dye to monitor the neutral lipid content of microalgae is a quick method. Under a fluorescence microscope, microalgae labeled with BODIPY and Nile Red were examined for the existence of intracellular lipid droplets. The green, red, and merge channels show dye fluorescence in the presence of cellular lipids of microalga *Scenedesmus* sp. BHU1 (**Figures 8B-D**) while bright field image does not show any cellular lipid (**Figure 8A**). The amount of lipid staining dye inside the cell and the size of the neutral lipid droplet determine the degree of the fluorescence. The occurrence of neutral lipids such as triglycerides and hydrocarbons was indicated by a sizable number of algal cells emitting red fluorescence in the field of the red channel between 590 and 650 nm wavelengths (**Figure 8C**). The presence of a considerable number of significant lipids that synthesizes in the cells of microalga *Scenedesmus* sp. BHU1 was confirmed by the intensity of the BODIPY and Nile Red emitted fluorescence. A remarkably similar study also showed that this fluorescence was found to be significantly linked to neutral lipids in microalgae like *Tetraselmis suecica*, *Nannochloropsis oculate*, and *Scenedesmus* sp. ISTGA1 (Wong et al., 2014; Balduyck et al., 2015; Tripathi et al., 2015). Hence, based on all these observations, the microalga *Scenedesmus* sp. BHU1 is a rich source of lipid which is a good indicator of biofuel feedstock.

CONCLUSION

The microalga *Scenedesmus* sp. emerged as a potential carbon uptake aspirant in the form of inorganic carbon, excess carbon is efficiently incorporated into the biomass for use in lipid accumulation and biofuel production. In the current study, the microalga isolated from wastewater habitat of Banaras Hindu University was identified to be *Scenedesmus* sp. BHU1. The growth of the strain BHU1 in terms of an optical density, pigments content, chlorophyll fluorescence, and biomass content was maximum under a surplus inorganic carbon, at 12 mM, sodium bicarbonate supplementation. The microalgal isolate *Scenedesmus* sp. BHU1 accumulated a significant amount of carbohydrate and intracellular neutral lipid as compared to other earlier reported microalgal species. As a result, it is an excellent aspirant for biofuel feedstock. Finally, it can be concluded that microalgal strain from wastewater environment can be beneficial in the field of inorganic carbon uptake and biofuel production. When sodium bicarbonate is added in the growing medium as a carbon source, the pH of the medium rises, inhibiting the growth of microalgae. Furthermore, investigation is required to optimize the pH of a bicarbonate-supplemented medium during Stage I cultivation and nutrient amelioration for Stage

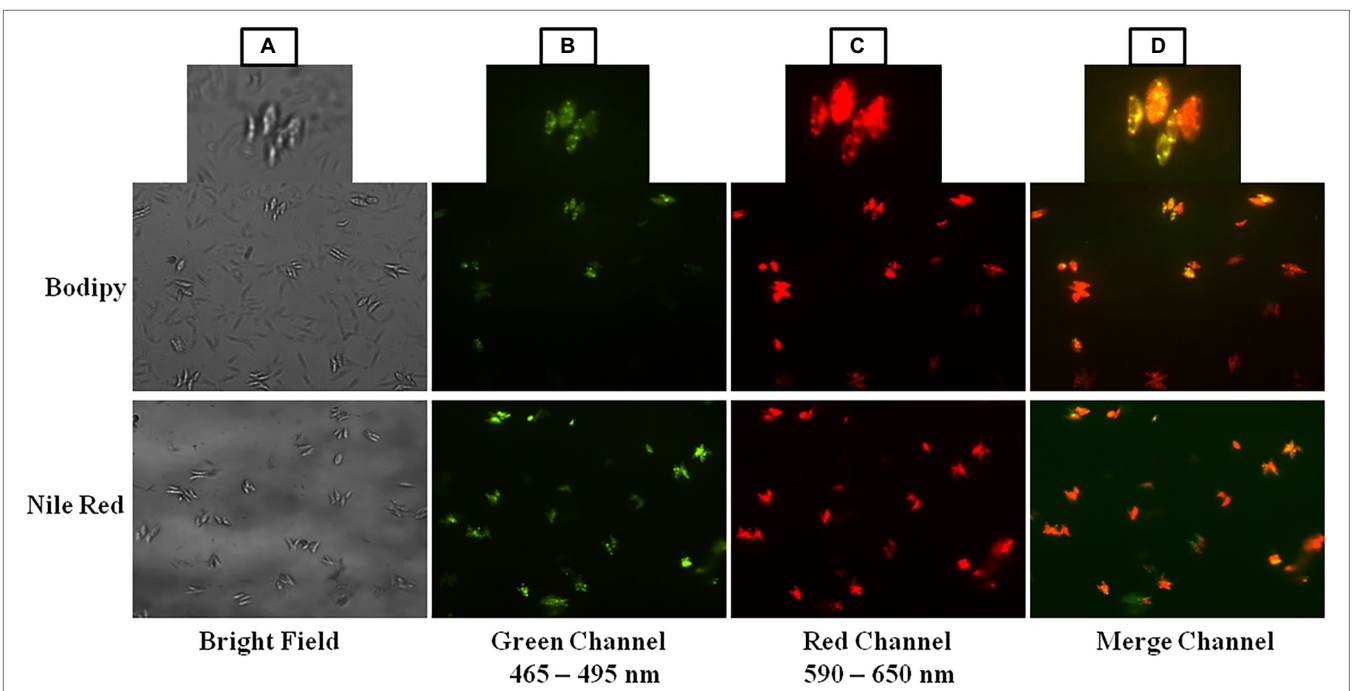

FIGURE 8 | BODIPY 505/515 and Nile Red stained cells of *Scenedesmus* sp. BHU1 under fluorescence microscope in different channels.

II cultivation to stimulate intracellular lipid synthesis, especially when bicarbonate is employed as a partial replacement for gaseous CO_2.

DATA AVAILABILITY STATEMENT

The raw data supporting the conclusions of this article will be made available by the authors, without undue reservation.

AUTHOR CONTRIBUTIONS

RG and RS designed the study, methodology, and investigation. RG, RS, PY, and AK wrote the manuscript. RG and EA_A acquired funding. RG, RS, and AK supervised the study. A-BA-A, AH, EA_A, and AD revised, edited, and provided valuable feedback to this study. All authors have read and agreed to the published version of the manuscript.

FUNDING

The authors would like to extend their sincere appreciation to the Researchers Supporting Project Number (RSP-2021/134), King Saud University, Riyadh, Saudi Arabia.

ACKNOWLEDGMENTS

We want to thank Central Instrumentation Library (CIL) Department of Botany, N.V. Chalapathi Rao, for SEM Facility Department of Geology, Interdisciplinary School of Life Science (ISLS), Banaras Hindu University, and DST-FIST, India, for providing the instrument facilities during the experiment. Finally, the authors (RS and PY) further thank New Delhi for providing a Junior/Senior Research Fellowship (JRF/SRF). The authors would like to extend their sincere appreciation to the Researchers Supporting Project Number (RSP-2021/134), King Saud University, Riyadh, Saudi Arabia.

REFERENCES

Aboul-Maaty, N. A. F., and Oraby, H. A. S. (2019). Extraction of high-quality genomic DNA from different plant orders applying a modified CTAB-based method. *Bull. Natl. Res. Cent.* 43, 1–10. doi: 10.1186/s42269-019-0066-1

Allakhverdiev, S. I., Nishiyama, Y., Miyairi, S., Yamamoto, H., Inagaki, N., Kanesaki, Y., et al. (2002). Salt stress inhibits the repair of photodamaged photosystem II by suppressing the transcription and translation of psbA genes in *Synechocystis*. *Plant Physiol.* 130, 1443–1453. doi: 10.1104/pp.011114

Apandi, N. M., Mohamed, R. M. S. R., Latiffi, N. A. A., Rozlan, N. F. M., and Al-Gheethi, A. A. S. (2017). "Protein and lipid content of microalgae Scenedesmus sp. biomass grown in wet market wastewater." in *MATEC Web Conf. Volume 103*, April 2017, 6. doi: 10.1051/matecconf/201710306011

Arenas, E. G., Rodriguez Palacio, M. C., Juantorena, A. U., Fernando, S. E. L., and Sebastian, P. J. (2017). Microalgae as a potential source for biodiesel production: techniques, methods, and other challenges. *Int. J. Energy Res.* 41, 761–789. doi: 10.1002/er.3663

Baker, N. R. (2008). Chlorophyll fluorescence: a probe of photosynthesis in vivo. *Annu. Rev. Plant Biol.* 59, 89–113. doi: 10.1146/annurev.arplant.59.032607.092759

Balduyck, L., Veryser, C., Goiris, K., Bruneel, C., Muylaert, K., and Foubert, I. (2015). Optimization of a Nile red method for rapid lipid determination in autotrophic, marine microalgae is species dependent. *J. Microbiol. Methods* 118, 152–158. doi: 10.1016/j.mimet.2015.09.009

Behera, S., Singh, R., Arora, R., Sharma, N. K., Shukla, M., and Kumar, S. (2015). Scope of algae as third generation biofuels. *Front. Bioeng. Biotechnol.* 2:90. doi: 10.3389/fbioe.2014.00090

Bligh, E. G., and Dyer, W. J. (1959). A rapid method of total lipid extraction and purification. *Can. J. Biochem. Physiol.* 37, 911–917. doi: 10.1139/o59-099

Borowitzka, M. A. (1992). Algal biotechnology products and processes: matching science and economics. *J. Appl. Psychol.* 4, 267–279. doi: 10.1007/BF02161212

Borowitzka, M. A. (2005). Culturing microalgae in outdoor ponds. In *Algal culturing techniques 2005. Vol. 206*. ed. R. A. Andersen (Burlington: Elsevier Academic Press).

Borowitzka, M. A., and Vonshak, A. (2017). Scaling up microalgal cultures to commercial scale. *Eur. J. Phycol.* 52, 407–418. doi: 10.1080/09670262.2017.1365177

Cheah, W. Y., Show, P. L., Juan, J. C., Chang, J. S., and Ling, T. C. (2018). Enhancing biomass and lipid productions of microalgae in palm oil mill effluent using carbon and nutrient supplementation. *Energy Convers. Manag.* 164, 188–197. doi: 10.1016/j.enconman.2018.02.094

Chen, W., Wang, J., Ren, Y., Chen, H., He, C., and Wang, Q. (2021). Optimized production and enrichment of α-linolenic acid by *Scenedesmus* sp. HSJ296. *Algal Res.* 60:102505. doi: 10.1016/j.algal.2021.102505

Chung, T. Y., Kuo, C. Y., Lin, W. J., Wang, W. L., and Chou, J. Y. (2018). Indole-3-acetic-acid-induced phenotypic plasticity in *Desmodesmus* algae. *Sci. Rep.* 8, 1–13. doi: 10.1038/s41598-018-28627-z

Devgoswami, C. R., Kalita, M. C., Talukdar, J., Bora, R., and Sharma, P. (2011). Studies on the growth behavior of *Chlorella*, *Haematococcus* and *Scenedesmus* sp. in culture media with different concentrations of sodium bicarbonate and carbon dioxide gas. *Afr. J. Biotechnol.* 10, 13128–13138. doi: 10.5897/AJB11.888

Fan, J., Yan, C., Andre, C., Shanklin, J., Schwender, J., and Xu, C. (2012). Oil accumulation is controlled by carbon precursor supply for fatty acid synthesis in *Chlamydomonas reinhardtii*. *Plant Cell Physiol.* 53, 1380–1390. doi: 10.1093/pcp/pcs082

Ferrigo, D., Galla, G., Sforza, E., Morosinotto, T., Barcaccia, G., and Berrini, C. (2015). Biochemical characterization and genetic identity of an oil rich *Acutodesmus obliquus* isolate. *J. Appl. Phycol.* 27, 149–161. doi: 10.1007/s10811-014-0315-5

Gargas, A., and DePriest, P. T. (1996). A nomenclature for fungal PCR primers with examples from intron-containing SSU rDNA. *Mycologia* 88, 745–748. doi: 10.1080/00275514.1996.12026712

Govender, T., Ramanna, L., Rawat, I., and Bux, F. (2012). BODIPY staining, an alternative to the Nile red fluorescence method for the evaluation of intracellular lipids in microalgae. *Bioresour. Technol.* 114, 507–511. doi: 10.1016/j.biortech.2012.03.024

Guiry, M. D., and Guiry, G. M. (2021). World-wide electronic publication, National University of Ireland, Galway. Algae Base. Available at: http://www.algaebase.org (Accessed November 20, 2021).

Han, W., Jin, W., Li, Z., Wei, Y., He, Z., Chen, C., et al. (2021). Cultivation of microalgae for lipid production using municipal wastewater. *Process. Saf. Environ. Prot.* 155, 155–165. doi: 10.1016/j.psep.2021.09.014

Ismagulova, T., Chekanov, K., Gorelova, O., Baulina, O., Semenova, L., Selyakh, I., et al. (2018). A new subarctic strain of *Tetradesmus obliquus*-part I: identification and fatty acid profiling. *J. Appl. Phycol.* 30, 2737–2750. doi: 10.1007/s10811-017-1313-1

Karemore, A., Pal, R., and Sen, R. (2013). Strategic enhancement of algal biomass and lipid in *Chlorococcum infusionum* as bioenergy feedstock. *Algal Res.* 2, 113–121. doi: 10.1016/j.algal.2013.01.005

Katayama, T., Kishi, M., Takahashi, K., Furuya, K., Abd Wahid, M. E., Khatoon, H., et al. (2019). Isolation of lipid-rich marine microalgae by flow cytometric screening with Nile red staining. *Aquaculture* 27, 509–518. doi: 10.1007/s10499-019-00344-y

Khoo, K. S., Chew, K. W., Yew, G. Y., Leong, W. H., Chai, Y. H., Show, P. L., et al. (2020). Recent advances in downstream processing of microalgae lipid recovery for biofuel production. *Bioresour. Technol.* 304:122996. doi: 10.1016/j.biortech.2020.122996

Kumar, N., Banerjee, C., and Jagadevan, S. (2021). Identification, characterization, and lipid profiling of microalgae *Scenedesmus* sp. NC1, isolated from coal mine effluent with potential for biofuel production. *Biotechnol. Rep.* 30:e00621. doi: 10.1016/j.btre.2021.e00621

Lee, K., Eisterhold, M. L., Rindi, F., Palanisami, S., and Nam, P. K. (2014). Isolation and screening of microalgae from natural habitats in the midwestern United States of America for biomass and biodiesel sources. *J. Nat. Sci. Biol. Med.* 5, 333–339. doi: 10.4103%2F0976-9668.136178

Lichtenthaler, H. K. (1987). Chlorophylls and carotenoids: pigments of photosynthetic biomembranes. *Methods Enzymol.* 148, 350–382. doi: 10.1016/0076-6879(87)48036-1

Loewus, F. A. (1952). Improvement in the anthrone method for determination of carbohydrates. *Ann. Chem.* 24, 219–223. doi: 10.1021/ac60061a050

López-Pacheco, I. Y., Castillo-Vacas, E. I., Castañeda-Hernández, L., Gradiz-Menjivar, A., Rodas-Zuluaga, L. I., Castillo-Zacarías, C., et al. (2021). CO_2 biocapture by *Scenedesmus* sp. grown in industrial wastewater. *Sci. Total Environ.* 790:148222. doi: 10.1016/j.scitotenv.2021.148222

Lowry, O. H., Rosenbrough, N. J., Farr, A. L., and Randall, R. J. (1951). Protein measurement with the folin phenol reagent. *J. Biol. Chem.* 193, 265–275. doi: 10.1016/S0021-9258(19)52451-6

Maheshwari, N., Krishna, P. K., Thakur, I. S., and Srivastava, S. (2020). Biological fixation of carbon dioxide and biodiesel production using microalgae isolated from sewage waste water. *Environ. Sci. Pollut. Res.* 27, 27319–27329. doi: 10.1007/s11356-019-05928-y

Mat Aron, N. S., Khoo, K. S., Chew, K. W., Show, P. L., Chen, W. H., and Nguyen, T. H. P. (2020). Sustainability of the four generations of biofuels: a review. *Int. J. Energy Res.* 44, 9266–9282. doi: 10.1002/er.5557

Mata, T. M., Melo, A. C., Simões, M., and Caetano, N. S. (2012). Parametric study of a brewery effluent treatment by microalgae *Scenedesmus obliquus*. *Bioresour. Technol.* 107, 151–158. doi: 10.1016/j.biortech.2011.12.109

Mokashi, K., Shetty, V., George, S. A., and Sibi, G. (2016). Sodium bicarbonate as inorganic carbon source for higher biomass and lipid production integrated carbon capture in *Chlorella vulgaris*. *Achiev. Life Sci.* 10, 111–117. doi: 10.1016/j.als.2016.05.011

Pancha, I., Chokshi, K., Ghosh, T., Paliwal, C., Maurya, R., and Mishra, S. (2015). Bicarbonate supplementation enhanced biofuel production potential as well as nutritional stress mitigation in the microalgae *Scenedesmus* sp. CCNM 1077. *Bioresour. Technol.* 193, 315–323. doi: 10.1016/j.biortech.2015.06.107

Pandey, A., Srivastava, S., and Kumar, S. (2019). Isolation, screening and comprehensive characterization of candidate microalgae for biofuel feedstock production and dairy effluent treatment: a sustainable approach. *Bioresour. Technol.* 293:121998. doi: 10.1016/j.biortech.2019.121998

Parichehreh, R., Gheshlaghi, R., Mahdavi, M. A., and Kamyab, H. (2021). Investigating the effects of eleven key physicochemical factors on growth and lipid accumulation of *Chlorella* sp. as a feedstock for biodiesel production. *J. Biotechnol.* 340, 64–74. doi: 10.1016/j.jbiotec.2021.08.010

Peng, X., Liu, S., Zhang, W., Zhao, Y., Chen, L., Wang, H., et al. (2014). Triacylglycerol accumulation of *Phaeodactylum tricornutum* with different supply of inorganic carbon. *J. Appl. Phycol.* 26, 131–139. doi: 10.1007/s10811-013-0075-7

Priyadharshini, S. D., Babu, P. S., Manikandan, S., Subbaiya, R., Govarthanan, M., and Karmegam, N. (2021). Phycoremediation of wastewater for pollutant removal: a green approach to environmental protection and long-term remediation. *Environ. Pollut.* 290:117989. doi: 10.1016/j.envpol.2021.117989

Rawat, I., Ranjith Kumar, R., Mutanda, T., and Bux, F. (2013). Biodiesel from microalgae: a critical evaluation from laboratory to large scale production. *Appl. Energy* 103, 444–467. doi: 10.1016/j.apenergy.2012.10.004

Renuka, N., Ratha, S. K., Kader, F., Rawat, I., and Bux, F. (2021). Insights into the potential impact of algae-mediated wastewater beneficiation for the circular bioeconomy: a global perspective. *J. Environ. Manag.* 297:113257. doi: 10.1016/j.jenvman.2021.113257

Rippka, R., Deruelles, J., Waterbury, J. B., Herdman, M., and Stanier, R. Y. (1979). Generic assignments, strain histories and properties of pure cultures of cyanobacteria. *Microbiology* 111, 1–61. doi: 10.1099/00221287-111-1-1

Sadiq, I. M., Dalai, S., Chandrasekaran, N., and Mukherjee, A. (2011). Ecotoxicity study of titania (TiO2) NPs on two microalgae species: *Scenedesmus* sp. and *Chlorella* sp. *Ecotoxicol. Environ. Saf.* 74, 1180–1187. doi: 10.1016/j.ecoenv.2011.03.006

Saitou, N., and Nei, M. (1987). The neighbor-joining method: a new method for reconstructing phylogenetic trees. *Mol. Biol. Evol.* 4, 406–425. doi: 10.1093/oxfordjournals. molbev.a040454

Sajjadi, B., Chen, W. Y., Raman, A. A. A., and Ibrahim, S. (2018). Microalgae lipid and biomass for biofuel production: a comprehensive review on lipid enhancement strategies and their effects on fatty acid composition. *Renew. Sust. Energ. Rev.* 97, 200–232. doi: 10.1016/j.rser.2018.07.050

Salbitani, G., Bolinesi, F., Affuso, M., Carraturo, F., Mangoni, O., and Carfagna, S. (2020). Rapid and positive effect of bicarbonate addition on growth and photosynthetic efficiency of the green microalgae *Chlorella sorokiniana* (Chlorophyta, Trebouxiophyceae). *Appl. Sci.* 10:4515. doi: 10.3390/app10134515

Sanger, F., Nicklen, S., and Coulson, A. R. (1977). DNA sequencing with chain-terminating inhibitors. *Proc. Natl. Acad. Sci.* 74, 5463–5467. doi: 10.1073/pnas.74.12.5463

Siddiki, S. Y. A., Mofijur, M., Kumar, P. S., Ahmed, S. F., Inayat, A., Kusumo, F., et al. (2022). Microalgae biomass as a sustainable source for biofuel, biochemical and biobased value-added products: an integrated biorefinery concept. *Fuel* 307:121782. doi: 10.1016/j.fuel.2021.121782

Singh, P., Khadim, R., Singh, A. K., Singh, U., Maurya, P., Tiwari, A., et al. (2019). Biochemical and physiological characterization of a halotolerant *Dunaliella salina* isolated from hypersaline Sambhar Lake, India. *J. Phycol.* 55, 60–73. doi: 10.1111/jpy.12777

Sitepu, I. R., Ignatia, L., Franz, A. K., Wong, D. M., Faulina, S. A., Tsui, M., et al. (2012). An improved high-throughput Nile red fluorescence assay for estimating intracellular lipids in a variety of yeast species. *J. Microbiol. Methods* 91, 321–328. doi: 10.1016/j.mimet.2012.09.001

Srinivasan, R., Mageswari, A., Subramanian, P., Suganthi, C., Chaitanyakumar, A., Aswini, V., et al. (2018). Bicarbonate supplementation enhances growth and biochemical composition of *Dunaliella salina* V-101 by reducing oxidative stress induced during macronutrient deficit conditions. *Sci. Rep.* 8, 6972–6914. doi: 10.1038/s41598-018-25417-5

Szabó, I., Bergantino, E., and Giacometti, G. M. (2005). Light and oxygenic photosynthesis: energy dissipation as a protection mechanism against photo-oxidation. *EMBO Rep.* 6, 629–634. doi: 10.1038/sj.embor.7400460

Tamura, K., Nei, M., and Kumar, S. (2004). Prospects for inferring very large phylogenies by using the neighbor-joining method. *Proc. Natl. Acad. Sci.* 101, 11030–11035. doi: 10.1073/pnas.0404206101

Tamura, K., Stecher, G., and Kumar, S. (2021). MEGA 11: molecular evolutionary genetics analysis version 11. *Mol. Biol. Evol.* 38, 3022–3027. doi: 10.1093/molbev/msab120

Tripathi, R., Singh, J., and Thakur, I. S. (2015). Characterization of microalga *Scenedesmus* sp. ISTGA1 for potential CO_2 sequestration and biodiesel production. *Renew. Energy* 74, 774–781. doi: 10.1016/j.renene.2014.09.005

Tu, Z., Liu, L., Lin, W., Xie, Z., and Luo, J. (2018). Potential of using sodium bicarbonate as external carbon source to cultivate microalga in non-sterile condition. *Bioresour. Technol.* 266, 109–115. doi: 10.1016/j.biortech.2018.06.076

Umetani, I., Janka, E., Sposób, M., Hulatt, C. J., Kleiven, S., and Bakke, R. (2021). Bicarbonate for microalgae cultivation: a case study in a chlorophyte, *Tetradesmus wisconsinensis* isolated from a Norwegian lake. *J. Appl. Phycol.* 33, 1341–1352. doi: 10.1007/s10811-021-02420-4

Valiente Moro, C., Crouzet, O., Rasconi, S., Thouvenot, A., Coffe, G., Batisson, I., et al. (2009). New design strategy for development of specific primer sets for PCR-based detection of Chlorophyceae and Bacillariophyceae in environmental samples. *Appl. Environ. Microbiol.* 75, 5729–5733. doi: 10.1128/AEM.00509-09

Vijay, A. K., Salim, S. A. M., Prabha, S., and George, B. (2021). Exogenous carbon source and phytohormone supplementation enhanced growth rate and metabolite production in freshwater microalgae *Scenedesmus obtusus* Meyen. *Bioresour. Technol. Rep.* 14:100669. doi: 10.1016/j.biteb.2021.100669

Ware, M. A., Belgio, E., and Ruban, A. V. (2015). Photoprotective capacity of non-photochemical quenching in plants acclimated to different light intensities. *Photosynth. Res.* 126, 261–274. doi: 10.1007/s11120-015-0102-4

White, S., Anandraj, A., and Bux, F. (2011). PAM fluorometry as a tool to assess microalgal nutrient stress and monitor cellular neutral lipids. *Bioresour. Technol.* 102, 1675–1682. doi: 10.1016/j.biortech.2010.09.097

White, D. A., Pagarette, A., Rooks, P., and Ali, S. T. (2013). The effect of sodium bicarbonate supplementation on growth and biochemical composition

of marine microalgae cultures. *J. Appl. Phycol.* 25, 153–165. doi: 10.1007/s10811-012-9849-6

Wong, D. M., Nguyen, T. T., and Franz, A. K. (2014). Ethylenediaminetetraacetic acid (EDTA) enhances intracellular lipid staining with Nile red in microalgae *Tetraselmis suecica*. *Algal Res.* 5, 158–163. doi: 10.1016/j.algal.2014.08.002

Yun, C. J., Hwang, K. O., Han, S. S., and Ri, H. G. (2019). The effect of salinity stress on the biofuel production potential of freshwater microalgae *Chlorella vulgaris* YH703. *Biomass Bioenergy* 127:105277. doi: 10.1016/j.biombioe.2019.105277

Conflict of Interest: The authors declare that the research was conducted in the absence of any commercial or financial relationships that could be construed as a potential conflict of interest.

Publisher's Note: All claims expressed in this article are solely those of the authors and do not necessarily represent those of their affiliated organizations, or those of the publisher, the editors and the reviewers. Any product that may be evaluated in this article, or claim that may be made by its manufacturer, is not guaranteed or endorsed by the publisher.

frontiers | Frontiers in Microbiology

ORIGINAL RESEARCH
published: 22 June 2022
doi: 10.3389/fmicb.2022.930357

Antibiotic-Induced Changes in Pigment Accumulation, Photosystem II, and Membrane Permeability in a Model Cyanobacterium

*Yavuz S. Yalcin, Busra N. Aydin, Mst Sayadujjhara and Viji Sitther**

Department of Biology, Morgan State University, Baltimore, MD, United States

Fremyella diplosiphon is a well-studied a model cyanobacterium for photosynthesis due to its efficient light absorption potential and pigment accumulation. In the present study, the impact of ampicillin, tetracycline, kanamycin, and cefotaxime on pigment fluorescence and photosynthetic capacity in *Fremyella diplosiphon* strains B481-WT and B481-SD was investigated. Our results indicated that both strains exposed to kanamycin from 0.2 to 3.2 mg/L and tetracycline from 0.8 to 12.8 mg/L enhanced growth and pigment accumulation. Additionally, B481-SD treated with 0.2–51.2 mg/L ampicillin resulted in a significant enhancement of pigment fluorescence. A detrimental effect on growth and pigmentation in both the strains exposed to 6.4–102.5 mg/L kanamycin and 0.8–102.5 mg/L cefotaxime was observed. Detection of reactive oxygen species revealed highest levels of oxidative stress at 51.2 and 102.5 mg/L kanamycin for B481-*SD* and 102.5 mg/L for B481-WT. Membrane permeability detected by lactate dehydrogenase assay indicated maximal activity at 0.8 mg/L ampicillin, kanamycin, and tetracycline treatments on day 6. Abundant vacuolation, pyrophosphate, and cyanophycin granule formation were observed in treated cells as a response to antibiotic stress. These findings on the hormetic effect of antibiotics on *F. diplosiphon* indicate that optimal antibiotic concentrations induce cellular growth while high concentrations severely impact cellular functionality. Future studies will be aimed to enhance cellular lipid productivity at optimal antibiotic concentrations to disintegrate the cell wall, thus paving the way for clean bioenergy applications.

Keywords: cyanobacteria, fluorescence yield, *Fremyella diplosiphon*, hormetic effect, lactate dehydrogenase, oxidative stress, β-lactams

OPEN ACCESS

Edited by:
Ajay Kumar,
Department of Postharvest Science of Fresh Produce, Agricultural Research Organization (ARO), Israel

Reviewed by:
Ashwani Rai,
Banaras Hindu University, India
Prashant Kumar Singh,
Pachhunga University College, India

***Correspondence:**
Viji Sitther
viji.sitther@morgan.edu

Specialty section:
This article was submitted to Microbiotechnology, a section of the journal Frontiers in Microbiology

Received: *27 April 2022*
Accepted: *25 May 2022*
Published: *22 June 2022*

Citation:
Yalcin YS, Aydin BN, Sayadujjhara M and Sitther V (2022) Antibiotic-Induced Changes in Pigment Accumulation, Photosystem II, and Membrane Permeability in a Model Cyanobacterium. Front. Microbiol. 13:930357. doi: 10.3389/fmicb.2022.930357

INTRODUCTION

In recent years, increased antibiotic contamination in surface and groundwater has drawn worldwide attention due to their potential consequences for the environmental ecosystem and health. Globally, antibiotic consumption has increased by 64% and at the rate of 39% over the past two decades (WHO, 2016; Browne et al., 2021). In the United States alone, about 10,000 tons per annum of antibiotics are consumed and account for ∼70% of the nation's annual antimicrobial consumption (U.S. Food and Drug Administration, 2019). Antibiotic residues excreted in urine and

feces after metabolism are directly introduced to the aquatic environments by poorly managed livestock that have direct access to surface water or indirectly by animal manure (Kümmerer, 2009; Bailey et al., 2015; Pan et al., 2021). While non-targeted antibiotic exposure on eukaryotes is minimal compared to prokaryotes, cyanobacteria are ten times more sensitive than algae to the harmful effects of antibiotics because of fragile cell structures (Norvill et al., 2016; Kulkarni et al., 2017). About 20 different kinds of antibiotics have been detected in the range of 1.26–127.49 ng/L in various aquatic environments (Kim et al., 2018). Of these, the β-lactam group, primarily the penicillin and cephalosporins, constitutes 50–60% of the most consumed antibiotics (Kapoor et al., 2017). Significant amount of β-lactams are directly excreted without any structural changes after metabolism (Snow et al., 2009). Besides, antibiotic residues are detrimental to microbial communities in aquatic ecosystems and are known to greatly impact cellular metabolism in cyanobacteria (González-Pleiter et al., 2013; Cui et al., 2020). The hormesis phenomenon (biphasic effect) in response to harmful environmental agents by low-dose stimulation and high-dose inhibition has been extensively studied (Kouda and Iki, 2010). Exposure of *Microcystis aeruginosa* to low dosages (< 20 mg/L) of erythromycin has been reported to trigger photosynthetic activity *(Fv/Fm)* (Wu et al., 2020).

Of the various cyanobacterial strains, *Fremyella diplosiphon* is a widely studied model organism known for its adaptive growth capability in varying light intensities. Besides, its ability to produce lipids and desirable essential fatty acids make it an ideal third generation biofuel agent. To our knowledge, the impact of antibiotics on *F. diplosiphon* growth and cell membrane permeability remains unknown. In this study, the impact of ampicillin, tetracycline, kanamycin, and cefotaxime on pigment accumulation, photosystem II (PSII) activity, reactive oxygen species (ROS) formation, and cell membrane permeability in *F. diplosiphon* strains B481-SD and B481-WT was investigated. Morphological alterations in cells exposed to antibiotics were observed by microscopic examinations.

MATERIALS AND METHODS

Cyanobacterial Strains and Growth Conditions

F. diplosiphon strains, B481-WT obtained from the UTEX algae repository (Austin, TX, United States), and B481-SD (overexpressed strain with the sterol desaturase gene; accession MH329183) were used in this study. Cultures were grown in liquid BG-11/HEPES medium under wide-spectrum red light (650 nm) with continuous shaking at 170 rpm at 28°C in an Innova 44R shaker (Eppendorf, Hamburg, Germany) for 6 days. Light fluence rate was adjusted to 30 μmol m^{-2} s^{-1} using the model LI-190SA quantum sensor (Li-Cor, United States). These conditions were kept constant during the study.

Antibiotic Treatment

Three classes of antibiotics: β-lactams (ampicillin, cefotaxime), aminoglycosides (kanamycin), and tetracycline, were tested in this study. Antibiotic stock solutions (25x–100x) were prepared according to the manufacturer's instructions and stored at -20°C. Working solutions in the range of 0.2–102.5 mg/L for ampicillin, kanamycin, cefotaxime and 410 mg/L for tetracycline were used in this study (Dias et al., 2015; Shang et al., 2015). Ampicillin, cefotaxime, and kanamycin working solutions were prepared immediately before use and diluted in ddH_2O to the desired concentrations (Baselga-Cervera et al., 2019). Each antibiotic concentration was mixed with 5 ml *F. diplosiphon* cells adjusted to OD750 nm. Assays were performed in 96-well clear polystyrene microplate (Corning®Inc., NY) and cultures grown under conditions mentioned above. Three replicate treatments were maintained and the experiment was repeated twice. In order to minimize the effects of light scattering, every other well was left blank. Plates were sealed with a Breathe-Easy sealing membrane (Sigma-Aldrich, MO, Lot#MKCP8263) to prevent evaporative water loss and decrease the risk of contamination.

Pigment and Photosynthesis Analysis in Antibiotic-Treated *Fremyella diplosiphon*

Phycocyanin and chlorophyll *a* fluorescence in antibiotic-treated and control *F. diplosiphon* were recorded every other day using a microplate reader (BioTek Synergy H1 Microplate Reader, Agilent, United States). While chlorophyll *a* fluorescence was recorded at an excitation of 420 nm and emission of 680 nm, phycocyanin was measured at an excitation of 590 nm and emissions of 650 nm (Rohaiček and Bartaìk, 1999). Fluorescence Epi-RGB mode was used for macro evaluation in 96 well plates on day 6 (Amersham Imager 680, GE Healthcare Bio-Sciences AB, Uppsala, Sweden). Minimal and maximal fluorescence yield (*Fo* and *Fm*) was measured using MINI-PAM (Walz, Effeltrich, Germany) every 48 h for 6 days after incubation in dark for 15 min. Based on these parameters PSII quantum yield (*Fv/Fo*) was calculated using the equation $Fv/Fo = (Fm - Fo)/Fo$ (Wan et al., 2015).

Reactive Oxygen Species Assay

Oxidative stress in antibiotic-treated *F. diplosiphon* strains was detected using 2',7'-dichlorofluorescein diacetate, also known as H_2DCFDA (EMD Chemicals, United States) (Ajiboye et al., 2017). After growth of cells in varying antibiotic concentrations for 6 days under conditions mentioned above, a fresh 20 mM DCFDA stock was prepared, and 50 μL added to 150 μl cells in a 96 well plate (Busch and Montgomery, 2015). Fluorescence intensity was measured at an excitation of 529 nm and emission of 495 nm using a microplate reader after incubation in the dark for 45 min at room temperature (BioTek Synergy H1 Microplate Reader, Agilent, United States). Three replicate treatments were maintained and the experiment repeated once.

Lactate Dehydrogenase Assay and Microscopic Observations

The toxicity of ampicillin, tetracycline, and kanamycin on *F. diplosiphon* was assessed using the Pierce™ (LDH Cytotoxicity Assay Kit, Thermo Fisher Scientific, United States) according to the manufacturer's protocol. Since cefotaxime resulted in

cell death on day 6, it was not included for this assay. Strains B481-WT and B481-SD were grown in liquid BG-11/HEPES medium containing 0.2–102.5 mg/L ampicillin, tetracycline, and kanamycin in 10 ml vented culture flasks. Cells at an optical density of 0.2 at OD750 nm were grown under continuous shaking at 70 rpm and 30 μmol m^{-2} s^{-1} at 28°C in an Innova 44R shaker. Cells grown in the absence of antibiotics served as control. The flasks were placed in an incubator at 37°C in the dark for 24 h prior to LDH measurement. On day 6, 50 μl cultures were transferred to a 96 well plate, and 50 μL of the reaction mixture (LDH Cytotoxicity Assay Kit, Thermo Fisher Scientific, United States) was added. After incubation for 30 min. at room temperature in the dark, 50 μL of stop solution was added and mixed gently (Wejnerowski et al., 2018). Absorbance was measured at 490 nm using a microplate reader (BioTek Synergy H1 Microplate Reader, Agilent, United States) after 2 h incubation in the dark at room temperature. Three replicates per treatment were maintained and the experiment was repeated. On day 6, microscopic observations were made using a cytation 5 Cell Imaging Multi-Mode reader (BioTek® Instruments, Inc., Winooski, United States).

Statistical Analysis

Repeated ANOVA and Tukey's multiple comparison tests including Pearson's correlation were used to analyze *F. diplosiphon* sensitivity to different antibiotic treatments at each sampling point. SPSS 28.0 (IBM Corporation, Armonk, United States) was also used to analyze and plot the data.

RESULTS

Antibiotics Impact Pigment Fluorescence in *Fremyella diplosiphon* Strains

Phycocyanin and chlorophyll *a* pigment autofluorescence was quantified to evaluate the effect of antibiotics on *F. diplosiphon* growth. Strain B481-SD treated with ampicillin ranging from 0.2 to 25.6 mg/L exhibited significant increases in phycocyanin and chlorophyll *a* autofluorescence; however, a significant decrease was detected at 51.2 and 102.5 mg/L ($p < 0.01$) (**Figures 1A**, **2A**). By contrast, B481-WT treated with ampicillin exhibited a significant decrease in pigment autofluorescence from 3.2 to 102.5 mg/L compared to the untreated control. We observed a significant reduction of pigment autofluorescence in B481-SD and B481-WT treated with cefotaxime ranging from 0.8 to 102.5 mg/L and 0.2 to 102.5 mg/L respectively (**Figures 1B,F**, **2B,F**). A significant reduction in phycocyanin and chlorophyll *a* autofluorescence was observed in both strains exposed to kanamycin from 6.4 to 102.5 mg/L when compared to the untreated control. However, a significant increase in B481-SD autofluorescence at lower kanamycin concentrations of 0.2–3.2 mg/L when compared to the control was observed (**Figures 1C**, **2C**). B481-SD treated with tetracycline reduced phycocyanin and chlorophyll *a* autofluorescence at concentrations ranging from 102.5 to 410 mg/L, while it ranged from 25.6 to 410 mg/L for B481-WT. A significant increase in pigment autofluorescence was observed in both strains treated with tetracycline from 0.8 to 12.8 mg/L on day 6 (**Figures 1D,H**, **2D,H**).

Photosynthetic Efficacy of *Fremyella diplosiphon* Exposed to Varying Antibiotic Concentrations

Quantification of photosynthetic efficiency (*Fv/Fo*) revealed a significant increase in B481-SD strain treated with ampicillin at 0.2–3.2 mg/L on day 4 compared to the control (**Figure 3A**). On the other hand, a significant reduction of *Fv/Fo* ratios was observed in B-481-SD treated with 51.2 and 102.8 mg/L ampicillin on day 6 (**Figures 3A,B**). A substantial reduction in the *Fv/Fo* ratios in cefotaxime-treated cells was observed, with no recovery of B481-SD and B481-WT at concentrations higher

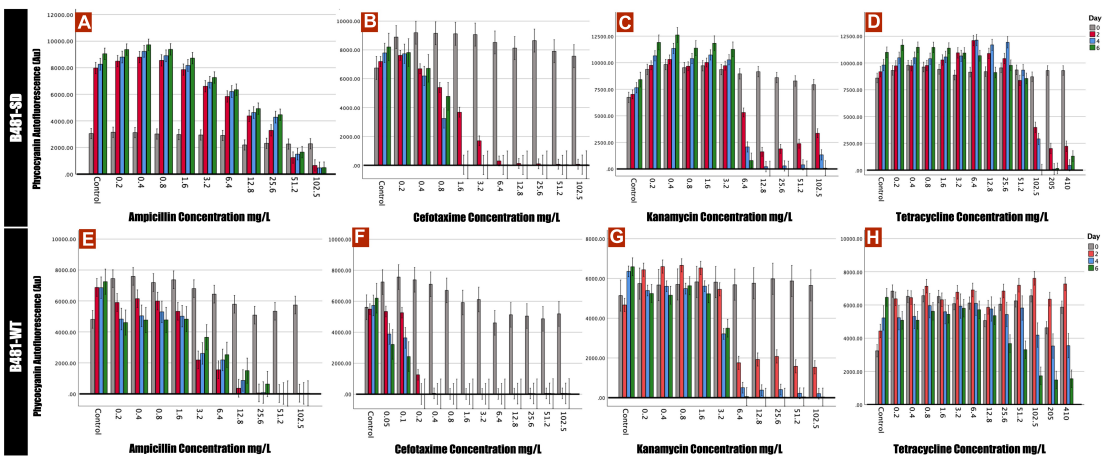

FIGURE 1 | Phycocyanin autofluorescense of B481-SD and B481-WT strains reflected by 590 nm excitation and 650 nm emission. B481-SD strain was exposed to concentrations ranging from 0.2 to 102.5 mg/L ampicillin, cefotaxime, kanamycin, and tetracycline **(A–D)**, and B481-WT strain to ampicillin and kanamycin concentrations ranging from 0.2 to 102.5 mg/L; 0.05–102.5 mg/L for cefotaxime and 0.2–410 mg/L for tetracycline **(E–H)**. Both strains were cultivated in antibiotics for 6 days at 28°C with a light intensity of 30 μmol m^{-2} s^{-1}. Mean and standard deviations are indicated by error bars.

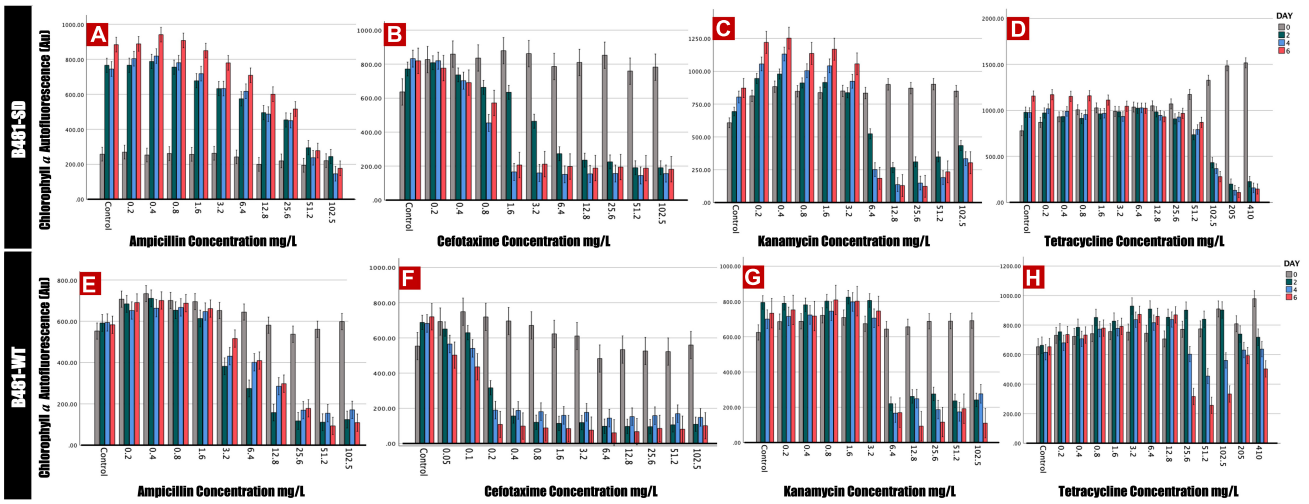

FIGURE 2 | Chlorophyll *a* autofluorescence of *Fremyella diplosiphon* strains B481-SD and B481-WT reflected by excitation of 420 nm and emission of 680 nm. B481-SD strain was exposed to ampicillin, cefotaxime, kanamycin, and tetracycline concentrations ranging from 0.2 to 102.5 mg/L **(A–D)**, B481-WT strain was exposed to ampicillin and kanamycin concentrations ranging from 0.2 to 102.5 mg/L; 0.05–102.5 mg/L for cefotaxime and 0.2–410 mg/L for tetracycline **(E–H)**. Both strains are cultivated with four antibiotics for 6 days at 28°C with a light intensity of 30 μmol m^{-2} s^{-1}. Mean and standard deviations are indicated by error bars.

than 1.6 mg/L and 0.05 mg/L respectively (**Figures 3C,D**). While we observed a significant decrease in *Fv/Fo* ratio in both strains treated with kanamycin from 1.6 to 102.5 mg/L, a significant increase in B481-WT at concentrations ranging from 0.2 to 1.6 mg/L kanamycin compared with the control group was noted (**Figure 3F**). We also observed a decrease in *Fv/Fo* ratios in both strains exposed to tetracycline concentrations higher than 102.5 mg/L ($p < 0.05$) (**Figures 3G,H**).

Detection of Reactive Oxygen Species in Antibiotic-Treated *Fremyella diplosiphon*

Antibiotic-induced ROS measured using the dichlorodihydrofluorescein revealed significantly higher levels ($p < 0.01$) in both strains treated with cefotaxime, kanamycin, and tetracycline from 0.2 to 102.5 mg/L compared to the untreated control (**Figures 4A,B**). While B481-SD treated with 102.5 mg/L ampicillin exhibited significantly higher ROS ($p < 0.01$), it ranged from 6.4 to 102.5 mg/L for B481-WT (**Figures 4A,B**). Highest levels of oxidative stress were observed at 51.2 and 102.5 mg/L kanamycin for B481-SD and 102.5 mg/L for B-481-WT.

Membrane Integrity in Antibiotic-Treated *Fremyella diplosiphon*

B481-SD and B481-WT strains treated with ampicillin, tetracycline, and kanamycin exhibited maximum LDH activity at the concentrations of 0.8 and 0.4 mg/L. Specifically, enhanced LDH activity ($p < 0.05$) was observed in B481-SD treated with tetracycline, ampicillin, and kanamycin from 0.2 to 0.8 mg/L (**Figure 5A**). The LDH activity of B481-WT was higher in kanamycin and tetracycline at 0.4 mg/L compared to ampicillin at the same concentration (**Figure 5B**). Microscopic observations such as filament fragmentation and alteration of cell shape were observed at concentrations higher than 25.6 mg/L ampicillin for B481-WT and 51.2 mg/L kanamycin for B481-SD and B481-WT (**Figures 6B–D**). In addition, cellular stress-related structures such as pyrophosphate granules (**Figure 6F**, green rectangle), akinetes (**Figure 6A**, yellow arrows), and cellular vacuoles (**Figures 6B–F**, red arrows) were observed in the strains exposed to higher antibiotic concentrations.

DISCUSSION

In the present study, we evaluated the effect of four different antibiotics on pigment autofluorescence and photosynthetic activity in two *F. diplosiphon* strains. Additionally, we observed membrane permeability and intracellular ROS production to determine the effect of antibiotic treatment on the strains.

Alterations of Pigment Autofluorescence in Antibiotic-Treated *Fremyella diplosiphon*

Of the four antibiotics tested in this study, ampicillin and cefotaxime belonged to the β-lactam group and are known to bind to the penicillin-binding protein of the prokaryotic cell (Stokes et al., 2019). The structural resemblance of the *F. diplosiphon* cell wall to gram-negative prokaryotes explains the sensitivity of cyanobacteria to β-lactam antibiotics (Springstein et al., 2020). Interestingly, phycocyanin and chlorophyll *a* autofluorescence in B481-SD was enhanced at lower ampicillin concentrations (0.2–25.6 mg/L); however, its growth was significantly inhibited at concentrations above 51.2 mg/L. On the other hand, a substantial decline in pigment fluorescence was observed in B481-WT at concentrations higher than 3.2 mg/L ampicillin. Thus, significantly higher pigment fluorescence in

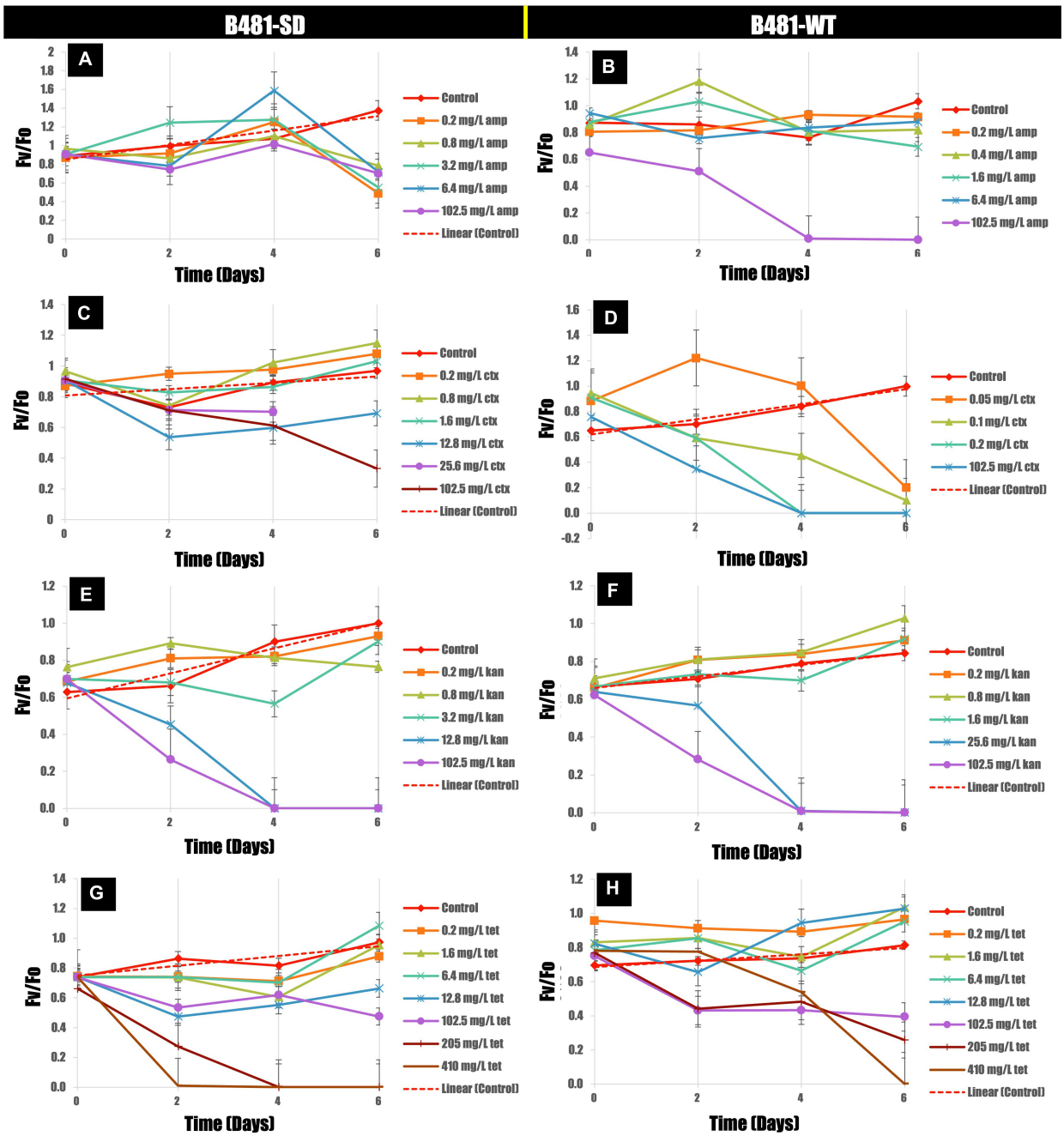

FIGURE 3 | Variance of *Fv/Fo* in B481-SD **(A,C,E,G)** and B481-WT **(B,D,F,H)** strains of *Fremyella diplosiphon* in response to ampicillin, cefotaxime, kanamycin, and tetracycline exposure for 6 days. Mean and standard deviations are indicated by error bars.

B481-SD at these concentrations provide further evidence of the sterol dehydrogenase gene overexpression associated with ampicillin resistance. It is also known that the molecular configuration against β-lactam antibiotics is a mechanism for acquiring bacterial resistance (Alpay-Karaoglu et al., 2007; Sanganyado and Gwenzi, 2019). The significant reduction of pigment accumulation observed in cefotaxime at concentrations above 1.6 mg/L for B481-SD and 0.2 mg/L for B481-WT indicate the higher sensitivity of B481-WT to cefotaxime. Additionally, enhanced fluorescence of the strains exposed to kanamycin (0.2–3.2 mg/L) and tetracycline (0.8–12.8 mg/L) on day 6 indicate the hormetic effect of these antibiotics on stimulation and inhibition. Our results are in accordance with the findings of Liu et al. (2015), who reported the toxic effect of amoxicillin at concentrations higher than 6.88 μg/L in *Microcystis aeruginosa,* while a growth-stimulating effect was

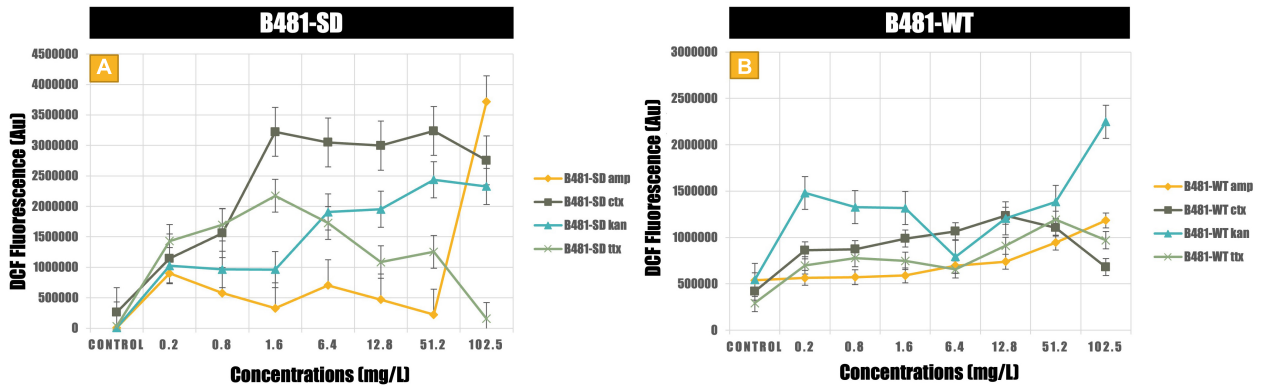

FIGURE 4 | Reactive oxygen species generated in B481-SD **(A)** and B481-WT **(B)** *Fremyella diplosiphon* strains exposed to ampicillin, cefotaxime, kanamycin, and tetracycline. Mean and standard deviations are indicated by error bars.

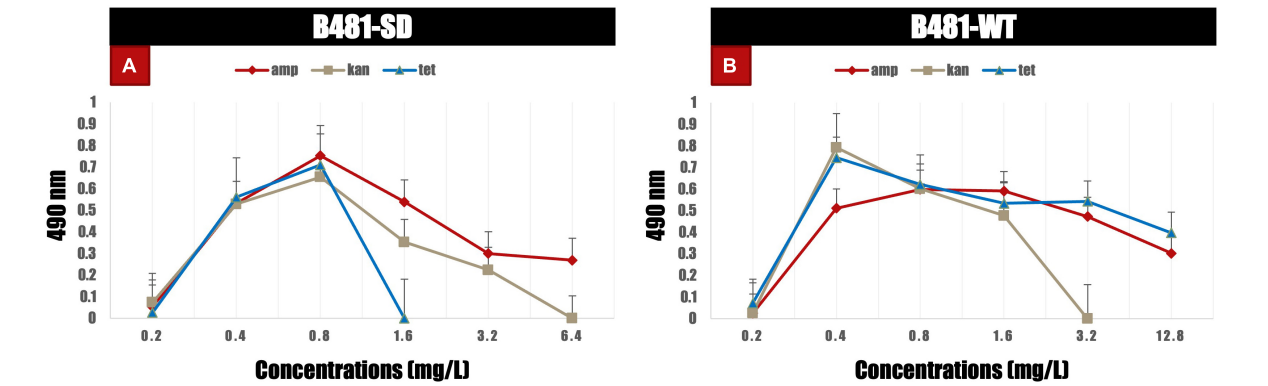

FIGURE 5 | Lactate dehydrogenase activity in B481-SD and B481-WT strains of *Fremyella diplosiphon* exposed to varying concentrations of ampicillin, kanamycin, and tetracycline **(A,B)** on day 6. Mean and standard deviations are indicated by error bars.

observed at concentrations below. A similar biphasic effect was reported in *Skeletonema costatum* where exposure to florfenicol at < 2.0 mg/L enhanced growth while inhibition was reported at > 2.0 mg/L (Liu et al., 2012). As noted in our study, ampicillin, kanamycin, and tetracycline at higher concentrations inhibited *F. diplosiphon* pigment autofluorescence (**Figures 1**, **2**). Despite lowering the cefotaxime concentrations to 0.05 mg/L (**Figures 1**, **2B,F**), we did not observe the hormetic effect in B481-WT. Exposure to kanamycin and tetracycline resulted in approximately twice more remarkable pigment fluorescence in B481-SD than B481-WT, indicating higher tolerance of B481-SD to harmful antibiotics regardless of β-lactam resistance. In a previous study by Fathabad et al. (2019), a 27.2% enhancement of total lipid content in B481-SD compared to B481-WT was reported, which was attributed to gene overexpression. The enhanced lipid production in B481-SD could be attributed to sustained membrane integrity, due to increased fatty acids that facilitates membrane repair in B48-SD (Sen, 2020). On the other hand, kanamycin and tetracycline inhibit protein synthesis by binding to the bacterial ribosomal subunit resulting in a misreading of the t-RNA. The inhibition of RNA translation could have resulted in protein-derived *F. diplosiphon* pigments as observed in our study. In a report by Daghrir and Drogui (2013), tetracycline at 100 mg/L was reported to be detrimental to aquatic organisms. Although photocatalytic degradation of tetracycline occurs in a few days, the byproducts anhydrotetracycline and 4-epianhydrotetracycline have been reported to be more toxic than the primary compound (Halling-Sørensen et al., 2002). Thus, high concentrations of tetracycline ranging from 205 to 410mg/L were selected in this study. These residues might have also contributed to the pigment fluorescence of *F. diplosiphon,* as observed in our study.

Antibiotic Exposure Enhance *Fremyella diplosiphon* Membrane Permeability

Assessment of membrane integrity as a measure of extracellular LDH enzyme activity revealed a linear correlation (data not shown). In both strains treated with antibiotics, LDH activity correlated to phycocyanin and chlorophyll *a* accumulation in a dose-dependent manner, indicating a positive correlation between increased metabolic activity and membrane permeability prior to complete cell destruction. Antimicrobial agents such as ampicillin and cefotaxime that target prokaryotic cell walls

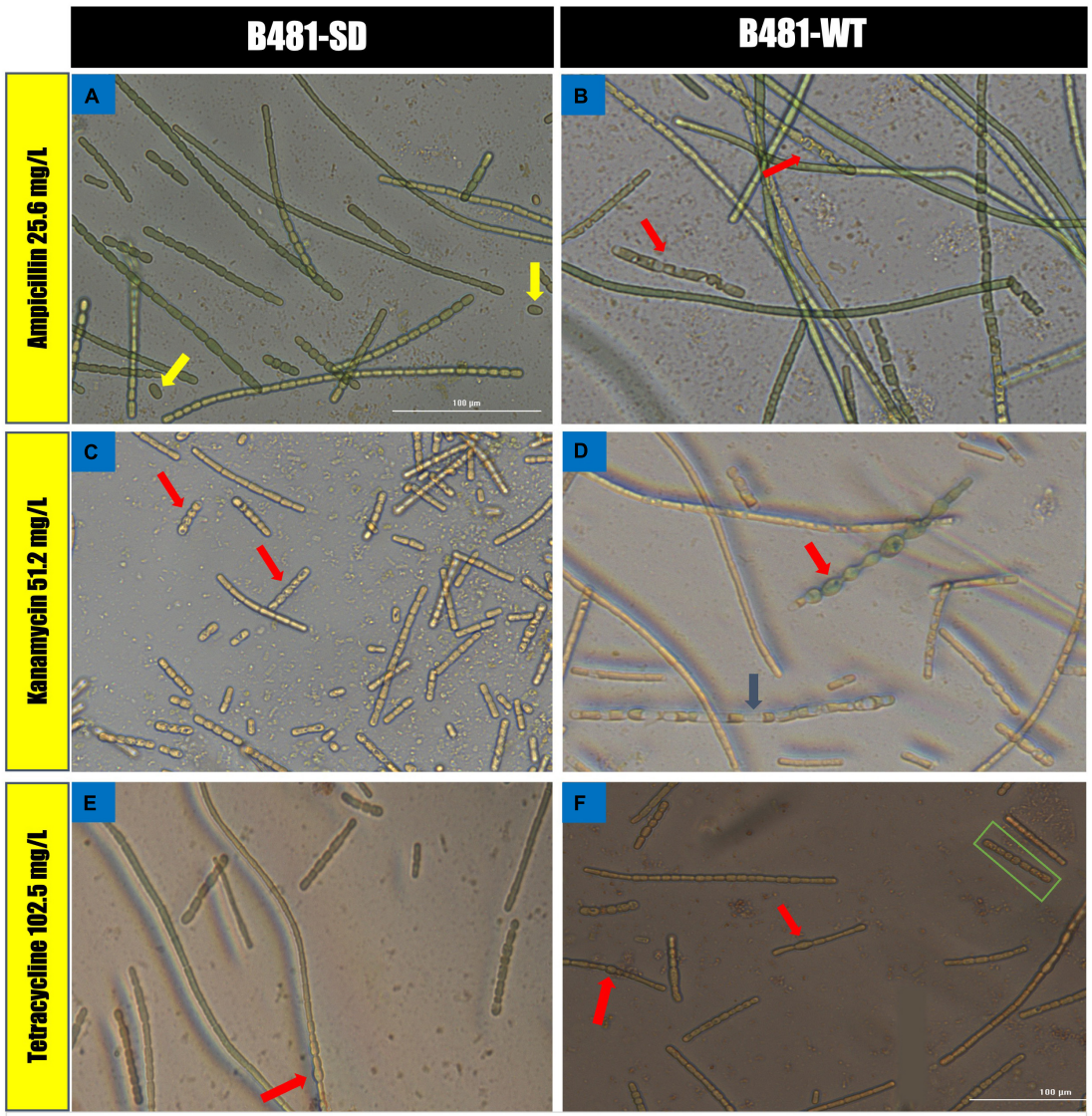

FIGURE 6 | Morphological alterations of *Fremyella diplosiphon* strains in concentrations at 25.6 mg/L ampicillin **(A,B)**, 51.2 mg/L kanamycin **(C,D)** and 102.5 mg/L tetracycline **(E,F)** treatments. Representative sections of color bright field images were captured using a cytation 5 Cell Imaging Multi-Mode reader at 40× magnification bars, 100 µm.

are reported to be more effective in weakening membranes than ribosomal inhibitor antibiotics such as kanamycin and tetracycline (Stokes et al., 2019). These compounds are known to trigger intracellular signaling *via* the shifting of metabolic compounds such as glucose, glycerol, and pyruvate to lipid synthesis. In a study by Liu et al. (2011) weakening of the cell wall by ampicillin was reported to facilitate free fatty acids (FFA) secretion by reducing feedback inhibition of enzymes involved in the synthesis of fatty acid precursors, thus resulting in an overall increase in FFA production (Alpay-Karaoglu et al., 2007). Enhanced lipid production in *Synechocystis* species was correlated to a loss in membrane components as well (Oliveira et al., 2016). Thus, we hypothesize that membrane damage could lead to permeability changes as indicated by increased metabolic activity stimulating lipid synthesis and accumulation.

Production of ROS is pertinent when antibiotic concentrations above the threshold level can onset cellular stress (Chen et al., 2019). In cellular metabolism, a dynamic equilibrium between ROS generation and elimination is maintained due to the operation of antioxidant defense systems. In addition, a tremendous increase of ROS may cause oxidative damage resulting in cell injury and ultimately cell death due to protein and lipid damage and impairment of cyanobacterial homeostasis (Du et al., 2018). The reactive oxygen radicals generated have the potential to react with membrane lipids and protein (phycocyanin, chlorophyll a) structures in cyanobacteria. Our results revealed maximal ROS levels in both strains treated

with ampicillin at 102.5 mg/L, with lower ROS levels in B481-SD compared to B481-WT. While B481-SD treated with cefotaxime at 0.2–102.5 mg/L exhibited higher levels of ROS, it was not detected in B481-WT (**Supplementary Figure 1D**). It is possible that a reduction in the number of viable cells could have lowered ROS production in B481-WT. We hypothesize that the detrimental effect of cefotaxime could have resulted in higher ROS levels in the first few days of the experiment, while the unstable structure of oxygen radicals due to easy loss of unpaired electrons and elimination could be responsible for lower ROS at the end of the testing period. Both strains exposed to kanamycin at 102.5 mg/L revealed maximum ROS on day 6 and exhibited a similar growth paradigm at the concentrations tested. ROS production is generally caused by the leakage of electrons from the photosystem electron transport chain as part of the metabolism of photosynthetic organisms and plays a dynamic equilibrium in the operation of antioxidant defense system. A study on the analysis of the impact of superoxide dismutase (SOD) enzymes in 149 cyanobacterial strains has shown diverse SOD enzyme isoforms, indicating that the antioxidant mechanism that eliminates ROS could vary in different cyanobacterial strains (Boden et al., 2021).

Chlorophyll *a* is an important light-harvesting photosynthetic pigment in cyanobacteria, which plays a crucial role in energy absorption and transduction (Latifi et al., 2009). The electron transport capacity of photosynthetic pigments such as chlorophyll *a* is closely related to the quality of the photosynthetic apparatus and indicated by PSII activity (*Fv/Fo*). As the pigment content of cyanobacteria decrease, the thylakoid membrane becomes the active site due to cell wall damaging antibiotics such as penicillin and cephalosporins (Liu et al., 2015). The decrease in PSII activity of both strains at higher ampicillin, cefotaxime, and kanamycin concentrations of 51.2 and 102.5 mg/L on day 6 as observed in our study could be attributed to enhanced ROS production. Therefore, it is possible that reduced pigment functions could have occurred due to ROS-induced damage to the thylakoid membranes, particularly chlorophyll *a*.

CONCLUSION

In this study, we investigated the effect of four antibiotics at varying concentrations on phycocyanin and chlorophyll *a* autofluorescence of *F. diplosiphon* strains. Significant increases in pigment accumulation at specific antibiotic concentrations pave the way for further studies to accomplish lipid synthesis for easy and efficient biofuel production. Future studies will aim toward enhancing membrane permeability in the B481-SD strain with antibiotics. In addition, the combined effect of antibiotics and zero-valent iron nanoparticles in enhancing specific lipid gene overexpression and transcript levels activity will be studied.

DATA AVAILABILITY STATEMENT

The original contributions presented in this study are included in the article/**Supplementary Material**, further inquiries can be directed to the corresponding author.

AUTHOR CONTRIBUTIONS

YY and BA designed and performed the experiments, analyzed, interpreted the data, and drafted the manuscript. MS gave critical comments on the article. VS designed, conceived the study, edited the manuscript, and obtained funding. All authors read and approved the final manuscript.

FUNDING

This research was funded by the National Science Foundation's Nanoscale Interactions Program (grant no. 1900966) and co-supported by Excellence in Research. Core support facilities partially provided by the National Institute of General Medical Sciences (grant no. 5UL1GM118973) and the National Institute on Minority Health and Health Disparities (grant no. 5U54MD013376) grants are acknowledged.

SUPPLEMENTARY MATERIAL

The Supplementary Material for this article can be found online at: https://www.frontiersin.org/articles/10.3389/fmicb.2022.930357/full#supplementary-material

REFERENCES

Ajiboye, T. O., Habibu, R. S., Saidu, K., Haliru, F. Z., Ajiboye, H. O., Aliyu, N. O., et al. (2017). Involvement of oxidative stress in protocatechuic acid-mediated bacterial lethality. *Microbiologyopen* 6:e00472. doi: 10.1002/mbo3.472

Alpay-Karaoglu, S., Birol Ozgumus, O., Sevim, E., Kolayli, F., Sevim, A., and Yesilgil, P. (2007). Investigation of antibiotic resistance profile and TEM-type β-lactamase gene carriage of ampicillin-resistant *Escherichia coli* strains isolated from drinking water. *Ann. Microbiol.* 57:281.

Bailey, C., Spielmeyer, A., Frings, R. M., Hamscher, G., and Schüttrumpf, H. (2015). From agricultural fields to surface water systems: the overland transport of veterinary antibiotics. *J. Soils Sediments* 15, 1630–1634. doi: 10.1007/s11368-015-1140-4

Baselga-Cervera, B., Cordoba-Diaz, M., García-Balboa, C., Costas, E., López-Rodas, V., and Cordoba-Diaz, D. (2019). Assessing the effect of high doses of ampicillin on five marine and freshwater phytoplankton species: a biodegradation perspective. *J. Appl. Psychol.* 31, 2999–3010. doi: 10.1007/s10811-019-01823-8

Boden, J. S., Konhauser, K. O., Robbins, L. J., and Sánchez-Baracaldo, P. (2021). Timing the evolution of antioxidant enzymes in cyanobacteria. *Nat. Commun.* 12:4742. doi: 10.1038/s41467-021-24396-y

Browne, A. J., Chipeta, M. G., Haines-Woodhouse, G., Kumaran, E. P. A., Hamadani, B. H. K., Zaraa, S., et al. (2021). Global antibiotic consumption and usage in humans, 2000–18: a spatial modelling study. *Lancet Planet. Health* 5, e893–e904. doi: 10.1016/S2542-5196(21)00280-1

Busch, A. W. U., and Montgomery, B. L. (2015). The tryptophan-rich sensory protein (TSPO) is involved in stress-related and light-dependent processes in the cyanobacterium fremyella diplosiphon. *Front. Microbiol.* 6:1393. doi: 10.3389/fmicb.2015.01393

Chen, X., Yin, H., Li, G., Wang, W., Wong, P. K., Zhao, H., et al. (2019). Antibiotic-resistance gene transfer in antibiotic-resistance bacteria under different light irradiation: implications from oxidative stress and gene expression. *Water Res.* 149, 282–291. doi: 10.1016/j.watres.2018.11.019

Cui, M., Liu, Y., and Zhang, J. (2020). Sulfamethoxazole and tetracycline induced alterations in biomass, photosynthesis, lipid productivity, and proteomic expression of Synechocystis sp. PCC 6803. *Environ. Sci. Pollut. Res.* 27, 30437–30447. doi: 10.1007/s11356-020-09327-6

Daghrir, R., and Drogui, P. (2013). Tetracycline antibiotics in the environment: a review. *Environ. Chem. Lett.* 11, 209–227. doi: 10.1007/s10311-013-0404-8

Dias, E., Oliveira, M., Jones-Dias, D., Vasconcelos, V., Ferreira, E., Manageiro, V., et al. (2015). Assessing the antibiotic susceptibility of freshwater cyanobacteria spp. *Front. Microbiol.* 6:799. doi: 10.3389/fmicb.2015.00799

Du, Y., Wang, J., Zhu, F., Mai, D., Xiang, Z., Chen, J., et al. (2018). Comprehensive assessment of three typical antibiotics on cyanobacteria (Microcystis aeruginosa): the impact and recovery capability. *Ecotoxicol. Environ. Saf.* 160, 84–93. doi: 10.1016/j.ecoenv.2018.05.035

Fathabad, G. S., Arumanayagam, A. C. S., Tabatabai, B., Chen, H., Lu, J., and Sitther, V. (2019). Augmenting Fremyella diplosiphon cellular lipid content and unsaturated fatty acid methyl esters via sterol desaturase gene overexpression. *Appl. Biochem. Biotechnol.* 189, 1127–1140. doi: 10.1007/s12010-019-03055-5

González-Pleiter, M., Gonzalo, S., Rodea-Palomares, I., Leganés, F., Rosal, R., Boltes, K., et al. (2013). Toxicity of five antibiotics and their mixtures towards photosynthetic aquatic organisms: implications for environmental risk assessment. *Water Res.* 47, 2050–2064. doi: 10.1016/j.watres.2013.01.020

Halling-Sørensen, B., Sengeløv, G., and Tjørnelund, J. (2002). Toxicity of tetracyclines and tetracycline degradation products to environmentally relevant bacteria, including selected tetracycline-resistant bacteria. *Arch. Environ. Contam. Toxicol.* 42, 263–271. doi: 10.1007/s00244-001-0017-2

Kapoor, G., Saigal, S., and Elongavan, A. (2017). Action and resistance mechanisms of antibiotics: a guide for clinicians. *J. Anaesthesiol. Clin. Pharmacol.* 33, 300–305. doi: 10.4103/joacp.JOACP_349_15

Kim, C., Ryu, H. D., Chung, E. G., and Kim, Y. (2018). Determination of 18 veterinary antibiotics in environmental water using high-performance liquid chromatography-q-orbitrap combined with on-line solid-phase extraction. *J. Chromatogr. B.* 1084, 158–165. doi: 10.1016/j.jchromb.2018.03.038

Kouda, K., and Iki, M. (2010). Beneficial effects of mild stress (Hormetic Effects): dietary restriction and health. *J. Physiol. Anthropol.* 29, 127–132. doi: 10.2114/jpa2.29.127

Kulkarni, P., Olson, N. D., Raspanti, G. A., Goldstein, R. E. R., Gibbs, S. G., Sapkota, A., et al. (2017). Antibiotic concentrations decrease during wastewater treatment but persist at low levels in reclaimed water. *Int. J. Environ. Res. Public Health* 14:668. doi: 10.3390/ijerph14060668

Kümmerer, K. (2009). Antibiotics in the aquatic environment - A review - Part I. *Chemosphere* 75, 417–434. doi: 10.1016/j.chemosphere.2008.11.086

Latifi, A., Ruiz, M., and Zhang, C. C. (2009). Oxidative stress in cyanobacteria. *FEMS Microbiol. Rev.* 33, 258–278. doi: 10.1111/j.1574-6976.2008.00134.x

Liu, W., Ming, Y., Huang, Z., and Li, P. (2012). Impacts of florfenicol on marine diatom Skeletonema costatum through photosynthesis inhibition and oxidative damages. *Plant Physiol. Biochem.* 60, 165–170. doi: 10.1016/j.plaphy.2012.08.009

Liu, X., Sheng, J., and Curtiss Iii, R. (2011). Fatty acid production in genetically modified cyanobacteria. *Proc. Natl. Acad. Sci. U. S. A.* 108, 6899–6904. doi: 10.1073/pnas.1103014108/-/DCSupplemental

Liu, Y., Chen, X., Zhang, J., and Gao, B. (2015). Hormesis effects of amoxicillin on growth and cellular biosynthesis of Microcystis aeruginosa at different nitrogen levels. *Microb. Ecol.* 69, 608–617. doi: 10.1007/s00248-014-0528-9

Norvill, Z. N., Shilton, A., and Guieysse, B. (2016). Emerging contaminant degradation and removal in algal wastewater treatment ponds: identifying the research gaps. *J. Hazard. Mater.* 313, 291–309. doi: 10.1016/j.jhazmat.2016.03.085

Oliveira, P., Martins, N. M., Santos, M., Pinto, F., Büttel, Z., Couto, N. A. S., et al. (2016). The versatile TolC-like Slr1270 in the cyanobacterium Synechocystis. *Environ. Microbiol.* 18, 486–502. doi: 10.1111/1462-2920.13172

Pan, M., Lyu, T., Zhan, L., Matamoros, V., Angelidaki, I., Cooper, M., et al. (2021). Mitigating antibiotic pollution using cyanobacteria: removal efficiency, pathways and metabolism. *Water Res.* 190:116735. doi: 10.1016/j.watres.2020.116735

Rohaìček, K., and Bartaìk, M. (1999). Technique of the modulated chlorophyll fluorescence: basic concepts, useful parameters, and Some applications. *Photosynthetica* 37:339.

Sanganyado, E., and Gwenzi, W. (2019). Antibiotic resistance in drinking water systems: occurrence, removal, and human health risks. *Sci. Total Environ.* 669, 785–797. doi: 10.1016/j.scitotenv.2019.03.162

Sen, S. (2020). Cyanobacterial membrane biology under environmental stresses with particular reference to photosynthesis and photomorphogenesis, in *Advances in Cyanobacterial Biology*. (Amsterdam: Elsevier), 73–84. doi: 10.1016/b978-0-12-819311-2.00006-1

Shang, A. H., Ye, J., Chen, D. H., Lu, X. X., Lu, H. D., Liu, C. N., et al. (2015). Physiological effects of tetracycline antibiotic pollutants on non-target aquatic Microcystis aeruginosa. *J. Environ. Sci. Health B Pestic.* 50, 809–818. doi: 10.1080/03601234.2015.1058100

Snow, D. D., Bartelt-Hunt, S. L., Devivo, S., Saunders, S., and Cassada, D. A. (2009). Detection, occurrence, and fate of emerging contaminants in agricultural environments. *Water Environ. Res.* 81, 941–958. doi: 10.2175/106143009x461573

Springstein, B. L., Nürnberg, D. J., Weiss, G. L., Pilhofer, M., and Stucken, K. (2020). Structural determinants and their role in cyanobacterial morphogenesis. *Life* 10, 1–33. doi: 10.3390/life10120355

Stokes, J. M., Lopatkin, A. J., Lobritz, M. A., and Collins, J. J. (2019). Bacterial Metabolism and Antibiotic Efficacy. *Cell Metabol.* 30, 251–259. doi: 10.1016/j.cmet.2019.06.009

U.S. Food and Drug Administration (2019). *Summary Report on Antimicrobials Sold or Distributed for Use in Food-Producing Animals.* Silver Spring, MD: U.S. Food and Drug Administration.

Wan, J., Guo, P., Peng, X., and Wen, K. (2015). Effect of erythromycin exposure on the growth, antioxidant system and photosynthesis of Microcystis flos-aquae. *J. Hazard. Mater* 283, 778–786. doi: 10.1016/j.jhazmat.2014.10.026

Wejnerowski, Ł, Rzymski, P., Kokociński, M., and Meriluoto, J. (2018). The structure and toxicity of winter cyanobacterial bloom in a eutrophic lake of the temperate zone. *Ecotoxicology* 27, 752–760. doi: 10.1007/s10646-018-1957-x

WHO (2016). *Report on Surveillance of Antibiotic Consumption*. Geneva: WHO.

Wu, Y., Wan, L., Zhang, W., Ding, H., and Yang, W. (2020). Resistance of cyanobacteria Microcystis aeruginosa to erythromycin with multiple exposure. *Chemosphere* 249:126147. doi: 10.1016/j.chemosphere.2020.126147

Conflict of Interest: The authors declare that the research was conducted in the absence of any commercial or financial relationships that could be construed as a potential conflict of interest.

Publisher's Note: All claims expressed in this article are solely those of the authors and do not necessarily represent those of their affiliated organizations, or those of the publisher, the editors and the reviewers. Any product that may be evaluated in this article, or claim that may be made by its manufacturer, is not guaranteed or endorsed by the publisher.

frontiers | Frontiers in Microbiology

REVIEW
published: 13 July 2022
doi: 10.3389/fmicb.2022.939347

Cyanobacteria as a Promising Alternative for Sustainable Environment: Synthesis of Biofuel and Biodegradable Plastics

Preeti Agarwal†, Renu Soni†, Pritam Kaur†, Akanksha Madan†, Reema Mishra†, Jayati Pandey, Shreya Singh and Garvita Singh†*

Department of Botany, Gargi College, University of Delhi, New Delhi, India

OPEN ACCESS

Edited by:
Prashant Kumar Singh, Pachhunga University College, India

Reviewed by:
Prashant Singh, Banaras Hindu University, India
Ashutosh Kumar Rai, Imam Abdulrahman Bin Faisal University, Saudi Arabia
Rajeshwar P. Sinha, Banaras Hindu University, India

***Correspondence:**
Garvita Singh
garvita.singh@gargi.du.ac.in

†These authors have contributed equally to this work and share first authorship

Specialty section:
This article was submitted to Microbial Physiology and Metabolism, a section of the journal Frontiers in Microbiology

Received: *09 May 2022*
Accepted: *09 June 2022*
Published: *13 July 2022*

Citation:
Agarwal P, Soni R, Kaur P, Madan A, Mishra R, Pandey J, Singh S and Singh G (2022) Cyanobacteria as a Promising Alternative for Sustainable Environment: Synthesis of Biofuel and Biodegradable Plastics. Front. Microbiol. 13:939347. doi: 10.3389/fmicb.2022.939347

With the aim to alleviate the increasing plastic burden and carbon footprint on Earth, the role of certain microbes that are capable of capturing and sequestering excess carbon dioxide (CO_2) generated by various anthropogenic means was studied. Cyanobacteria, which are photosynthetic prokaryotes, are promising alternative for carbon sequestration as well as biofuel and bioplastic production because of their minimal growth requirements, higher efficiency of photosynthesis and growth rates, presence of considerable amounts of lipids in thylakoid membranes, and cosmopolitan nature. These microbes could prove beneficial to future generations in achieving sustainable environmental goals. Their role in the production of polyhydroxyalkanoates (PHAs) as a source of intracellular energy and carbon sink is being utilized for bioplastic production. PHAs have emerged as well-suited alternatives for conventional plastics and are a parallel competitor to petrochemical-based plastics. Although a lot of studies have been conducted where plants and crops are used as sources of energy and bioplastics, cyanobacteria have been reported to have a more efficient photosynthetic process strongly responsible for increased production with limited land input along with an acceptable cost. The biodiesel production from cyanobacteria is an unconventional choice for a sustainable future as it curtails toxic sulfur release and checks the addition of aromatic hydrocarbons having efficient oxygen content, with promising combustion potential, thus making them a better choice. Here, we aim at reporting the application of cyanobacteria for biofuel production and their competent biotechnological potential, along with achievements and constraints in its pathway toward commercial benefits. This review article also highlights the role of various cyanobacterial species that are a source of green and clean energy along with their high potential in the production of biodegradable plastics.

Keywords: biodegradable, bioplastics, biofuel, biopolymer, clean energy, polyhydroxyalkanoates, sustainable

INTRODUCTION

There is an unprecedented increase in carbon footprint due to increased toxicant levels in the atmosphere and excessive use of fossil fuels as well as their plastic derivatives, which are being discarded in landfill sites and will persist in the environment for more than the next 100 years. It has drastically posed new environmental challenges for nature and the survival of living organisms. Rapid climate change, along with ever-increasing billions of tons of plastic products in almost every inch of the planet, has posed serious threats to the Earth and would contribute to a massive global environmental hazard (Borrelle et al., 2020; Silva et al., 2020). The marine ecosystem is facing severe impacts because of accumulation of plastic debris with minimal degradation properties (Jambeck et al., 2015). Continuous accumulation of plastics in various strata of water bodies has led to the origin of a new ecosystem acknowledged as the "plastisphere." This is an outcome of the long shelf life and hydrophobic nature of non-degradable plastics being accumulated as debris, which could be the cause of replacement of natural ecosystems leading to unknown natural disasters (Zettler et al., 2013; Bergmann et al., 2017). Another outcome is the fragmentation of plastics to microplastics to the level that they mark a presence in the food chain imposing a threat to the whole ecosystem (Chen, 2015; Giacovelli and Environment: Technology for Environment, 2018). This is further being aggravated because of the prevailing COVID-19 situation across the globe, which has led to an uncalculated increase in single-use plastics in various forms and is another upcoming threat we are going to observe in the environment in the coming times (Ammendolia et al., 2021; Mejjad et al., 2021). Moreover, the energy crisis that the world is facing because of continuous depletion of fossil fuels could spark a misbalance in the world economy and progress. This further leads to new challenges to attain environmental goals wherein an unfiltered usage of non-biodegradable plastics from various unconventional resources is another major issue for a sustainable future. A recent study from IPCC (2014), the Intergovernmental Panel on Climate Change, projects a worrisome image wherein climate change could result in more severe impacts if we fail to abate GHG (greenhouse gas) emission in the near future. Biodiversity is shrinking as a result of prominent desert spread and choking of warmer oceans with plastic waste. In reality, the plastic industry consumes around 6% of world oil and is anticipated to grow up to 20% by 2050, as stated by IEA (International Energy Agency, 2017), which needs attention (Giacovelli and Environment: Technology for Environment, 2018). A continuous assessment conducted by World Economic Forum has put up an image wherein plastic production across the globe will further increase by 2-fold in the coming 20 years. This production of plastic would be accompanied by generation of enormous amounts of GHG emission. Combustion of fossil fuels is estimated to have caused a rise in atmospheric CO_2 from 300 to 400 ppm in the past century (Jambeck et al., 2015). These elevated carbon dioxide levels have led to a huge loss of glacial mass in polar regions such as Greenland and Antarctic belts, portraying unrequited human behavior toward the environment. Apart from these alarming scenarios, climate change is likely to be accompanied by rising sea levels that could cause higher precipitation and submergence in various regions (Pachauri et al., 2014).

There is an acute need to identify new sustainable substrates that could pace up with both energy demands in the form of biofuels as commercial products and biodegradable plastics as clean and green resources. Thoughtful calculations to attain carbon neutrality have predicted that cutting down on fossil fuel usage by 6–7 percent every year until 2030 is the only way to stop cataclysmic after-effects generated by fossil fuels and non-degradable and non-recyclable plastics. The environmental and economic costs associated with fossil fuel consumption both for energy requirements and commercial resources such as plastics have been garnering immense criticism, pushing a massive interest in biofuels and bioplastics for a sustainable future.

With great success, biofuels and bioplastics have been produced commercially from terrestrial plants (both monocots and dicots). However, the cultivation of these crops for biofuel or bioplastic derivation creates an immense competition for agricultural land against edible crops. In contrast to terrestrial plants currently being exploited for biofuel and bioplastic production, bacteria, yeast, and cyanobacteria prove to be more efficient and feasible alternatives. Bacterial cultivation, being a heterotrophic model, entails higher expenses in lieu of the costly input of organic nutrients required to accumulate crucial metabolites. The rate-limiting usage of organic substrates for the fermentation process in the production of bacterial bioplastic is one of the major cost additions, the second-largest expense is the energy-intensive procedures involved in polyhydroxyalkanoate (PHA) extraction. The bacterial, heterotrophic model for bioplastic production is therefore far from becoming economically feasible (Markou and Nerantzis, 2013; Karan et al., 2019).

However, now, the world is not only talking about reducing CO_2 but also about employing microalgae and cyanobacteria for the biological fixation of atmospheric CO_2, which provides an efficient and feasible strategy to sequester excess carbon. Cyanobacteria are being studied for biological life support systems in various forms and means. Growth patterns, cell assembly, and targeted genetic modulations are being conducted in order to get the desired industrial products (Rosenboom et al., 2022). Several common cyanobacterial species such as *Anabaena cylindrica*, *Anabaena muscorum*, *Anabaena doliolum*, and *Synechocystis* sp. have been tested for their potential role in the production of various industrial compounds including biofuel and bioplastics. Various identification measures including phase contrast microscopy and scanning electron microscopy (SEM) along with fluorescence microscopic images (**Figure 1**) reveal their nature and alignment of cells and elaborate autoflourescent compounds as phycobiliproteins and chlorophylls. These organisms are quite promising, with biofixation efficiency estimated to be ∼10-fold more than that of terrestrial plants (Cheah et al., 2015; Cuellar-Bermudez et al., 2015). In the last 15 years, from the very first pivotal steps of detecting chemicals of industrial assets expressed from exogenous genes in cyanobacteria, algal biotechnology has advanced in several prospects. Through robust studies on

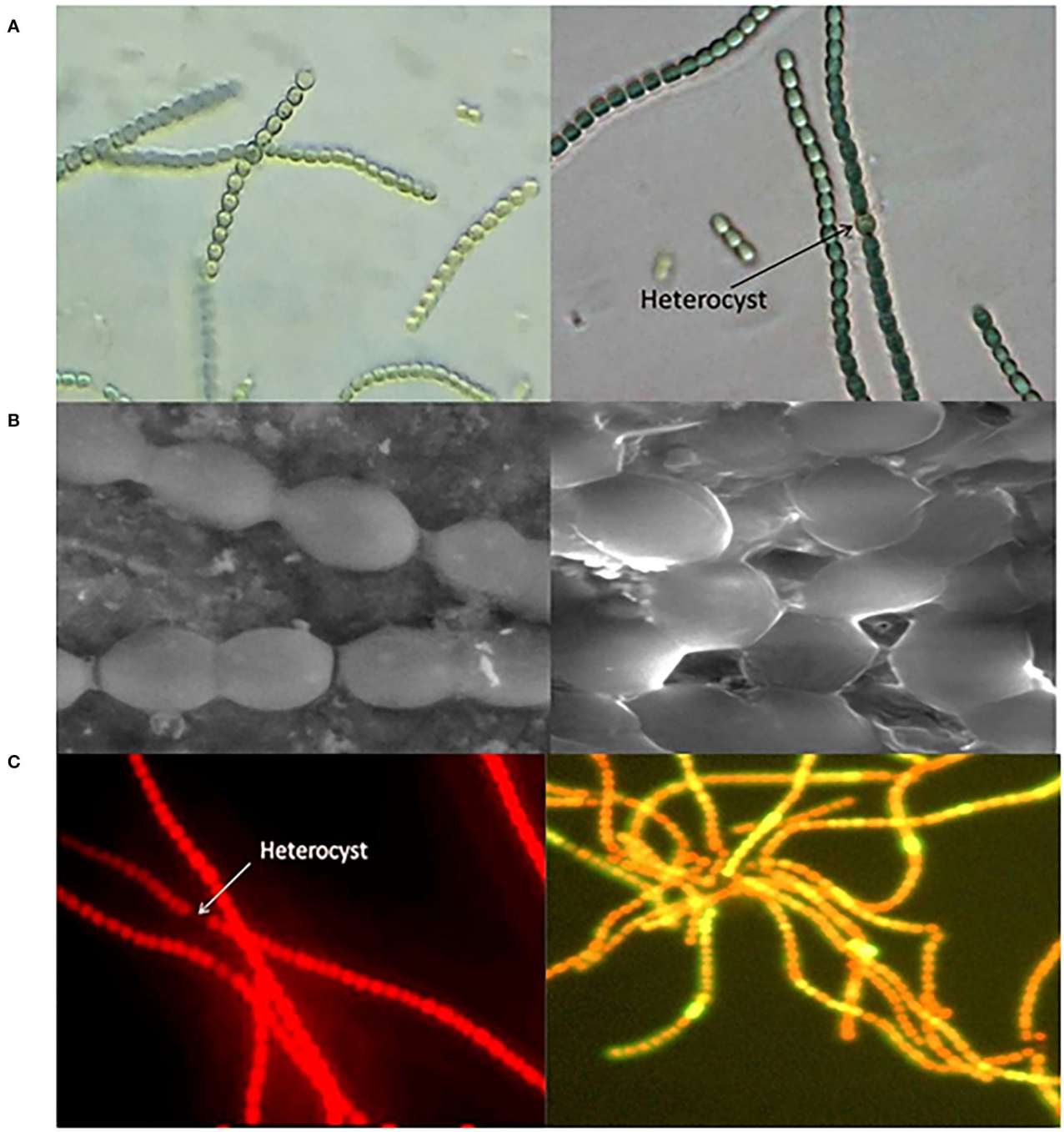

FIGURE 1 | Mic of Cyanobacterium *Anabaena* sp. **(A)** Phase contrast microscopic images, **(B)** scanning electron microscopic (SEM) images, and **(C)** fluorescence microscopic image showing auto-fluorescent pigments.

photosynthetic pathways in cyanobacteria, desired products on a commercial scale for understanding the metabolic machinery of host organisms have been attained (Oliver et al., 2013). Next, there is a need to overcome various challenges posed for sustainable biofuel and bioplastic production by cyanobacteria. Engineering cyanobacterial strains for enhancing yield is challenging as the metabolic pathway involves oxygen-sensitive enzymes. Selection and optimization of strains that possess the ability to metabolize both fatty acid content and precursors, play a significant role in commercializing cyanobacterium-derived biofuels and bioplastics for a sustainable future. As mentioned earlier, these organisms show a much higher photosynthetic efficiency of up to 10% than terrestrial plants possessing an efficiency of 4% (Lewis and Nocera, 2006); furthermore, they

require minimal land and nutrient input. To attain a sustainable economy, there is an urgent need for the replacement of fossil fuel substrates for various commercial products such as plastics and other polymers. An interdisciplinary approach involving an understanding of synergistic actions and selection of feedstock biomass to useful compounds like biofuels or bioplastics is ultimately the only roadmap that could help in attaining a better environmental prospect.

This review aims to highlight the potential role of cyanobacteria as a green sustainable methodology for biofuel and bioplastic production and enhance their yield by modifying metabolic pathways by genetic engineering. This review also features scope and constraints related to large-scale industrial production of biofuel and bioplastics. The dynamic metabolic versatility of cyanobacteria offers potential to overcome hurdles related to first-generation biofuel that utilizes plant resources as a substrate which has large land and water requirements. This has put considerable trust and interest in exploring cyanobacteria, a step toward sustainability for biofuels and bioplastics. The purpose of this study, therefore, is to portray a suitable approach toward the production of green energy as biofuels (generations III and IV) and bioplastics for a sustainable environment utilizing cyanobacteria as a biomass source.

CYANOBACTERIA: A SUSTAINABLE BIOFACTORY FOR BIOFUEL AND BIOPLASTIC PRODUCTION

Cyanobacteria, prokaryotic photosynthetic organisms and ancestors of present-day chloroplasts, are extremely potential microbes that are being selected for their efficiency for production of biofuels and biodegradable plastics because of their promising attributes such as mitigation strategy for atmospheric CO_2 absorption and fixation, utilizing it for its growth in adverse climatic conditions such as saline water and barren unfertile land, with a potential to fix atmospheric nitrogen. Their high specific growth rate, abundant fatty acid and oil content, and other active metabolites make them a better-suited alternative to other resources (Gouveia and Oliveira, 2009). **Figure 2** illustrates a schematic representation of the innate efficiency of cyanobacteria to convert nutrients and CO_2 into high-value cell constituents that can be harnessed for commercial-scale production of industrially and commercially relevant chemicals like biofuels (especially bioethanol and butanol) and materials like bioplastics (PHB and PHBV).

Thus, among various resources available for biofuel and bioplastic production, cyanobacteria have long been considered as energy-rich sources because of production of diacylglycerol (DAG) and triacylglycerol (TAG) that can be utilized as precursors of biodiesel. The availability of genetic sequence information of these microbes further makes them efficient in being utilized for generation of renewable biofuels (Wijffels et al., 2013; Halfmann et al., 2014; Savakis and Hellingwerf, 2015). According to research conducted in the past, cyanobacteria and algae produce a wide range of chemical intermediates and hydrocarbons that act as precursors for biofuels. As a result, cyanobacterium-derived fuel holds a great promise as a possible replacement for present fossil-fuel-derived goods (Nozzi et al., 2013). The biomass obtained from cyanobacteria can be utilized as a food source or as a variety of feedstock, and antioxidants, coloring agents, medicines, and bioactive chemicals are just a few of the significant biomolecules that may be extracted from cyanobacteria. Various types of biofuels obtained from cyanobacteria include bioethanol, isobutanol, ethylene, 1-butanol, biomethane, biodiesel, and biohydrogen (Schenk et al., 2008).

Cyanobacteria also possess the metabolism for producing economically useful and sustainable biopolymer polyhydroxyalkanoates, PHAs, and their various copolymers including polyhydroxybutyrate (PHB). The biopolymeric PHB exhibits material properties similar to polypropylene, a conventional plastic derived from fossil fuels such as petroleum. However, in contrast to conventional plastics, PHB is biodegradable; therefore, its usage as an alternative to conventional plastics can help in mitigating the severe environmental impacts of fossil fuel overconsumption as well as the non-biodegradability of plastics. Thus, cyanobacteria such as *Anabaena*, *Synechocystis*, *Nostoc muscorum*, *Spirulina* and many other species can act as biofactories for bioplastic and biofuel production (Kiran et al., 2014).

Cyanobacteria as Source of Renewable Energy: Tremendous Potential

Bioenergy is a form of energy that is obtained biologically from biomass. Biofuel (either bioethanol or biodiesel) is the only substitute source of energy that can currently replace the transportation fuel in automobiles without requiring extensive engine changes (Kaygusuz, 2009). Biofuel research must include not only the determination of the best material to utilize and its conversion to biofuel but also the ecologically safe and economical use of by-products created during the processing and production of these biofuels in a sustainable manner (Parmar et al., 2011). Development of alternative energy fuel sources is urgently needed, as majority of the world's current fuel supply is reliant on fossil fuels. One of the most challenging problems is the creation of sustainable and clean energy supplies for the future, which is ultimately linked to economic success and stability, as well as higher standards of living on a global scale (Posten and Schaub, 2009). The massive usage of non-renewable fuel sources to meet energy requirements has prompted researchers to look into alternative energy sources (Misra et al., 2013). As a result, biofuels have gained a bigger share of the fuel industry, and their future potential will pave the way for energy security.

Sunflower, rapeseed, switchgrass, peanuts, wheat, soybean, and sesame are among the most popularly utilized feedstock for the first and second generations of bioenergy. Vegetable oil and alcohols (ethanol, butanol, and propanol) are among the liquid forms of energy generated from these sources. As previously stated, the primary restriction for these energy crops is the competition for acreage and water with our food sources. To alleviate this restriction, third-generation sources are considered

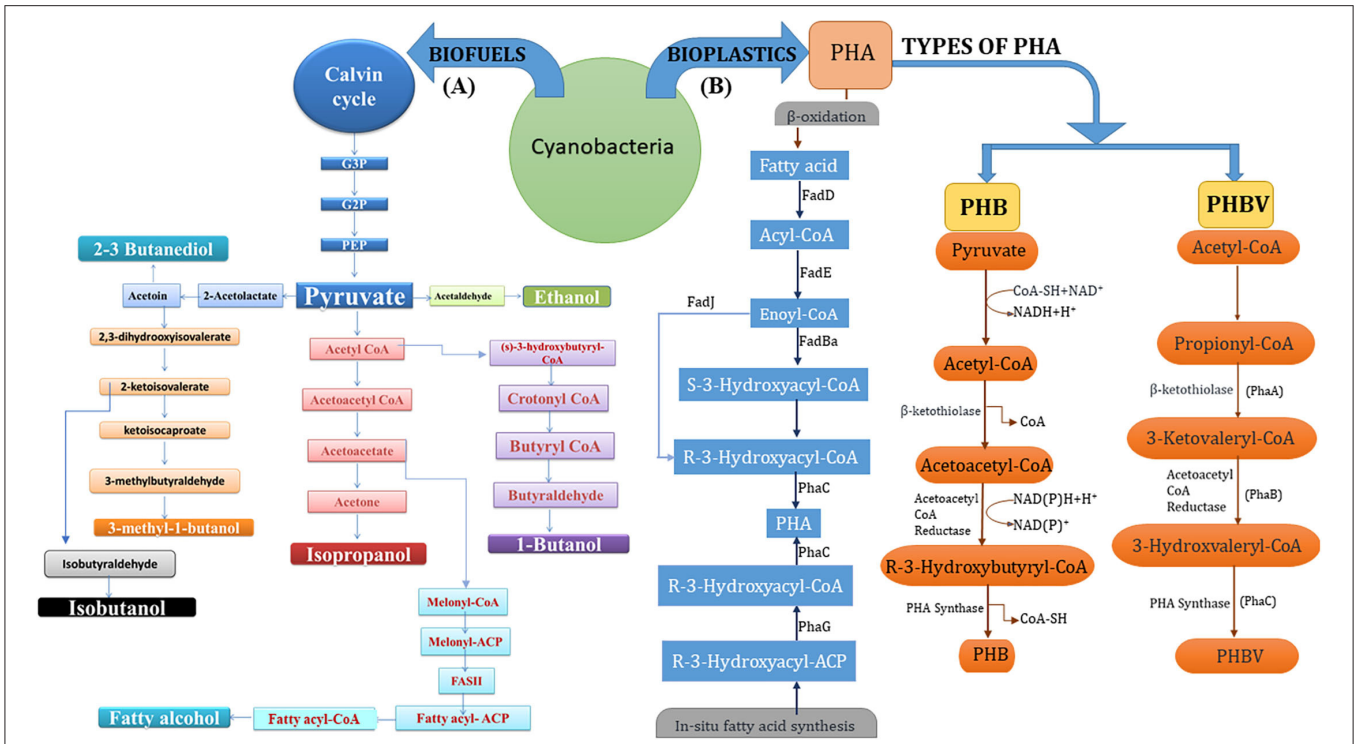

FIGURE 2 | (A) Schematic representation of cyanobacterial metabolic pathways leading to biofuel (bioethanol) derivatives *viz.* ethanol, butanol, isobutanol, isopropanol, 2,3-butanediol, and fatty alcohol; all derived from Calvin cycle and associated intermediate biomolecules (especially pyruvate). **(B)** Synthesis of PHA copolymers (PHB and PHBV) through enzyme-mediated 3-step pathway i.e., condensation, reduction, and polymerization with precursor acetyl-CoA molecules and through fatty acid β-oxidation pathway.

as a non-food biomass origin for energy supply (Quintana et al., 2011) (**Figure 3**).

Cyanobacteria can transform up to 10% of solar energy into biomass, in comparison to the 5% by eukaryotic algae and the 1% by traditional energy crops like sugarcane and maize (Parmar et al., 2011). They also convert CO_2 into biological components that may be used to make foods, biofuels, feedstock, and highly valued biologically active substances throughout this process (Pereira et al., 2011). Cyanobacteria are viewed as a possible feedstock for carbon-neutral biofuels owing to their high biomass production, quick growing capacity, and ability to manufacture and accumulate considerable quantities (∼20–50% of dry weight) of neutral lipids deposited in lipid bodies present in the cytosol (Halim et al., 2013). Overall, cyanobacteria outperform plants and algae in terms of photosynthetic efficiency, although algae produce far more oil. Cyanobacterial species *viz. Synechococcus elongatus* PCC 7942 and *Synechocystis* sp. PCC 6803 are widely utilized and identified as a potential biofuel source. As a result, photosynthetic microorganisms like cyanobacteria can better serve the goal of bioenergy generation in a more cost-effective and ecologically friendly manner, potentially replacing a large amount of fossil fuel consumption (Farrokh et al., 2019). They have a high amount of lipids, mostly found in thylakoid membranes. In comparison to higher plants and other algae, they have higher photosynthetic output and growth rates. Cyanobacteria may grow readily if given only the most basic dietary requirements: air, water, nitrogen, carbon dioxide, and mineral salts (particularly salts having phosphorous) with photons of light as the sole source of energy. As a result, cultivation is straightforward and economical (Quintana et al., 2011). Cyanobacteria have a comparatively short genome, and many of them have already been entirely sequenced, making system biology methods less difficult in these species than in eukaryotic algae (Rittmann, 2008). Cyanobacteria have been genetically modified to create a variety of substances related to biofuel (Machado and Atsumi, 2012; **Table 1**). *Synechococcus elongatus* sp. strain PCC 7942 was effectively designed to make ethanol by adding a gene for enzymes, alcohol dehydrogenase, and pyruvate decarboxylase, diverting carbon from pyruvate to ethanol (Deng and Coleman, 1999).

Cyanobacteria are an excellent alternative for producing solar-powered biofuels from water, sunlight, and CO_2. However, several difficulties for biofuel generation and development in cyanobacteria are investigated by extending natural biosynthetic pathways. Several initiatives have been undertaken to increase biofuel production by expanding natural biochemical routes, including hydrogen, fatty acids, ethanol, isoprene, and butanol. Currently, metabolic engineering techniques and synthetic biology are employed in cyanobacteria to produce high-level

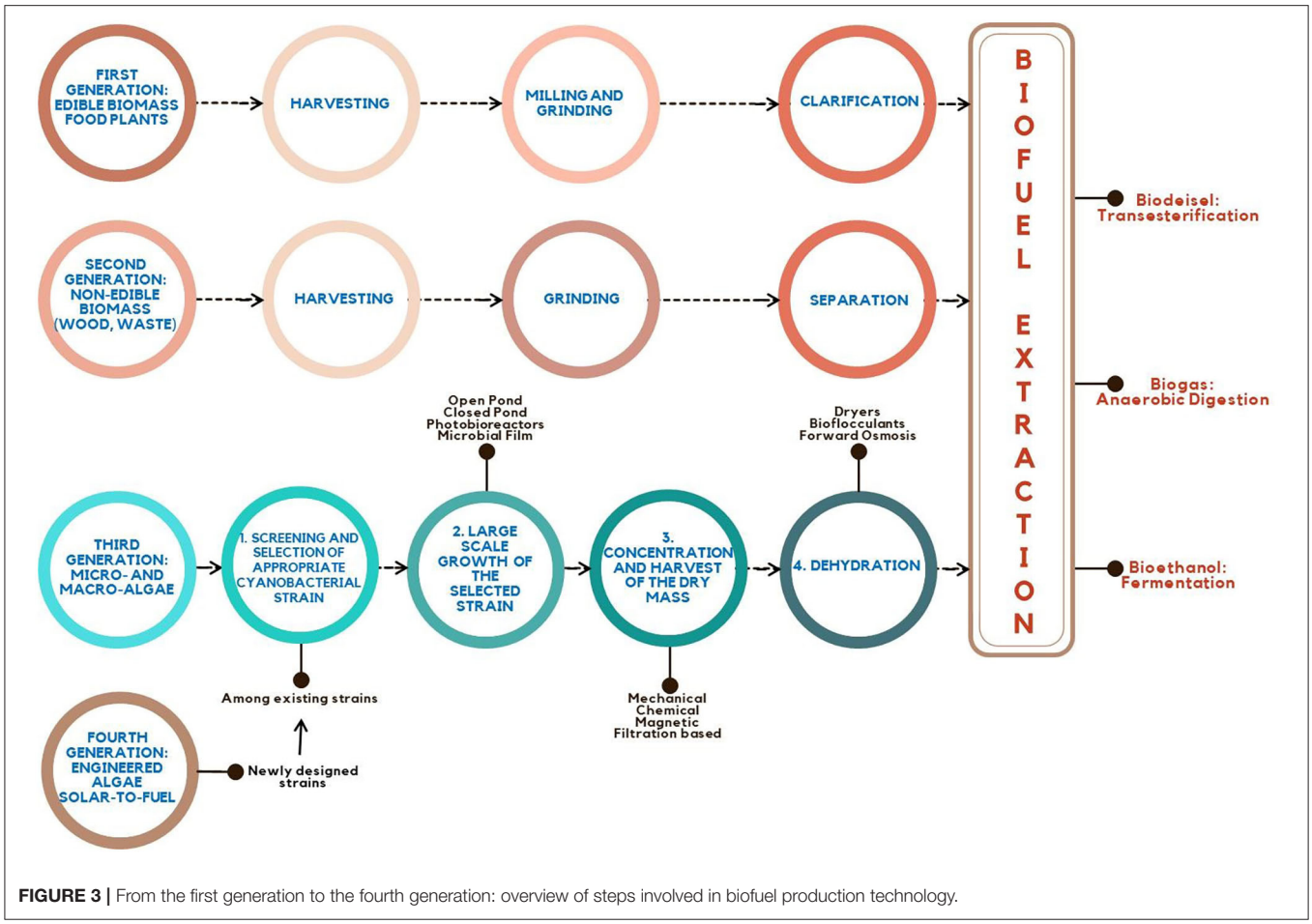

FIGURE 3 | From the first generation to the fourth generation: overview of steps involved in biofuel production technology.

biofuels. Different types of biofuels obtained from cyanobacteria are discussed below.

Ethanol

Glucose and sucrose are two of the major sugar moieties easily obtained from cyanobacteria. Anaerobic fermentation of these simple sugars in the dark produces ethanol or ethyl alcohol. It is a colorless, flammable, and volatile liquid created by microbes by sugar fermentation. The ethanol made from renewable sources is a desirable source of energy, since it can be combined with diesel and utilized without requiring further modifications to present diesel engines (Kaygusuz, 2009). In the production of ethanol, cyanobacteria have an advantage over conventional energy crops, since they ferment naturally without any need for yeast cultures (fermentation initiators) that are needed by the latter, therefore making cyanobacteria better candidates for ethanol generation. Most algae and cyanobacteria do not need fermentation as their major source of energy. Fermentation occurs at a low level in these species, thus helping them to survive. Genetic modification may be a viable option for overcoming this difficulty and increasing ethanol output from engineered cyanobacteria that are a reliable source for ethanol production (Quintana et al., 2011). *Synechococcus* sp. PCC 7942 was the first genetically engineered cyanobacterial species utilized to produce ethanol. Coding sequences of *Zymomonas mobilis* pyruvate decarboxylase (*PDC*) and alcohol dehydrogenase II (*ADH*) were cloned in the pCB4 vector and utilized to transform *Synechococcus* sp. strain PCC 7942. The promoter from the *rbcLS* operon, which encodes cyanobacterial ribulose-1,5-bisphosphate carboxylase/oxygenase, increased the expression of the *PDC* and *ADH* genes (Deng and Coleman, 1999). Modifying various abiotic parameters like light intensity, carbon source, CO_2 concentration, pH, and medium composition can boost the production of certain molecules (Gao et al., 2012). In many situations, optimizing these abiotic and biotic elements together has led to increased yields (Andrews et al., 2021). Carrieri et al. (2010) evaluated the influence of salt stress on cyanobacterial fermentation rate. High salt concentration in a medium led to a 100-fold increase in ethanol production as compared to low salt concentration. The amount of ethanol released by cyanobacteria has a significant impact on two parameters, the amount of energy used and GHG emission. Cyanobacteria derived ethanol do not produce any remnant, ash, smoke and greenhouse gases in any form therefore serves as an eco-friendly fuel (Luo et al., 2010). Multiple ethanologenic cassette insertions inside the *Synechocystis* genome have been shown to be a

successful technique for increasing ethanol titers (Gundolf et al., 2019; Wang et al., 2020). However, in cyanobacteria, plasmid-based ethanol-generating systems have been highly effective and have frequently resulted in rather large ethanol titers (Dühring et al., 2017). Using a plasmid-based system, the patented strain ABICyanol1 has attained an ethanol output of 0.55 g/L/d (Piven et al., 2015). According to an *in silico* study, the maximal amount of ethanol produced by *Synechocystis* sp. PCC 6803 was found to be 235 percent more than what was produced experimentally on the laboratory scale. The researchers were able to do this by developing a combined ethanol/biomass system (Lasry Testa et al., 2019). Cyanobacteria have the potential to produce lipids, which may be utilized as biofuel feedstock (Anahas and Muralitharan, 2018). Recently, Roussou et al. (2021) investigated the combined effects of Calvin-Benson-Bassham (CBB) enzymes like transketolase (TK), aldolase (FBA), and fructose-1,6/sedoheptulose-1,7-bisphosphatase (FBP/SBPase) on ethanol production in *Synechocystis* PCC 6803. The strain that overexpressed a combination of FBA and TK CBB enzymes produced the maximum amount of ethanol.

Butanol

Butanol (butyl alcohol) is a 4-carbon alcohol (C_4H_9OH) that forms the main bulk chemical and an effective blend-in fuel sourced from non-renewable fossil resources (Liu et al., 2021). 1-Butanol is gaining interest as a potential fuel alternative and an important chemical feedstock. It can be produced by both the coenzyme A (CoA)-dependent route (Ezeji et al., 2007) and the ketoacid pathway (Shen and Liao, 2008) (**Figure 2**). There are also biological pathways for fermentative butanol synthesis (Wichmann et al., 2021). Natural cyanobacterial strains do not synthesize isobutanol or 1-butanol, suggesting that butanol metabolic genes and related pathways are missing. For heterotrophic 1-butanol synthesis, the clostridial route, a natural 1-butanol-generating pathway from *Clostridium*, was introduced into *E. coli* (Shen et al., 2011). In *Synechococcus* 7942, Atsumi et al. (2008) created a synthetic isobutanol pathway that generates isobutyraldehyde and isobutanol. Similarly, an alternative acetoacetyl-CoA biosynthesis pathway (ATP-driven) has been created in *Synechococcus* by overexpression of acetoacetyl-CoA synthase (*NphT7*) that condenses malonyl-CoA and acetyl CoA. In *Synechococcus*, the overexpression of three enzymes (phosphoglycerate mutase, enolase, and pyruvate kinase) from the three stages between 3-phosphoglycerate and the pyruvate of the Calvin–Benson–Bassham cycle boosted overall carbon output by 1.8-fold and 2,3-butanediol synthesis by 2.4-fold (Oliver and Atsumi, 2015). Miao et al. (2018) reported a maximum 1-butanol and isobutanol production in *Synechocystis* PCC 6803 during a long-lasting culture (0.9 g/L in 46 days). CRISPR interference (CRISPRi) was conducted in another investigation to repress the enzyme citrate synthase gltA, which arrests growth but increases carbon partitioning leading to the production of 1-butanol in *Synechocystis* (Shabestary et al., 2018).

Furthermore, the synthesis of 1-butanol was boosted by overexpressing a heterogeneous phosphoketolase (PK) route, one of the natural acetyl-CoA supporting routes in *Synechocystis* (Xiong et al., 2015; Liu et al., 2019). Wichmann et al. (2021) recently showed that photosynthetic butanol is created directly from CO_2, with a carbon partitioning of 60% to 1-butanol.

Biodiesel

Biodiesel, unlike petroleum diesel, is biodegradable and non-toxic, and when burnt as a fuel, it considerably decreases toxicants and other emissions (Yusuf et al., 2011). Cyanobacteria are photosynthetic microorganisms that can convert solar energy and CO_2 into biofuels in a single biological system. Synthesizing fatty acid-based compounds using solar energy as the energy source, CO_2 as the carbon source, and cyanobacteria as the biological system would be a potential technique for developing sustainable biofuels (Quintana et al., 2011). In combined liquid–gaseous fuel-processing solutions, S*pirulina* also demonstrated the greatest overall utilization efficiency. In cyanobacteria, overproduction and transesterification of fatty acids to generate fatty acid methyl esters, fatty alcohols, or fatty alkanes are the two processes involved in the production of fatty acid-based biofuels (Mata et al., 2010). These lipid feedstocks are made up of 90–98 percent triglycerides and trace quantities of monoglycerides and diglycerides, 1–5 percent free fatty acids, and small amounts of phosphatides, phospholipids, carotenes, sulfur compounds, tocopherols, and water (Chisti, 2007). Because of their high fatty acid content, Hossain et al. (2020) discovered that cyanobacteria represent a promising source for the biodiesel sector. Cyanobacteria have high lipid content, with Oscillatoriales having the greatest overall lipid concentration. More studies are needed to improve the mass culture conditions for increasing the lipid content of cyanobacterial biomass, and research on value addition of residual biomass is also required. Nagappan et al. (2020) evaluated numerous nitrogen-fixing cyanobacteria for biodiesel production based on biomass production, lipid productivity, lipid profile, and harvesting capability. The evaluation resulted in the selection of *Nostoc* sp. MCC41, a nitrogen-fixing cyanobacterium and a promising species. It contains a high proportion of palmitic acid, indicating its applicability for biodiesel production. *Nostoc* sp. *MCC41* can be regarded as a promising and eco-friendly resource for efficient biodiesel production because of its ease of harvesting, capacity to grow under mixotrophic conditions, and ability to fix atmospheric nitrogen. To investigate the activity of certain enzymes used in saturated fatty acid production in cyanobacteria, genetically altered *Synechococcus elongatus* PCC 7942 was generated by overexpression or deletion of genes coding for fatty acid synthase system enzymes; its lipid profile was evaluated, and it was found that the functioning of some of these enzymes differed. Modifications resulting from gene overexpression or deletion were then conducted to increase the production of alpha-linolenic acid in cyanobacterium. When combined with the overexpression of *Synechococcus* sp. *desA* and *desB* desaturase genes, the mutant generated by *fabF* overexpression and *fadD* deletion, PCC 7002, generated the most omega-3 fatty acids (Santos-Merino et al., 2018).

Hydrogen

Because it is non-polluting and infinite, hydrogen (H_2) is a more appealing biofuel candidate for upcoming usage (Srirangan et al.,

TABLE 1 | Different cyanobacterial strains genetically engineered for biofuel production.

S. No.	Cyanobacterial strain	Organic Carbon utilization	Cultivation conditions	Specific growth rate	Biofuel/biofuel precursor	Product concentration	Engineered status	Reference
1.	*Cyanothece* sp. ATCC 51142	Oxygenic photo-autotrophic	Chemostat culture-ASP-2 medium, Nitrogen deprivation, Continuous white light illumination	Variable	Hydrogen	400 mmol H_2/mg Chl. H	Disruption of uptake *hydrogenase* gene	Masukawa et al., 2002
2.	*Synechococcus elongatus* 7942	Photoautotrophic	Modified BG-11 Medium	0.161 day^{-1}	Iso-butanol	450 mg/L	Overexpression of ribulose 1,5-bisphosphate carboxylase/oxygenase (Rubisco)	Atsumi et al., 2009
3.	*Synechocystis* sp. PCC 6803	Photo-auto/heterotrophic	BG11 medium	1.7∼2.5 day^{-1}	Ethanol	5.5 g/L	*pdc-adh* genes set expressed under *PpsbA2* promoter	Dexter and Fu, 2009
4.	*Synechocystis* sp. PCC 6803	-	Dark, Nitrogen limiting	1.7∼2.5 day^{-1}	Hydrogen	186 nmol/mg chl a/h	*nitrate reductase (ΔnarB), nitrite reductase (ΔnirA)*	Baebprasert et al., 2011
5.	*Synechococcus elongatus* 7942	Photoautotrophic	Modified BG-11 medium	0.161 day^{-1}	1-butanol	30 mg/L	substitution of bifunctional aldehyde/alcohol dehydrogenase (*AdhE2*) with separate butyraldehyde dehydrogenase (*Bldh*) and NADPH-dependent alcohol dehydrogenase (*YqhD*)	Lan and Liao, 2012
6.	*Synechococcus elongatus* 7942	Photoautotrophic	BG-11 medium	0.161 day^{-1}	2,3 butanediol	2.4 g/L	Integrated *alsS*, *alsD*, and *adh*	Oliver et al., 2013
7.	*Synechocystis* sp. PCC 6803	Mixoautotrophic	BG11 medium	1.7∼2.5 day^{-1}	Isobutanol	114 mg/L	*kivd* and *adhA* gene set of Ehrlich pathway expressed under P_{tac}	Varman et al., 2013
8.	*Synechococcus* sp. PCC 7002	Photoautotrophic	Agar plates of medium A^+	0.2 h^{-1}	Fatty acids	130 mg/L	*fadD* gene knockout, overexpression of *tesA* and *rbcLS*	Ruffing, 2014

(Continued)

TABLE 1 | Continued

S. No.	Cyanobacterial strain	Organic Carbon utilization	Cultivation conditions	Specific growth rate	Biofuel/biofuel precursor	Product concentration	Engineered status	Reference
9.	*Synechocystis* sp. PCC 6803	Photoautotrophic	BG11 medium	1.7∼2.5 day^{-1}	Fatty alcohol for biodiesel	761 μg /g dry cell weight	Overexpression of fatty *acyl-CoA reductase* gene and disruption of the native glycogen/poly-β-hydroxybutyrate biosynthesis pathways	Qi et al., 2013
10.	*Synechococcus* sp. PCC 7002	Photolitho-autotrophic	CO_2 enriched seawater medium	0.2 h^{-1}	Ethanol	0.25% (v/v)	Pyruvate decaroxylase (PDC) gene from *Zymomonas mobilis* and Alcohol Dehydrogenase (ADH) gene from *Synechocystis* 6803	Kopka et al., 2017
11.	*Synechococcus* sp. PCC 11901	Photoautotrophic	MAD, MAD2 medium.	≈100 mgDW h^{-1}	Fatty acids	≈1.54 g L^{-1}	*tesA* under $P_{clac143}$ promoter, *fadD* knockout	Włodarczyk et al., 2020
12.	*Synechocystis* sp. PCC 6803	Photoautotrophic	BG11 medium	1.7∼2.5 day^{-1}	3-Methyl 1-Butanol	75 mg/L	Keto-acid Decarboxylase *(kdc)*-Alcohol Dehydrogenase *(adh)* gene set expressed under *CcaS/CcaR* system	Kobayashi et al., 2022

2011). According to Kruse et al. (2005), many cyanobacteria spontaneously create hydrogen as a secondary metabolite that balances redox energetics, and many other strains can create hydrogen by the reversible action of hydrogenase. The most significant impediment to cyanobacterial H_2 production is that hydrogenases are particularly sensitive to the O_2 produced during photosynthesis. Furthermore, the presence of reducing agents like ferredoxin and NADPH is a barrier, since they are involved in other processes such as respiration. To boost hydrogen generation, it will be necessary to reroute some of the electron flow to hydrogen-producing enzymes and to develop hydrogenases tolerant to oxygen (Weyman, 2010). When cyanobacteria are cultured under nitrogen-deficient conditions, H_2 evolves as a by-product of nitrogen fixation. It was also discovered that non-heterocystous cyanobacteria produce lesser hydrogen than heterocystous species. Several studies have looked at cyanobacterial species that can produce H_2 as a source of clean biofuel (Abed et al., 2009). Multiple attempts have been made to boost H_2 production rather than carbon flow to augment electron flux. Nitrogenase-based generation systems of H_2 have been created in *Nostoc* sp. PCC 7120 by inhibiting hydrogenase (Hup) absorption, resulting in increased hydrogen (Masukawa et al., 2002). *Synechococcus* 7002 mutants deficient in lactate dehydrogenase showed a 5-fold increase in total H_2 generation when compared with the wild type (McNeely et al., 2010). The production of an exogenous ferredoxin by *Clostridium acetobutylicum* during the fermentation process might boost electron flow to the hydrogenase (HydA). In light-dependent anoxic circumstances, H_2 production was increased twice its original amount (Ducat et al., 2011). Several initiatives have been launched to hinder competitive pathways for reductant usage and to promote H_2 production. As a consequence, the *ldhA* gene was inactivated in *Synechococcus* sp. 7002, NADH/NAD ratios were significantly increased, and H_2 production was significantly enhanced when native bidirectional [*NiFe*] hydrogenase was increased (five-fold in anoxic and dark circumstances) (McNeely et al., 2010). Engineered *Anabaena variabilis* ATCC 29413, *Nostoc* sp. PCC 7422, and *Nostoc linckia* HA-46 generated more H_2 than *Synechococcus* sp. PCC 7002, *Synechocystis* sp. PCC 6803, and *Nostoc punctiforme* ATCC 29133. In contrast, the lowest H_2 producers have been found to be *Synechococcus elongatus* PCC 7942, *Synechococcus* sp. PCC 7002, and *Synechocystis* sp. PCC 6803d. It implies that during H_2 synthesis, oxygen may function as an inhibitor in these cyanobacteria. As a consequence, an artificial oxygen-consuming device for O_2 consumption may be built in the near future, resulting in enhanced H_2 production in *Synechocystis* sp. PCC 6803 and *Synechococcus* sp. PCC 7002 (Srirangan et al., 2011). Khetkorn et al. (2012) used multiple inhibitors to promote electron flow toward nitrogenase and bidirectional Hox-hydrogenase in *Anabaena siamensis* TISTR 8012 to study the downregulation of those competing for metabolic pathways. Increased H_2 generation produced by inhibitors corresponded to increase in respective Hox-hydrogenase activity and nif D transcript levels and decrease in hupL transcript levels. The NiFe-hydrogenase HoxYH from the cyanobacterium *Synechocstis* sp. PCC 6803 was coupled with the photosystem I component PsaD. The resultant psaD-hoxYH mutant grew photoautotrophically, accumulated a large concentration of photosynthetically produced hydrogen in the light under anaerobic conditions, and did not consume hydrogen. According to the findings, psaD-hoxYH photosynthetic hydrogen production is most likely a mix of anoxygenic and oxygenic photosynthesis (Appel et al., 2020).

Conversion and Downstream Processing for Large-Scale Production of Eco-Friendly Cyanobacterial Biofuels

Steps of Conversion of Cyanobacterial Biomass to Biofuels

The scientific community is continuously looking for alternatives and optimizations to improvise and achieve an efficient, practical, and economically viable bioenergy process (**Figure 3**). However, the general pathway is as follows:

Selection and Screening of Cyanobacterial Strains With Desirable Fatty Acid Profiles. It will determine the quality of the biofuel produced eventually. Not only selection from among the existing cyanobacterial strains but many promising strains designed by genome modeling strategies have also been developed, especially in a popular cyanobacterium, *Synechocystis* sp. PCC 6803 (Erdrich et al., 2014), to yield an economically feasible level of biofuel.

Large-Scale Growth of Cyanobacterial Strain. Multiple approaches have been adopted for achieving high biomass productivity (Jorquera et al., 2010) viz: (a) Open pond systems where open waters with nutrients are supplied for algal growth. However, such systems are prone to bacterial and protest contamination. (b) Closed pond systems that utilize closed chambers to provide round-the-year cultivation owing to full control over light and temperature conditions. (c) Photobioreactors that are high on investment and need technology optimization but tend to maximize the photosynthetic surface area. (d) Microbial biofilm method wherein the microbial paste is applied on a suitable substratum to directly produce the biomass, thereby omitting the harvesting step.

A few prerequisites must be fulfilled to achieve viable biomass and include sufficient nutrient inputs, maintenance of sterile conditions to prevent contamination from other microbes, and optimization and maintenance of strain-conducive environmental conditions of light and temperature (Sitther et al., 2020).

Harvest/Collection Through Concentration and Dry Mass Production. Strategies including batch centrifugation (mechanical separation method), flocculation (inorganic vs. organic separation methods), use of magnetic nanoparticles, reverse and/or direct vacuuming (filtration-based method), and flotation (natural formation of gas vesicles) have been constantly employed for harvesting biomass (Parmar et al., 2011; Sitther et al., 2020).

Drying/Dewatering/Dehydration. Dehydration is carried out to prepare the biomass for extraction of biofuel using huge drums

with oven dryers. This dewatering process can be performed either by addition of bioflocculants (usually bacterial cells) in the cyanobacterial culture, which saves the additional costs of chemical flocculants, but increases the chances of contamination and interference with cyanobacterial metabolic processes, or another efficient technology of forwarding osmosis could be employed that works on creating a pressure gradient across a semi-permeable membrane. This method is highly efficient and can recover cyanobacterial cells from dilute cultures as well (Anyanwu et al., 2018).

Extraction and Purification. Extraction and purification of third-generation biofuels are accomplished using multiple techniques *viz*:

a. Transesterification for biodiesel production is the most conventional process for optimized generation of lipid-based biofuel. In this process, fatty acids (triglycerides) and methanol are converted into glycerol and FAMEs (fatty acid methyl esters), in the presence of a strong alkali or a strong acid (Bhatia et al., 2021). Conventional 2-step transesterification, which involves sequential lysis and transesterification, does not yield ample FAMEs from cyanobacteria; therefore, a highly efficient single-step method has been developed where cell lysis and transesterification of fatty acids occur simultaneously, which can be chemically separated by phase separation. This direct transesterification (also called *in situ* transesterification) allows for quantification and characterization of fatty acids without involving a separate method of extraction (Wahlen et al., 2011).

b. Fermentation for bioethanol production: cellular fermentable sugars and polysaccharide glycogen are present in cyanobacteria that can be optionally enzymatically hydrolyzed and converted to ethanol and carbon dioxide in the complete absence of oxygen (Lakatos et al., 2019).

c. Anaerobic digestion for biogas production: various conversion pathways have been standardized to obtain gas-based cyanobacterial fuels where cyanobacterial residual biomass (post-liquid fuel extraction or direct from culture/sludge) can be anaerobically digested by hydrolysis (conversion of initial biomolecules into soluble sugars), fermentation (sugar conversion to alcohol and intermediary biomolecules), and methanogenesis (conversion to biogas mixture comprising up to 70 percent methane using methanogens) (Fardinpoor et al., 2021). Cyanobacterial biohydrogen is produced under nitrogen-deficient conditions because of the reverse activity of enzyme hydrogenase. Some strains of *Anabaena* spp. are known to have a maximum potential to produce the highest amounts of biohydrogen (Sadvakasova et al., 2020).

Analysis, Testing for Marketability and Approvals for Commercialization of the Biofuel Product: In Terms of Rate of Titer Production, Its Quality, and Steadiness. International standards and specifications are continually being introduced to harmonize the quality and testing methodologies of biofuel products globally (Gadonneix et al., 2010). ISO (International Organization for Standardization) keeps developing and updating these standards to help in efficient development and global acceptance of biofuel products.

Light-Mediated (Direct) Use of Cyanobacteria as Biofuels

Cyanobacteria have an upper hand over other biofuel candidates because of their inbuilt efficiency to utilize sunlight and convert biomass into fuels. Light-driven conversion works smoothly without any additional processing steps. Therefore, by employing multiple interdisciplinary approaches, we can alter and improvise metabolic pathways directly achieving high yields of the fourth-generation drop-in biofuels (Johnson et al., 2016). The basic raw materials (carbon dioxide, water, and light) are provided, and the modified genetic makeup leads to the direct production of high-value biofuel derivatives such as ethanol and butanol. This is a rapidly growing field of study where new ways of altering the genetic makeup of cyanobacterial strains can be conducted resulting in not only improved yields but also single step biofuel production. *Synechococcus* sp. PCC 7002, with overexpression of native sodium-dependent bicarbonate transporters SbtA and BicA, yielded a 50% increase in growth/biomass and intracellular glycogen yield (Gupta et al., 2020). Fan et al. (2022) worked on *Synechocystis* sp. PCC 6803 and studied variations in the efficiency of substrate conversion into aromatic alcohol by optimizing permutations and combinations of parameters like temperature, light, substrates, and cell concentrations. They successfully achieved higher NADPH regeneration and, hence, improved reaction rates in terms of alcohol production.

The advent of fourth-generation biofuels from inexhaustible raw material sources like cyanobacteria, which are cheap and easily available, has opened new hopes. A photosynthetic mechanism involving water oxidation can lead to large-scale fuel production either by an artificial photosynthetic process (Inganäs and Sundström, 2016) or by directly opting for methods of solar biofuel production that is a much cleaner source of energy. This will not just take up hydrogen production but will certainly minimize the generation of reduced carbon-based biofuels by concomitant atmospheric CO_2 fixation and by designing synthetic pathways for enhanced biofuel outputs (Mund et al., 2022; Sebesta et al., 2022). An approach toward designer cyanobacterial strains with edited metabolic pathways can troubleshoot many environmental concerns at the industrial level for biofuel production. The biggest challenge to be resolved is identifying controlled expression systems in designer cyanobacteria. To sum up, the fourth generation biofuels, which are a by-product of the designer microbes including cyanobacteria, are utilized as photobiological solar fuels designed to work in coalition with photovoltaics or electro biofuels. Cyanobacterial strains having their metabolism tailored specifically for enhanced biofuel production is going to take up the mere future. Additionally, using computational modeling methods for identification of the complex interplay of potential pathways, the flux can be manipulated in order to achieve higher and efficient biofuel yields (Misra et al., 2013).

Bioplastics: Bio-Based, Biodegradable, and Eco-Friendly Plastics

Plastics are primarily composed of polymers and include a wide range of semisynthetic and synthetic materials. Moreover,

because of plasticity, plastic objects can be remolded into a wide range of solid shapes by pressurizing them. Fossil fuels such as natural gas and petroleum are used to make plastics recently; however, industrial methods use renewable materials, namely, corn or cotton derivatives. Flexibility and other properties like being lightweight, durability, and low production cost have led to their extensive use worldwide. Plastic objects, having lower weight and cost, have an additional advantage and wide applications in industries and markets (ACC, 2013; Lane, 2015). In industries, plastics are used to meet numerous requirements that are very specific in having a high strength-to-density ratio. In plastics, polymers have a high degree of chain branching and cross-linking that makes them rigid; and for transparency, polymers with variable glass transition temperatures are used. Different polymers can be blended to make products with desired properties. Therefore, depending on density and high resistance under different ambient suitable conditions, the most widely produced thermoplastics that have multiple uses in industries are polyethylene terephthalate (PET), low-density polyethylene (LDPE) and high-density polyethylene (HDPE), polyvinyl chloride (PVC), polypropylene (PP), and polystyrene (PS) (ACC, 2007). These properties and ability to be remolded provide long shelf life to numerous plastic products; therefore, plastic polymers can be used in packaging, storing, and transportation of materials even to long distances. Production of plastic polymers is increasing worldwide and was reported to be more than 300 million tons in the past few years (Plastics, 2019). Conventional petrochemical-based plastics impose serious environmental hazards. On the contrary, unrestrained usage of non-durable goods made from plastic polymers generated a vast amount of uncalculated waste in the environment. It also imposes a severe threat to ecosystems because of their slow decomposition process in the natural ecosystem, and it is one of the global concerns that the world needs to address. However, plastic polymers are non-biodegradable, they rely on the population boom and demand. As minimum plastic waste is known to be recycled therefore, reducing the demand at an individual level, lowering human pressure on environment and creating interest to develop the better disposal mechanisms can be the ways for sustainable future.

Now, bioplastics are a better-known option, sustainable, and a suitable alternative to conventional synthetic chemical-based plastics and are well-recommended by the United Nations (UN) recently. Because of environmental safety concerns, many agencies including the UN Food and Agriculture Organization (FAO) assessed the sustainability of bio-based plastic materials and strongly recommended bio-based polymers that can be biologically degraded over conventional non-biodegradable polymers. Plant-based biodegradable bioplastics can be an alternative sustainable source of plastics. However, land requirement for proper plant growth can be a limitation in developing nations where no well-equipped land use pattern is followed (European Bioplastics, 2021).

Bioplastics (bio-based plastics) are synthesized at least partially from biological matters as well as plastics that can be biologically degraded. Biodegradable or biologically degradable plastics are broken down or completely degraded or decomposed by microbes under particular conditions in due space within a certain period. As observed and based on composition, it is a very interesting fact that every plastic product that is bio-based cannot be biodegradable, and all biodegradable plastics products cannot always be bio-based. Moreover, under all environmental conditions, biodegradable plastics cannot be degraded biologically. Renewable resources used for obtaining bioplastics, are recycled *via* varied natural biological phenomena and can help in reducing fossil fuel consumption (Ashter, 2016).

The potential studies conducted by "Organization for Economic Co-operation and Development" (OECD) further provided many definitions for plastic polymers such as bioplastics are bio-based, and while their production generates very less and cleaner residues, their decomposition mechanisms are less detrimental than conventional chemical-based plastics to the environment (Reis et al., 2003; Schlebusch and Forchhammer, 2010; Jim, 2014). Despite of their origin, bioplastics can also be referred based on how they can be degraded by different organisms namely, bacteria, fungi and algae (Rutkowska et al., 2002). Polysaccharides, namely, cellulose and starch, and various polyesters like polyhydroxyalkanoates (PHAs) are bioplastics that can be the potential and most promising source of environmentally safe polymers (Storz and Vorlop, 2013).

Until now, bio-based and non-biodegradable plastics are being manufactured in the market; however, biodegradable polymers are not leading; therefore, creating biopolymers with high performance and reasonable cost is a matter of highest environmental concern (Iles and Martin, 2013). Consequently, because of an urgent need to find an alternative to conventional plastics, and likely PHAs and PHBs, bio-based and biodegradable polymers will require high production capacities at considerate rates in the near future (Aeschelmann et al., 2016). As to growing environmental safety concerns, industries are more attracted to biodegradable plastics that are short-lived and that can be suitably disposed of. In the degradation of plastic polymers, various microorganisms decompose the polymers in the following order as PHAs = PCL (polycaprolactone) > PBS (polybutylene succinate) > PLA (polylactic acid) (Tokiwa et al., 2009; De Paula et al., 2018). Among the plastic polymers, PCL is fossil-based; however, PBS is not fully bio-based, and PLA has gained a growing amount of interest (Lackner, 2015). However, the production capacity of PHAs is still small but is speculated to grow exponentially in the near future (Aeschelmann et al., 2016).

Among PHAs, PHBs are widely studied and comprise the most common PHA. To date, PHBs are the only widespread PHAs produced under photo-autotrophic conditions (Troschl et al., 2018). Polymers such as PHAs, and especially PHBs, have physicochemical characteristics similar to those of petrochemical plastic and can have wide applications. PHBs are crystalline and are comparatively rigid having a methyl group as a side chain. PHBs decompose at ∼200°C, i.e., near their melting temperature, show poor melt stability, and turn brittle within a few days of manufacturing. Blending and incorporating other co-monomers can change the chemical properties and other characteristics like decreasing the aging process and, hence, increasing their applications widely. PHBs display less resistance to solvents and high natural resistance against photodegradation (Lane, 2015;

Gomes Gradíssimo et al., 2020). Therefore, it is an emergent need to use microorganisms such as cyanobacteria that have low nutritional requirements to produce useful, environmentally safe, bio-based, and biodegradable PHAs.

PHA and PHB Structure

PHAs are linear polyesters having 3–6 hydroxy acids and more than 150 monomers accounting for around 2 million Daltons (**Figure 4**) (Chen and Wu, 2005; Gomes Gradíssimo et al., 2020). Alcohol, sugar, and alkane production can act as a substrate for the formation of polymers. The varied physical properties are due to the different chemical structures of PHAs produced from different bacterial genera becoming more suitable for wide applications (Raza et al., 2018). PHAs, however, are one of the largest categories of natural bio-based polyesters composed of more than 150 different monomers of PHAs (Pittman et al., 2011). Varied changes in structural configurations and variations of monomers can form homopolymers of PHAs and copolymers of PHAs, and an example of a homopolymer is PHB and a copolymer is poly(3-hydroxybutyrate-co-3-hydroxyvalerate) (PHVB) (Chen, 2009). Based on polymerization, PHAs can be of different lengths such as short-chain length (SCL) including PHB, poly(3-hydroxyvalerate)-PHV, and their copolymer PHBV, while another type of PHAs is medium chain length (MCL) that includes poly(3-hydroxynonanoate)-PHN and poly(3-hydroxyoctanoate)-PHO.

Properties of PHAs

Cyanobacterial PHAs exhibit thermostability and physical properties like those of conventional plastics derived from fossil origin (Gadgil et al., 2017). The physical and chemical properties are determined by their chemical structure, i.e., the number of monomers. The shorter PHA is brittle and shows high crystallinity, while polymers with more number of monomers are flexible and elastic. It covers biopolymers that are biodegradable as well as biocompatible (Chen and Wu, 2005; Tokiwa et al., 2009; Tan et al., 2014; Gomes Gradíssimo et al., 2020). The decomposition of PHAs under natural conditions or by bacterial action depends on various factors like polymer composition, humidity, and temperature of the surrounding. It also depends on the type of decomposing microorganism, as it affects the duration of degradation because different bacteria express diverse types of PHA-depolymerase that degrades the biopolymer. Moreover, the chemical and physical properties of bioplastics result in sinking of these bioplastics in an aquatic environment that facilitates their transformation into carbon and water by decomposers (Tokiwa et al., 2009; Raza et al., 2018).

Interestingly, PHAs like synthetic plastics can be customized and thus are attractive biomaterials, as they can be designed to suit a specific function. Blending PHAs with other biodegradable polymers can considerably improve the physical properties like crystallinity, glass transition temperature, and mechanical properties (Li et al., 2016). Owing to their unique versatility and ecologically friendly biodegradable properties, PHAs are of great use, as they have a wide range of applications and show to be a promising substitute to petrochemical polymers. Usually, petrochemical plastic wastes are either fragmented into microplastics or are being collected into the oceans as garbage patches. However, bioplastics have met the standard specifications for marine degradability. Based on growing needs, PHAs nowadays are most attractive to producers, and the bioplastic market is expected to strongly increase the production capacity of PHAs by many folds in the future (Aeschelmann et al., 2016; Rosenboom et al., 2022). They are widely used in industries to manufacture biodegradable water-resistant surfaces, for controlled pesticide delivery, nanocomposite materials, mulch films, medical devices, tissue scaffolding, plastic packaging, etc. (Philip et al., 2007; Gomes Gradíssimo et al., 2020).

PHAs producing organisms are categorized into two groups: one group that produces PHAs during their growth period and another group that synthesizes PHAs when they grow under limited nutrient conditions (Basnett et al., 2017). Cyanobacteria are the only prokaryotic species known to produce the homopolymer of PHB naturally in photoautotrophic and chemoheterotrophic environments (Rani and Sharma, 2021). The unsteady growth during the fermentation process promotes PHA production. The accumulation depends on the presence of various elements in the growth medium as well as the ionic strength of the medium (Chen, 2009). Recently, cyanobacteria were genetically transformed with PHB and PHA synthesis encoding genes (Noreen et al., 2016).

Biosynthetic Pathway for PHA Production in Cyanobacteria

Three biosynthetic pathways are involved in the assimilation of carbon into different polymers. The foremost well-described pathway found in cyanobacteria for PHA production, especially PHB, is similar to earlier documented pathways in heterotrophic and other archaebacteria species (Lim et al., 2002; Lee et al., 2005; Singh and Mallick, 2017). Among cyanobacteria, *Synechocystis* PCC6803 is widely used as a model organism for gaining insight into the generation of PHBs. PHB biosynthesis involves majorly three enzyme-mediated steps: condensation, reduction, and polymerization. Step one includes reversible condensation (Claisen type) of the precursor, i.e., two molecules of acetyl-CoA derived from the tricarboxylic acid (TCA) cycle with an enzyme, ketothiolase, and produces acetoacetyl-CoA. The first step is followed by reduction of acetoacetyl-CoA (encoded by gene *phaA*) with NADPH-linked enzyme acetoacetyl-CoA reductase (encoded by *phaB*) and produces d(-)-3-hydroxybutyryl-CoA. Furthermore, in the last step, d (-)-3-hydroxybutyrate-CoA gets polymerized by the PHA-synthase enzyme (encoded by genes *phaC* and *phaE*) and finally produces poly(3-hydroxybutyrate) biopolymer (PHB) (**Figure 2**). The four genes, slr1993- *phaA*, slr1994- *phaB*, slr1830- *phaC*, and slr1829- *phaE* encoding the three enzymes are involved in PHB synthesis. In anoxygenic purple sulfur bacteria, the PHA synthase coding mediated by genes *phaC* and *phaE* is similar to that in a cyanobacterium (Lane and Benton, 2015). The role of Rubisco in CO_2 assimilation is additionally observed in the production of PHB involving the conversion of glycolate to 2-phosphoglycolate synthesis under photosynthetic conditions. Along with the conjugation of PHB synthesis, the substrate propionic acid is used in the synthesis of PHBV copolymer (Balaji et al., 2013). Reportedly,

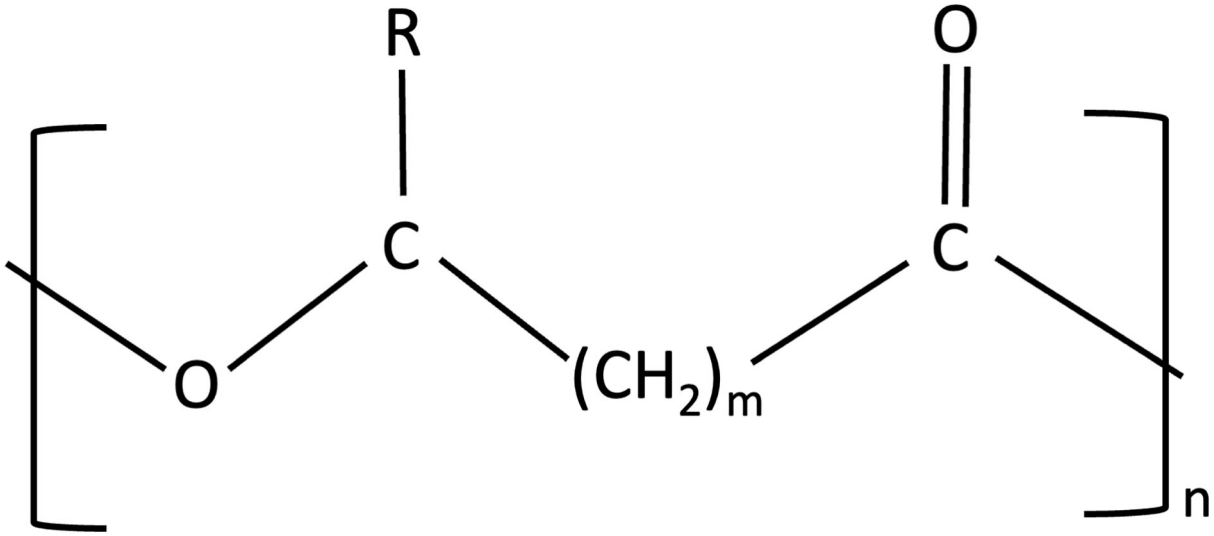

FIGURE 4 | Structure of PHAs (polyhydroxyalkanoates). In homopolymers, m can vary from 1 to 3 {polyhydroxybutyrate (PHB) - m = 1}, n can vary from 100 to 30,000 monomers, where R is a varied chain length alkyl group.

different conditions showed different production rates of PHBs. Under photo-autotrophic conditions in *Synechocystis* sp., the production of these biopolymers was up to 20% (DCW, dry cell weight); however, under heterotrophic conditions, acetate supplementation, and phosphorus deprivation, the production was 28.8% (DCW), and when genetically modified organisms were supplemented with acetate, they showed a higher yield of PHB at 35% (DCW). Interestingly, the highest yield of 55% was obtained when *Synechococcus* sp. MA19 was grown with $Ca_3(PO_4)_2$ (Panda et al., 2006; Khetkorn et al., 2016; Kamravamanesh et al., 2017; Gomes Gradíssimo et al., 2020).

However, another interesting biosynthetic pathway involves metabolism of lipids and transformation of different alkanes, alkenes, and alkanoates to generate MCL-PHA polymers. Furthermore, PHA synthase enzymes polymerize different hydroxyalkanoate monomers during the fatty acid oxidation pathway (Hein et al., 2002; Lim et al., 2002).

In the next and third biosynthetic low production cost involved pathway, MCL-PHAs are polymerized from monomers that are produced from glucose, fructose, and sucrose (Philip et al., 2007). Here, with a glycolic precursor and intermediates of the fatty acid biosynthesis pathway, lipids and carbohydrates are used in the generation of PHAs. PHA generation, accumulation, and growth of microbes are also affected by the availability or deprivation of many nutrients and their concentrations, mainly including nitrogen, phosphate, sulfur, and oxygen. Optimum changes in carbon-to-nitrogen ratio are used for culture optimization, whereas abundant carbon is favorable for the production of biomass, and limiting the concentration of phosphorus and/or nitrogen is found to beneficial for the generation of polymers of PHAs (Salehizadeh and Van Loosdrecht, 2004; Wen et al., 2010; Montiel-Jarillo et al., 2017). In cells, nitrogen is required for manufacturing proteins and nucleic acids, and the availability and deprivation of nitrogen levels influence NAD(P)H concentration, NAD(P)H/NAD(P) ratio, and, hence, the TCA cycle (Lee et al., 2005; Albuquerque et al., 2010; Reddy and Mohan, 2015). In a balanced well-supplemented nutrient culture, the TCA cycle is maintained as the concentration of NAD(P)H, and NAD(P)H/NAD(P) ratio remains constant. On the contrary, in nitrogen deficiency, amino acid synthesis, α-ketoglutarate conversion into glutamate, assimilation of ammonium ions, and NAD(P)H accumulation get affected (Panda et al., 2006; Liu et al., 2011) and, hence, influence PHB production.

In cyanobacteria, other than nitrogen, the availability and deprivation effect of phosphorus are found to be more significant. Despite the role in cell maintenance and lipid and carbohydrate assimilation, mainly the inorganic form of phosphorous is a part of protein and nucleic acid (Reddy and Mohan, 2015; Gomes Gradíssimo et al., 2020). Therefore, in well-balanced culture, nutritional growth conditions with a suitable concentration of phosphorous and high coenzyme-A (CoA-SH) concentration inhibit the synthesis of PHA, whereas during phosphorous deprivation, the Krebs cycle gets restricted (Montiel-Jarillo et al., 2017). The deprivation metabolism of nitrogen and phosphorous promotes the reducing factor, NADH accumulation; citrate synthase concentration decreases and isocitrate dehydrogenase and acetyl-CoA precursor concentration increases and, hence, influence PHA biosynthesis (Singh and Mallick, 2017; Gomes Gradíssimo et al., 2020).

Genetic Engineering of Cyanobacteria for Enhanced Bioplastic Production

Cyanobacteria serve as a promising and sustainable substitute to produce biopolymers like PHB and offer several advantages in comparison to heterotrophic bacteria (Khetkorn et al., 2016).

Despite various advantages, still, they have not found acceptance in the market as cyanobacterial strains are still not optimized for industrial processes. Genetic engineering is one of the techniques that have been exploited to improve the production of PHBs. There have been numerous research studies on genetic engineering in plants for the production of bioplastics, which are referred to as first- and second-generation bioplastics, but now the third generation that is commonly known as "algal bioplastics" is gaining immense importance as it offers a substitute for sustainable production of bioplastics. Genetic studies on cyanobacteria have a major advantage in terms of genetic manipulation in comparison to plants as their genome is less complex and, thus, is easy to manipulate (Koksharova and Wolk, 2002; Koller, 2020). However, most studies on biosynthesis and metabolic engineering of cyanobacterial PHB have been conducted with restricted strains of cyanobacteria. Out of all, *Synechocystis* sp. PCC 6803 is a largely applied model organism. It was the first phototrophic organism to be completely sequenced with mutant variants readily available and thus is largely used in gene manipulation to improve PHA production. There are a number of reports where it has been efficiently transformed for the production of PHBs and for the synthesis of biohydrogen, isoprene, and other compounds (Kaneko and Tabata, 1997; Kamravamanesh et al., 2017; Yashavanth et al., 2021).

Photosynthetic prokaryotes can be genetically engineered by transformation with genes encoding the enzymes required for PHB biosynthesis like acetoacetyl-CoA reductase, β-ketothiolase, and PHB synthase. The wild type cyanobacterial strains like *Aulosira fertilissima*, *Nostoc muscorum*, and *Synechocystis* sp. PCC 6803, which exhibit native PHB biosynthesis pathway, can be genetically engineered for achieving high yield and PHB productivity (Bhati et al., 2010). Mobilization of complete operons or genes from some other microorganisms that produce PHBs into the cyanobacteria can also boost PHB biosynthesis. In addition to the genes associated with the PHB pathway, the overexpression or deletion of other genes has been found to amplify the level of acetyl-CoA and PHB (Yashavanth et al., 2021). Takahashi et al. (1998) reported that recombinant *Synechococcus* sp. PCC7942 obtained by transformation with genes from *Alcaligenes eutrophus* that encode poly-3-hydroxybutyrate (PHB)-synthesizing enzymes showed improved PHB content in response to CO_2 enrichment under photoautotrophic conditions and nitrogen starvation. Moreover, the addition of acetate enhanced PHB content by more than 25% under conditions of nitrogen starvation. Miyake et al. (2000) found that inserting the PHB synthase gene obtained from *Ralstonia eutropha* in *Synechococcus* sp. MA19 resulted in the production of soluble PHB synthase that led to the synthesis of PHB granules with no pigment. In another study by Akiyama et al. (2011), *Synechococcus* PCC7002 was transformed with PHA genes from *Cupriavidus necator* enhancing PHB production by up to 52% under heterotrophic conditions. In another study by Wang et al. (2013), synthetic metabolic pathways were constructed, and *Synechocystis* 6803 was standardized to synthesize (S)- and (R)-3-hydroxybutyrate (3HB) using CO_2 directly. It was observed that *Synechocystis* cells easily secreted both forms of 3HB molecules without overexpressing the transporters. Furthermore, the competing pathway was suppressed by deleting the genes coding for PHB polymerase (*slr1829* and *slr1830*) from the genome of *Synechocystis,* which led to enhanced production of 3HB. The photosynthetic cultivation of recombinant *Synechocystis* TABd (for 21 days) produced 533.4 mg/L of 3HB. The accumulation of PHB is reported to increase under the conditions of nitrogen deficiency, and *sigE (*the Sigma factor) is also found to induce PHB synthesis and carbohydrate metabolic pathways. The *sigE* overexpression in *Synechocystis* 6803 improved PHB biosynthesis under nitrogen-deficient conditions. Interestingly, the monomer units and molecular weight of produced PHB are identical to those of PHB from the wild type (Osanai et al., 2013). Similarly, in another report, the recombinant *Synechocystis* sp. PCC 6803 obtained by transformation with the PHA synthase gene from *Cupriavidus necator* displayed enhanced activity of the PHA synthase enzyme; however, the total PHB content was not found to increase (Sudesh et al., 2002; Katayama et al., 2018). *Synechocystis* 6803 transformed with *pha* genes was found to be effective, and the recombinant cells had higher PHB content (12-fold high) in comparison to the wild type in response to nitrogen stress (Hondo et al., 2015). In *Synechocystis* 6803, phaAB overexpression and use of acetate (4 mM) were found to increase PHB content by 35% (DCW) (Khetkorn et al., 2016). In *Synechocystis*, overexpressing the acetoacetyl-CoA reductase gene improved the production of R-3-hydroxybutyrate to 1.84 g L^{-1}, and maximum volumetrical production was 263 mgL^{-1} day^{-1} in *Synechocystis* (Wang et al., 2018). In another study, deletion of the *agp* gene encoding for ADP-glucose pyrophosphorylase from *Synechocystis* sp. PCC 6803 altered the partitioning of cellular carbon, and that consequently led to increased PHB production (18.6%), titer (232 mg/L), and productivity (7.3 mg/L/day) (Wu et al., 2002). Enzymes like acetyl-CoA hydrolase, phosphotransacetylase, and phosphoketolase control the level of acetyl-CoA in microbial cells. Acetyl-CoA can be converted into a large number of compounds based on the cell's requirement by employing different enzymes, particularly those that are used for PHB biosynthesis. Phosphotransacetylase (*pta* gene) and acetyl-CoA hydrolase (*ach* gene) are enzymes that convert acetyl-CoA into acetate. Phosphoketolase (encoded by *xfpk* gene) is an enzyme that, on the other hand, increases the level of acetyl-CoA in cells. Carpine et al. (2017) used a different strategy to amplify the production of PHB. For this experiment, recombinant *Synechocystis* PCC 6803 was designed by engineering central carbon metabolism instead of overexpressing or introducing PHB synthesis genes such that the PHB synthesis pathway gets downregulated and acetyl-CoA level increases. For this, seven diverse mutants were constructed that harbored individually or in the arrangement of three dissimilar genetic modifications to the metabolic pathway of *Synechocystis*. These included deletions of acetyl-CoA hydrolase-*Ach* and phosphotransacetylase-*Pta* and expression of heterologous phosphoketolase-*XfpK* (*Bifidobacterium breve).* It was observed that a strain having all the three recombinations in consolidation, i.e., *xfpk* overexpression in a background of double deletion (*pta*, *ach*), displayed a maximum PHB production of 12% PHB yield, titer of 232 mg/L, and productivity of 7.3

mg/L/day. Koch et al. (2020) engineered a strain that lacked PirC (the regulatory protein, product of sll0944) that exhibited high phosphoglycerate mutase activity and increased level of PHB in response to nutrient stress. This was further modified to produce more PHBs by transferring *phaA* and *phaB* (PHA metabolism genes) from a PHB-synthesizing bacterium, *Cupriavidus necator*. This strain was termed as PPT1 (ΔpirC-REphaAB), and the production of PHB was found to be high (constant light as well under day-night conditions). Under nitrogen- and phosphorus-deficient conditions, it produced 63% of PHBs, and this level further increased by 81 percent when acetate was added (under identical culture conditions). The PHB production achieved by PPT1 was the maximum ever documented for any known cyanobacteria. Thus, the above studies indicate that genetic modification can be a promising tool in cyanobacteria to achieve sustainable and cost-effective PHB production on an industrial scale. Some of the wild-type and recombinant cyanobacterial strains used for biosynthesis of the polymer are listed in **Table 2**.

CHALLENGES AND CONSTRAINTS IN PRODUCTION OF BIOFUEL AND BIOPLASTICS FROM CYANOBACTERIA

Challenges at different steps in large-scale production appear, because outdoor cultivation may vary from ideal indoor conditions. These might occur at basic steps like insufficient light or nutrients, contamination in open pond cultivation systems, or the extraction, purification, and harvest stages. At times, the harvest is not efficient enough to be scaled up at a commercial level. Therefore, there is always a need for competent cyanobacterial strains by manipulation of metabolism to enhance fuel and bioplastic production and minimize raw material inputs and cost. There are multiple bottlenecks at various steps including operations and logistics, which need to be addressed to get the desired quality and quantity of biofuel and bioplastics.

High Inputs of Resources (Space, Nutrients and Water)

The impact will directly be seen on land use pattern and agricultural inputs if the acceptance of algal biofuels increases in the near future. Preparedness for a future where acceptance of eco-friendly fuels will become imperative needs a well-planned cultivation model (Nozzi et al., 2013). Investment for setting up the initial infrastructure for the development of cost-effective scaling-up and harvest technology needs an upgrade.

Technical and Economic Limitations

These include maintenance of optimal growth conditions throughout the culture until the harvest, fine-tuning the metabolic needs of strains, various aspects of boosting biosynthesis efficiency, biomass production (Lau et al., 2015), and efficient pre-treatment optimization with least emissions and high yield (Khan et al., 2018) along with the process of dewatering (Anyanwu et al., 2018). Other issues include analysis of nutrient consumption rate and its flux and continuous mining of efficient indigenous strains with better photosynthetic efficiency and higher productivity.

As discussed in many research studies, the use of native and genetically engineered heterotrophic microorganisms (*Bacillus megaterium*, *Cupriavidus necator*, *Escherichia coli*, *Pseudomonas aeruginosa*, *Ralstonia eutropha*, and *Saccharomyces cerevisiae*) has been the prime focus for producing PHAs (Pandian et al., 2010; Agnew et al., 2012; Ienczak et al., 2013). However, the fermentation process normally involves high production costs and hence limits their applicability for PHA production. This elevated cost is primarily due to the carbon source that is used to maintain the fermentation, productivity, downstream processing, and purification processes. It has been found that agricultural and industrial wastes along with other cheap carbon sources can help in lowering the cost of production, but this compromises the yield and requires redesigning of unit operation (Ienczak et al., 2013). There are studies indicating that the application of cyanobacteria in the production of industrial PHAs can help in lowering the cost of nutritional inputs as they have fewer nutritional requirements in contrast to heterotrophic bacteria (Asada et al., 1999; Sharma et al., 2007). Thus, PHA production *via* cyanobacteria would be effective in producing biodegradable bioplastics by sequestering CO_2 as a costless source of carbon and thus can significantly contribute in lowering PHA production costs. However, these cyanobacteria normally give lower yield than heterotrophic organisms. Therefore, extensive inputs by research and development are required to upscale the yield of using cyanobacteria for industrial purposes.

Transitioning From Pilot Phase to Industrial-Scale Production

In the urge of rising global energy and economic crises, cyanobacteria are emerging as a potential source for biofuels and bioplastics. Various studies are going on to take these bio-factories from laboratories to industries, and extensive research is focused on industrial upscale of a large variety of products, especially biofuels and bioplastics, from cyanobacteria under outdoor conditions. Additionally, many products like pigments can also be derived from the leftover residue after PHB extraction and can be used in a wide variety of downstream processes (Forchhammer and Koch, 2022). Along with industrial-level advantages, using cyanobacteria can help in reducing the cost related to production, increasing yield, managing waste, and producing energy-rich livestock that can, therefore, lead to sustainable production and environmental conservation (Gomes Gradíssimo et al., 2020). Many research studies have strongly recommended the development and use of improved recombinant strains of cyanobacteria that can accumulate high levels of acetate and polymer either by gene silencing or gene transfer. Additionally, whole production or reactor units are required to be innovatively redesigned. By this, several challenges related to low production of polymer can be solved (Drosg et al., 2015). However, with increasing and uncertain demands and supplies, industries are yet to report to derive maximum profits as compared to their high operational costs, and greenhouse gas emission and contamination during production of bioplastics

TABLE 2 | List of wild-type and recombinant cyanobacterial strains used for the production of polymers.

Cyanobacterial strains	PHB content (% DCW)	Substrate and culture conditions	PHA composition	References
Spirulina platensis	6.0	CO_2	PHB	Campbell and Balkwill, 1982
Spirulina maxima	7–9	CO_2, N and P limitation	PHB	De Philippis et al., 1992
Synechocystis PCC 7942	3.0	CO_2, N limitation	PHB	Takahashi et al., 1998
	25.6	Acetate, N limitation		
Synechocystis sp. PCC 6803	38	Phosphate deficiency, gas exchange limitation, acetate, fructose	PHB	Panda and Mallick, 2007
	9.5	Photoautotrophic, N-limitation		
	11.2	Photoautotrophic, P-limitation		
Arthrospira platensis UMACC 161	1.0	CO_2	PHB	Toh et al., 2008
	10	Acetate, CO_2, N starvation		
Nostoc moscorum Agardh	60	Acetate and Valerate, N deficiency	PHB-co-PHV	Bhati and Mallick, 2012
Nostoc moscorum	22	CO_2, P starvation	PHB	Haase et al., 2012
Aulosira fertilissima CCC444	85	Citrate and Acetate, P deficiency	PHB	Samantaray and Mallick, 2012
Aulosira fertilissima CCC 444	76.9	Fructose, Valerate	P (3HB-co-3HV)	Samantaray and Mallick, 2014
	65.7	Fructose, Valerate, P deficiency		
Caltorix scytonemicola TISTR 8095	25	CO_2, N deficiency	PHB	Kaewbai-Ngam et al., 2016; Monshupanee et al., 2016
Synechocystis sp. PCC 6714	16	CO_2, N and P limitation	PHB	Kamravamanesh et al., 2017
Synechococcus elongates	17.2	CO_2, sucrose, N deficiency	Not specified	Mendhulkar and Laukik, 2017
Synechocystis sp. CCALA192	12.5	CO_2, N limitation	PHB	Troschl et al., 2018
Recombinant cyanobacterial strains used for the production of the polymer				
Synechococcus sp. PCC 7942	25.6	Acetate, nitrogen limitation	PHB	Takahashi et al., 1998
Synechocystis sp. PCC 6803	11	Acetate, nitrogen limitation	PHB	Sudesh et al., 2002
Synechococcus sp. PCC 7942	1.0	CO_2	PHB	Suzuki et al., 2010
Synechocystis sp. PCC 6803	14	Direct photosynthesis	PHB	Lau et al., 2014
Synechocystis sp. PCC 6803	7.0	CO_2	PHB	Hondo et al., 2015
Synechococcus sp. PCC 7002	~4.5%	Light, CO_2 (photoautotrophy)	P (3HB-co-4HV)	Zhang et al., 2015
Synechocystis sp. PCC 6803	26	CO_2, N deprivation, photoautotrophic	PHB	Khetkorn et al., 2016
	35	Acetate, N deficiency		
Synechocystis sp. PCC 6803	12	CO_2, photoautotrophic	PHB	Carpine et al., 2017
Synechocystis sp.	35	CO_2	PHB	Wang et al., 2018

on a large-scale industrial level pose challenges in using cyanobacteria for production of biopolymers (Priyadarshini et al., 2022; Rosenboom et al., 2022; Samadhiya et al., 2022). Interestingly, more focus on simultaneous degradation of petrochemical plastics and production of biodegradable plastics could be a promising approach (Priyadarshini et al., 2022).

Marketing and Acceptance

Once the product obtained manages the scope and implementation inconsistencies, various hurdles need to be surpassed in order to reach economically feasible quality and quantity of biofuel (Gupta et al., 2020). These hurdles include the cost barriers, trade limitations, and issues with engines' fuel interface to meet the standards of global energy demand (Rodionova et al., 2017).

ADVANCEMENTS, FUTURE PERSPECTIVES, AND NOVEL APPROACHES FOR ECO-FRIENDLY CYANOBACTERIAL BIOFUEL AND BIOPLASTIC PRODUCTION

To overcome the abovementioned challenges and scale up biofuel production and use, strategies for overcoming each hurdle need to be optimized. In comparison to terrestrial plants, their tiny

genome size, short development cycle, and simple metabolic activities have made their genetic manipulation more efficient (Singh et al., 2017). A huge amount of data on cyanobacterial genome sequencing has aided in the building of genome-scale models (GSMs) for a wide range of species, from model species *viz. Synechocystis* sp. PCC6803 to industrially promising strains like *Arthrospira platensis* NIES-39 (Yoshikawa et al., 2015). As a result, cyanobacterial genetics and metabolic control systems are elaborately characterized. This information has opened new vistas for genetic engineering of cyanobacteria to make biofuels. Cyanobacteria are employed as microbial model systems to focus on production of various biofuel forms. Strategies and improvements on genome-scale networks and modeling are enhanced and used for efficient cyanobacterial-based biofuels using the systems metabolic engineering method (Klanchui et al., 2016).

Ever-progressing genomics and systems biology have resulted in the recognition of new paradigms for systems metabolic engineering. Because of breakthroughs in metabolic engineering, the industrial production of cyanobacterial biofuels has recently become a reality. To capitalize on the usage of these organisms for better biofuel production, strategies to improve lipid productivity, salt tolerance, and other value-added parameters or design features have been devised (Sitther et al., 2020). Cultivation efficiency is observed to be maximized by the addition of waste paper (which enhances degradation) and co-cultivation/co-culture of autotrophic cyanobacteria with heterotrophic bacteria (which adds secondary metabolites to the cultivation system) (Luan and Lu, 2018).

Cyanobacteria have a great potential in the field of industrial biotechnology, which deals with the manufacture of a broad variety of bio-products such as hydrogen, isoprenoids, alcohols, and other high-value bioactive substances. Several innovative strategies have recently been applied in the discovery and development phases for the commercial application of cyanobacteria.

The demand for polymers in developed countries is expected to rise by 2–3 folds, and a lot of current studies are largely focused on finding a substitute to synthetic plastics. Heterotrophic bacteria produce 17–90% (DCW) of PHBs depending on nutrient supply and growth conditions. However, heterotrophs require carbon from heavily irrigated arable lands, and a huge cost is involved in the fermentation of heterotrophic bacteria, thus limiting their application in large-scale production of PHBs (Balaji et al., 2013). Cyanobacteria possess the ability to synthesize PHAs under mixotrophic and photoautotrophic growth conditions when supplemented with substrates such as acetate, propionate, and glucose. They can serve as an alternative for the biosynthesis of PHB, as 50% of the biomass of cyanobacteria is made of carbon and they utilize carbon sources from industrial effluents that permit the assimilation process by photo-biorefineries. The cyanobacterial cultivation in open systems like the one conducted for *Spirulina* sp. may further help in reducing the cost, as these systems are easy to build and function (Klinthong et al., 2015; Slocombe and Benemann, 2017; Meixner et al., 2018). The isolation and purification of PHBs from cyanobacteria are almost same as those conducted for PHA production *via* Gram-negative heterotrophic bacteria. Thus, by simplifying the design of photobioreactors, the applied material and decreasing the energy consumption can help in reducing the cost of bioreactors and subsequently will further lessen the cost of cyanobacterial PHB production (Drosg et al., 2015; Singh and Mallick, 2017; Costa et al., 2018). Besides this, other factors that contribute to increased cost of production are the cost involved in the procurement of raw material and extraction and purification processes. The method for PHAs recovery from the cell biomass plays a considerable role in the quality of PHA materials obtained as well as the cost involved in the process. Thus, various innovative methods like quick extraction methods for biomass disruption *via* enzymatic or chemical, mechanical methods, and high temperature and pressure for cell disruption are required for studying various PHA-synthesizing archaeal and eubacterial species (Madkour et al., 2013; Riedel et al., 2013; Samorì et al., 2015). Moreover, the costs involved in the procurement of raw materials for cyanobacterial cultivation surpass 50% of the entire expenditure involved in the production of PHBs *via* the heterotrophic method of production. The carbon source corresponds to 60% of the total expenditure on nutrients required for the cultivation of cyanobacteria under autotrophic conditions. Thus, to decrease the expenditure, there is a need to find a cheap alternative of carbon or nutritional sources like agro-industrial waste, carbon enriched wastewater, CO_2 from cement plants, oil refineries, and thermoelectric combustion gas for cyanobacteria or heterotrophic bacteria. In addition to this, the use of residues and cheap nitrogen sources for culture like ammonium salts, urea, and nitrogen-enriched wastewater can further decrease the cost of nutrients (Borges et al., 2013; Costa et al., 2018).

Thus, there is a need to modify the cultivation, harvesting, and extraction methods, develop improved photobioreactor, find environment friendly and cost-effective recovery substitutes or downstream processes for cyanobacterial PHAs that can significantly boost PHA productivity and thereby would facilitate lowering the price associated with it (Singh and Mallick, 2017; Costa et al., 2018). In addition to this, the application of metabolic inhibitors has also been recommended to improve cyanobacterial PHA yield. The optimization of PHB production in cyanobacteria can be achieved by isolating strains that exhibit high capability of PHB biosynthesis. Genetic engineering is reported to be one of the promising methods to achieve cost-effective and sustainable PHA production from cyanobacteria. Cyanobacterial strains can be engineered with PHB synthase, acetoacetyl-CoA reductase, 3-ketothiolase genes, etc (Chen and Wu, 2005; Tao et al., 2008). Furthermore, the identification of SigE (RNA polymerase sigma factor) (Rre37), response regulator and presence of cyanobacterial entire Krebs cycle is found to be of great value in increasing the PHA synthesis in cyanobacteria (Singh and Mallick, 2017). Thus, cyanobacteria offer a promising photosynthetic platform to enhance PHA production. This has received immense attention as a result of current advancements in

cultivation and metabolic engineering methods (Oliver et al., 2016).

Exploring the cyanobacterial "omics" research and technology is a current achievement that includes advancements in genetic modification and synthetic biology. These methodologies aided in the creation of complex metabolic engineering programs aimed at creating strains tailored for specific industrial biotechnology applications. Furthermore, emerging approaches such as Clustered Regularly Interspaced Short Palindromic Repeats associated protein (CRISPR/Cas) and CRISPRi (CRISPR interference) study in cyanobacteria (Gale et al., 2019) hold a lot of promise. To evaluate and design cyanobacteria for increased production, a well-studied model system and integration of synthetic biology approaches like metabolic models and genomic models, omics approach and genetic tools, and use of genetic manipulation are required to achieve enhanced bioplastic production (Santos-Merino et al., 2019). These models have emerged as a result of high-throughput omics investigation in cyanobacteria, which includes the use of practically applicable omics technologies in *Synechocystis*, a representative strain for cyanobacteria. Strategy on a large scale requires the expression of several genes that, in turn, has led to the innovation of more competent genetic tools in recent years like a system based on CRISPR (Santos-Merino et al., 2019). With the completion of a CRISPRi-gene repression library and a novel enhanced natural transformation method in cyanobacteria, the prospective execution of research advancements for production by biosynthesis can be hastened (Pope et al., 2020). The results of more extensive techniques and technology are encouraging in terms of establishing efficient cyanobacterial production systems. CRISPR/Cas tools are known to produce a large number of mutant knock-in and knock-out strains with desired traits (Sreenikethanam and Bajhaiya, 2021). These gene-editing tools are yet to be extensively investigated in algal systems, predominantly in the field of bioplastic research. It is also suggested that increasing the basic understanding related to cellular structure, metabolism, photosynthesis of cyanobacteria, and application of molecular tools can help in increasing PHA biosynthesis and productivity, as the *Synechocystis* sp. PCC 6803 genome sequence is available and there are various molecular and systems biology methods accessible to study this bacterium. Biosynthetic pathway engineering requires an in-depth understanding of cellular metabolism. High-throughput omics tools have been applied to understand the dynamic process of *Synechocystis* 6803 in response to several physiological conditions (Yu et al., 2013). Approaches based on synthetic biology to identify as well as develop new, fast-growing, tolerant cyanobacterial strains by simultaneously and critically considering genetic transformation, computational biology aspects, and scale-up techniques are continually being pursued to fast-forward the mass production of efficient cyanobacterial biofuels (Liang et al., 2018).

CONCLUSIONS

Known as blue-green algae, prokaryotic, photosynthetic, Gram-negative organisms, cyanobacteria are of immense biological value. Among the various alternatives to reduce GHG emission by the usage of low carbon-based fuels, biofuels and bioplastics can help in lessening the atmospheric carbon footprint and can further lessen the oil dependence on finite resources for sustainable growth and development. The circular economy suggests the pattern of production and consumption by reducing the demand, reusing, repairing, recycling, and resource extraction or recovery from existing materials and their products for a long time. By this, the use of cyanobacteria in deriving biofuels and bioplastics using metabolites in different industries can be of help in the circular economy and achieve sustainable goals as suggested by Rosenboom et al. (2022). Most of the applications of cyanobacteria for sustainable production are still marked by low product yield. In this regard, computational methods for scheming and designing a suitable strain based on genome-scale metabolic models hold an enormous potential to appreciably enhance product yield. Integration of progressing system biology and synthetic biology would help in finding and developing new and economical methods to achieve eco-friendly, cost-effective, and sustainable biofuel and bioplastic production from cyanobacteria.

AUTHOR CONTRIBUTIONS

PA, RS, PK, AM, and RM helped in drafting, writing, and editing manuscript, including figures and table. JP and SS helped in making figures and tables and were involved in editing. GS generated the idea, designed the manuscript, and involved in writing and editing manuscript. All authors contributed to the article and approved the submitted version.

ACKNOWLEDGMENTS

The authors are thankful to the Botany Department of Gargi College, University of Delhi for providing continuous support during the preparation of this manuscript.

REFERENCES

Abed, R. M., Dobretsov, S., and Sudesh, K. (2009). Applications of cyanobacteria in biotechnology. *J. Appl. Microbiol.* 106, 1–12. doi: 10.1111/j.1365-2672.2008.03918.x

ACC (2007). *Plastic Packaging Resins (Resin Codes)*. Arlington, VA: American Chemistry Council. Available online at: https://www.carrollcountymd.gov/media/3284/plastic-codes.pdf

ACC (2013). *Plastic Resins in the United States: American Chemistry Council: Economics and Statistics Department*. Washington, DC: American Chemistry Council.

Aeschelmann, F., Carus, M., Baltus, W., Carrez, D., de Guzman, D., Käb, H., et al. (2016). *Bio-Based Building Blocks and Polymers. Global Capacities and Trends 2016–2021*. Hurth: Nova-Institut GmBH. Available online at: https://renewable-carbon.eu/publications/product/bio-based-building-blocks-and-polymers-global-capacities-and-trends-2016-2021/

Agnew, D. E., Stevermer, A. K., Youngquist, J. T., and Pfleger, B. F. (2012). Engineering *Escherichia coli* for production of C12–C14 polyhydroxyalkanoate from glucose. *Metab. Eng.* 14, 705–713. doi: 10.1016/j.ymben.2012.08.003

Akiyama, H., Okuhata, H., Onizuka, T., Kanai, S., Hirano, M., Tanaka, S., et al. (2011). Antibiotics-free stable polyhydroxyalkanoate (PHA) production from carbon dioxide by recombinant cyanobacteria. *Bioresour. Technol.* 102, 11039–11042. doi: 10.1016/j.biortech.2011.09.058

Albuquerque, M. G. E., Torres, C. A. V., and Reis, M. A. M. (2010). Polyhydroxyalkanoate (PHA) production by a mixed microbial culture using sugar molasses: effect of the influent substrate concentration on culture selection. *Water Res.* 44, 3419–3433. doi: 10.1016/j.watres.2010.03.021

Ammendolia, J., Saturno, J., Brooks, A. L., Jacobs, S., and Jambeck, J. R. (2021). An emerging source of plastic pollution: environmental presence of plastic personal protective equipment (PPE) debris related to COVID-19 in a metropolitan city. *Environ. Pollut.* 269, 116160. doi: 10.1016/j.envpol.2020.116160

Anahas, A. M. P., and Muralitharan, G. (2018). Characterization of heterocystous cyanobacterial strains for biodiesel production based on fatty acid content analysis and hydrocarbon production. *Energy. Convers. Manag.* 157, 423–437. doi: 10.1016/j.enconman.2017.12.012

Andrews, F., Faulkner, M., Toogood, H. S., and Scrutton, N. S. (2021). Combinatorial use of environmental stresses and genetic engineering to increase ethanol titres in cyanobacteria. *Biotechnol. Biofuels.* 14, 1–17. doi: 10.1186/s13068-021-02091-w

Anyanwu, R. C., Rodriguez, C., Durrant, A., and Olabi, A. G. (2018). Optimisation of tray drier microalgae dewatering techniques using response surface methodology. *Energies* 11, 2327. doi: 10.3390/en11092327

Appel, J., Hueren, V., Boehm, M., and Gutekunst, K. (2020). Cyanobacterial *in vivo* solar hydrogen production using a photosystem I–hydrogenase (PsaD-HoxYH) fusion complex. *Nat. Energy*. 5, 458–467. doi: 10.1038/s41560-020-0609-6

Asada, Y., Miyake, M., Miyake, J., Kurane, R., and Tokiwa, Y. (1999). Photosynthetic accumulation of poly-(hydroxybutyrate) by cyanobacteria—the metabolism and potential for CO_2 recycling. *Int. J. Biol. Macromol.* 25, 37–42. doi: 10.1016/S0141-8130(99)00013-6

Ashter, S. A. (2016). *Introduction to Bioplastics Engineering*. Merrimack, NH: William Andrew. R&D Endovascular, Maquet Getinge Group. doi: 10.1016/B978-0-323-39396-6.00001-4

Atsumi, S., Hanai, T., and Liao, J. C. (2008). Non-fermentative pathways for synthesis of branched-chain higher alcohols as biofuels. *Nature* 451, 86–89. doi: 10.1038/nature06450

Atsumi, S., Higashide, W., and Liao, J. C. (2009). Direct photosynthetic recycling of carbon dioxide to isobutyraldehyde. *Nat. Biotechnol.* 27, 1177–1180. doi: 10.1038/nbt.1586

Baebprasert, W., Jantaro, S., Khetkorn, W., Lindblad, P., and Incharoensakdi, A. (2011). Increased H_2 production in the cyanobacterium *Synechocystis* sp. strain PCC 6803 by redirecting the electron supply via genetic engineering of the nitrate assimilation pathway. *Metab. Eng.* 13, 610–616. doi: 10.1016/j.ymben.2011.07.004

Balaji, S., Gopi, K., and Muthuvelan, B. (2013). A review on production of poly β hydroxybutyrates from cyanobacteria for the production of bioplastics. *Algal. Res.* 2, 278–285. doi: 10.1016/j.algal.2013.03.002

Basnett, P., Lukasiewicz, B., Marcello, E., Gura, H. K., Knowles, J. C., and Roy, I. (2017). Production of a novel medium chain length poly (3-hydroxyalkanoate) using unprocessed biodiesel waste and its evaluation as a tissue engineering scaffold. *Microb. Biotechnol.* 10, 1384–1399. doi: 10.1111/1751-7915.12782

Bergmann, M., Wirzberger, V., Krumpen, T., Lorenz, C., Primpke, S., Tekman, M. B., et al. (2017). High quantities of microplastic in arctic deep-sea sediments from the HAUSGARTEN observatory. *Environ. Sci. Technol.* 51, 11000–11010. doi: 10.1021/acs.est.7b03331

Bhati, R., and Mallick, N. (2012). Production and characterization of poly (3-hydroxybutyrate-co-3-hydroxyvalerate) co-polymer by a N_2-fixing cyanobacterium, *Nostoc muscorum* Agardh. *Chem. Technol. Biotechnol.* 87, 505–512. doi: 10.1002/jctb.2737

Bhati, R., Samantaray, S., Sharma, L., and Mallick, N. (2010). Poly-β-hydroxybutyrate accumulation in cyanobacteria under photoautotrophy. *Biotechnol. J.* 5:1181–1185. doi: 10.1002/biot.201000252

Bhatia, S. K., Bhatia, R. K., Jeon, J. M., Pugazhendhi, A., Awasthi, M. K., Kumar, D., et al. (2021). An overview on advancements in biobased transesterification methods for biodiesel production: oil resources, extraction, biocatalysts, and process intensification technologies. *Fuel.* 285, 119117. doi: 10.1016/j.fuel.2020.119117

Borges, J. A., Rosa, G. M. D., Meza, L. H. R., Henrard, A. A., Souza, M. D. R. A. Z. D., and Costa, J. A. V. (2013). *Spirulina* sp. LEB-18 culture using effluent from the anaerobic digestion. *Braz. J. Chem. Eng.* 30, 277–287. doi: 10.1590/S0104-66322013000200006

Borrelle, S. B., Ringma, J., Law, K. L., Monnahan, C. C., Lebreton, L., McGivern, A., et al. (2020). Predicted growth in plastic waste exceeds efforts to mitigate plastic pollution. *Science* 369, 1515–1518. doi: 10.1126/science.aba3656

Campbell, J. III, Stevens Jr, S. E., and Balkwill, D. L. (1982). Accumulation of poly-beta-hydroxybutyrate in *Spirulina platensis*. *J. Bacteriol.* 149, 361–363. doi: 10.1128/jb.149.1.361-363.1982

Carpine, R., Du, W., Olivieri, G., Pollio, A., Hellingwerf, K. J., Marzocchella, A., et al. (2017). Genetic engineering of *Synechocystis* sp. PCC6803 for poly-β-hydroxybutyrate overproduction. *Algal. Res.* 25, 117–127. doi: 10.1016/j.algal.2017.05.013

Carrieri, D., Momot, D., Brasg, I. A., Ananyev, G., Lenz, O., Bryant, D. A., et al. (2010). Boosting autofermentation rates and product yields with sodium stress cycling: application to production of renewable fuels by cyanobacteria. *Appl. Environ. Microbiol.* 76, 6455–6462. doi: 10.1128/AEM.00975-10

Cheah, W. Y., Show, P. L., Chang, J. S., Ling, T. C., and Juan, J. C. (2015). Biosequestration of atmospheric CO_2 and flue gas-containing CO_2 by microalgae. *Bioresour Technol.* 184, 190–201. doi: 10.1016/j.biortech.2014.11.026

Chen, C. L. (2015). "Regulation and management of marine litter," in *Marine Anthropogenic Litter*. eds M. Bergmann, L. Gutow, and M. Klages (Cham: Springer), 395–428. doi: 10.1007/978-3-319-16510-3_15

Chen, G. Q. (2009). A microbial polyhydroxyalkanoates (PHA) based bio-and materials industry. *Chem Soc Rev.* 38, 2434–2446. doi: 10.1039/b812677c

Chen, G. Q., and Wu, Q. (2005). The application of polyhydroxyalkanoates as tissue engineering materials. *Biomaterials* 26, 6565–6578. doi: 10.1016/j.biomaterials.2005.04.036

Chisti, Y. (2007). Biodiesel from microalgae. *Biotechnol. Adv.* 25, 294–306. doi: 10.1016/j.biotechadv.2007.02.001

Costa, J. A. V., Moreira, J. B., Lucas, B. F., Braga, V. D. S., Cassuriaga, A. P. A., and Morais, M. G. D. (2018). Recent advances and future perspectives of PHB production by cyanobacteria. *Ind Biotechnol.* 14, 249–256. doi: 10.1089/ind.2018.0017

Cuellar-Bermudez, S. P., Aguilar-Hernandez, I., Cardenas-Chavez, D. L., Ornelas-Soto, N., Romero-Ogawa, M. A., and Parra-Saldivar, R. (2015). Extraction and purification of high-value metabolites from microalgae: essential lipids, astaxanthin and Psychobilly phycobiliproteins. *Microb. Biotechnol.* 8, 190–209. doi: 10.1111/1751-7915.12167

De Paula, F. C., de Paula, C. B., and Contiero, J. (2018). "Prospective biodegradable plastics from biomass conversion processes," in *Biofuels - State of Development*, ed K. Biernat (London: IntechOpen), 245–272. doi: 10.5772/intechopen.75111

De Philippis, R., Sili, C., and Vincenzini, M. (1992). Glycogen and poly-β-hydroxybutyrate synthesis in *Spirulina maxima*. *Microbiology* 138, 1623–1628. doi: 10.1099/00221287-138-8-1623

Deng, M. D., and Coleman, J. R. (1999). Ethanol synthesis by genetic engineering in cyanobacteria. *Appl. Environ. Microbiol.* 65, 523–528. doi: 10.1128/AEM.65.2.523-528.1999

Dexter, J., and Fu, P. (2009). Metabolic engineering of cyanobacteria for ethanol production. *Energy. Environ. Sci.* 2, 857–864. doi: 10.1039/b811937f

Drosg, B., Fritz, I., Gattermayr, F., and Silvestrini, L. (2015). Photo-autotrophic production of poly (hydroxyalkanoates) in cyanobacteria. *Chem. Biochem. Eng. Q.* 29, 145–156. doi: 10.15255/CABEQ.2014.2254

Ducat, D. C., Sachdeva, G., and Silver, P. A. (2011). Rewiring hydrogenase-dependent redox circuits in cyanobacteria. *Proc. Natl. Acad. Sci. U. S. A.* 108, 3941–3946. doi: 10.1073/pnas.1016026108

Dühring, U., Baier, K., Germer, F., and Shi, T. (2017). *Genetically enhanced Cyanobacteria for the production of a first chemical compound harbouring Zn^{2+}, CO^{2+} or Ni^{2+}-inducible promoters.* U.S. Patent No. 9,551,014. Washington, DC: U.S. Patent and Trademark Office.

Erdrich, P., Knoop, H., Steuer, R., and Klamt, S. (2014). Cyanobacterial biofuels: new insights and strain design strategies revealed by computational modeling. *Microbial Cell Fact*. 13, 1–15. doi: 10.1186/s12934-014-0128-x

European Bioplastics (2021). *United Nations recommends bioplastics as a sustainable alternative to conventional plastics*. Available online at: https://www.european-bioplastics.org/united-nations-recommends-bioplastics-as-a-sustainable-alternative-to-conventional-plastics/. (accessed April 24, 2022).

Ezeji, T. C., Qureshi, N., and Blaschek, H. P. (2007). Bioproduction of butanol from biomass: from genes to bioreactors. *Curr. Opin. Biotechnol*. 18, 220–227. doi: 10.1016/j.copbio.2007.04.002

Fan, J., Zhang, Y., Wu, P., Zhang, X., and Bai, Y. (2022). Enhancing cofactor regeneration of cyanobacteria for the light-powered synthesis of chiral alcohols. *Bioorg. Chem.* 118, 105477. doi: 10.1016/j.bioorg.2021.105477

Fardinpoor, M., Perendeci, N. A., Yilmaz, V., Taştan, B. E., and Yilmaz, F. (2021). Effects of hydrodynamic cavitation-assisted NaOH pretreatment on biofuel production from Cyanobacteria: promising approach. *BioEnergy. Res.* 15, 289–302. doi: 10.1007/s12155-021-10286-0

Farrokh, P., Sheikhpour, M., Kasaeian, A., Asadi, H., and Bavandi, R. (2019). Cyanobacteria as an eco-friendly resource for biofuel production: a critical review. *Biotechnol. Prog.* 35, p.e2835. doi: 10.1002/btpr.2835

Forchhammer, K., and Koch, M. (2022). *Bacteria Produce Bioplastics: Resource-Saving and Very Environmentally Friendly*. Bioeconomy, BW. Available online at: https://www.biooekonomie-bw.de/en/articles/news/bacteria-produce-bioplastics-resource-saving-and-very-environmentally-friendly (accessed May 18, 2022).

Gadgil, B. S. T., Killi, N., and Rathna, G. V. (2017). Polyhydroxyalkanoates as biomaterials. *Med. Chem. Comm*. 8, 1774–1787. doi: 10.1039/C7MD00252A

Gadonneix, P., de Castro, F. B., de Medeiros, N. F., Drouin, R., Jain, C. P., Kim, Y. D., et al. (2010). *Biofuels: Policies, Standards and Technologies*. London: World Energy Council.

Gale, G. A., Schiavon Osorio, A. A., Mills, L. A., Wang, B., Lea-Smith, D. J., and McCormick, A. J. (2019). Emerging species and genome editing tools: future prospects in cyanobacterial synthetic biology. *Microorganisms* 7, 409. doi: 10.3390/microorganisms7100409

Gao, Z., Zhao, H., Li, Z., Tan, X., and Lu, X. (2012). Photosynthetic production of ethanol from carbon dioxide in genetically engineered cyanobacteria. *Energy. Environ. Sci*. 5, 9857–9865. doi: 10.1039/C2EE22675H

Giacovelli, U. N., and Environment: Technology for Environment (2018). *Single-Use Plastics: A Roadmap for Sustainability*. Available online at: https://stg-wedocs.unep.org/handle/20.500.11822/25496 (accessed May 5, 2021).

Gomes Gradíssimo, D., Pereira Xavier, L., and Valadares Santos, A. (2020). Cyanobacterial polyhydroxyalkanoates: a sustainable alternative in a circular economy. *Molecules* 25, 4331. doi: 10.3390/molecules25184331

Gouveia, L., and Oliveira, A. C. (2009). Microalgae as a raw material for biofuels production. *J. Ind. Microb. Biotechnol*. 36, 269–274. doi: 10.1007/s10295-008-0495-6

Gundolf, R., Oberleitner, S., and Richter, J. (2019). Evaluation of new genetic toolkits and their role for ethanol production in cyanobacteria. *Energies* 12, 3515. doi: 10.3390/en12183515

Gupta, J. K., Rai, P., Jain, K. K., and Srivastava, S. (2020). Overexpression of bicarbonate transporters in the marine cyanobacterium *Synechococcus* sp. PCC 7002 increases growth rate and glycogen accumulation. *Biotechnol. Biofuels*. 13, 1–12. doi: 10.1186/s13068-020-1656-8

Haase, S. M., Huchzermeyer, B., and Rath, T. (2012). PHB accumulation in *Nostoc muscorum* under different carbon stress situations. *J. Appl. Phycol.* 24, 157–162. doi: 10.1007/s10811-011-9663-6

Halfmann, C., Gu, L., Gibbons, W., and Zhou, R. (2014). Genetically engineering cyanobacteria to convert CO_2, water, and light into the long-chain hydrocarbon farnesene. *Appl. Microbiol. Biotechnol*. 98, 9869–9877. doi: 10.1007/s00253-014-6118-4

Halim, R., Harun, R., Webley, P. A., and Danquah, M. K. (2013). "Bioprocess engineering aspects of biodiesel and bioethanol production from microalgae," in *Advanced Biofuels and Bioproducts* (New York, NY: Springer), 601–628. doi: 10.1007/978-1-4614-3348-4_25

Hein, J., Paletta, A., and Steinbchel, S., Cloning. Characterization and comparison of the Pseudomonas mendocina polyhydroxyalkanoate synthases PhaC1 and PhaC2. (2002). Appl. *Microbiol. Biotechnol*. 58, 229–236. doi: 10.1007/s00253-001-0863-x

Hondo, S., Takahashi, M., Osanai, T., Matsuda, M., Hasunuma, T., Tazuke, A., et al. (2015). Genetic engineering and metabolite profiling for overproduction of polyhydroxybutyrate in cyanobacteria. *J. Biosci. Bioeng.* 120, 510–517. doi: 10.1016/j.jbiosc.2015.03.004

Hossain, M. F., Ratnayake, R. R., Mahbub, S., Kumara, K. W., and Magana-Arachchi, D. N. (2020). Identification and culturing of cyanobacteria isolated from freshwater bodies of Sri Lanka for biodiesel production. *Saudi J. Biol. Sci.* 27, 1514–1520. doi: 10.1016/j.sjbs.2020.03.024

Ienczak, J. L., Schmidell, W., and de Aragão, G. M. F. (2013). High-cell-density culture strategies for polyhydroxyalkanoate production: a review. *J. Ind. Microbiol. Biotechnol*. 40, 275–286. doi: 10.1007/s10295-013-1236-z

Iles, A., and Martin, A. N. (2013). Expanding bioplastics production: sustainable business innovation in the chemical industry. *J. Clean. Prod.* 45, 38–49. doi: 10.1016/j.jclepro.2012.05.008

Inganäs, O., and Sundström, V. (2016). Solar energy for electricity and fuels. *Ambio* 45, 15–23. doi: 10.1007/s13280-015-0729-6

International Energy Agency (2017). "Global shifts in the energy system," in *World Energy Outlook 2017*. Available online at: https://www.iea.org/weo2017/ (accessed April 15, 2022).

IPCC (2014). *Climate Change 2014: Synthesis Report. Contribution of Working Groups I, II and III to the Fifth Assessment Report of the Intergovernmental Panel on Climate Change [R.K. Pachauri and L.A. Meyer (eds.)]*. IPCC, Geneva, Switzerland, 151.

Jambeck, J. R., Geyer, R., Wilcox, C., Siegler, T. R., Perryman, M., and Andrady, A., et al. (2015). Plastic waste inputs from land into the ocean. *Science* 347, 768–771. doi: 10.1126/science.1260352

Jim, P. (2014). OECD policies for bioplastics in the context of a bioeconomy. *Ind. Biotechnol*. 10, 19–21. doi: 10.1089/ind.2013.1612

Johnson, T. J., Gibbons, J. L., Gu, L., Zhou, R., and Gibbons, W. R. (2016). Molecular genetic improvements of cyanobacteria to enhance the industrial potential of the microbe: a review. *Biotechnol. Prog.* 32, 1357–1371. doi: 10.1002/btpr.2358

Jorquera, O., Kiperstok, A., Sales, E. A., Embiruçu, M., and Ghirardi, M. L. (2010). Comparative energy life-cycle analyses of microalgal biomass production in open ponds and photobioreactors. *Bioresour Technol*. 101, 1406–1413. doi: 10.1016/j.biortech.2009.09.038

Kaewbai-Ngam, A., Incharoensakdi, A., and Monshupanee, T. (2016). Increased accumulation of polyhydroxybutyrate in divergent cyanobacteria under nutrient-deprived photoautotrophy: an efficient conversion of solar energy and carbon dioxide to polyhydroxybutyrate by *Calothrix scytonemicola* TISTR 8095. *Bioresour. Technol.* 212, 342–347. doi: 10.1016/j.biortech.2016.04.035

Kamravamanesh, D., Pflügl, S., Nischkauer, W., Limbeck, A., Lackner, M., and Herwig, C. (2017). Photosynthetic poly-β-hydroxybutyrate accumulation in unicellular cyanobacterium *Synechocystis* sp. PCC 6714. *AMB Express* 7, 1–12. doi: 10.1186/s13568-017-0443-9

Kaneko, T., and Tabata, S. (1997). Complete genome structure of the unicellular cyanobacterium *Synechocystis* sp. PCC6803. *Plant Cell Physiol.* 38, 1171–1176. doi: 10.1093/oxfordjournals.pcp.a029103

Karan, H., Funk, C., Grabert, M., Oey, M., and Hankamer, B. (2019). Green bioplastics as part of a circular bioeconomy. *Trends. Plant. Sci.* 24, 237–249. doi: 10.1016/j.tplants.2018.11.010

Katayama, N., Iijima, H., and Osanai, T. (2018). Production of bioplastic compounds by genetically manipulated and metabolic engineered cyanobacteria. *Adv. Exp. Med. Biol.*1080, 155–169. doi: 10.1007/978-981-13-0854-3_7

Kaygusuz, K. (2009). Bioenergy as a clean and sustainable fuel. *Energy Sources*. 31, 1069–1080. doi: 10.1080/15567030801909839

Khan, M. I., Shin, J. H., and Kim, J. D. (2018). The promising future of microalgae: current status, challenges, and optimization of a sustainable and renewable industry for biofuels, feed, and other products. *Microb. Cell Fact*. 17, 1–21. doi: 10.1186/s12934-018-0879-x

Khetkorn, W., Incharoensakdi, A., Lindblad, P., and Jantaro, S. (2016). Enhancement of poly-3-hydroxybutyrate production in *Synechocystis* sp. PCC 6803 by overexpression of its native biosynthetic genes. *Bioresour. Technol.* 214, 761–768. doi: 10.1016/j.biortech.2016.05.014

Khetkorn, W., Lindblad, P., and Incharoensakdi, A. (2012). Inactivation of uptake hydrogenase leads to enhanced and sustained hydrogen production with high

nitrogenase activity under high light exposure in the cyanobacterium *Anabaena siamensis* TISTR 8012. *J. Biol. Eng.* 6, 1–11. doi: 10.1186/1754-1611-6-19

Kiran, B., Kumar, R., and Deshmukh, D. (2014). Perspectives of microalgal biofuels as a renewable source of energy. *Energy. Convers. Manag.* 88, 1228–1244. doi: 10.1016/j.enconman.2014.06.022

Klanchui, A., Raethong, N., Prommeenate, P., Vongsangnak, W., and Meechai, A. (2016). Cyanobacterial biofuels: strategies and developments on network and modeling. *Netw. Biol.* 160, 75–102. doi: 10.1007/10_2016_42

Klinthong, W., Yang, Y. H., Huang, C. H., and Tan, C. S. (2015). A review: microalgae and their applications in CO_2 capture and renewable energy. *Aerosol Air Qual. Res.* 15, 712–742. doi: 10.4209/aaqr.2014.11.0299

Kobayashi, S., Atsumi, S., Ikebukuro, K., Sode, K., and Asano, R. (2022). Light-induced production of isobutanol and 3-methyl-1-butanol by metabolically engineered cyanobacteria. *Microbial. Cell Fact.* 21, 1–11. doi: 10.1186/s12934-021-01732-x

Koch, M., Bruckmoser, J., Scholl, J., Hauf, W., Rieger, B., and Forchhammer, K. (2020). Maximizing PHB content in *Synechocystis* sp. PCC 6803: a new metabolic engineering strategy based on the regulator PirC. *Microb. Cell Fact.* 19, 1–12. doi: 10.1186/s12934-020-01491-1

Koksharova, O., and Wolk, C. (2002). Genetic tools for cyanobacteria. *Appl. Microbiol. Biotechnol.* 58, 123–137. doi: 10.1007/s00253-001-0864-9

Koller, M. (2020). "Bioplastics from microalgae"—Polyhydroxyalkanoate production by cyanobacteria," in *Handbook of Microalgae-Based Processes and Products*, eds E. Jacob-Lopes, M. I. Queiroz, M. M. Maroneze, and L. Q. Zepka (Amsterdam: Academic Press), 597–645. doi: 10.1016/B978-0-12-818536-0.00022-1

Kopka, J., Schmidt, S., Dethloff, F., Pade, N., Berendt, S., Schottkowski, M., et al. (2017). Systems analysis of ethanol production in the genetically engineered cyanobacterium *Synechococcus* sp. PCC 7002. *Biotechnol. Biofuels* 10, 56. doi: 10.1186/s13068-017-0741-0

Kruse, O., Rupprecht, J., Bader, K. P., Thomas-Hall, S., Schenk, P. M., Finazzi, G., et al. (2005). Improved photobiological H_2 production in engineered green algal cells. *J. Biol. Chem.* 280, 34170–34177. doi: 10.1074/jbc.M503840200

Lackner, M. (2015). "Bioplastics-biobased plastics as renewable and/or biodegradable alternatives to petroplastics," in *Kirk-Othmer Encyclopedia of Chemical Technology, 6th Edn* (Wiley), 1–41. doi: 10.1002/0471238961.koe00006

Lakatos, G. E., Ranglová, K., Manoel, J. C., Grivalský, T., Kopecký, J., and Masojídek, J. (2019). Bioethanol production from microalgae polysaccharides. *Folia. Microbiol.* 64, 627–644. doi: 10.1007/s12223-019-00732-0

Lan, E. I., and Liao, J. C. (2012). ATP drives direct photosynthetic production of 1-butanol in cyanobacteria. *Proc. Natl. Acad. Sci. U. S. A.* 109, pp.6018–6023. doi: 10.1073/pnas.1200074109

Lane, C. E. (2015). *Bioplastic Production in Cyanobacteria and Consensus Degenerate PCR Probe Design* (LSU Doctoral Dissertations). 2777. Etd-11082015-141227.

Lane, C. E., and Benton, M. G. (2015). Detection of the enzymatically-active polyhydroxyalkanoate synthase subunit gene, phaC, in cyanobacteria via colony PCR. *Mol. Cell. Probes* 29, 454–460. doi: 10.1016/j.mcp.2015.07.001

Lasry Testa, R., Delpino, C., Estrada, V., and Diaz, S. M. (2019). In silico strategies to couple production of bioethanol with growth in cyanobacteria. *Biotechnol Bioeng.* 116, 2061–2073. doi: 10.1002/bit.26998

Lau, N. S., Foong, C. P., Kurihara, Y., Sudesh, K., and Matsui, M. (2014). RNA-Seq analysis provides insights for understanding photoautotrophic polyhydroxyalkanoate production in recombinant *Synechocystis* sp. *PLoS ONE* 9, e86368. doi: 10.1371/journal.pone.0086368

Lau, N. S., Matsui, M., and Abdullah, A. A. A. (2015). Cyanobacteria: photoautotrophic microbial factories for the sustainable synthesis of industrial products. *Biomed. Res. Int.* 2015, 754934. doi: 10.1155/2015/754934

Lee, S. Y., Hong, S. H., Park, S. J., van Wegen, R., and Middelberg, A. P. J. (2005). *Metabolic Flux Analysis on the Production of Poly(3-hydroxybutyrate) Biopolymers*. New York, NY: Wiley, 249–257.

Lewis, N. S., and Nocera, D. G. (2006). Powering the planet: chemical challenges in solar energy utilization. *Proc. Natl. Acad. Sci. U. S. A.* 103, 15729–15735. doi: 10.1073/pnas.0603395103

Li, W. C., Tse, H. F., and Fok, L. (2016). Plastic waste in the marine environment: a review of sources, occurrence and effects. *Sci. Total Environ.* 566-567, 333–349. doi: 10.1016/j.scitotenv.2016.05.084

Liang, F., Englund, E., Lindberg, P., and Lindblad, P. (2018). Engineered cyanobacteria with enhanced growth show increased ethanol production and higher biofuel to biomass ratio. *Metab. Eng.* 46, 51–59. doi: 10.1016/j.ymben.2018.02.006

Lim, S.-J., Jung, Y.-M., Shin, H. D., and Lee, Y.-H. (2002). Amplification of the NADPH-related genes zwf and gnd for the oddball biosynthesis of PHB in an *E. coli* transformant harboring a cloned phbCAB operon. *J. Biosci. Bioeng.* 93, 543–549. doi: 10.1016/S1389-1723(02)80235-3

Liu, X., Miao, R., Lindberg, P., and Lindblad, P. (2019). Modular engineering for efficient photosynthetic biosynthesis of 1-butanol from CO_2 in cyanobacteria. *Environ. Sci. Technol.* 12, 2765–2777. doi: 10.1039/C9EE01214A

Liu, X., Xie, H., Roussou, S., Miao, R., and Lindblad, P. (2021). "2 Engineering cyanobacteria for photosynthetic butanol production," in *Photosynthesis: Biotechnological Applications with Micro-Algae* (De Gruyter), 33–56. doi: 10.1515/9783110716979-002

Liu, Z., Wang, Y., He, N., Huang, J., Zhu, K., Shao, W., et al. (2011). Optimization of polyhydroxybutyrate (PHB) production by excess activated sludge and microbial community analysis. *J. Hazard. Mater.* 185, 8–16. doi: 10.1016/j.jhazmat.2010.08.003

Luan, G., and Lu, X. (2018). Tailoring cyanobacterial cell factory for improved industrial properties. *Biotechnol. Adv.* 36, 430–442. doi: 10.1016/j.biotechadv.2018.01.005

Luo, D., Hu, Z., Choi, D. G., Thomas, V. M., Realff, M. J., and Chance, R. R. (2010). Life cycle energy and greenhouse gas emissions for an ethanol production process based on blue-green algae. *Environ. Sci. Technol.* 44, 8670–8677. doi: 10.1021/es1007577

Machado, I. M., and Atsumi, S. (2012). Cyanobacterial biofuel production. *J. Biotechnol.* 162, 50–56. doi: 10.1016/j.jbiotec.2012.03.005

Madkour, M. H., Heinrich, D., Alghamdi, M. A., Shabbaj, I. I., and Steinbchel, A. (2013). PHA recovery from biomass. *Biomacromolecules* 14, 2963–2972. doi: 10.1021/bm4010244

Markou, G., and Nerantzis, E. (2013). Microalgae for high-value compounds and biofuels production: a review with focus on cultivation under stress conditions. *Biotechnol. Adv.* 31, 1532–1542. doi: 10.1016/j.biotechadv.2013.07.011

Masukawa, H., Mochimaru, M., and Sakurai, H. (2002). Disruption of the uptake hydrogenase gene, but not of the bidirectional hydrogenase gene, leads to enhanced photobiological hydrogen production by the nitrogen-fixing cyanobacterium *Anabaena* sp. PCC 7120. *Appl. Microbiol. Biotechnol.* 58, 618–624. doi: 10.1007/s00253-002-0934-7

Mata, T. M., Martins, A. A., and Caetano, N. S. (2010). Microalgae for biodiesel production and other applications: a review. *Renew. Sust. Energy Rev.* 14, 217–232. doi: 10.1016/j.rser.2009.07.020

McNeely, K., Xu, Y., Bennette, N., Bryant, D. A., and Dismukes, G. C. (2010). Redirecting reductant flux into hydrogen production via metabolic engineering of fermentative carbon metabolism in a cyanobacterium. *Appl. Environ. Microbiol.* 76, 5032–5038. doi: 10.1128/AEM.00862-10

Meixner, K., Kovalcik, A., Sykacek, E., Gruber-Brunhumer, M., Zeilinger, W., Markl, K., et al. (2018). Cyanobacteria Biorefinery—Production of poly (3-hydroxybutyrate) with *Synechocystis salina* and utilisation of residual biomass. *J Biotechnol.* 265, 46–53. doi: 10.1016/j.jbiotec.2017.10.020

Mejjad, N., Cherif, E. K., Rodero, A., Krawczyk, D. A., El Kharraz, J., and Moumen, A., et al. (2021). Disposal behaviour of used masks during the COVID-19 pandemic in the moroccan community: potential environmental impact. *Int. J. Environ. Res. Public Health* 18, 4382. doi: 10.3390/ijerph18084382

Mendhulkar, V. D., and Laukik, A. S. (2017). Synthesis of biodegradable polymer Polyhydroxyalkanoate (PHA) in Cyanobacteria *Synechococcus* elongates under mixotrophic nitrogen- and phosphate-mediated stress conditions. *Ind. Biotechnol.* 13, 85–93. doi: 10.1089/ind.2016.0021

Miao, R., Xie, H., Ho, F. M., and Lindblad, P. (2018). Protein engineering of α-ketoisovalerate decarboxylase for improved isobutanol production in *Synechocystis* PCC 6803. *Metab. Eng.* 47, 42–48. doi: 10.1016/j.ymben.2018.02.014

Misra, N., Panda, P. K., and Parida, B. K. (2013). Agrigenomics for microalgal biofuel production: an overview of various bioinformatics resources and recent studies to link OMICS to bioenergy and bioeconomy. *OMICS Int. J. Integr. Biol.* 17, 537–549. doi: 10.1089/omi.2013.0025

Miyake, M., Takase, K., Narato, M., Khatipov, E., Schnackenberg, J., Shirai, M., et al. (2000). "Polyhydroxybutyrate production from carbon

dioxide by cyanobacteria," in *Twenty-First Symposium on Biotechnology for Fuels and Chemicals* (Totowa, NJ: Humana Press), 991–1002. doi: 10.1007/978-1-4612-1392-5_78

Monshupanee, T., Nimdach, P., and Incharoensakdi, A. (2016). Two-stage (photoautotrophy and heterotrophy) cultivation enables efficient production of bioplastic poly-3-hydroxybutyrate in auto-sedimenting cyanobacterium. *Sci. Rep.* 6, 37121. doi: 10.1038/srep37121

Montiel-Jarillo, G., Carrera, J., and Suárez-Ojeda, M. E. (2017). Enrichment of a mixed microbial culture for polyhydroxyalkanoates production: Effect of pH and N and P concentrations. *Sci. Total Environ.* 583, 300–307. doi: 10.1016/j.scitotenv.2017.01.069

Mund, N. K., Liu, Y., and Chen, S. (2022). Advances in metabolic engineering of cyanobacteria for production of biofuels. *Fuel* 322, 124117. doi: 10.1016/j.fuel.2022.124117

Nagappan, S., Bhosale, R., Nguyen, D. D., Pugazhendhi, A., Tsai, P. C., Chang, S. W., et al. (2020). Nitrogen-fixing cyanobacteria as a potential resource for efficient biodiesel production. *Fuel* 279, 118440. doi: 10.1016/j.fuel.2020.118440

Noreen, A., Zia, K. M., Zuber, M., Ali, M., and Mujahid, M. (2016). A critical review of algal biomass: a versatile platform of bio-based polyesters from renewable resources. *Int. J. Biol. Macromol.* 86, 937–949. doi: 10.1016/j.ijbiomac.2016.01.067

Nozzi, N. E., Oliver, J. W., and Atsumi, S. (2013). Cyanobacteria as a platform for biofuel production. *Front. Bioeng. Biotechnol.* 1, 7. doi: 10.3389/fbioe.2013.00007

Oliver, J. W., and Atsumi, S. (2015). A carbon sink pathway increases carbon productivity in cyanobacteria. *Metab. Eng.* 29, 106–112. doi: 10.1016/j.ymben.2015.03.006

Oliver, J. W. K., Machado, I. M. P., Yoneda, H., and Atsumi, S. (2013). Cyanobacterial conversion of carbon dioxide to 2,3-butanediol. *Proc. Natl. Acad. Sci. U. S. A.* 110, 1249–1254. doi: 10.1073/pnas.1213024110

Oliver, N. J., Rabinovitch-Deere, C. A., Carroll, A. L., Nozzi, N. E., Case, A. E., and Atsumi, S. (2016). Cyanobacterial metabolic engineering for biofuel and chemical production. *Curr. Opin. Chem. Biol.* 35, 43–50. doi: 10.1016/j.cbpa.2016.08.023

Osanai, T., Numata, K., Oikawa, A., Kuwahara, A., Iijima, H., Doi, Y., et al. (2013). Increased bioplastic production with an RNA polymerase sigma factor SigE during nitrogen starvation in *Synechocystis* sp. PCC 6803. *DNA Res.* 20, 525–535. doi: 10.1093/dnares/dst028

Pachauri, R. K., Allen, M. R., Barros, V. R., Broome, J., Cramer, W., Christ, R., et al. (2014). *Climate change 2014: synthesis report. Contribution of Working Groups I, II and III to the fifth assessment report of the Intergovernmental Panel on Climate Change* (p. 151). IPCC.

Panda, B., Jain, P., Sharma, L., and Mallick, N. (2006). Optimization of cultural and nutritional conditions for accumulation of poly- -hydroxybutyrate in *Synechocystis* sp. PCC 6803. *Bioresour. Technol.* 97, 1296–1301. doi: 10.1016/j.biortech.2005.05.013

Panda, B., and Mallick, N. (2007). Enhanced poly-β-hydroxybutyrate accumulation in a unicellular cyanobacterium, *Synechocystis* sp. PCC 6803. *Lett. Appl. Microbiol.* 44, 194–198. doi: 10.1111/j.1472-765X.2006.02048.x

Pandian, S. R., Deepak, V., Kalishwaralal, K., Rameshkumar, N., Jeyaraj, M., and Gurunathan, S. (2010). Optimization and fed-batch production of PHB utilizing dairy waste and sea water as nutrient sources by *Bacillus megaterium* SRKP-3. *Bioresour. Technol.* 101, 705–711. doi: 10.1016/j.biortech.2009.08.040

Parmar, A., Singh, N. K., Pandey, A., Gnansounou, E., and Madamwar, D. (2011). Cyanobacteria and microalgae: a positive prospect for biofuels. *Bioresour. Technol.* 102, 10163–10172. doi: 10.1016/j.biortech.2011.08.030

Pereira, H., Barreira, L., Mozes, A., Florindo, C., Polo, C., Duarte, C. V., et al. (2011). Microplate-based high throughput screening procedure for the isolation of lipid-rich marine microalgae. *Biotechnol. Biofuels* 4, 1–12. doi: 10.1186/1754-6834-4-61

Philip, S., Keshavarz, T., and Roy, I. (2007). Polyhydroxyalkanoates: biodegradable polymers with a range of applications. *J. Chem. Technol. Biotechnol.* 82, 233–247. doi: 10.1002/jctb.1667

Pittman, J. K., Dean, A. P., and Osundeko, O. (2011). The potential of sustainable algal biofuel production using wastewater resources. *Bioresour. Technol.* 102, 17–25. doi: 10.1016/j.biortech.2010.06.035

Piven, I., Friedrich, A., Dühring, U., Uliczka, F., Baier, K., Inaba, M., et al. (2015). *Cyanobacterium sp. for production of compounds*. Patent EP2935566A4. United States.

Plastics—The Facts (2019). Available online at: https://issuu.com/plasticseuropeebook/docs/final_web_version_plastics_the_facts2019_14102019 (accessed June 24, 2020).

Pope, M. A., Hodge, J. A., and Nixon, P. J. (2020). An improved natural transformation protocol for the cyanobacterium *Synechocystis* sp. PCC 6803. *Front. Plant Sci.* 11, 372. doi: 10.3389/fpls.2020.00372

Posten, C., and Schaub, G. (2009). Microalgae and terrestrial biomass as source for fuels—a process view. *J. Biotechnol.* 142, 64–69. doi: 10.1016/j.jbiotec.2009.03.015

Priyadarshini, R., Palanisami, T., Pugazhendi, A., Gnanamani, A., and Parthiba Karthikeyan, O. (2022). Editorial: plastic to bioplastic (P2BP): a green technology for circular bioeconomy. *Front. Microbiol.* 13, 851045.doi: 10.3389/fmicb.2022.851045

Qi, F., Yao, L., Tan, X., and Lu, X. (2013). Construction, characterization and application of molecular tools for metabolic engineering of *Synechocystis* sp. *Biotechnol. Lett.* 10, 1655–1661. doi: 10.1007/s10529-013-1252-0

Quintana, N., Van der Kooy, F., Van de Rhee, M. D., Voshol, G. P., and Verpoorte, R. (2011). Renewable energy from Cyanobacteria: energy production optimization by metabolic pathway engineering. *Appl. Microbiol. Biotechnol.* 91, 471–490. doi: 10.1007/s00253-011-3394-0

Rani, G. U., and Sharma, S. (2021). "Biopolymers, bioplastics and biodegradability: an introduction," in *Book: Reference Module in Materials Science and Materials Engineering*. doi: 10.1016/B978-0-12-820352-1.00131-0

Raza, Z. A., Abid, S., and Banat, I. M. (2018). Polyhydroxyalkanoates: characteristics, production, recent developments and applications. *Int. Biodeterior. Biodegrad.* 126, 45–56. doi: 10.1016/j.ibiod.2017.10.001

Reddy, M. V., and Mohan, S. V. (2015). Polyhydroxyalkanoates production by newly isolated bacteria *Serratia ureilytica* using volatile fatty acids as substrate: bio-electro kinetic analysis. *J. Microb. Biochem. Technol.* 7, 26–32. doi: 10.4172/1948-5948.1000177

Reis, M. A. M., Serafim, L. S., Lemos, P. C., Ramos, A. M., Aguiar, F. R., and Van Loosdrecht, M. C. M. (2003). Production of polyhydroxyalkanoates by mixed microbial cultures. *Bioprocess. Biosyst. Eng.* 25, 377–385. doi: 10.1007/s00449-003-0322-4

Riedel, S. L., Brigham, C. J., Budde, C. F., Bader, J., Rha, C., Stahl, U., et al. (2013). Recovery of poly (3- hydroxybutyrate-co-3-hydroxyhexanoate) from *Ralstonia eutropha* cultures with non-halogenated solvents. *Biotechnol Bioeng.* 110, 461–470. doi: 10.1002/bit.24713

Rittmann, B. E. (2008). Opportunities for renewable bioenergy using microorganisms. *Biotechnol Bioeng.* 100, 203–212. doi: 10.1002/bit.21875

Rodionova, M. V., Poudyal, R. S., Tiwari, I., Voloshin, R. A., Zharmukhamedov, S. K., Nam, H. G., et al. (2017). Biofuel production: challenges and opportunities. *Int. J. Hydrog. Energy* 42, pp.8450–8461. doi: 10.1016/j.ijhydene.2016.11.125

Rosenboom, J. G., Langer, R., and Traverso, G. (2022). Bioplastics for a circular economy. *Nat. Rev. Mater.* 7, 117–137. doi: 10.1038/s41578-021-00407-8

Roussou, S., Albergati, A., Liang, F., and Lindblad, P. (2021). Engineered cyanobacteria with additional overexpression of selected Calvin-Benson-Bassham enzymes show further increased ethanol production. *Metab. Eng. Commun.* 12, e00161. doi: 10.1016/j.mec.2021.e00161

Ruffing, A. M. (2014). Improved free fatty acid production in cyanobacteria with *Synechococcus* sp. PCC 7002 as host. *Front. Bioen. Biotechnol.* 2, 17. doi: 10.3389/fbioe.2014.00017

Rutkowska, M., Heimowska, A., Krasowska, K., and Janik, H. (2002). Biodegradability of polyethylene starch blends in sea water. *Pol. J. Environ. Stud.* 11. 267–271.

Sadvakasova, A. K., Kossalbayev, B. D., Zayadan, B. K., Bolatkhan, K., Alwasel, S., Najafpour, M. M., et al. (2020). Bioprocesses of hydrogen production by cyanobacteria cells and possible ways to increase their productivity. *Renew. Sust. Energy Rev.* 133, 110054. doi: 10.1016/j.rser.2020.110054

Salehizadeh, H., and Van Loosdrecht, M. C. M. (2004). Production of polyhydroxyalkanoates by mixed culture: recent trends and biotechnological importance. *Biotechnol. Adv.* 22, 261–279. doi: 10.1016/j.biotechadv.2003.09.003

Samadhiya, K., Sangtani, R., Nogueira, R., and Bala, K. (2022). Insightful advancement and opportunities for microbial bioplastic production. *Front. Microbiol.* 12, 674864–674864. doi: 10.3389/fmicb.2021.674864

Samantaray, S., and Mallick, N. (2012). Production and characterization of poly-β-hydroxybutyrate (PHB) polymer from *Aulosira fertilissima*. *J. Appl. Phycol.* 24, 803–814. doi: 10.1007/s10811-011-9699-7

Samantaray, S., and Mallick, N. (2014). Production of poly (3-hydroxybutyrate-co-3-hydroxyvalerate) co-polymer by the diazotrophic cyanobacterium *Aulosira fertilissima* CCC 444. *J. Appl. Phycol.* 26, 237–245. doi: 10.1007/s10811-013-0073-9

Samorì, C., Basaglia, M., Casella, S., Favaro, L., Galletti, P., Giorgini, L., et al. (2015). Dimethyl carbonate and switchable anionic surfactants: two effective tools for the extraction of polyhydroxyalkanoates from microbial biomass. *Green Chem.* 17, 1047–1056. doi: 10.1039/C4GC01821D

Santos-Merino, M., Garcillán-Barcia, M. P., and de la Cruz, F. (2018). Engineering the fatty acid synthesis pathway in *Synechococcus elongatus* PCC 7942 improves omega-3 fatty acid production. *Biotechnol. Biofuels* 11, 1–13. doi: 10.1186/s13068-018-1243-4

Santos-Merino, M., Singh, A. K., and Ducat, D. C. (2019). New applications of synthetic biology tools for cyanobacterial metabolic engineering. *Front. Bioeng. Biotechnol.* 7, 33. doi: 10.3389/fbioe.2019.00033

Savakis, P., and Hellingwerf, K. J. (2015). Engineering cyanobacteria for direct biofuel production from CO_2. *Curr. Opin. Biotechnol.* 33, 8–14. doi: 10.1016/j.copbio.2014.09.007

Schenk, P. M., Thomas-Hall, S. R., Stephens, E., Marx, U., Mussgnug, J. H., Posten, C., et al. (2008). Second generation biofuels: high-efficiency microalgae for biodiesel production. *Bioenergy Res.* 1, 20–43. doi: 10.1007/s12155-008-9008-8

Schlebusch, M., and Forchhammer, K. (2010). Requirement of the nitrogen starvation-induced protein Sll0783 for polyhydroxybutyrate accumulation in *Synechocystis* sp. strain PCC 6803. *AEM* 76, 6101–6107. doi: 10.1128/AEM.00484-10

Sebesta, J., Xiong, W., Guarnieri, M. T., and Yu, J. (2022). Biocontainment of genetically engineered algae. *Front. Plant Sci.* 13, 839446. doi: 10.3389/fpls.2022.839446

Shabestary, K., Anfelt, J., Ljungqvist, E., Jahn, M., Yao, L., and Hudson, E. P. (2018). Targeted repression of essential genes to arrest growth and increase carbon partitioning and biofuel titers in cyanobacteria. *ACS Synth. Biol.* 7, 1669–1675. doi: 10.1021/acssynbio.8b00056

Sharma, L., Kumar Singh, A., Panda, B., and Mallick, N. (2007). Process optimization for poly-β- hydroxybutyrate production in a nitrogen fixing cyanobacterium, *Nostoc muscorum* using response surface methodology. *Bioresour. Technol.* 98, 987–993. doi: 10.1016/j.biortech.2006.04.016

Shen, C. R., Lan, E. I., Dekishima, Y., Baez, A., Cho, K. M., and Liao, J. C. (2011). Driving forces enable high-titer anaerobic 1-butanol synthesis in *Escherichia coli*. *Appl. Environ. Microbiol.* 77, 2905–2915. doi: 10.1128/AEM.03034-10

Shen, C. R., and Liao, J. C. (2008). Metabolic engineering of *Escherichia coli* for 1-butanol and 1-propanol production via the keto-acid pathways. *Metab. Eng.* 10, 312–320. doi: 10.1016/j.ymben.2008.08.001

Silva, A. L. P., Prata, J. C., Walker, T. R., Duarte, A. C., Ouyang, W., Barcelò, D., et al. (2020). Increased plastic pollution due to COVID-19 pandemic: challenges and recommendations. *Chem. Eng. J.* 405, 126683. doi: 10.1016/j.cej.2020.126683

Singh, A. K., and Mallick, N. (2017). Advances in cyanobacterial polyhydroxyalkanoates production. *FEMS Microbiol. Lett.* 364, fnx189. doi: 10.1093/femsle/fnx189

Singh, S. P., Pathak, J., and Sinha, R. P. (2017). Cyanobacterial factories for the production of green energy and value-added products: an integrated approach for economic viability. *Renew. Sust. Energy Rev.* 69, 578–595. doi: 10.1016/j.rser.2016.11.110

Sitther, V., Tabatabai, B., Fathabad, S. G., Gichuki, S., Chen, H., and Arumanayagam, A. C. S. (2020). Cyanobacteria as a biofuel source: advances and applications. *Adv. Cyanobacterial Biol.* 49, 269–289. doi: 10.1016/B978-0-12-819311-2.00018-8

Slocombe, S. P., and Benemann, J. R. (Eds.). (2017). *Microalgal Production for Biomass and High-Value Products*. Boca Raton, FL: CRC Press, 32. doi: 10.1201/b19464

Sreenikethanam, A., and Bajhaiya, A. (2021). *Algae Based Bio-Plastics: Future of Green Economy*, ed K. Biernat. London. doi: 10.5772/intechopen.100981

Srirangan, K., Pyne, M. E., and Chou, C. P. (2011). Biochemical and genetic engineering strategies to enhance hydrogen production in photosynthetic algae and cyanobacteria. *Bioresour. Technol.* 102, 8589–8604. doi: 10.1016/j.biortech.2011.03.087

Storz, H., and Vorlop, K.-D. (2013). Bio-based plastics: Status, challenges and trends. Landbauforsch. *Appl. Agric. Res.* 4, 321–332. doi: 10.3220/LBF_2013_321-332

Sudesh, K., Taguchi, K., and Doi, Y. (2002). Effect of increased PHA synthase activity on polyhydroxyalkanoates biosynthesis in *Synechocystis* sp. PCC6803. *Int. J. Biol. Macromol.* 30, 97–104. doi: 10.1016/S0141-8130(02)00010-7

Suzuki, E., Ohkawa, H., Moriya, K., Matsubara, T., Nagaike, Y., Iwasaki, I., et al. (2010). Carbohydrate metabolism in mutants of the cyanobacterium *Synechococcus elongatus* PCC 7942 defective in glycogen synthesis. *Appl. Environ. Microbiol.* 76, 3153–3159. doi: 10.1128/AEM.00397-08

Takahashi, H., Miyake, M., Tokiwa, Y., and Asada, Y. (1998). Improved accumulation of poly-3-hydroxybutyrate by a recombinant cyanobacterium. *Biotechnol Lett*. 20, 183–186. doi: 10.1023/A:1005392827791

Tan, G. Y. A., Chen, C. L., Ge, L., Li, L., Wang, L., Zhao, L., et al. (2014). Enhanced gas chromatography-mass spectrometry method for bacterial polyhydroxyalkanoates analysis. *J. Biosci. Bioeng.* 117, 379–382. doi: 10.1016/j.jbiosc.2013.08.020

Tao, Y., He, Y., Wu, Y., Liu, F., Li, X., Zong, W., et al. (2008). Characteristics of a new photosynthetic bacterial strain for hydrogen production and its application in wastewater treatment. *Int J Hydrogen Energ*. 33, 963–973. doi: 10.1016/j.ijhydene.2007.11.021

Toh, P. S., Jau, M. H., Yew, S. P., Abed, R. M., and Sudesh, K. (2008). Comparison of polyhydroxyalkanoates biosynthesis, obilization and the effects on cellular morphology in *Spirulina platensis* and *Synechocystis* sp. uniwg. *J Biosci.* 19, 21–38.

Tokiwa, Y., Calabia, B. P., Ugwu, C. U., and Aiba, S. (2009). Biodegradability of plastics. *Int. J. Mol. Sci.* 10, 3722–3742. doi: 10.3390/ijms10093722

Troschl, C., Meixner, K., Fritz, I., Leitner, K., Romero, A. P., Kovalcik, A., et al. (2018). Pilot-scale production of poly-hydroxybutyrate with the cyanobacterium *Synechocytis* sp. CCALA192 in a non-sterile tubular photobioreactor. *Algal Res.* 34, 116–125. doi: 10.1016/j.algal.2018.07.011

Varman, A. M., Xiao, Y., Pakrasi, H. B., and Tang, Y. J. (2013). Metabolic engineering of *Synechocystis* sp. strain PCC 6803 for isobutanol production. *Appl. Environ. Microbiol.* 79, 908–914. doi: 10.1128/AEM.02827-12

Wahlen, B. D., Willis, R. M., and Seefeldt, L. C. (2011). Biodiesel production by simultaneous extraction and conversion of total lipids from microalgae, cyanobacteria, and wild mixed-cultures. *Bioresour. Technol.* 102, 2724–2730. doi: 10.1016/j.biortech.2010.11.026

Wang, B., Pugh, S., Nielsen, D. R., Zhang, W., and Meldrum, D. R. (2013). Engineering cyanobacteria for photosynthetic production of 3-hydroxybutyrate directly from CO_2. *Metab. Eng.* 16, 68–77. doi: 10.1016/j.ymben.2013.01.001

Wang, B., Xiong, W., Yu, J., Maness, P. C., and Meldrum, D. R. (2018). Unlocking the photobiological conversion of CO_2 to (R)-3-hydroxybutyrate in cyanobacteria. *Green Chem.* 20, 3772–3782. doi: 10.1039/C8GC01208C

Wang, M., Luan, G., and Lu, X. (2020). Engineering ethanol production in a marine cyanobacterium *Synechococcus* sp. PCC7002 through simultaneously removing glycogen synthesis genes and introducing ethanolgenic cassettes. *J. Biotechnol.* 317, 1–4. doi: 10.1016/j.jbiotec.2020.04.002

Wen, Q., Chen, Z., Tian, T., and Chen, W. (2010). Effects of phosphorus and nitrogen limitation on PHA production in activated sludge. *J. Environ. Sci.* 22, 1602–1607. doi: 10.1016/S1001-0742(09)60295-3

Weyman, P. D. (2010). "Expression of oxygen-tolerant hydrogenases in Synechococcus elongatus," in *10th Cyanobacterial Molecular Biology Workshop* (Lake Arrowhead, CA).

Wichmann, J., Lauersen, K. J., Biondi, N., Christensen, M., Guerra, T., Hellgardt, K., et al. (2021). Engineering biocatalytic solar fuel production: the PHOTOFUEL consortium. *Trends Biotechnol.* 39, 323–327. doi: 10.1016/j.tibtech.2021.01.003

Wijffels, R. H., Kruse, O., and Hellingwerf, K. J. (2013). Potential of industrial biotechnology with cyanobacteria and eukaryotic microalgae. *Curr. Opin. Biotechnol.* 24, 405–413. doi: 10.1016/j.copbio.2013.04.004

Włodarczyk, A., Selão, T. T., Norling, B., and Nixon, P. J. (2020). Newly discovered *Synechococcus* sp. PCC 11901 is a robust cyanobacterial strain for high biomass production. *Commun Biol.* 3, 1–14. doi: 10.1038/s42003-020-0910-8

Wu, G. F., Shen, Z. Y., and Wu, Q. Y. (2002). Modification of carbon partitioning to enhance PHB production in *Synechocystis* sp. PCC6803. *Enzyme Microb. Technol.* 30, 710–715. doi: 10.1016/S0141-0229(02)00044-3

Xiong, W., Lee, T. C., Rommelfanger, S., Gjersing, E., Cano, M., Maness, P. C., et al. (2015). Phosphoketolase pathway contributes to carbon metabolism in cyanobacteria. *Nat. Plants* 2, 1–8. doi: 10.1038/nplants.2015.187

Yashavanth, P. R., Das, M., and Maiti, S. K. (2021). Recent progress and challenges in cyanobacterial autotrophic production of polyhydroxybutyrate (PHB), a bioplastic. *J. Environ. Chem. Eng.* 9, 105379. doi: 10.1016/j.jece.2021.105379

Yoshikawa, K., Aikawa, S., Kojima, Y., Toya, Y., Furusawa, C., Kondo, A., et al. (2015). Construction of a genome-scale metabolic model of *Arthrospira platensis* NIES-39 and metabolic design for cyanobacterial bioproduction. *PLoS ONE* 10, e0144430. doi: 10.1371/journal.pone.0144430

Yu, Y., You, L., Liu, D., Hollinshead, W., Tang, Y. J., and Zhang, F. (2013). Development of *Synechocystis* sp. PCC 6803 as a phototrophic cell factory. *Mar. Drugs* 11, 2894–2916. doi: 10.3390/md11082894

Yusuf, N. N. A. N., Kamarudin, S. K., and Yaakub, Z. (2011). Overview on the current trend in biodiesel production. *Energy. Convers. Manag.* 52, 2741–2751. doi: 10.1016/j.enconman.2010.12.004

Zettler, E. R., Mincer, T. J., and Amaral-Zettler, L. A. (2013). Life in the "Plastisphere": microbial communities on plastic marine debris. *Environ. Sci. Technol.* 47, 7137–7146. doi: 10.1021/es401288x

Zhang, S., Liu, Y., and Bryant, D. A. (2015). Metabolic engineering of *Synechococcus* sp. PCC 7002 to produce poly-3-hydroxybutyrate and poly-3-hydroxybutyrate-co-4-hydroxybutyrate. *Metab. Eng.* 32, 174–83. doi: 10.1016/j.ymben.2015.10.001

Conflict of Interest: The authors declare that the research was conducted in the absence of any commercial or financial relationships that could be construed as a potential conflict of interest.

Publisher's Note: All claims expressed in this article are solely those of the authors and do not necessarily represent those of their affiliated organizations, or those of the publisher, the editors and the reviewers. Any product that may be evaluated in this article, or claim that may be made by its manufacturer, is not guaranteed or endorsed by the publisher.

frontiers | Frontiers in Microbiology

REVIEW
published: 19 July 2022
doi: 10.3389/fmicb.2022.932459

Therapeutical and Nutraceutical Roles of Cyanobacterial Tetrapyrrole Chromophore: Recent Advances and Future Implications

*Kshetrimayum Birla Singh[1], Kaushalendra[2] and Jay Prakash Rajan[3]**

[1] Department of Life Science, Manipur University, Imphal, India, [2] Department of Zoology, Pachhunga University College, Mizoram University, Aizawl, India, [3] Department of Chemistry, Pachhunga University College, Mizoram University, Aizawl, India

Cyanobacteria have attracted the attention of researchers because of their promising role as primary and secondary metabolites in functional food and drug design. Due to an ever-increasing awareness of health and the use of natural products to avoid the onset of many chronic and lifestyle metabolic diseases, the global demand for the use of natural drugs and food additives has increased in the last few decades. There are several reports about the highly valuable cyanobacterial products such as carotenoids, vitamins, minerals, polysaccharides, and phycobiliproteins showing antioxidant, anti-cancerous, anti-inflammatory, hypoglycemic, and antimicrobial properties. Recently, it has been shown that allophycocyanin increases longevity and reduces the paralysis effect at least in *Caenorhabditis elegans*. Additionally, other pigments such as phycoerythrin and phycocyanin show antioxidative properties. Because of their high solubility in water and zero side effects, some of the cyanobacterial tetrapyrrole derivatives, i.e., pigments, facilitate an innovative and alternative way for the beverage and food industries in place of synthetic coloring agents at the commercial level. Thus, not only are the tetrapyrrole derivatives essential constituents for the synthesis of most of the basic physiological biomolecules, such as hemoglobin, chlorophyll, and cobalamin, but also have the potential to be used for the synthesis of synthetic compounds used in the pharmaceutical and nutraceutical industries. In the present review, we focused on the different aspects of tetrapyrrole rings in the drug design and food industries and addressed its remaining limitations to be used as natural nutrient supplements and therapeutic agents.

Keywords: tetrapyrrole, antioxidants, phycobiliprotein, phycocyanin, therapeutic agent

OPEN ACCESS

Edited by:
Vijay Pratap Singh,
University of Allahabad, India

Reviewed by:
Alok Singh,
University of Allahabad, India
Lalit Kumar Pandey,
Mahatma Jyotiba Phule Rohilkhand University, Bareilly, India

***Correspondence:**
Jay Prakash Rajan
rajanpuc@yahoo.com

Specialty section:
This article was submitted to Microbiotechnology, a section of the journal Frontiers in Microbiology

Received: *29 April 2022*
Accepted: *22 June 2022*
Published: *19 July 2022*

Citation:
Singh KB, Kaushalendra and Rajan JP (2022) Therapeutical and Nutraceutical Roles of Cyanobacterial Tetrapyrrole Chromophore: Recent Advances and Future Implications. Front. Microbiol. 13:932459. doi: 10.3389/fmicb.2022.932459

INTRODUCTION

Cyanobacteria are the earliest inhabitants of the earth and flourish in almost every habitat such as soil, rock, fresh water, and marine water, including some of the toughest environments such as hot springs. The secret behind their universal distribution in each and every corner of the globe lies in their ability to produce a wide range of bioactive compounds that evolved to protect them from various exogenous and endogenous environmental insults. Recently, with the advanced biotechnological route, humans have started to use the same cyanobacterial compounds in agriculture, pharmacology, and formulation of functional foods because of their ability to be

used as an alternative source of cytoprotective, nutritive, and therapeutic compounds that may be present at suboptimal levels in human body under certain pathological conditions (Fernández-Rojas et al., 2014a; Pagels et al., 2019). This is the reason why researchers have started to pay attention to extracting the novel bioactive components from cyanobacteria at a low cost and in an efficient way. It has been established already that most cyanobacterial compounds have tetrapyrrole rings in the heart of their supermolecular structure. Tetrapyrrole pigments are closely related to bilirubin molecules showing potent antioxidative and anti-proliferative properties when used as food supplements (Dillon et al., 1995; Konícková et al., 2014). There are several reports that most of the cyanobacterial species are laden with a higher quantity of essential amino acids, proteins, vitamins, flavonoids, unsaturated fatty acids, vitamins, and minerals as compared to traditional food such as milk, vegetables, fruits, soybean, egg, fish, and meat (Pervushkin et al., 2001; Khan et al., 2005; Jin et al., 2021). Therefore, due to their enriched nutritional value, the extraction of bioactive components from cyanobacteria has been proven as a boon for health. They serve as a sustainable source of raw material for drug development for the cure of various diseases and nutrient-related deficiencies (Ferris and Hirsch, 1991; Pyne et al., 2001; Soares et al., 2015). In recent years, researchers are focused on the biocompatibility of these compounds, especially with proteins in the nanosystem of host cells, to maintain human's cellular health along with the correction of lifestyle and dietary-related diseases.

One of the most important natural antioxidant compounds present in cyanobacteria is its pigment, a tetrapyrrole linear derivative, along with a rich source of vitamins and minerals; however, their primary biological role is to do photosynthesis, thus contributing to the production of a major amount of biomass in the ecosystem (Romay et al., 1998, 2003; Romay and Gonzalez, 2000; Remirez et al., 2002; Eriksen, 2008; Thangam et al., 2013; Zhang et al., 2022). Among the functional components identified in cyanobacteria, natural pigments such as chlorophylls, carotenoids, and phycobilins have received attention due to their linear tetrapyrrolic structure. The tetrapyrrolic derivatives have many potential applications in the cosmetics, pharmaceutical food, and textile industries. In fact, the derivatives of tetrapyrrole form a battery of novel bioactive compounds that may be used to improve the human health as they show the antibacterial, antiviral, antiarthritic, cytotoxic, and immunoregulative properties (Ou et al., 2010; Zheng et al., 2013; Young et al., 2016). The aim of the present review was to discuss the use of tetrapyrrole pigment of cyanobacterial origin for nutraceutical and therapeutical purposes.

TETRAPYRROLE PIGMENT IN THE NUTRACEUTICAL INDUSTRY

Due to the ever-increasing population throughout the entire globe, it has become a challenging task to help the population maintain a balanced nutritional state. Since agricultural production cannot be increased with the pace of the increasing population, researchers now have started to look toward alternative food sources to fulfill the global demand for healthier food products. They have started to focus on the cyanobacteria being a rich source of proteins, the most important food component for a balanced diet. One of the cyanobacterial species, i.e., *Spirulina*, has made its way to the dining table because of its high nutritional values. The other bioactive compounds present in *Spirulina* show antioxidative, antimicrobial, anti-cancer, antiviral, and anti-inflammatory activities (Hayashi et al., 1994; Bath and Madyastha, 2000; Carmichael et al., 2000; Hirata et al., 2000). There is scientific evidence that *Spirulina*'s is a novel food supplement and is well-recognized for preventing and managing certain diseases such as hypercholesterolemia and cancer. A number of cyanobacterial species host a wide range of secondary metabolites and natural pigments such as β carotene, scytonemin, phycoerythrin, phycocyanin, and phycobilisomes. These pigments have been proved as healthy bioactive constituents of cyanobacterial species and are being utilized by researchers' disease diagnostics, supplementary food, and herbal medicines (Sielaff et al., 2006; Tan, 2007; Gademann and Portmann, 2008; Ghosh et al., 2016). Phycocyanin extracted from *S. platensis* widely used as a cosmetic colorant and food additive. Recently, researchers have moved their focus to the use of cyanobacterial pigments such as phycobiliprotein as food supplements in the nutraceutical industry. The dried contents of *Arthrospira platensis* may play an important role in functional foods because of the bioactive compounds showing immunoregulative and antioxidative properties. *A. platensis* also suppresses the inflammation, viral infection, cancer progression, and maturity of cholesterol-related diseases (Jensen et al., 2001; Matsui et al., 2012).

ANTITUMOR EFFECT OF TETRAPYRROLE PIGMENT

Cancer is the worst result of harmful mutations in the nuclear and mitochondrial genes along with the foul games of free radicals in the cellular ecosystem, causing several unwelcomed molecular changes. Many of the cyanobacterial compounds are reported to check cancer and tumor progression. Natural compounds obtained from *Spirulina platensis* exhibit antiproliferative properties (Mysliwa-Kurdziel and Solymosi, 2017). The possible paths of this mechanism lie in the activity of tetrapyrrole compounds, such as phycobiliproteins and phycocyanin, being nucleophilic in nature and thus being able to prevent the cellular damage by neutralizing the excess reactive oxygen species. Thangam et al. (2013) investigated in detail the effectiveness of phycobiliprotein in the inhibition of colon cancer (HT-29) and lung cancer (A549). Gupta and Gupta (2012) suggested that phycobiliprotein may have suppressive effects on TPA-induced tumors on mice skin. Jiang et al. (2017) reported that phycocyanin is effective in checking the entry of HeLa cancerous cells into the G2 phase of the cell cycle. Recently, Liu et al. (2012) noted that phycocyanin promotes the release of cytochrome c (Cyt c), which in turn repair the damaged DNA and promote apoptosis in Hepal-6 cells. A cyanobacterial tetrapyrrole pigment also ameliorates the

cellular damage in normal cells done by chemotherapy and radiotherapy by reducing the oxidative stress and enhancing the antioxidative defense system.

NEPHROPROTECTIVE EFFECT OF TETRAPYRROLE PIGMENT

Kidney disease and failure occur under several pathophysiological conditions such as severe diabetes, pesticides, and heavy metal contamination (nephrotoxins) and due to sepsis syndrome, cardiorenal syndrome, and obstruction of the urinary tract. Renal diseases are diagnosed by the Renal Function Test in which abnormal serum creatinine level and urine output are the most important parameters. It is reported that oxidative load in such critical conditions acts synergistically enhancing nephrotoxicity. The nephroprotective effects of phycoerythrins and phycobiliproteins, which contain tetrapyrrole, play a key role in lowering oxidative stress and minimizing damage to renal cells. *Spirulina* and its extracted components have the potential to improve the glomerular functions in renal cells by maintaining the normal redox environment under oxidative stress conditions. Natural pigments from cyanobacteria are involved in the regulation of mitochondrial activity especially in renal cells *via* energy production and control the apoptosis progression. Experimental pieces of evidence suggest that oxidative load is one of the major causes of nephrotoxicity and renal dysfunction which can be determined by measurement of biomarkers by the level of malondialdehyde, glutathione, and activity of superoxide dismutase, and catalase. It is quite evident that *Spirulina* extract can diminish the level of malondialdehyde and glutathione while enhancing the biosynthesis and activity of superoxide dismutase and catalase in mesangial renal cells restoring the normal functions of the kidney. Phycocyanins from *Spirulina* are reported to modify the physicochemical forces such as oncotic and hydrostatic pressures which are suspected to influence the pressure along with the glomerular filter (Europa et al., 2010; Lim et al., 2012; Fernández-Rojas et al., 2014b; Liu et al., 2017; Mysliwa-Kurdziel and Solymosi, 2017). Phycocyanins from *Spirulina* also prevent the formation of oxalic acid which may form the calcium oxalate in renal calculi. Additionally, phycocyanins down-regulate the ROS production and lipid peroxidation in kidney cells (Riss et al., 2007; Zheng et al., 2013; Farooq et al., 2014).

HEPATOPROTECTIVE EFFECT OF TETRAPYRROLE PIGMENT

Liver diseases are caused by different etiological conditions such as viral infections, metabolic syndrome, alcohol and drug abuse, autoimmune diseases, and toxins, including pesticides, heavy metal contamination, and microplastics. The cyanobacterial extract is reported to have excellent hepatoprotective bioactive compounds that inhibit the kinases activity, a key protein of the cell cycle that cures the hyperproliferative disease without any chemical toxicity. Vadiraja et al. (1998) noted the pharmacological activities of phycocyanin and reported that it could neutralize the effect of ROS in liver cells. Cyanobacterial phycocyanin is also branded to control the synthesis and activity of many hepatic enzymes such as microsomal cytochrome P450, aminopyrine-N-demethylase, and glucose-6-phosphatase. Phycocyanin can suppress inflammation by blocking the hepatocyte growth factor (Vadiraja et al., 1998; Riss et al., 2007). Further, along with phycocyanin, phycocyanobilin also exhibits free radical scavenging activity (Bath and Madyastha, 2000; Ou et al., 2010).

CARDIO-PROTECTIVE EFFECT OF TETRAPYRROLE PIGMENT

Arterial thrombotic stress such as myocardial infarction and heart stroke is the foremost cause of cardiovascular diseases, ranking at the first position in the list of causes of human mortality worldwide. The platelet activity, particularly the aggregation and activation of platelets, significantly controls the debut of atherothrombotic disease. In traditional and modern medical practices, cyanobacterial extracts, particularly from *Spirulina*, are known to lower the serum cholesterol level as phycocyanin is involved in regulating the cholesterol absorption and the bile acid reabsorption process (Iwata et al., 1990; Shibata et al., 2001; Nagaoka et al., 2005; Radibratovic et al., 2016). Also, phycocyanin's constituent compounds, a class of covalently bonded open-chain tetrapyrrole derivatives, work as a pro-drug after its break down due to gastrointestinal enzymes and extend its therapeutic effects (Radibratovic et al., 2016). Tetrapyrrole pigments are well-established in preventing redox environmental disturbances, thus increasing the myocardial enzymatic activity. On the one hand, phycocyanin downregulates the signaling pathways, leading to inflammation by inhibiting the phospho-NFκB p65 enzyme while decreasing the synthesis of mRNAs of proinflammatory cytokines (Hao et al., 2018). On the other hand, the same pigment is also known to promote the heme oxygenase-1 molecular pathway enhancing the anti-inflammatory processes. It also diminishes the activity of caspase, thus minimizing the cell death but endorsing the synthesis of antioxidant enzymes (Gao et al., 2016; Kim et al., 2018).

ANTIDIABETIC EFFECT OF TETRAPYRROLE PIGMENT

Diabetes mellitus is a metabolic disorder in which lifelong hyperglycemia is manifested due to a decline in glycogen synthesis, leading to abnormal glucose levels in the blood. Prolonged hyperglycemia leads to other chronic diseases such as heart disease, kidney failure, and blindness. In 2010, Ou et al. showed that cyanobacterial pigments, especially phycocyanin, significantly enhance the muscular and hepatic glycogen synthesis, restoring the glucose homeostasis. Insulin secretion is directly related to the bio efficiency of α cells whose hormonal synthesis and secretion decrease significantly

under stress, hypertension, inflammation, obesity, and aging. deKoning et al. (2008) reported that phycocyanin can control the size of the endocrine portion of the pancreas, influencing insulin secretion significantly (Yu et al., 2013). Ghosh et al. (2016) found that glucose metabolism is influenced by oxidative stress, which in turn is dropped off by the free radical scavenging activity of cyanobacterial pigments. Further, extracted pigments from *Synechocystis*, *Lyngbya*, and *Microcoleus* species inhibit the α-glycosidase and α-amylase activities, leading to hypoglycemic conditions. Additionally, the α-amylase and α-glucosidase inhibitions also decline the occurrence of diarrhea and flatulence, both of which are linked to indigestion of food in the gastrointestine tract. Cyanobacterial pigments enhance the digestion *via* fermentation done by lactic acid bacteria. The crude as well as purified phycoerythrin and phycocyanin play a dual role as hypoglycemic and antioxidative activities and could be used as food additives in food industries.

CONCLUSION

The successful use of cyanobacteria in nutraceutical and pharmaceutical applications will depend on its novel tetrapyrrole-derived bioactive compounds which encompass antiallergic, anticarcinogenic, antibacterial, anticoagulant, antifungal, antihypertensive, anti-inflammatory, antinociceptive, antioxidant, antipyretic, cholesterol-lowering, hepatoprotective, and immune enhancement properties. Positive health effects have been related to the fact that the structure of phycocyanorubin and bilirubin resembles each other. In addition to their valuable role in medicinal and functional food, this group of natural pigments from cyanobacteria represents an attractive source of bioactive sustainable compounds. Tetrapyrrole-derived compounds in cyanobacteria have been used as a food additive in chewing gum, candies, food supplements, beverages such as soft drinks, and cosmetics products such as lipsticks and eyeliners. They also show therapeutic properties such as antitumor, nephroprotective, hepatoprotective, anti-diabetes, and antioxidant activities. These scientific studies announce that the consumption of edible cyanobacteria may be a safe alternative approach in the therapeutic and nutraceutical industries without any side effect.

AUTHOR CONTRIBUTIONS

JR wrote this article. Ka collected the research article. KS edited and corrected this article. All authors contributed to the article and approved the submitted version.

ACKNOWLEDGMENTS

We acknowledge partial funding from the Department of Biotechnology (DBT), New Delhi under their "DBT-BUILDER-Manipur University Interdisciplinary Life Science Programme for Advanced Research and Education" to carry out advanced research related to this study.

REFERENCES

Bath, V. B., and Madyastha, K. M. (2000). C-phycocyanin: a potent peroxyl radical scavenger *in vivo* and *in vitro*. *Biochem. Biophys. Res. Commun.* 275, 20–25. doi: 10.1006/bbrc.2000.3270

Carmichael, W. W., Drapeau, C., and Anderson, D. M. (2000). Harvesting of *Aphanizomenon* flos-aquae Ralfs ex Born & Flah. var. flos-aquae (*Cyanobacteria*) from Klamath Lake for human dietary use. *J. Appl. Phycol.* 12, 585–595. doi: 10.1023/A:1026506713560

deKoning, E. J., Bonner-Weir, S., and Rabelink, T. J. (2008). Preservation of beta-cell functions by targeting beta-cell mass. *Trends Pharmacol. Sci.* 29, 218–227. doi: 10.1016/j.tips.2008.02.001

Dillon, J. C., Phuc, A. P., and Dubacq, J. P. (1995). Nutritional value of the alga Spirulina. *World Rev. Nutr. Diet.* 77, 32–46. doi: 10.1159/000424464

Eriksen, N. T. (2008). Production of phycocyanin–a pigment with applications in biology, biotechnology, foods and medicine. *Appl. Microbiol. Biotechnol.* 80, 1–14. doi: 10.1007/s00253-008-1542-y

Europa, C. E., Butron, R. O., Gallardo-Casas, C. A., Blas-Valdivia, V., Pineda-Reynoso, M., Olvera-Ramírez, R., et al. (2010). Phycobiliproteins from Pseudanabaena tenuisrich in c-phycoerythrin protect against HgCl2-caused oxidative stress and cellular damage in the kidney. *J. Appl. Phycol.* 22, 495–501. doi: 10.1007/s10811-009-9484-z

Farooq, S. M., Boppana, N. B., Devarajan, A., Sekaran, S. D., and Shankar, E. M. (2014). C-phycocyanin confers protection against oxalate-mediated oxidative stress and mitochondrial dysfunctions in MDCK cells. *PLoS One* 9:e93056. doi: 10.1371/journal.pone.0093056

Fernández-Rojas, B., Medina-Campos, O. N., Hernández-Pando, R., Negrette-Guzmán, M., Huerta-Yepez, S., and Pedraza-Chaverri, J. (2014a). C-Phycocyanin prevents cisplatin-induced nephro-toxicity through inhibition of oxidative stress. *Food Funct.* 5, 480–490. doi: 10.1039/c3fo60501a

Fernández-Rojas, B., Hernández-Juárez, J., and Pedraza-Chaverri, J. (2014b). Nutraceutical properties of Phycocyanin. *J. Funct. Foods* 11, 375–392. doi: 10.1016/j.jff.2014.10.011

Ferris, M. J., and Hirsch, C. F. (1991). Method for isolation and purification of *Cyanobacteria*. *Appl. Environ. Microbiol.* 57, 1448–1452. doi: 10.1128/aem.57.5

Gademann, K., and Portmann, C. (2008). Secondary metabolites from *Cyanobacteria*: complex structure and powerful bioactivities. *Curr. Org. Chem.* 12, 326–330. doi: 10.2174/13852720878374 3750

Gao, Y., Liu, C., Wan, G., Wang, X., Cheng, X., and Ou, Y. (2016). Phycocyanin prevents methylglyoxal-induced mitochondrial-dependent apoptosis in INS-1 cells by Nrf2. *Food Funct.* 7, 1129–1137. doi: 10.1039/c5fo01548k

Ghosh, T., Bhayani, K., Paliwal, C., Maurya, R., Chokshi, K., Pancha, I., et al. (2016). *Cyanobacterial* pigments as natural anti-hyperglycemic agents: an *in vitro* study. *Front. Marine Sci.* 3, 146. doi: 10.3389/fmars.2016.00 146

Gupta, N. K., and Gupta, K. P. (2012). Effects of C-Phycocyanin on the representative genes of tumor development in mouse skin exposed to 12-O-tetradecanoyl-phorbol-13-acetate. *Environ. Toxicol. Pharmacol.* 34, 941–948. doi: 10.1016/j.etap.2012.08.001

Hao, S., Yan, Y., Huang, W., Gai, F., Wang, J., Liu, L., et al. (2018). C-Phycocyanin reduces inflammation by inhibiting NF-κB activity through down regulating PDCD5 in lipopolysaccharide-induced RAW 264.7 macrophages. *J. Funct. Foods* 42, 21–29.

Hayashi, O., Katoh, T., and Okuwaki, Y. (1994). Enhancement of anti-body production in mice by dietary *Spirulina platensis*. *J. Nutr. Sci. Vitaminol.* 40, 431–441. doi: 10.3177/jnsv.40.431

Hirata, T., Tanaka, M., Ooike, M., Tsunomura, T., and Sakaguchi, M. (2000). Antioxidant activities of phycocyanobilin prepared from *Spirulina platensis*. *J. Appl. Phycol.* 12, 435–439.

Iwata, K., Inayama, T., and Kato, T. (1990). Effects of *Spirulina platensis* on plasma lipoprotein lipase activity in fructose-induced hyperlipidemic rats. *J. Nutr. Sci. Vitaminol.* 36, 165–171. doi: 10.3177/jnsv.36.165

Jensen, G. S., Ginsberg, D. I., and Drapeau, C. (2001). Blue-green algae as an immuno-enhancer and biomodulator. *J. Am. Nutraceut. Ass.* 3, 24–30. doi: 10.3389/fenvs.2018.00007

Jiang, L., Wang, Y., Yin, Q., Liu, G., Liu, H., Huang, Y., et al. (2017). Phycocyanin: a Potential Drug for Cancer Treatment. *J. Cancer* 8, 3416–3429. doi: 10.7150/jca.21058

Jin, H., Wang, Y., Zhao, P., Wang, L., Zhang, S., Meng, D., et al. (2021). Potential of producing flavonoids using *Cyanobacteria* as a sustainable chassis. *J. Agric. Food Chem.* 69, 12385–12401. doi: 10.1021/acs.jafc.1c04632

Khan, Z., Bhadouria, P., and Bisen, P. (2005). Nutritional and therapeutic potential of spirulina, Curr. Pharm. *Biotechnology* 6, 373–379.

Kim, K. M., Lee, J. Y., Im, A.-R., and Chae, S. (2018). Phycocyanin protects against UVB-induced apoptosis through the PKC α/βII-Nrf-2/HO-1 dependent pathway in human primary skin cells. *Molecules* 23:478. doi: 10.3390/molecules23020478

Konícková, R., Vanková, K., Vaníková, J., Vánová, J., Muchová, L., Subhanová, I., et al. (2014). Anti-cancer effects of blue-green alga *Spirulina platensis*, a natural source of bilirubin-like tetrapyrrolic compounds, Annals of Hept. *Ann. Hepatol.* 13, 273–283.

Lim, B. J., Jeong, J. Y., Chang, Y. K., Na, K. R., Lee, K. W., Shin, Y. T., et al. (2012). C-phycocyanin attenuates cisplatin-induced nephrotoxicity in mice. *Ren. Fail.* 34, 892–900. doi: 10.3109/0886022X.2012.690925

Liu, C., Fu, Y., Li, C. E., Chen, T., and Li, X. (2017). Phycocyanin-functionalized selenium nanoparticles reverse palmitic acid-induced pancreatic b-cell apoptosis by enhancing cellular uptake and blocking reactive oxygen species (ROS)-mediated mitochondria dysfunction. *J. Agri. Food Chem.* 65, 4405–4413. doi: 10.1021/acs.jafc.7b00896

Liu, S. F., Wang, T. Y., and Gao, Y. (2012). Effects of phycocyanin on Hepa1-6 cells and immune function of mice bearing tumor. *Chin. J. Public Health* 3, 342–349.

Matsui, K., Nazifi, E., Hirai, Y., Wada, N., Matsugo, S., and Sakamoto, T. (2012). The *Cyanobacterial* UV-absorbing pigment scytonemin displays radical-scavenging activity. *J. Gen. Appl. Microbiol.* 58, 137–144. doi: 10.2323/jgam.58.137

Mysliwa-Kurdziel, B., and Solymosi, K. (2017). Phycobilins and phycobiliproteins used in food industry and medicine. *Mini. Rev. Med. Chem.* 17, 1173–1193. doi: 10.2174/1389557516666160912180155

Nagaoka, S., Shimizu, K., Kaneko, H., Shibayama, F., Morikawa, K., Kanamura, Y., et al. (2005). Novel protein C-phycocyanin plays a crucial role in the hypocholesterolomic action of *Spirulina platenis* concentrate in rats. *J. Nutr.* 135, 2425–2430. doi: 10.1093/jn/135.10.2425

Ou, Y., Zheng, S., Lin, L., Jiang, Q., and Yang, X. (2010). Protective effect of C-phycocyanin against carbon tetrachloride-induced hepatocyte damage *in vitro* and *in vivo*. *Chem. Bio. Interact.* 185, 94–100. doi: 10.1016/j.cbi.2010.03.013

Pagels, F., Guedes, A. C., Amaro, H. M., Kijjoa, A., and Vasconcelos, V. (2019). Phycobiliproteins from *Cyanobacteria*: chemistry and Biotechnological Applications. *Biotechnol. Adv.* 37, 422–443. doi: 10.1016/j.biotechadv.2019.02.010

Pervushkin, S. V., Voronin, A. V., Kurkin, V. A., Sokhina, A. A., and Shatalaev, I. F. (2001). Proteins from *Spirulina platensis* biomass. *Chem. Nat. Comp.* 37, 476–480.

Pyne, P. K., Bhattacharjee, and Srivastav, P. (2001). Microalgae (*Spirulina platensis*) and its bioactive molecules: review. *Indian J. Nutr.* 4, 160–165.

Radibratovic, M., Minic, S., Stanic-Vucinic, D., Nikolic, M., Milcic, M., and Cirkovic Velickovic, T. (2016). Stabilization of human serum albumin by the binding of phycocyanobilin, a bioactive chromophore of blue-green alga Spirulina: molecular dynamics and experimental study. *PLoS One* 11:e0167973. doi: 10.1371/journal.pone.0167973

Remirez, D., Ledón, N., and González, R. (2002). Role of histamine in the inhibitory effects of phycocyanin in experimental models of allergic inflammatory response. *Mediators Inflamm.* 11, 81–85. doi: 10.1080/09629350220131926

Riss, J., Décordé, K., Sutra, T., Delage, M., Baccou, J. C., Jouy, N., et al. (2007). Phycobiliprotein C-phycocyanin from *Spirulina platensisis* powerfully responsible for reducing oxidative stress and NADPH oxidase expression induced by an atherogenic diet in hamsters. *J. Agri. Food Chem.* 55, 7962–7967. doi: 10.1021/jf070529g

Romay, C., Armesto, J., Remirez, D., Gonzalez, R., Ledon, L., and Garcia, I. (1998). Antioxidant and anti-inflammatory properties of C-phycocyanin from blue-green algae. *Inflamm. Res.* 47, 36–41. doi: 10.1007/s000110050256

Romay, C., and Gonzalez, R. (2000). Phycocyanin is an antioxidant protector of human erythrocytes against lysis by peroxyl radicals. *J. Pharm. Pharmacol.* 52, 367–368. doi: 10.1211/0022357001774093

Romay, C. H., González, R., Ledón, N., Remirez, D., and Rimbau, V. (2003). C-phycocyanin: a biliprotein with antioxidant, anti-inflammatory and neuroprotective effects. *Curr. Protein Pept. Sci.* 4, 207–216. doi: 10.2174/1389203033487216

Shibata, S., Oda, K., Onodera-Masuoka, N., Matsubara, S., Kikuchi Hayakawa, H., Ishikawa, F., et al. (2001). Hypocholesterolemic effect of indigestible fraction of Chlorella regularis in cholesterol-fed rats. *J. Nutr. Sci. Vitaminol.* 47, 373–377. doi: 10.3177/jnsv.47.373

Sielaff, H., Christiansen, G., and Schwecke, T. (2006). Natural products from *Cyano-bacteria*: exploiting a new source for drug discovery. *IDrugs* 9, 119–127.

Soares, A. R., Engene, N., Gunasekera, S. P., Sneed, J. M., and Paul, V. J. (2015). Carriebowlinol, an antimicrobial tetrahydroquinolinol from an assemblage of marine *Cyanobacteria* containing a novel taxon. *J. Nat. Prod.* 78, 534—-538. doi: 10.1021/np500598x

Tan, L. T. (2007). Bioactive natural products from marine *Cyanobacteria* for drug discovery. *Phytochemistry* 68, 954–979. doi: 10.1016/j.phytochem.2007.01.012

Thangam, R., Suresh, V., Asenath, P. W., Rajkumar, M., Senthilkumar, N., Gunasekaran, P., et al. (2013). C-Phycocyanin from Oscillatoria tenuis exhibited an antioxidant and *in vitro* antiproliferative activity through induction of apoptosis and G0/G1 cell cycle arrest. *Food Chem.* 140, 262–272. doi: 10.1016/j.foodchem.2013.02.060

Vadiraja, B. B., Gaikwad, N. W., and Madyastha, K. M. (1998). Hepatoprotective effect of C-phycocyanin: protection for carbon tetrachloride and R-(+)-pulegone-mediated hepatotoxicty in rats. *Bioch. Biophy. Res. Commun.* 249, 428–431. doi: 10.1006/bbrc.1998.9149

Young, I., Chuang, S., Hsu, C., Sun, Y., and Lin, F. (2016). C-phycocyanin alleviates osteoarthritic injury in chondrocytes stimulated with H2O2 and compressive stress. *Int. J. Biol. Macromol.* 93, 852–859. doi: 10.1016/j.ijbiomac.2016.09.051

Yu, O., Lin, L., Xuegan, Y., Qin, P., and Xiaodong, C. (2013). Antidiabetic potential of phycocyanin: effects on KKAy mice. *Pharmac. Biol.* 51, 539–544. doi: 10.3109/13880209.2012.747545

Zhang, L., Kong, D., Huang, J., Wang, Q., and Shao, L. (2022). The therapeutic effect and the possible mechanism of C-phycocyanin in lipopolysaccharide and seawater-induced acute lung injury. *Drug Des. Devel. Ther.* 6, 1025–1040. doi: 10.2147/DDDT.S347772

Zheng, J., Inoguchi, T., Sasaki, S., Maeda, Y., McCarty, M. F., Fujii, M., et al. (2013). Phycocyanin and phycocyanobilin from *Spirulina platensis* protect against diabetic nephropathy by inhibiting oxidative stress. *Am. J. Physiol. Regul. Integr. Comp. Physiol.* 304, 110–120. doi: 10.1152/ajpregu.00648.2011

Conflict of Interest: The authors declare that the research was conducted in the absence of any commercial or financial relationships that could be construed as a potential conflict of interest.

frontiers | Frontiers in Microbiology

TYPE Original Research
PUBLISHED 13 October 2022
DOI 10.3389/fmicb.2022.1038136

OPEN ACCESS

EDITED BY
Prashant Kumar Singh,
Mizoram University,
India

REVIEWED BY
Gulab Chand Arya,
Agricultural Research Organization (ARO),
Israel
Avinash Singh,
New York University, United States
Deepanker Yadav,
Guru Ghasidas Vishwavidyalaya,
India

*CORRESPONDENCE
Sijun Huang
huangsijun@scsio.ac.cn

SPECIALTY SECTION
This article was submitted to Microbial Physiology and Metabolism, a section of the journal Frontiers in Microbiology

RECEIVED 06 September 2022
ACCEPTED 27 September 2022
PUBLISHED 13 October 2022

CITATION
He X, Liu H, Long L, Dong J and Huang S (2022) Acclimation and stress response of *Prochlorococcus* to low salinity.
Front. Microbiol. 13:1038136.
doi: 10.3389/fmicb.2022.1038136

Acclimation and stress response of *Prochlorococcus* to low salinity

Xiayu He[1,2], Huan Liu[1,2], Lijuan Long[1,3], Junde Dong[1,3] and Sijun Huang[1,3]*

[1]Key Laboratory of Tropical Marine Bio-resources and Ecology, South China Sea Institute of Oceanology, Chinese Academy of Sciences, Guangzhou, China, [2]College of Earth and Planetary Sciences, University of Chinese Academy of Sciences, Huairou, Beijing, China, [3]Southern Marine Science and Engineering Guangdong Laboratory (Guangzhou), Guangzhou, China

Prochlorococcus is an obligate marine microorganism and the dominant autotroph in tropical and subtropical open ocean. However, the salinity range for growing and response to low salinity exposure of *Prochlorococcus* are still unknown. In this study, we found that low-light adapted *Prochlorococcus* stain NATL1A and high-light adapted strain MED4 could be acclimated in the lowest salinity of 25 and 28psu, respectively. Analysis of the effective quantum yield of PSII photochemistry (F_v/F_m) indicated that both strains were stressed when growing in salinity lower than 34psu. We then compared the global transcriptome of low salinity (28psu) acclimated cells and cells growing in normal seawater salinity (34psu). The transcriptomic responses of NATL1A and MED4 were approximately different, with more differentially expressed genes in NATL1A (525 genes) than in MED4 (277 genes). To cope with low salinity, NATL1A down-regulated the transcript of genes involved in translation, ribosomal structure and biogenesis and ATP-production, and up-regulated photosynthesis-related genes, while MED4 regulated these genes in an opposite way. In addition, both strains up-regulated an iron ABC transporter gene, *idiA*, suggesting low salinity acclimated cells could be iron limited. This study demonstrated the growing salinity range of *Prochlorococcus* cells and their global gene expression changes due to low salinity stress.

KEYWORDS

***Prochlorococcus*, transcriptome, low salinity acclimation, low salinity stress, RNAseq**

Introduction

Cyanobacterium *Prochlorococcus* is the smallest and most abundant photosynthetic, oxygen-evolving organism on Earth, playing a significant role in carbon fixation and biogeochemical cycles in the ocean (Guillard et al., 1985; Goericke and Welschmeyer, 1993; Liu et al., 1997). The prokaryotic *Prochlorococcus* cells contain divinyl-chlorophyll a and both monovinyl and divinyl-chlorophyll b as their primary photosynthetic pigments, which are unique to other cyanobacteria that contain chlorophyll a and phycobiliprotein

(Chisholm et al., 1992; Hess et al., 1996). *Prochlorococcus* is believed to be an obligate marine organism that is predominantly found in oligotrophic open oceans, as well as in some coastal waters, but barely seen in low salinity estuarine waters (Flombaum et al., 2013). *Prochlorococcus* thrives throughout the euphotic zone in the tropical and subtropical oceans from 45° N to 40° S (Scanlan et al., 2009). This genus of marine picocyanobacteria is divided into high-light (HL) adapted and low-light (LL) adapted ecotypes, which are also phylogenetically distinct (Ferris and Palenik, 1998; Moore and Chisholm, 1999). HL ecotypes are usually distributed in upper euphotic zone, while LL ecotypes are generally distributed in the lower to bottom euphotic zone (Johnson et al., 2006; Zinser et al., 2007). Besides the light-related niche partitioning of HL and LL ecotypes, two HL ecotypes, HLI and HLII, also display temperature-related niche partitioning that HLII ecotypes dominate the warmer oceans between 30° N and 30° S while HLI ecotypes dominate the higher latitude oceans (West et al., 2001; Rocap et al., 2003; Mühling, 2012; Voigt et al., 2014). Despite comprising diverse phylogenetic lineages, *Prochlorococcus* is monophyletic on the phylogenetic tree built on 16S rRNA sequences of cyanobacteria (Rocap et al., 2002). *Synechococcus* is the sister genus of *Prochlorococcus*. However, *Synechococcus* is a provisional genus containing polyphyletic clusters which are scattering on the phylogenetic tree of cyanobacteria (Robertson et al., 2001). Marine *Synechococcus* is affiliated with cluster 5, which comprises subclusters 5.1, 5.2 and 5.3. In contrast to *Prochlorococcus*, marine *Synechococcus* is much more widely distributed, existing from estuary to open ocean and from equatorial to polar regions (Partensky et al., 1999; Zwirglmaier et al., 2008).

Salinity is a crucial factor affecting the growth and biogeography of cyanobacteria (Scanlan et al., 2009). There were plenty of studies on cyanobacteria's salt acclimation and salt stress response (Hagemann, 2011). However, most of those studies were conducted mainly on freshwater cyanobacteria such as the euryhaline *Synechococcus* strain PCC 7002 and moderately halotolerant *Synechocystis* strain PCC 6803 rather than typical marine cyanobacteria such as *Prochlorococcus* or marine *Synechococcus* (Hagemann, 2011). For example, when growing at high salinity, *Synechococcus* PCC 7002 had increased expression of genes involved in compatible solute biosynthesis and electron transport, while only minor changes were observed when cells were grown at low salinity (Ludwig and Bryant, 2012). It also has been revealed that 200–300 genes were up-regulated and a comparable number of genes were down-regulated after the addition of salt in *Synechocystis* PCC 6803 (Kanesaki et al., 2002; Marin et al., 2003). Secondly, very few studies focus on the acclimation and stress response of marine cyanobacteria to low salinity. Lastly, compared to *Synechococcus*, salinity-related physiological studies on *Prochlorococcus* are even more seldom. A recent study showed that *Prochlorococcus* strain AS9601 could be acclimated to a high salt concentration of 5% (w/v; Al-Hosani et al., 2015). The authors compared the growth rate and transcriptome of AS9601 at salinities 3.8% (w/v) and 5% (w/v), and found that, under high salt concentration, approximately one-third of the genome expressed differentially.

The strict biogeographic distribution of *Prochlorococcus* in oceanic waters suggests that this organism cannot be adapted to low salinity. However, what is the lowest salinity that *Prochlorococcus* can survive and what is the stress response of *Prochlorococcus* cells to low salinity are still unclear. In this study we first tested the salinity range of two *Prochlorococcus* strains, NATL1A and MED4, and then acclimatized the two strains under different salinities. We found that the lowest acclimation salinity is 25 psu for MED4 and 28 psu for NATL1A. Both NATL1A and MED4 cells were stressed when growing in salinities lower than 34 psu. We also found that the transcriptomic response of the two strains to low salinity stress were highly different.

Materials and methods

Strains and growth conditions

Prochlorococcus strains MED4 and NATL1A were obtained from Jiao Nianzhi Lab, Xiamen University. Cultures were maintained in Pro99 natural seawater medium with a salinity of 34 psu, at 21°C and under a constant light intensity of 10 μE m^{-2} s^{-1}. We used canted neck polystyrene flasks (Corning Inc., Corning, NY, United States) of different volumes to culture the *Prochlorococcus* strains.

Experiment setup and growth rate calculation

Preparation of Pro99 medium followed the protocol from the Chisholm Laboratory.[1] The seawater from the South China Sea basin was filtered through 0.22 μm polycarbonate membrane, and the salinity was pre-adjusted to 22 psu ~ 60 psu with a 2 psu interval using ddH_2O or NaCl. Salinity was measured using an ATAGO PAL-06S refractometer (ATAGO, Japan). These seawaters were autoclaved at 121°C for 15 min. Macronutrient (NH_4Cl and NaH_2PO_4) stocks and the trace metal stock were prepared in advance, and they were added into the above seawater base. *Prochlorococcus* cultures growing in the Pro99 medium of salinity 34 psu were inoculated into the salinity gradient mediums. The salinity was finally adjusted to 22 psu ~ 60 psu using the ddH_2O with Pro99 nutrients. *Prochlorococcus* growth was monitored every day for 2 weeks by measuring the OD440 absorbance using a multimode plate reader (PerkinElmer, Waltham, MA, United States) and measuring the cell abundance using a flow cytometer (BD Accuri C6, BD Biosciences, CA, United States). Three biological replicates were set up for the experiment. Growth rate was calculated based on the two monitoring methods,

1 https://chisholmlab.mit.edu

respectively. Growth rate was calculated according to Mackey et al. (2013): $T_d = \mathrm{Ln}\,(N_{i+1}/N_i)$, N_{i+1} is the number of cells on day i + 1, N_i is the number of cells on day i, T_d is the growth rate of cells. The average growth rate of cells was calculated during the logarithmic phase.

Low salinity acclimation

Prochlorococcus strains MED4 and NATL1A were acclimated to different salinities (24 psu, 25 psu, 26 psu, 27 psu, 28 psu, 30 psu, 32 psu, 34 psu) by consecutive transfers from exponential growing cultures to fresh media. Three biological replicates were set up for each salinity. Five rounds of transfer were conducted for each strain. Using flow cytometry, cell abundance was monitored at day 0, day 5 and day 10. To assess the stress to low salinity, each strain's dark-adapted photochemical efficiency (F_v/F_m) was monitored on day 10 in each round, using a handheld fluorometer (AquaPen AP 110/C, Photon Systems Instruments). To measure F_v/F_m, 1 ml culture was dark-adapted in the sample cuvette for 15–30 min. The maximal fluorescence levels (F_m) were measured in the dark and under bright purple light (455 nm, 100 $\mu Em^{-2}\,s^{-1}$), where F_0 is the basal fluorescence level and F_v is the variable fluorescence. The PSII quantum yield was calculated as $F_v/F_m = (F_m - F_0)/F_m$.

RNAseq analysis

To acclimate the *Prochlorococcus* strains, MED4 and NATL1A were growing in the Pro99 medium of salinity 28 psu and 34 psu for five rounds of inoculation. Then the acclimated cultures were inoculated in fresh medium of salinity 28 psu and 34 psu, with salinity 34 psu being the control. Three biological replicates were set up. During the exponential growth phase, 100 ml cultures were filtered onto 0.22 μm polycarbonate membrane to collect cells and the membranes were immediately flash frozen in RNAlater by liquid nitrogen and stored at −80°C until RNA extraction. Total RNA was extracted from the membrane using the MagZol Reagent (Magen Biotech, Guangzhou, China). Sequencing libraries were prepared using VAHTS™ Stranded mRNA-seq Library Prep Kit for Illumina® (Vazyme biotech co., Ltd., Nanjing, China) following the manufacturer's instructions. Libraries were multiplexed and sequencing was carried out on an Illumina HiSeq system with the 2 × 150 paired-end (PE) configuration (GENEWIZ). Cutadapt (v1. 9. 1) was used to remove adapters, primers, and reads with a base quality <20 based on FASTQ files. Clean data were aligned to the MED4 and NATL1A genomes *via* Bowtie2 software (v2. 1. 0). HTSeq (v0. 6. 1p1) was used to estimate gene expression levels from clean data. Differential expression analysis was performed using the DESeq Bioconductor package, a model based on negative binomial distribution. After adjusting using Benjamini and Hochberg's approach for controlling the false discovery rate, differentially expressed genes were considered significant at value of $p < 0.05$. Highly induced or suppressed genes were considered as meeting both false discovery rate $p < 0.05$ and magnitude of log2fold change with values greater than 1 (highly induced) or less than −1 (highly suppressed). These two different criterions were also used in a previous study (Al-Hosani et al., 2015). Transcriptomic data have been deposited in NCBI Gene Expression Omnibus (GEO) under the accession number GSE195946.

Results and discussion

Salinity range and acclimation to low salinity of *Prochlorococcus*

High-light adapted *Prochlorococcus* strain MED4 and low-light adapted strain NATL1A were tested for growth in different salinities ranging from 22 psu to 60 psu. Cell counting through flow cytometry (Figure 1A) and absorbance measurement

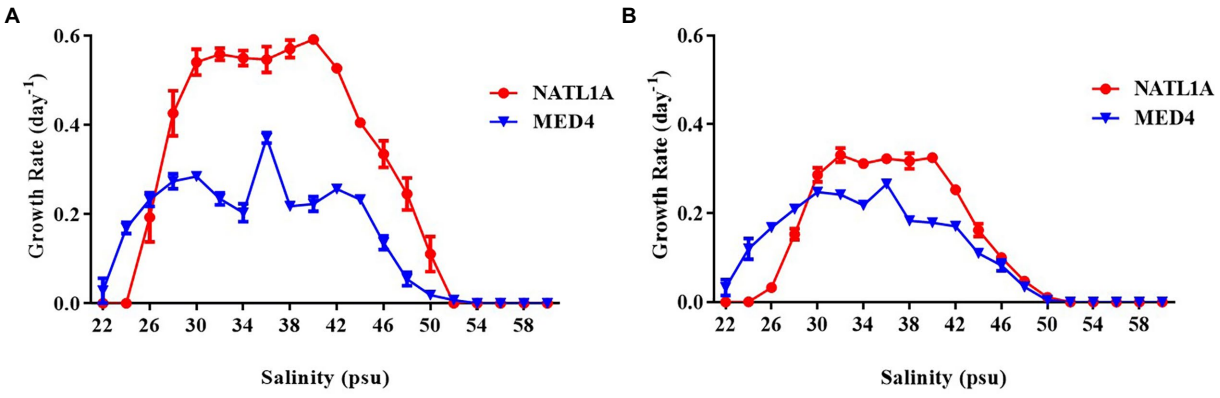

FIGURE 1
Growth rate of *Prochlorococcus* strains NATL1A and MED4 growing in Pro99 medium with salinities from 22psu to 60psu. Flow cytometry **(A)** and absorbance (OD440) measurement of chlorophyll **(B)** were used to monitor growth.

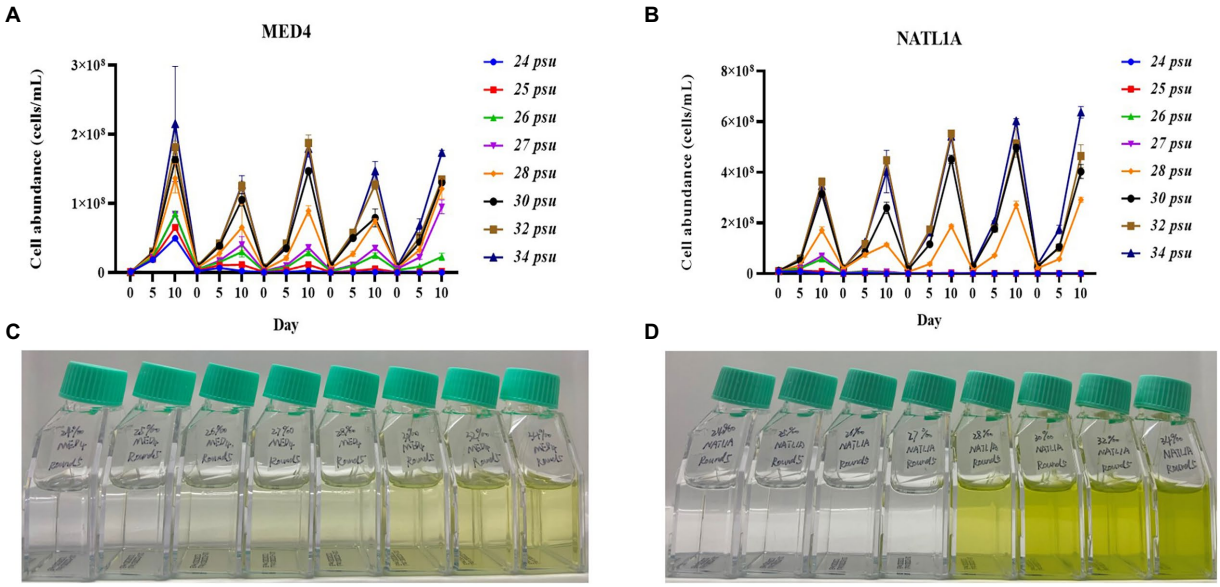

FIGURE 2
Acclimation of *Prochlorococcus* strains NATL1A and MED4 in different salinities. Five rounds of transfers were carried out and the growth **(A,B)** were monitored by flow cytometry. The pictures **(C,D)** showed the last round of cultures.

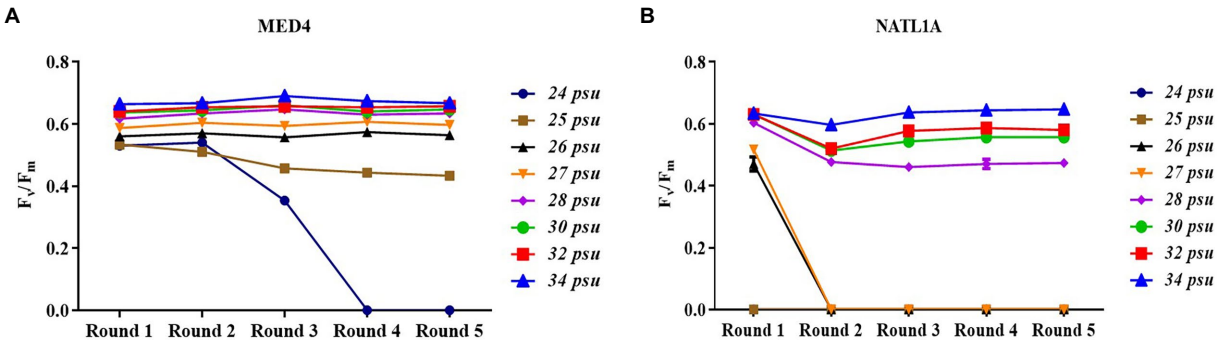

FIGURE 3
Dark-adapted photochemical efficiency (Fv/Fm) of *Prochlorococcus* strains MED4 **(A)** and NATL1A **(B)** growing in different salinities during acclimation.

at 440 nm (Figure 1B) were used to monitor the growth of *Prochlorococcus* cells. MED4 could grow in the salinity range from 22 psu to 50 psu and NATL1A could grow in the range from 26 psu to 50 psu. The optimal salinity ranges of MED4 and NATL1A were similar, from 30 psu to 40 psu. This result came from the first transfer of cultures from salinity 34 psu to other salinities. Under the same growing temperature (21°C) and light intensity (10 $\mu E\, m^{-2}\, s^{-1}$), the LL strain NATL1A grew faster than the HL strain MED4.

During the acclimation experiment, NATL1A could grow in salinities higher than 26 psu in the first round, but could not survive in salinity lower than 28 psu in the last round (Figure 2B). Interestingly, MED4 showed a gradually changing growth rate in the salinity gradient from 25 psu to 28 psu, while NATL1A showed a sharp change between salinity 27 psu and salinity 28 psu (Figures 2C,D). The effective quantum yield of PSII photochemistry (F_v/F_m) was measured on the 10th day at the end of each incubation round (Figure 3). Both strains showed reduced yield when growing in low salinities from 24 psu to 32 psu, compared to the yield when growing in salinity 34 psu, and the lower the salinity resulted in lower yield. The yield of MED4 growing in salinity 24 psu was not detectable after round 4, while the yield of NATL1A growing in salinities 27 psu and below was not detectable after round 2. Together, these data showed that *Prochlorococcus* MED4 and NATL1A could be acclimated in salinities 25 psu and 28 psu, respectively. Interesting, the high-light adapted strain MED4 and low-light adapted strain NATL1A showed different tolerance to low salinity.

It is well known that *Prochlorococcus* is an oceanic microorganism (Partensky et al., 1999), although a few studies claimed that *Prochlorococcus*-like populations existed in estuarine and even freshwater environments (Corzo et al., 1999; Shang et al.,

TABLE 1 Functional categorization of differentially expressed genes (p <0.05) in low salinity acclimated cells of NATL1A and MED4.

Function categories	Total no.		Total no. differential expressed		No. induced		No. repressed		Prevalent expression profile	
	NATL1A	MED4	NATL1A	MED4	NATL1A	MED4	NATL1A	MED4	NATL1A	MED4
Translation, ribosomal structure and biogenesis	128	130	38	25	5	24	33	1	Repressed	Induced
Transcription	26	27	10	6	7	5	3	1	Induced	Induced
Signal transduction mechanisms	26	24	7	3	3	2	4	1	Equal	Equal
Secondary metabolites biosynthesis, transport, and catabolism	18	22	4	7	3	2	1	5	Equal	Repressed
Replication, recombination, and repair	4	4	2	1	2	1	0	0	Equal	Equal
Posttranslational modification, protein turnover, chaperones	87	82	23	19	13	5	10	14	Induced	Repressed
Nucleotide transport and metabolism	48	50	14	5	8	4	6	1	Equal	Induced
Lipid metabolism	29	31	10	6	3	3	7	3	Repressed	Equal
Intracellular trafficking and secretion	14	12	4	2	2	1	2	1	Equal	Equal
Inorganic ion transport and metabolism	58	57	8	6	5	2	3	4	Equal	Equal
Energy production and conversion	77	78	28	14	19	8	9	6	Induced	Equal
DNA replication, recombination, and repair	68	65	12	7	7	5	5	2	Equal	Induced
Defense mechanisms	17	16	2	1	2	0	0	1	Equal	Equal
Coenzyme metabolism	105	101	20	11	6	4	14	7	Repressed	Repressed
Cell wall/ membrane/envelope biogenesis	1	2	1	1	1	0	0	1	Equal	Equal
Cell envelope biogenesis, outer membrane	93	91	30	10	16	6	14	4	Equal	Equal
Cell division and chromosome partitioning	14	16	4	3	3	1	1	2	Equal	Equal
Cell cycle control, cell division, chromosome partitioning	2	2	0	1	0	1	0	0	Equal	Equal
Carbohydrate transport and metabolism	46	48	10	10	4	6	6	4	Equal	Equal
Amino acid transport and metabolism	128	118	38	17	19	11	19	6	Equal	Induced
Function unknown	86	88	18	13	10	4	8	9	–	–
General function prediction only	137	132	44	13	23	8	21	5	–	–
Others	6	5	2	0	0	0	2	0	–	–
Not in COGs	1,021	841	196	96	125	43	71	53	–	–
Total	2,239	2042	525	277	286	146	239	131	–	–

2007; Mitbavkar et al., 2012; Zhang et al., 2013). However, these studies all only depended on flow cytometry investigation, and could not confirm that those "populations" on the flow cytometry diagram were indeed *Prochlorococcus*. Our acclimation study suggests that *Prochlorococcus* cannot live in salinity lower than 25 psu for a long time period (50 days in this study). This study provides evidence supporting that *Prochlorococcus* is an oceanic organism.

Differentially expressed genes in low salinity acclimated *Prochlorococcus* cells

RNA-seq was performed to assess the response of acclimated *Prochlorococcus* cells to low salinity (28 psu), with the salinity 34 psu being the control. When the filter criteria of significance meet the *value of p* <0.05, there were 525 differentially expressed genes in the low salinity acclimated cells of NATL1A, with 286 genes being induced and 239 genes being repressed (Table 1). By contrast, MED4 appears to be less fluctuant under low salinity stress, with only 277 differentially expressed genes, among which 146 were induced and 131 were repressed (Table 1). A previous study compared the transcriptomes of *Prochlorococcus* AS9601 under high salt stress (5.0%) and under normal salt concentration (3.8%), and found 627 differentially expressed genes (Al-Hosani et al., 2015). Together, these results suggest that *Prochlorococcus* is sensitive to salinity changes.

Subsequently, the differentially expressed genes of these two strains were functionally classified according to Cyanobase definitions (Fujisawa et al., 2014). Firstly, the numbers of induced and repressed genes were equal for most functional modules

(60–70%) in each of the two strains. Secondly, compared to the control group, the changed prevalent expression profiles between the two strains were different. In low salinity acclimated NATL1A, some genes involved in translation, ribosomal structure and biogenesis, lipid metabolism and coenzyme metabolism were down-regulated, while genes involved in transcription, posttranslational modification, protein turnover, chaperones and energy production and conversion were up-regulated (Table 1). However, in MED4, regulation profile of the functions mentioned above is different from NATL1A, except for coenzyme metabolism.

Contrasting regulation between NATL1A and MED4

Most interestingly, among the genes involved in translation, ribosomal structure and biogenesis, five were up-regulated and 33 were down-regulated in low salinity acclimated NATL1A cells compared to control (Tables 1, 2). However, in MED4, 24 genes of those genes were up-regulated and only one was down-regulated (Tables 1, 3). Strikingly, the regulation of genes involved in energy production and conversion were also in distinct patterns between NATL1A and MED4. In low salinity acclimated NATL1A cells, the ATP-producing genes were down-regulated (*atpA*, *atpC*, *atpD*, *atpH* and other ATP synthase genes), while many genes involved in photosynthesis (*psaC*, *psb27*, *rbcS*), cytochrome oxidation (*cyoA*, *cyoB*, *ctaE*), NADH dehydrogenase (*ndhA*, *ndhH*) were up-regulated (Table 2). However, in low salinity acclimated MED4 cells, genes for photosynthesis were down-regulated, such as photosystems II (*psbA*, *psbB*, *psbD*, *psbN*), cytochrome F (*petA*), and electron transport chain intermediate (*ndhD*), while most ATP-producing genes (*acnB*, *atpG*, *atpF*, *atpH*, *atpD*) were up-regulated. This striking contrasting transcriptional regulation indicated the two strains processed different response mechanisms to low salinity stress. It is likely that, to respond to low salinity stress, NATL1A enhanced photosynthesis but repressed ATP production and translation and biosynthesis. In contrast, MED4 repressed photosynthesis but enhanced ATP production, translation and biosynthesis. The reason is possible that NATL1A and MED4 were in different stress level under the salinity 28 psu, which appears to be slightly stressful for MED4, but extremely stressful for NATL1A. This is the reason why the differentially expressed genes of NATL1A were more than those of MED4.

It has been pointed out that the response of photosystem gene expression to high salt stress might be dependent on the organism under study, based on the investigations on *Prochlorococcus* strain AS9601, *Synechocystis* PCC 6803 and *Synechococcus* PCC 7002 (Al-Hosani et al., 2015). In high salt acclimated AS9601 cells, many genes coding for components of Photosystem I, Photosystem II and chlorophyll were down-regulated. By contrast, in high salt acclimated PCC 7002, PSI genes were down-regulated but PSII genes were not changed significantly (Ludwig and Bryant, 2012). Similarly, in this study, NATL1A and MED4 also showed heterogeneity in response to low salinity stress.

Compatible solute and transporters

Cyanobacteria generally use the salt-out strategy for salt acclimation, in which cells maintain low intracellular ion concentration and accumulate compatible solutes to establish turgor (Hagemann, 2011). Compatible solutes are low-molecular-weight organic compounds, with sucrose, glucosylglycerol (GG), glucosylglycerate (GGA) and glycine betaine (GB) being the most common ones utilized by cyanobacteria (Klähn and Hagemann, 2011). *Prochlorococcus* cells probably use GGA and sucrose as their main compatible solutes (Scanlan et al., 2009). In NATL1A, we observed significant decrease in transcript abundance of the GGA synthesis genes (*gpgP*, encoding glucosyl-phosphoglycerate phosphatase, and *gpgS*, encoding glucosyl-phosphoglycerate synthase) in the low salinity acclimated cells compared to control cells (Table 4). However, we did not observe significant change on the sucrose synthesis gene *spsA* (encoding sucrose phosphate synthase). Moreover, in MED4, all the three genes did not show significant change in transcript abundance. These results suggest that, to cope with low salinity stress, NATL1A probably reduced the concentration of intracellular compatible solute GGA, while MED4 did not reduce the concentration of the compatible solutes. Again, this different observations may be due to that the two strains were at different stress level when growing in the medium with salinity 28 psu. In another study, high salt acclimated *Prochlorococcus* AS9601 cells up-regulated the *gpgS* gene and a sodium transporter, suggesting that active extrusion of sodium ions and accumulation of GGA are involved in AS9601 acclimation to high salt stress (Al-Hosani et al., 2015). Together, these results suggests that compatible solute GGA may play an important role in the adaptation of *Prochlorococcus* to salinity changes.

Na^+/H^+ antiporter is closely related to plant salinity tolerance, and it is one of the critical factors of plant salt tolerance. To adapt to a high salt environment, plants will reduce the plasma membrane Na^+ level through Na^+/H^+ antiporter (Apse et al., 1999; Hasegawa et al., 2000). Besides, cyanobacteria cells involved in salt stress tolerance was correlated with the activity of Na^+/H^+ antiporter (Allakhverdiev et al., 1999, 2000). However, in this study, the transcript level of Na^+/H^+ antiporter (*nhaP*) was increased under low salinity stress in NATL1A cells (Table 2). It is not clear what is the mechanism involved in this phenomenon. Perhaps the increasing expression of Na^+/H^+ antiporter would help to reduce the cytoplasm Na^+ level which has already adapted to high salinity level of seawater.

Iron transporter and molecular chaperone

Interestingly, a periplasmic ABC-type Fe^{3+} transporter (*afuA/idiA/futA*) was up-regulated in low salinity acclimated cells of

TABLE 2 List of a part of differentially expressed genes (p <0.05) in low salinity acclimated *Prochlorococcus* NATL1A.

Gene ID	Gene name	Product	p-Value	$\log_2$FC
Energy production and conversion				
gene-NATL1_05001	*cyoA*	putative cytochrome c oxidase, subunit 2	< 0.001	1.249
gene-NATL1_17081	*acoA*	Pyruvate dehydrogenase E1 alpha subunit	< 0.001	0.979
gene-NATL1_04991	*cyoB*	Cytochrome c oxidase, subunit I	< 0.001	0.897
gene-NATL1_06051	*rbcS*	Ribulose bisphosphate carboxylase, small chain	0.010	0.780
gene-NATL1_02471	*ndhH*	putative NADH dehydrogenase subunit	< 0.001	0.770
gene-NATL1_20041	NATL1_20041	NADH dehydrogenase I subunit N	< 0.001	0.723
gene-NATL1_05651	*psb27*	possible Photosystem II reaction center Psb27 protein	< 0.001	0.6925
gene-NATL1_05981	*chlN*	Light-independent protochlorophyllide reductase subunit N	< 0.001	0.650
gene-NATL1_20591	*psaC*	Photosystem I subunit PsaC	0.004	0.633
gene-NATL1_04561	*pdhC*	Dihydrolipoamide acetyltransferase	0.001	0.607
gene-NATL1_04981	*ctaE*	Cytochrome c oxidase, subunit III	0.002	0.580
gene-NATL1_20451	*icd*	Isocitrate dehydrogenase	0.002	0.547
gene-NATL1_04171	*petB*	Cytochrome b6	0.006	0.532
gene-NATL1_02331	*ndhA*	putative respiratory-chain NADH dehydrogenase subunit	0.006	0.498
gene-NATL1_17231	NATL1_17231	FAD/FMN-containing dehydrogenases	0.024	0.484
gene-NATL1_03751	*rub*	probable rubredoxin	0.0158	0.453
gene-NATL1_21811	*acnB*	Aconitate hydratase B	0.0188	0.394
gene-NATL1_03311	*psbI*	photosystem II reaction center PsbI protein	0.0263	−0.446
gene-NATL1_19381	NATL1_19381	Fe-S oxidoreductase	0.021	−0.482
gene-NATL1_18501	*atpH*	ATP synthase, delta (OSCP) subunit	0.008	−0.497
gene-NATL1_18491	*atpA*	ATP synthase F1, alpha subunit	0.006	−0.565
gene-NATL1_19601	*psaI*	photosystem I subunit VIII (PsaI)	0.008	−0.574
gene-NATL1_00561	NATL1_00561	Flavoprotein, FldA	0.009	−0.647
gene-NATL1_18481	NATL1_18481	ATP synthase gamma subunit	< 0.001	−0.668
gene-NATL1_18511	NATL1_18511	ATP synthase B/B′ *CF*(0)	< 0.001	−0.671
gene-NATL1_18381	*atpD*	ATP synthase F1, beta subunit	< 0.001	−0.723
gene-NATL1_14931	*gldA*	putative glycerol dehydrogenase	0.004	−0.755
gene-NATL1_18391	*atpC*	ATP synthase, Epsilon subunit	< 0.001	−1.089
Inorganic ion transport and metabolism				
gene-NATL1_16181	*afuA*	putative iron ABC transporter, substrate binding protein	< 0.001	1.208
gene-NATL1_19031	NATL1_19031	Ferric uptake regulator family	< 0.001	0.853
gene-NATL1_05281	*nhaP*	putative Na^+/H^+ antiporter, CPA1 family	0.005	0.597
gene-NATL1_20831	*mgtE*	MgtE family, putative magnesium transport protein	0.009	0.501
gene-NATL1_03411	*amtB*	Ammonium transporter family	0.022	0.414
gene-NATL1_03071	*met3*	ATP-sulfurylase	0.002	−0.582
gene-NATL1_15081	*petH*	ferredoxin-NADP oxidoreductase (FNR)	< 0.001	−0.687
Molecular chaperone				
gene-NATL1_09851	NATL1_09851	Molecular chaperone DnaK, heat shock protein hsp70	0.001	0.668
gene-NATL1_21861	NATL1_21861	Molecular chaperone DnaK2, heat shock protein hsp70-2	0.010	0.624
Translation, ribosomal structure and biogenesis				
gene-NATL1_18631	NATL1_18631	FtsJ cell division protein: S4 domain:Hemolysin A	0.001	0.837
gene-NATL1_04781	NATL1_04781	tRNA/rRNA methyltransferase (SpoU)	0.006	0.573
gene-NATL1_00131	NATL1_00131	tRNA-dihydrouridine synthase	0.040	0.566
gene-NATL1_04521	*lrtA*	light repressed protein A-like protein	0.002	0.563
gene-NATL1_03171	*ileS*	Isoleucyl-tRNA synthetase	0.016	0.425
gene-NATL1_04021	*rps1a*	30S ribosomal protein S1, protein A	0.036	−0.379
gene-NATL1_17711	*rplU*	50S ribosomal protein L21	0.025	−0.445
gene-NATL1_16641	*rpsN*	30S Ribosomal protein S14	0.011	−0.455

(Continued)

TABLE 2 (Continued)

Gene ID	Gene name	Product	*p*-Value	log_2FC
gene-NATL1_05781	*frr*	Ribosome recycling factor	0.022	−0.457
gene-NATL1_19971	*rpsC*	30S ribosomal protein S3	0.016	−0.480
gene-NATL1_07951	*glyS*	Glycyl-tRNA synthetase beta subunit	0.013	−0.485
gene-NATL1_19921	*rplX*	50S ribosomal protein L24	0.022	−0.490
gene-NATL1_07891	*rpsB*	30S ribosomal protein S2	0.015	−0.497
gene-NATL1_02771	*rplL*	50S ribosomal protein L7/L12	0.004	−0.564
gene-NATL1_19481	*rpsJ*	30S ribosomal protein S10	0.001	−0.568
gene-NATL1_21621	*aspS*	Aspartyl-tRNA synthetase	0.005	−0.570
gene-NATL1_19521	*rpsL*	30S ribosomal protein S12	0.001	−0.582
gene-NATL1_19871	*rpsE*	30S ribosomal protein S5	0.001	−0.605
gene-NATL1_02781	*rplJ*	50S ribosomal protein L10	0.002	−0.610
gene-NATL1_19991	*rpsS*	30S Ribosomal protein S19	0.001	−0.616
gene-NATL1_19891	*rplF*	50S ribosomal protein L6	< 0.001	−0.623
gene-NATL1_09331	*gatA*	Glutamyl-tRNA (Gln) amidotransferase A subunit	0.001	−0.631
gene-NATL1_05331	*map*	putative methionine aminopeptidase	< 0.001	−0.635
gene-NATL1_16221	*glyQ*	glycyl-tRNA synthetase，alpha subunit	0.034	−0.637
gene-NATL1_20021	*rplD*	50S ribosomal protein L4	< 0.001	−0.705
gene-NATL1_19881	*rplR*	50S ribosomal protein L18	< 0.001	−0.736
gene-NATL1_19951	*rpmC*	50S ribosomal protein L29	< 0.001	−0.752
gene-NATL1_00581	*alaS*	Alanyl-tRNA synthetase	0.002	−0.756
gene-NATL1_10481	*fmt*	putative Methionyl-tRNA formyltransferase	0.008	−0.777
gene-NATL1_17561	*tyrS*	Tyrosyl-tRNA synthetase	0.026	−0.777
gene-NATL1_03281	*pth*	Peptidyl-tRNA hydrolase	0.050	−0.785
gene-NATL1_20011	*rplW*	50S ribosomal protein L23	< 0.001	−0.791
gene-NATL1_07901	*tsf*	putative Elongation factor Ts	< 0.001	−0.821
gene-NATL1_19511	*rpsG*	30S ribosomal protein S7	< 0.001	−0.868
gene-NATL1_21311	*rplT*	50S ribosomal protein L20	< 0.001	−0.883
gene-NATL1_06131	*tdcF*	Putative translation initiation inhibitor，yjgF family	0.001	−0.939
gene-NATL1_10131	*rpsR*	30S Ribosomal protein S18	0.001	−1.140
gene-NATL1_10191	*cspR*	putative tRNA/rRNA methyltransferase (SpoU family)	0.009	−1.690

both NATL1A and MED4, compared to control cells. Moreover, NATL1A also up-regulated a ferric uptake regulator (NATL1_19031). It has been demonstrated that the transcript levels of *idiA* gene in *Synechococcus* PCC 6301 and *Prochlorococcus* MED4 were increased under iron deficiency conditions (Michel et al., 1999; Webb et al., 2001; Thompson et al., 2011). This suggests that cells may be iron-limited under low salt-stress. Previously, *afuA* was found to be down-regulated in high salt stressed cells of *Prochlorococcus* AS9601 (Al-Hosani et al., 2015). The authors attributed this to the reduced expression of iron required proteins under high salt condition. They also concluded that AS9601 was not iron limited because no difference in ferredoxin expression level was found between salt acclimated cells and control cells. It has been also revealed that iron requirement and siderophore production in cells is lower under high salinity (Boyle et al., 1977; Ruebsam et al., 2018). Together, these results indicates that there is a tight link between iron requirement and salt conditions in *Prochlorococcus*. However, the gene *isiB* (flavodoxin), which was induced in low iron stress (Erdner and Anderson, 1999; McKay et al., 1999), was not observed to be up-regulated in this study (Table 3). Hence, the specific relationship between low salinity stress and iron homeostasis remains to be investigated.

Up-regulated expression of *dnaK* was observed in both MED4 and NATL1A, which suggests that this gene could play a role in low salinity acclimation (Tables 2, 3). However, the molecular chaperone *dnaK* is one of the key factors for salt stress tolerance in halophiles, and over expression of *dnaK* can greatly reduce the growth lag period of the bacteria, allowing them to grow normally under salt stress (Sugimoto et al., 2003). Fukuda et al. (2001, 2002) cloned the *dnaK* gene from *Tetragenococcus halophila* JCM5888 and introduced it into *E. coli*, and found that the *dnaK* transcript abundance was increased approximately 3.5-fold under salt stress. Meanwhile, *dnaK* was also found to be present in the halotolerant cyanobacterium *Aphanothece halophytica* (Hibino et al., 1999). The gene product of *dnaK*, heat shock protein hsp70, likely plays an important role in stress resistance, no matter it is low salinity stress or high salt stress.

TABLE 3 List of a part of differentially expressed genes (p <0.05) in low salinity acclimated *Prochlorococcus* MED4.

Gene ID	Gene name	Product	p-Value	$\log_2$FC
Energy production and conversion				
gene-PMM0930	*pdhB*	Pyruvate dehydrogenase E1 beta subunit	< 0.001	0.691
gene-PMM0317	*psbM*	possible Photosystem II reaction center M protein (PsbM)	0.033	0.590
gene-PMM0544	*chlB*	Light-independent protochlorophyllide reductase subunit B	0.004	0.507
gene-PMM1452	*atpH,atpD*	ATP synthase, delta (OSCP) subunit	0.042	0.476
gene-PMM0785	*prk,cbbP*	phosphoribulokinase	0.007	0.475
gene-PMM1700	*acnB*	Aconitate hydratase B	0.009	0.460
gene-PMM1454	*atpG*	ATP synthase B/B′ *CF*(0)	0.019	0.411
gene-PMM1453	*atpF*	ATP synthase B/B′ *CF*(0)	0.038	0.392
gene-PMM0223	*psbA*	Photosystem II PsbA protein (D1)	0.018	−0.427
gene-PMM1157	*psbD*	Photosystem II PsbD protein (D2)	0.008	−0.470
gene-PMM0315	*psbB*	Photosystem II PsbB protein (CP47)	0.014	−0.476
gene-PMM0461	*petA*	Cytochrome f	0.021	−0.477
gene-PMM1171	*isiB*	Flavodoxin	0.045	−0.522
gene-PMM1229	PMM1229	Dehydrogenase, E1 component	0.009	−0.577
gene-PMM0594	*ndhD*	putative NADH Dehydrogenase (complex I) subunit (chain 4)	0.001	−0.663
gene-PMM0252	*psbN*	Photosystem II reaction center N protein (psbN)	0.001	−0.919
gene-PMM0366	PMM0366	Type-1 copper (blue) domain	0.002	−0.960
gene-PMM0316	PMM0316	possible ferredoxin	< 0.001	−1.358
gene-PMM0926	*psb28*	possible Photosystem II reaction center Psb28 protein	0.041	−1.707
Inorganic ion transport and metabolism				
gene-PMM1032	PMM1032	ABC transporter, substrate binding protein, possibly Mn.	0.006	0.751
gene-PMM1164	*futA/afuA/idiA*	putative iron ABC transporter, substrate binding protein	< 0.001	0.950
gene-PMM0808	PMM0808	Rieske iron–sulfur protein 2Fe-2S subunit	0.019	−0.501
gene-PMM0227	*cysD*	ATP-sulfurylase	< 0.001	−0.893
gene-PMM1701	PMM1701	putative chloride channel	< 0.001	−0.984
gene-PMM0504	PMM0504	CutA1 divalent ion tolerance protein	0.004	−2.817
Molecular chaperone				
gene-PMM1704	*dnaK2*	Molecular chaperone DnaK2, heat shock protein hsp70-2	0.047	0.360
Translation, ribosomal structure and biogenesis				
gene-PMM1537	*rps13, rpsM*	30S ribosomal protein S13	0.001	1.774
gene-PMM1538	*rpmJ, rpl36*	50S Ribosomal protein L36	< 0.001	1.081
gene-PMM1688	*aspS*	Aspartyl-tRNA synthetase	0.002	0.952
gene-PMM1507	*rpsJ, rps10*	30S ribosomal protein S10	< 0.001	0.844
gene-PMM0068	*def*	putative formylmethionine deformylase	0.025	0.745
gene-PMM1661	*rpl35, rpmI*	50S ribosomal protein L35	0.006	0.724
gene-PMM1534	*rpl17, rplQ*	50S ribosomal protein L17	0.002	0.697
gene-PMM1550	*rpl29, rpmC*	50S ribosomal protein L29	0.041	0.609
gene-PMM1545	*rps8, rpsH*	30S ribosomal protein S8	0.001	0.599
gene-PMM1191	*pnp*	polyribonucleotide nucleotidyltransferase	0.003	0.592
gene-PMM0597	*thrS*	Threonyl-tRNA synthetase	0.016	0.561
gene-PMM0312	*rps1a, rpsA1*	30S ribosomal protein S1，homolog A	0.002	0.560
gene-PMM1548	*rpl14, rplN*	50S Ribosomal protein L14	0.047	0.539
gene-PMM1280	PMM1280	putative bifuntional enzyme: tRNA methyltransferase: 2-C-methyl-D-erythritol 2，4-cyclodiphosphate synthase	0.029	0.551
gene-PMM0202	*rpl10, rplJ*	50S ribosomal protein L10	0.002	0.507
gene-PMM1662	*rpl20, rplT*	50S ribosomal protein L20	0.017	0.498
gene-PMM0870	*rpl33, rpmG*	50S Ribosomal protein L33	0.030	0.467
gene-PMM1706	*rps6, rpsF*	30S ribosomal protein S6	0.041	0.465
gene-PMM1508	*tufA*	Elongation factor Tu	0.006	0.459
gene-PMM0238	*ileS*	Isoleucyl-tRNA synthetase	0.027	0.429
gene-PMM1532	*rpl13, rplM*	50S ribosomal protein L13	0.044	0.425
gene-PMM0203	*rpl1, rplA*	50S ribosomal protein L1	0.021	0.420
gene-PMM1546	*rpl5, rplE*	50S ribosomal protein L5	0.028	0.384
gene-PMM1509	*fusA*	Elongation factor G	0.030	0.370

TABLE 4 Expression change on genes responsible for compatible solute biosynthesis.

	NATL1A			MED4		
	Locus	*p*-Value	log_2FC	Locus	*p*-Value	log_2FC
gpgP	NATL1_05721	0.001	−0.809	PMM0515	0.367	0.214
gpgS	NATL1_09131	0.012	−0.431	PMM0962	0.476	−0.132
spsA	NATL1_21951	0.421	−0.147	PMM1711	0.143	−0.371

Highly differentially expressed genes

When the filter criterion was changed from only meeting the value of p ($p < 0.05$) to meeting both value of p and log2fold change with values greater than 1 (high induction) or less than-1 (high inhibition), there were 81 and 30 highly differentially expressed genes in NATL1A and MED4, respectively. These number are comparable to the previous study on *Prochlorococcus* AS9601, in which 69 highly differentially expressed genes were found in high salt acclimated cells compared to control cells (Al-Hosani et al., 2015). In NATL1A, 22 genes were down-regulated and 59 were up-regulated, while in MED4, 17 genes were down-regulated and 13 were up-regulated. There was no apparent gene enrichment pattern observed among these highly differentially expressed genes (Supplementary Tables S1, S2). For example, in low-salinity stress cells of NATL1A, many genes were highly inhibited, which were related to posttranslational modification (NATL1_02111 and NATL1_13731), signal transduction mechanisms (*typA*), cell envelope biogenesis, outer membrane (NATL1_08371 and NATL1_04491), translation, ribosomal structure and biogenesis (*rpsR*), coenzyme metabolism (*folE*), energy production and conversion (*atpC*), and amino acid transport and metabolism (*proA*). Nevertheless, in salinity acclimated cells of MED4, some other genes appear to be repressed, which were those involved in energy production and conversion (PMM0316), secondary metabolites biosynthesis, transport, and catabolism (PMM0280), DNA replication, recombination, and repair (*ruvC*), lipid metabolism (*des, yocE*) and posttranslational modification (PMM1006).

Conclusion

Prochlorococcus is the most abundant phototroph in the ocean. This organism has been adapted to open ocean areas with stable salt concentrations, and barely found in nearshore and estuarine waters with lower and variable salt concentrations. In this study, we showed that the lowest salinities for acclimation of high-light adapted *Prochlorococcus* strain MED4 and low-light adapted strain NATL1A were 25 psu and 28 psu, respectively. The optimal growing salinity of both MED4 and NATL1A were from 30 to 40 psu. Global transcriptome analysis showed that the two strains responded differently to low salinity stress. First, far more genes of NATL1A were impacted than those of MED4 in low salinity acclimated cells, suggesting NATL1A was more intensively stressed than MED4 under salinity 28 psu. Second, compared to control, low salinity acclimated cells of NATL1A repressed the expression of genes involved in translation, ribosomal structure and biogenesis and ATP production, but enhanced photosynthesis, while MED4 regulated these pathways in an opposite way. To cope with low salinity, NATL1A also reduced the transcript abundance of genes involved in compatible solute GGA, while MED4 did not. Interpreting from a previous study and this study, a tight link between iron transportation and salt condition was verified, with high salinity stressed cells coupling with up-regulation of iron transporters and low salinity stressed cells coupling with down-regulation of iron transporters. This study demonstrated the regulations of global transcriptome of *Prochlorococcus* under low salinity stress and the mechanisms within those regulations warrant further investigation.

Data availability statement

The datasets presented in this study can be found in online repositories. The names of the repository/repositories and accession number(s) can be found below: https://www.ncbi.nlm.nih.gov/geo/query/acc.cgi?acc=GSE195946.

Author contributions

SH, JD, and LL designed the experiments. XH and HL performed the experiments and analyzed the data. SH and XH wrote the manuscript. JD and LL provided resources and supervision. All authors contributed to the article and approved the submitted version.

Funding

This study was funded by the National Natural Science Foundation of China [grant number 42176116, 41576126]; Key Special Project for Introduced Talents Team of Southern Marine Science and Engineering Guangdong Laboratory (Guangzhou) [GML2019ZD0404]; the Natural Science Foundation of Guangdong Province [grant number 2017A030306020]; the Youth Innovation Promotion Association [grant number 2018377]; and the Rising Star Foundation of the South China Sea Institute of Oceanology [grant number NHXX2019ST0101].

Acknowledgments

We thank Rui Zhang and Xilin Xiao for sharing the *Prochlorococcus* strains.

Conflict of interest

The authors declare that the research was conducted in the absence of any commercial or financial relationships that could be construed as a potential conflict of interest.

Publisher's note

All claims expressed in this article are solely those of the authors and do not necessarily represent those of their affiliated organizations, or those of the publisher, the editors and the reviewers. Any product that may be evaluated in this article, or claim that may be made by its manufacturer, is not guaranteed or endorsed by the publisher.

Supplementary material

The Supplementary material for this article can be found online at: https://www.frontiersin.org/articles/10.3389/fmicb.2022.1038136/full#supplementary-material

References

Al-Hosani, S., Oudah, M. M., Henschel, A., and Yousef, L. F. (2015). Global transcriptome analysis of salt acclimated *Prochlorococcus* AS9601. *Microbiol. Res.* 176, 21–28. doi: 10.1016/j.micres.2015.04.006

Allakhverdiev, S. I., Nishiyama, Y., Suzuki, I., Tasaka, Y., and Murata, N. (1999). Genetic engineering of the unsaturation of fatty acids in membrane lipids alters the tolerance of *Synechocystis* to salt stress. *Proc. Natl. Acad. Sci.* 96, 5862–5867. doi: 10.1073/pnas.96.10.5862

Allakhverdiev, S. I., Sakamoto, A., Nishiyama, Y., Inaba, M., and Murata, N. (2000). Ionic and osmotic effects of NaCl-induced inactivation of photosystems I and II in *Synechococcus* sp. *Plant Physiol.* 123, 1047–1056. doi: 10.1104/pp.123.3.1047

Apse, M. P., Aharon, G. S., Snedden, W. A., and Blumwald, E. (1999). Salt tolerance conferred by overexpression of a vacuolar Na+/H+ antiport in *Arabidopsis*. *Science* 285, 1256–1258. doi: 10.1126/science.285.5431.1256

Boyle, E. A., Edmond, J. M., and Sholkovitz, E. R. (1977). The mechanism of iron removal in estuaries. *Geochim. Cosmochim. Acta* 41, 1313–1324. doi: 10.1016/0016-7037(77)90075-8

Chisholm, S. W., Frankel, S. L., Goericke, R., Olson, R. J., Palenik, B., Waterbury, J. B., et al. (1992). *Prochlorococcus marinus* nov. gen. Nov. sp.: an oxyphototrophic marine prokaryote containing divinyl chlorophyll a and b. *Arch. Microbiol.* 157, 297–300. doi: 10.1007/BF00245165

Corzo, A., Jimenez-Gomez, F., Gordillo, F. J. L., Garcia-Ruiz, R., and Niell, F. X. (1999). *Synechococcus* and *Prochlorococcus*-like populations detected by flow cytometry in a eutrophic reservoir in summer. *J. Plankton Res.* 21, 1575–1581. doi: 10.1093/plankt/21.8.1575

Erdner, D. L., and Anderson, D. M. (1999). Ferredoxin and flavodoxin as biochemical indicators of iron limitation during open-ocean iron enrichment. *Limnol. Oceanogr.* 44, 1609–1615. doi: 10.4319/lo.1999.44.7.1609

Ferris, M. J., and Palenik, B. (1998). Niche adaptation in ocean cyanobacteria. *Nature* 396, 226–228. doi: 10.1038/24297

Flombaum, P., Gallegos, J. L., Gordillo, R. A., Rincon, J., Zabala, L. L., Jiao, N. Z., et al. (2013). Present and future global distributions of the marine cyanobacteria *Prochlorococcus* and *Synechococcus*. *Proc. Natl. Acad. Sci.* 110, 9824–9829. doi: 10.1073/pnas.1307701110

Fujisawa, T., Okamoto, S., Katayama, T., Nakao, M., Yoshimura, H., Kajiya-Kanegae, H., et al. (2014). CyanoBase and RhizoBase: databases of manually curated annotations for cyanobacterial and rhizobial genomes. *Nucleic Acids Res.* 42, D666–D670. doi: 10.1093/nar/gkt1145

Fukuda, D., Watanabe, M., Shino, S., Sonomoto, K., and Ishizaki, A. (2001). Cloning and characterization of dnaK operon of *Tetragenococcus halophila*. *J. Fac. Agric. Kyushu Univ.* 46, 229–241. doi: 10.5109/24435

Fukuda, D., Watanabe, M., Sonezaki, S., Sugimoto, S., Sonomoto, K., and Ishizaki, A. (2002). Molecular characterization and regulatory analysis of dnaK operon of halophilic lactic acid bacterium *Tetragenococcus halophila*. *J. Biosci. Bioeng.* 93, 388–394. doi: 10.1016/S1389-1723(02)80072-X

Goericke, R., and Welschmeyer, N. A. (1993). The marine prochlorophyte *Prochlorococcus* contributes significantly to phytoplankton biomass and primary production in the Sargasso Sea. *Deep-Sea Res. I Oceanogr. Res. Pap.* 40, 2283–2294. doi: 10.1016/0967-0637(93)90104-B

Guillard, R. R. L., Murphy, L. S., Foss, P., and Liaaen-Jensen, S. (1985). *Synechococcus* spp. as likely zeaxanthin-dominant ultraphytoplankton in the North Atlantic. *Limnol. Oceanogr.* 30, 412–414. doi: 10.4319/lo.1985.30.2.0412

Hagemann, M. (2011). Molecular biology of cyanobacterial salt acclimation. *FEMS Microbiol. Rev.* 35, 87–123. doi: 10.1111/j.1574-6976.2010.00234.x

Hasegawa, P. M., Bressan, R. A., Zhu, J. K., and Bohnert, H. J. (2000). Plant cellular and molecular responses to high salinity. *Annu. Rev. Plant Biol.* 51, 463–499. doi: 10.1146/annurev.arplant.51.1.463

Hess, W. R., Partensky, F., Van der Staay, G. W., Garcia-Fernandez, J. M., Börner, T., and Vaulot, D. (1996). Coexistence of phycoerythrin and a chlorophyll a/b antenna in a marine prokaryote. *Proc. Natl. Acad. Sci.* 93, 11126–11130. doi: 10.1073/pnas.93.20.11126

Hibino, T., Kaku, N., Yoshikawa, H., Takabe, T., and Takabe, T. (1999). Molecular characterization of DnaK from the halotolerant cyanobacterium *Aphanothece halophytica* for ATPase, protein folding, and copper binding under various salinity conditions. *Plant Mol. Biol.* 40, 409–418. doi: 10.1023/A:1006273124726

Johnson, Z. I., Zinser, E. R., Coe, A., McNulty, N. P., Woodward, E. M. S., and Chisholm, S. W. (2006). Niche partitioning among *Prochlorococcus* ecotypes along ocean-scale environmental gradients. *Science* 311, 1737–1740. doi: 10.1126/science.1118052

Kanesaki, Y., Suzuki, I., Allakhverdiev, S. I., Mikami, K., and Murata, N. (2002). Salt stress and hyperosmotic stress regulate the expression of different sets of genes in *Synechocystis* sp. PCC 6803. *Biochem. Biophys. Res. Commun.* 290, 339–348. doi: 10.1006/bbrc.2001.6201

Klähn, S., and Hagemann, M. (2011). Compatible solute biosynthesis in cyanobacteria. *Environ. Microbiol.* 13, 551–562. doi: 10.1111/j.1462-2920.2010.02366.x

Liu, H., Nolla, H. A., and Campbell, L. (1997). *Prochlorococcus* growth rate and contribution to primary production in the equatorial and subtropical North Pacific Ocean. *Aquat. Microb. Ecol.* 12, 39–47. doi: 10.3354/ame012039

Ludwig, M., and Bryant, D. A. (2012). *Synechococcus* sp. strain PCC 7002 transcriptome: acclimation to temperature, salinity, oxidative stress, and mixotrophic growth conditions. *Front. Microbiol.* 3:354. doi: 10.3389/fmicb.2012.00354

Mackey, K. R., Paytan, A., Caldeira, K., Grossman, A. R., Moran, D., McIlvin, M., et al. (2013). Effect of temperature on photosynthesis and growth in marine *Synechococcus* spp. *Plant Physiol.* 163, 815–829. doi: 10.1104/pp.113.221937

Marin, K., Suzuki, I., Yamaguchi, K., Ribbeck, K., Yamamoto, H., Kanesaki, Y., et al. (2003). Identification of histidine kinases that act as sensors in the perception of salt stress in *Synechocystis* sp. PCC 6803. *Proc. Natl. Acad. Sci.* 100, 9061–9066. doi: 10.1073/pnas.1532302100

McKay, R. M. L., La Roche, J., Yakunin, A. F., Durnford, D. G., and Geider, R. J. (1999). Accumulation of ferredoxin and flavodoxin in a marine diatom in response to Fe. *J. Phycol.* 35, 510–519. doi: 10.1046/j.1529-8817.1999.3530510.x

Michel, K. P., Krüger, F., Pühler, A., and Pistorius, E. K. (1999). Molecular characterization of idiA and adjacent genes in the cyanobacteria *Synechococcus* sp. strains PCC 6301 and PCC 7942. *Microbiology* 145, 1473–1484. doi: 10.1099/13500872-145-6-1473

Mitbavkar, S., Rajaneesh, K. M., Anil, A. C., and Sundar, D. (2012). Picophytoplankton community in a tropical estuary: detection of *Prochlorococcus*-like populations. *Estuar. Coast. Shelf Sci.* 107, 159–164. doi: 10.1016/j.ecss.2012.05.002

Moore, L. R., and Chisholm, S. W. (1999). Photophysiology of the marine cyanobacterium *Prochlorococcus*: ecotypic differences among cultured isolates. *Limnol. Oceanogr.* 44, 628–638. doi: 10.4319/lo.1999.44.3.0628

Mühling, M. (2012). On the culture-independent assessment of the diversity and distribution of *Prochlorococcus*. *Environ. Microbiol.* 14, 567–579. doi: 10.1111/j.1462-2920.2011.02589.x

Partensky, F., Blanchot, J., and Vaulot, D. (1999). Differential distribution and ecology of *Prochlorococcus* and *Synechococcus* in oceanic waters: a review. *Bull. Inst. Oceanogr. Monaco* 19, 457–476.

Robertson, B. R., Tezuka, N., and Watanabe, M. M. (2001). Phylogenetic analyses of *Synechococcus* strains (cyanobacteria) using sequences of 16S rDNA and part of the phycocyanin operon reveal multiple evolutionary lines and reflect phycobilin content. *Int. J. Syst. Evol. Microbiol.* 51, 861–871. doi: 10.1099/00207713-51-3-861

Rocap, G., Distel, D. L., Waterbury, J. B., and Chisholm, S. W. (2002). Resolution of *Prochlorococcus* and *Synechococcus* ecotypes by using 16S-23S ribosomal DNA internal transcribed spacer sequences. *Appl. Environ. Microbiol.* 68, 1180–1191. doi: 10.1128/AEM.68.3.1180-1191.2002

Rocap, G., Larimer, F. W., Lamerdin, J., Malfatti, S., Chain, P., Ahlgren, N. A., et al. (2003). Genome divergence in two *Prochlorococcus* ecotypes reflects oceanic niche differentiation. *Nature* 424, 1042–1047. doi: 10.1038/nature01947

Ruebsam, H., Kirsch, F., Reimann, V., Erban, A., Kopka, J., Hagemann, M., et al. (2018). The iron-stress activated RNA 1 (IsaR1) coordinates osmotic acclimation and iron starvation responses in the cyanobacterium *Synechocystis* sp. PCC 6803. *Environ. Microbiol.* 20, 2757–2768. doi: 10.1111/1462-2920.14079

Scanlan, D. J., Ostrowski, M., Mazard, S., Dufresne, A., Garczarek, L., Hess, W. R., et al. (2009). Ecological genomics of marine picocyanobacteria. *Microbiol. Mol. Biol. Rev.* 73, 249–299. doi: 10.1128/MMBR.00035-08

Shang, X., Zhang, L. H., and Zhang, J. (2007). *Prochlorococcus*-like populations detected by flow cytometry in the fresh and brackish waters of the Changjiang estuary. *J. Mar. Biol. Assoc. U. K.* 87, 643–648. doi: 10.1017/S0025315407055191

Sugimoto, S., Nakayama, J., Fukuda, D., Sonezaki, S., Watanabe, M., Tosukhowong, A., et al. (2003). Effect of heterologous expression of molecular chaperone DnaK from *Tetragenococcus halophilus* on salinity adaptation of *Escherichia coli*. *J. Biosci. Bioeng.* 96, 129–133. doi: 10.1016/S1389-1723(03)90114-9

Thompson, A. W., Huang, K., Saito, M. A., and Chisholm, S. W. (2011). Transcriptome response of high-and low-light-adapted *Prochlorococcus* strains to changing iron availability. *ISME J.* 5, 1580–1594. doi: 10.1038/ismej.2011.49

Voigt, K., Sharma, C. M., Mitschke, J., Lambrecht, S. J., Voß, B., Hess, W. R., et al. (2014). Comparative transcriptomics of two environmentally relevant cyanobacteria reveals unexpected transcriptome diversity. *ISME J.* 8, 2056–2068. doi: 10.1038/ismej.2014.57

Webb, E. A., Moffett, J. W., and Waterbury, J. B. (2001). Iron stress in open-ocean cyanobacteria (*Synechococcus*, *Trichodesmium*, and *Crocosphaera* spp.): identification of the IdiA protein. *Appl. Environ. Microbiol.* 67, 5444–5452. doi: 10.1128/AEM.67.12.5444-5452.2001

West, N. J., Schönhuber, W. A., Fuller, N. J., Amann, R. I., Rippka, R., Post, A. F., et al. (2001). Closely related *Prochlorococcus* genotypes show remarkably different depth distributions in two oceanic regions as revealed by in situ hybridization using 16S rRNA-targeted oligonucleotides. *Microbiology* 147, 1731–1744. doi: 10.1099/00221287-147-7-1731

Zhang, X., Shi, Z., Ye, F., Zeng, Y., and Huang, X. (2013). Picophytoplankton abundance and distribution in three contrasting periods in the Pearl River estuary, South China. *Mar. Freshw. Res.* 64, 692–705. doi: 10.1071/MF12303

Zinser, E. R., Johnson, Z. I., Coe, A., Karaca, E., Veneziano, D., and Chisholm, S. W. (2007). Influence of light and temperature on *Prochlorococcus* ecotype distributions in the Atlantic Ocean. *Limnol. Oceanogr.* 52, 2205–2220. doi: 10.4319/lo.2007.52.5.2205

Zwirglmaier, K., Jardillier, L., Ostrowski, M., Mazard, S., Garczarek, L., Vaulot, D., et al. (2008). Global phylogeography of marine *Synechococcus* and *Prochlorococcus* reveals a distinct partitioning of lineages among oceanic biomes. *Environ. Microbiol.* 10, 147–161. doi: 10.1111/j.1462-2920.2007.01440.x

frontiers | Frontiers in Microbiology

TYPE Original Research
PUBLISHED 07 November 2022
DOI 10.3389/fmicb.2022.1046388

OPEN ACCESS

EDITED BY
Prashant Kumar Singh,
Mizoram University,
India

REVIEWED BY
Shivam Yadav,
Patliputra University,
India
Shweta Rai,
Babasaheb Bhimrao Ambedkar Bihar University, India
Naveen Kumar Sharma,
Indira Gandhi National Tribal University, India

*CORRESPONDENCE
Nils Schuergers
nils.schuergers@biologie.uni-freiburg.de
Annegret Wilde
annegret.wilde@biologie.uni-freiburg.de

SPECIALTY SECTION
This article was submitted to Microbial Physiology and Metabolism, a section of the journal Frontiers in Microbiology

RECEIVED 16 September 2022
ACCEPTED 18 October 2022
PUBLISHED 07 November 2022

CITATION
Ding J, Schuergers N, Baehre H and Wilde A (2022) Enzymatic properties of CARF-domain proteins in *Synechocystis* sp. PCC 6803.
Front. Microbiol. 13:1046388.
doi: 10.3389/fmicb.2022.1046388

Enzymatic properties of CARF-domain proteins in *Synechocystis* sp. PCC 6803

Jin Ding[1], Nils Schuergers[1]*, Heike Baehre[2] and Annegret Wilde[1]*

[1]Molecular Genetics of Prokaryotes, Institute of Biology III, University of Freiburg, Freiburg, Germany, [2]Research Core Unit Metabolomics, Hannover Medical School, Hannover, Germany

Prokaryotic CRISPR-Cas (clustered regularly interspaced short palindromic repeats and CRISPR-associated genes) systems provide immunity against invading genetic elements such as bacteriophages and plasmids. In type III CRISPR systems, the recognition of target RNA leads to the synthesis of cyclic oligoadenylate (cOA) second messengers that activate ancillary effector proteins *via* their CRISPR-associated Rossmann fold (CARF) domains. Commonly, these are ribonucleases (RNases) that unspecifically degrade both invader and host RNA. To mitigate adverse effects on cell growth, ring nucleases can degrade extant cOAs to switch off ancillary nucleases. Here we show that the model organism *Synechocystis* sp. PCC 6803 harbors functional CARF-domain effector and ring nuclease proteins. We purified and characterized the two ancillary CARF-domain proteins from the III-D type CRISPR system of this cyanobacterium. The Csx1 homolog, SyCsx1, is a cyclic tetraadenylate(cA4)-dependent RNase with a strict specificity for cytosine nucleotides. The second CARF-domain protein with similarity to Csm6 effectors, SyCsm6, did not show RNase activity *in vitro* but was able to break down cOAs and attenuate SyCsx1 RNase activity. Our data suggest that the CRISPR systems in *Synechocystis* confer a multilayered cA4-mediated defense mechanism.

KEYWORDS

CRISPR, cyclic oligoadenylate signaling, CARF, HEPN, cyanobacteria

Introduction

The majority of archaeal and almost half of all bacterial genomes encode CRISPR-Cas (clustered regularly interspaced short palindromic repeats and CRISPR-associated genes) systems which provide immunity against invading genetic elements such as bacteriophages or plasmids (Makarova et al., 2020a). These systems acquire short sequences of foreign DNA that are integrated as new spacers between repeat sequences of CRISPR loci. Once transcribed and matured, CRISPR RNAs (crRNA) serve as guides for effector complexes composed of a single or multiple Cas protein(s) that can recognize and degrade foreign nucleic acids (Sorek et al., 2013; Marraffini, 2015; Mohanraju et al., 2016). CRISPR-Cas systems, which show an exceptional diversity in gene composition and modular organization, can be classified into two classes with six distinct types (Types I–VI) and over

30 subtypes (Makarova et al., 2015, 2020a). Intriguingly, a single organism can contain multiple and diverse CRISPR-Cas systems.

The hallmark of the widespread Type III CRISPR-Cas systems is the presence of the large subunit Cas10 in the effector complex that targets both invader RNA transcripts and invader DNA. Most Cas10 proteins have two enzymatic activities related to the defense function of CRISPR systems. A histidine-aspartate (HD) nuclease domain was shown to provide immunity by degrading single-stranded target DNA in a transcription-dependent manner (Samai et al., 2015; Elmore et al., 2016; Kazlauskiene et al., 2016). Moreover, using ATP as substrate, a pair of composite Palm domains in Cas10 generates cyclic oligoadenylates (cOAs) with various ring sizes, containing between three and six 3′–5′ linked AMP units (cA3-cA6). This polymerase/cyclase activity depends on an intact GGDD motif in the Palm domain and is inhibited as soon as the target RNA is degraded (Kazlauskiene et al., 2017; Niewoehner et al., 2017; Rouillon et al., 2018).

The cOA molecules constitute key second messengers which activate Type III ancillary proteins, typically Csm6 or related Csx1 family RNases. These RNases harbor a CRISPR-associated Rossmann fold (CARF) nucleotide-binding domain, which upon binding of the cOA ligand, allosterically activates the promiscuous RNase activity of a nucleotide-binding (HEPN) effector domain (Kazlauskiene et al., 2017; Niewoehner et al., 2017). Indiscriminate RNA degradation of host and invader transcripts constitutes an additional interference mechanism that boosts immunity and invader DNA clearance by preventing invader replication, arresting cell growth, and inducing cell dormancy or cell death (Jiang et al., 2016; Foster et al., 2019; Rostøl and Marraffini, 2019). To switch off these RNases and limit self-toxicity, cOA must be removed from the cell once the invading genetic elements have been cleared. Several organisms evolved ring nucleases which are CARF domain containing enzymes that cleave the cOA messenger in a metal-independent mechanism and convert it into two molecules of di-adenylate containing a 2′,3′-cyclic phosphate (A2 > P; Athukoralage et al., 2018; Molina et al., 2019). However, not all prokaryotes that harbor Type III CRISPR-Cas systems encode a dedicated CARF domain ring-nuclease. Several organisms employ dual-function RNases with a CARF domain that acts as a cOA sensor and has ring-nuclease activity (Athukoralage et al., 2019; Jia et al., 2019b; Garcia-Doval et al., 2020; Smalakyte et al., 2020). Others encode homologs of Csx3 in their CRISPR III ancillary modules. This Mn-dependent exoribonuclease has a structure which is distinct from the Rossmann fold and has been characterized as a ring nuclease that degrades cA4 (Athukoralage et al., 2020a).

About two thirds of all sequenced cyanobacterial genomes encode a CRISPR-Cas system (Makarova et al., 2020a). The model organism *Synechocystis* sp. PCC 6803 (from here on *Synechocystis*) contains three CRISPR-Cas systems (named CRISPR1-3), which are encoded on the stably transmitted plasmid pSYSA (Figure 1). With the exception of CRISPR2 which has not been characterized in detail, these systems were shown to efficiently mediate immunity against invading plasmids (Behler et al., 2018; Shah et al., 2019). According to their gene composition, CRISPR1 can be classified as a I-D system, whereas CRISPR2 and CRISPR3 are type III-D and type III-B systems, respectively harboring two Palm domains in the large effector complex subunits (Hein et al., 2013; Scholz et al., 2013; Reimann et al., 2017). Adjacent to the Type III-D interference complex, two accessory genes encoding CARF domain proteins have been identified (Shah et al., 2019). The last ORF (*sll7062*) in the CRISPR2 effector complex operon [transcriptional unit TU7058 (Kopf et al., 2014)] encodes a Csm6 family protein. This Csm6 homolog (hereafter SyCsm6) has an N-terminal CARF domain of the CARF7 family fused to a RelE domain, a nonspecific RNase found in numerous toxin-antitoxin systems (Griffin et al., 2013; Makarova et al., 2020b). This domain architecture is strongly linked to Type III CRISPR-Cas systems (Shah et al., 2019). Next to *sll7062* on the opposite strand, *slr7061* encodes a Csx1 family protein (SyCsx1) with a CARF-HEPN domain structure, the most abundant ancillary protein architecture associated with Type III (A, B, or D) CRISPR–Cas systems (Shah et al., 2019; Makarova et al., 2020b). Furthermore, a *csx3* homolog (*slr7080*) is encoded upstream of the CRISPR3 module. Deletion of the putative *csx3* gene did not affect the ability of the system to defend against an invader plasmid (Shah et al., 2019).

Considering the presence of these genes, we hypothesize that *Synechocystis* harbors a functional cOA-signaling pathway. Therefore, we heterologously expressed and purified the CRISPR-associated CARF-domain proteins from *Synechocystis* to characterize their enzymatic properties. We show that SyCsx1, but not SyCsm6, has a cA4-dependent RNase activity *in vitro*. However, SyCsm6 was able to degrade cOA and abolished the RNase activity of SyCsx1. Our results suggested that both CARF-domain proteins orchestrate cOA-dependent ribonucleolytic activity in tandem.

Results

SyCsx1 is a cA4-activated RNase with a preference for cytosines

The gene *csx1* from the *Synechocystis* CRISPR2 locus (Figure 1) encodes a CARF-domain protein whose function has not yet been elucidated. Sequence comparison to biochemically characterized Csx1 homologs showed that the distinct DxTHG motive, which is part of the ligand-binding surface of the CARF domain (Makarova et al., 2020b) and the HEPN active site residues (RXXXXH; R-X4-6-H) (Anantharaman et al., 2013) are conserved in SyCsx1 (Figure 2A). To confirm that SyCsx1 functions as a cOA-dependent RNase, we expressed and purified recombinant His-tagged SyCsx1 (49.3 kDa). Size exclusion chromatography revealed a monodisperse peak at around ~89 kDa (Figure 2B), suggesting that SyCsx1 forms a dimer in solution. Dimerization is typically observed in solved CARF-domain protein structures and is important for cOA binding and RNA

10.3389/fmicb.2022.1046388

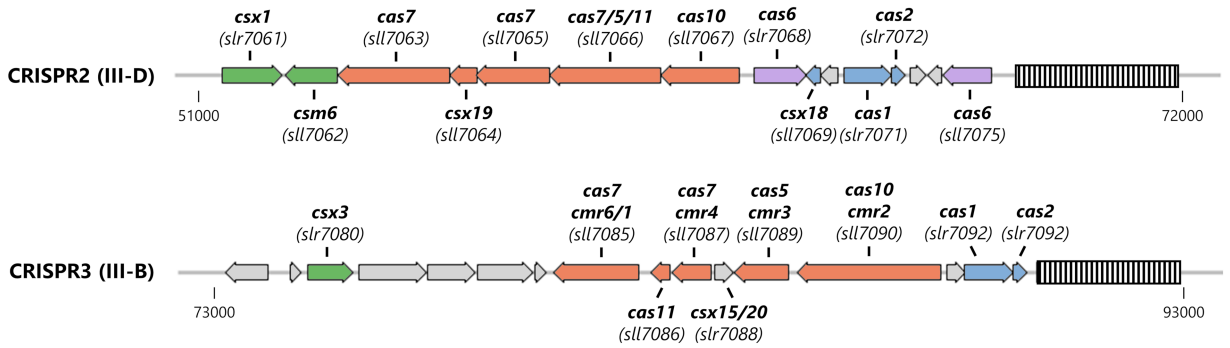

FIGURE 1
Organization of the Type III CRISPR-Cas systems encoded on the large plasmid pSYSA in *Synechocystis*. The CRISPR arrays are shown as striped boxes. Genes are color-coded: adaptation-associated genes (blue), effector complex components (salmon), pre-crRNA processing (purple), and ancillary genes putatively involved in cOA-signaling (green).

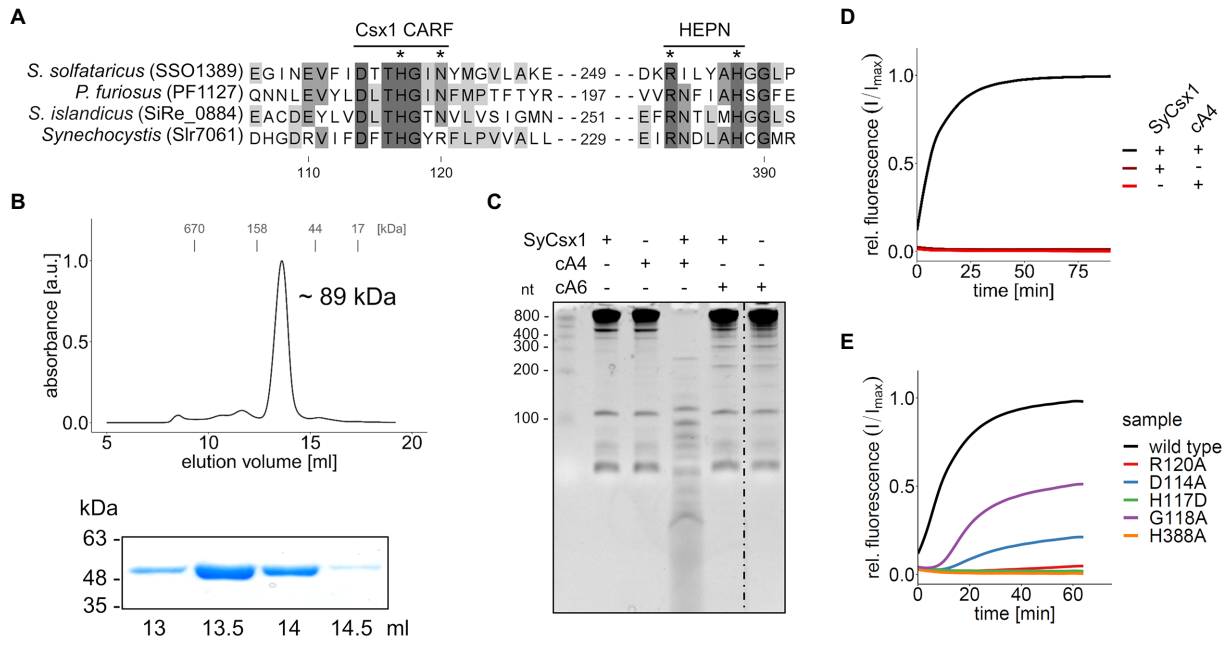

FIGURE 2
SyCsx1 shows cA4-dependent ribonuclease activity. **(A)** Multiple sequence alignment of SyCsx1 and homologous Csx1 proteins showing the conserved DxTHG motif from the CARF domain and the RxxxxH active site of the HEPN domain. An asterisk marks residues that were shown to impact protein function. **(B)** His-tagged SyCsx1 (48.7kDa) was isolated from *E. coli* by affinity chromatography and further purified by size-exclusion chromatography on a Superdex 200 10/300 column (upper panel). Elution fractions were analyzed by SDS-PAGE (lower panel, see Supplementary Figure S1). **(C)** 400 ng of *Synechocystis* total RNA were incubated in the presence or absence of SyCsx1 and 300 nM cOAs for 1 h and subsequently separated on a 12% denaturing PAA gel. The dotted line indicates a non-contiguous sample that was omitted from the gel. **(D)** A fluorogenic ribonuclease activity assay measuring the cleavage of 40 nM RNaseAlert substrate by SyCsx1 depending on the addition of 300 nM cA4 (excitation 490 nm; emission 520 nm). The cleavage of the RNaseAlert substrate separates a fluorophore/quencher pair, generating a fluorescent signal. **(E)** Fluorogenic ribonuclease activity assay of SyCsx1 variants with point mutations in the ligand-binding site of the CARF domain or the active site of the HEPN domain. All fluorogenic assays were performed in triplicates and mean values of relative fluorescence normalized to the maximum substrate turnover are shown.

decay (Kim et al., 2013; Molina et al., 2019). We tested RNase activity of SyCsx1 on *Synechocystis* total RNA in the presence or absence of cA4 and cA6, which are the most common CARF-domain ligands that activate effector domains (Athukoralage and White, 2021). Analysis of RNA cleavage by denaturing polyacrylamide (PAA) gel electrophoresis (Figure 2C) demonstrated that SyCsx1 without a specific activator does not degrade total RNA. Only if it is stimulated by the second messenger cA4, but not by cA6, it shows RNase activity that leads to a substantial degradation of total RNA. Additionally, we assayed

the cOA-dependent cleavage of a fluorogenic RNA substrate (Figure 2D). SyCsx1 is clearly inactive in the absence of cOAs, while the addition of cA4 leads to a significant increase of the fluorescence signal and presumably the complete turnover of the substrate.

To confirm the role of the ligand-binding CARF and the HEPN effector domain for SyCsx1 function, we performed RNase activity assays with recombinant protein variants in which we exchanged conserved residues in the CARF and HEPN domains (Figure 2E). In the presence of cA4, mutations in the conserved DxTHG motif (D114A, G118A) attenuated RNase activity and replacement of residues (H117D, R120A) that are known to participate in cOAs binding in other CARF domain proteins (Molina et al., 2019), reduced RNA cleavage to barely measurable levels. Furthermore, mutating an active site residue of the conserved HEPN-associated RxxxxH motif (H388A) completely abolished RNase activity of SyCsx1. Taken together, these results confirm that cA4-binding by the CARF domain allosterically regulates the nuclease activity of the C-terminal HEPN domain in SyCsx1.

To narrow down the substrate specificity of SyCsx1, we analyzed the cleavage of single (ss) and double-stranded (ds) RNA and DNA substrates (Figure 3A). Denaturing PAA gel electrophoresis revealed that in the presence of cA4 only the ssRNA substrate but neither dsRNA nor the DNA substrates were degraded. The accumulation of a distinct ssRNA cleavage product hints at a sequence-specific cleavage mechanism. To analyze the base specificity of SyCsx1, we performed cleavage assays with the 25mer homooligonucleotides poly(A/U/C/G). SyCsx1 degraded poly(C) completely within 120 min, while the other three homopolymers were stable in the presence of the protein (Figure 3B). These results demonstrate that Csx1 is a cA4-dependent ssRNA RNase with strict specificity for cytosine nucleotides.

SyCsm6 does not show RNase activity *in vitro*

The other CARF domain protein found in *Synechocystis* is SyCsm6. The respective ORF *sll7062* is transcribed as part of the CRISPR2 effector complex operon (Kopf et al., 2014). To determine enzymatic activity, recombinant His-tagged SyCsm6 was expressed and purified from *Escherichia coli*. In size exclusion chromatography, SyCsm6 (43.5 kDa) eluted at a volume corresponding to around ~72 kDa (Figure 4B), suggestive of dimer formation similar to SyCsx1 and other CARF domain proteins. First, we performed cleavage assays of purified SyCsm6 with *Synechocystis* total RNA in the presence or absence of cA4 and cA6. Separation of the reaction products on denaturing PAA gels did not reveal any degradation of total RNA (Figure 4C), implying that SyCsm6 does not possess RNase activity under the tested conditions. However, SyCsm6 does not encompass a HEPN domain at its C-terminus but a putative RelE-like effector domain. The *E. coli* toxin RelE and homologous proteins are ribosome-dependent endoribonucleases that inhibit translation, leading to growth arrest (Pedersen et al., 2003). Therefore, it is conceivable that SyCsm6 can degrade actively translated mRNA in a cOA-dependent manner *in vivo*.

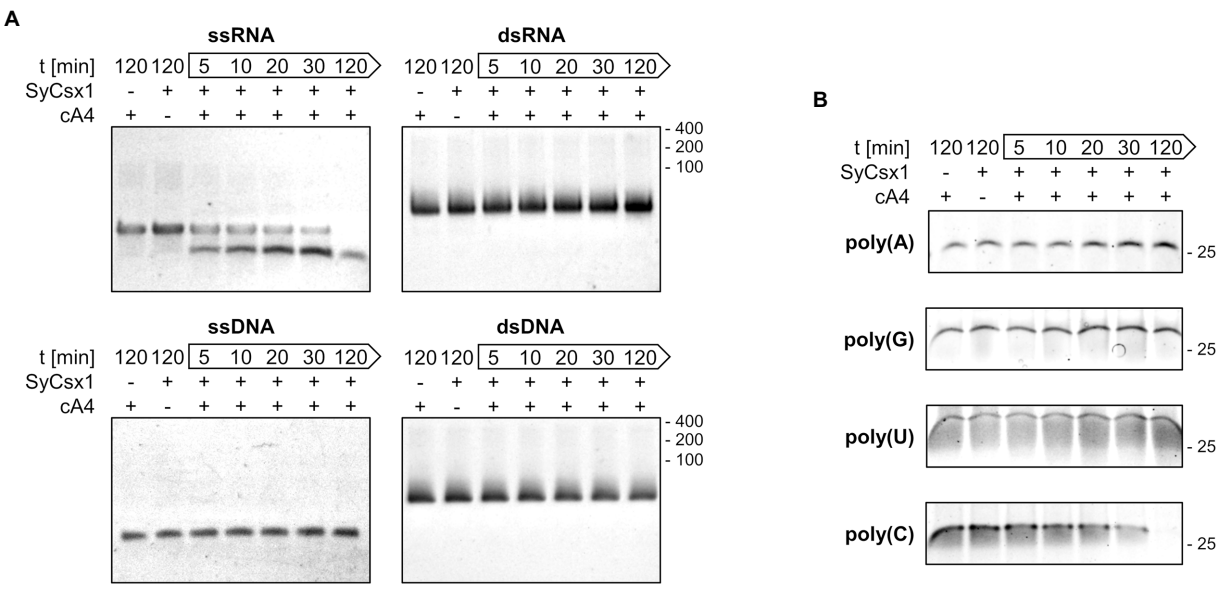

FIGURE 3
SyCsx1 is a single-strand-specific ribonuclease with a strict preference for cytosine bases. **(A)** Cleavage of 5 μM single- and double-stranded RNA or DNA oligonucleotides (40 nt) by SyCsx1 at 30°C after the addition of 300 nM cA4. 10 μl aliquots of were sampled at indicated time points, separated on 12% denaturing PAA gels, and stained with ethidium bromide. **(B)** 25 nt RNA-homopolymers were incubated with SyCsx1 and cA4 at 30°C and analyzed as before, except that SybrGold was used for staining.

10.3389/fmicb.2022.1046388

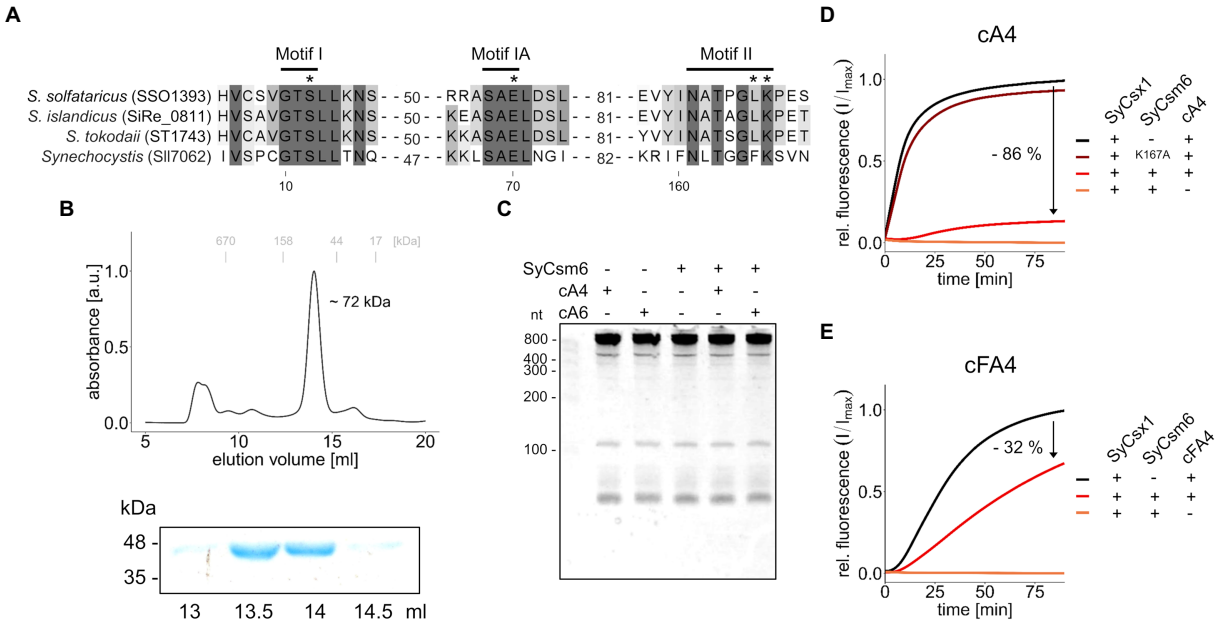

FIGURE 4
SyCsm6 has ring-nuclease activity but does not cleave RNA *in vitro*. **(A)** Multiple sequence alignment of SyCsm6 (Sll7062) and homologous Csm6/Crn1 proteins showing conserved CARF domain motives implicated in cOA-binding and cleavage. An asterisk marks residues that were shown or predicted to impact ring nuclease activity. **(B)** His-tagged SyCsm6 (43.5 kDa) was isolated from *E. coli* by affinity chromatography and further purified by size-exclusion chromatography on a Superdex 200 10/300 column (upper panel). Elution fractions were analyzed by SDS-PAGE (lower panel, see Supplementary Figure S1). **(C)** 400 ng of *Synechocystis* total RNA were incubated in the presence or absence of SyCsm6 and 300 nM cOAs for 1 h and subsequently separated on a 12% denaturing PAA gel. **(D)** A fluorogenic ribonuclease activity assay measuring RNA cleavage by SyCsx1 after pre-treatment of 30 pmol cA4 with either wild-type SyCsm6, the putatively inactive K167A variant, or a control without protein. After the pre-treatment for 60 min at 30°C and inactivation of SyCsm6 by heating to 95°C for 5 min, the reaction was started by adding SyCsx1 and 20 nm RNaseAlert substrate (excitation 490 nm; emission 520 nm). **(E)** The same assay as before using tetrafluoro-c-tetraAMP (cFA4) as the substrate. All fluorogenic assays were performed in triplicates and mean values of relative fluorescence normalized to the maximum substrate turnover are shown.

SyCsm6 is a ring nuclease degrading cOA

Sequence- and structure-based classification revealed that the CARF domain of SyCsm6 is similar to the corresponding domains of CRISPR ring nucleases 1 (Crn1) from crenarchaea of the genus *Sulfolobus* (Makarova et al., 2020b). A direct sequence comparison (Figure 4A) shows that critical residues in two motives implicated in ligand-binding (K167) and ring-nuclease activity (E70, S12) of cOA-degrading CARF-domain proteins are present in *Synechocystis* SyCsm6 (Athukoralage et al., 2018, 2019; Garcia-Doval et al., 2020; Makarova et al., 2020b). Hence, we speculated that SyCsm6 might have ring nuclease activity. To evaluate cOA degradation, we incubated cA4 with SyCsm6 and tested whether the pre-incubated cA4 could activate SyCsx1 in a cleavage assay. Figure 4D shows that after denaturation and removal of SyCsm6, the pre-treated cA4 sample activated SyCsx1 to a much lower extent compared to a cA4 sample receiving only a mock treatment. In contrast, complete SyCsx1 activation and therefore no putative cleavage of cA4 was observed when the cyclic molecule was pre-treated with the SyCsm6(K167A) variant. This lysine residue is thought to be crucial for cA4 binding. This is in line with data from *Sulfolobus solfataricus* showing that the corresponding mutation in Sso1393 leads to a catalytic inactive enzyme (Athukoralage et al., 2018). To further validate that the differences in SyCsx1 activation are linked to cA4 degradation, the assays were repeated with the cA4 analog tetrafluoro-c-tetraAMP (cFA4) that is resistant to cleavage. Overall, cFA4 is a less potent activator of SyCsx1 as seen by the slower substrate turnover (Figure 4E). This is consistent with data showing that the 2′-fluoro modifications in hexafluoro-c-hexaAMP (cFA6) lead to a weaker activation of Csm6 from *Enterococcus italicus*, likely due to lower binding affinity of the modified activator (Garcia-Doval et al., 2020). Importantly, pre-incubation with active SyCsm6 decreases the ability of cFA4 to activate SyCsx1 much less when compared to unmodified cA4 implying that the observed effect is caused by cOA cleavage.

To identify potential cleavage products, we analyzed the turnover of cOAs by liquid chromatography coupled with high-resolution mass spectrometry. After incubating cA4 for 120 min with SyCsm6, the substrate peak was gone and cA4 was converted to a product with a retention time of 7.8 min. This was identified as a linear diadenylate with a cyclic 2′,3 terminus (A2 > P), as we were able to show high agreement in the fragment pattern as well as in the exact mass, drift time, collision cross-section (CCS) value and retention time compared to a standard (Supplementary Figure S2). Similarly, cA6 was cleaved to A2 > P

and an additional product. This is likely a triadenylate as it has the exact mass as well as drift time and CCS value as a c-tri-AMP standard (Supplementary Figure S3). However, it differs in both the retention time and fragment spectra and we speculate that it is the linear form carrying a 2′,3′-cyclic phosphate group (A3 > P). No accumulation of these cleavage products of cA4 or cA6 were observed when these substrates were incubated with the SyCsm6(K167A) mutant (Supplementary Figure S4). Together, these results indicate that SyCsm6 catalyzes cOA cleavage producing the same linear An>P forms that are generated by the CARF domain of stand-alone ring nucleases and self-inactivating Csm6 homologs (Athukoralage et al., 2018; Garcia-Doval et al., 2020; Smalakyte et al., 2020).

Discussion

A new mechanism by which CRISPR systems provide immunity against invading genetic elements has emerged in the past few years. Studies in different bacteria and archaea have shown how type III CRISPR-mediated cOA signaling activates ancillary nucleases that enhance antiviral defense and how enzymes with ring nuclease activity cleave cOA to switch off these nonspecific nucleases to facilitate cell recovery (Athukoralage and White, 2021). To our knowledge, cOA signaling *via* type III CRISPR systems was not shown for cyanobacteria yet, though these phototrophic bacteria are very rich in various type III CRISPR systems (Makarova et al., 2015; Shah et al., 2019). Here we characterized two ancillary CRISPR proteins in a cyanobacterial model organism and showed that cyanobacteria encode proteins that harbor enzymatic activities required for cOA-mediated defense against invading genetic elements.

SyCsx1 is a CARF-family effector protein harboring a HEPN domain with RNase activity specifically activated by cA4 but not by cA6 (Figures 2C–E). While we cannot exclude activation by cyclic nucleotides of different sizes, most characterized CARF domain effectors specifically recognize one of these two second messengers (Kazlauskiene et al., 2017; Niewoehner et al., 2017; Rouillon et al., 2018; Molina et al., 2019; Garcia-Doval et al., 2020; McMahon et al., 2020). Although there is no experimental evidence that cA4 is synthesized by the Cas10 homolog of the CRISPR2 (III-D) system in *Synechocystis*, sequence analysis indicates that it harbors conserved Palm1 and Palm2 domains which are required for cOA synthesis (Supplementary Figure S5; Kazlauskiene et al., 2017; Niewoehner et al., 2017; You et al., 2019; Jia et al., 2019a). In addition, it is plausible that the Cas10 homolog of the CRISPR3 (III-B) system generates cOAs. Once activated, SyCsx1 specifically degrades single-stranded RNA with a stark preference for phosphodiester bonds involving cytosine nucleotides (Figure 3). Such nucleotide-specificity is known from other Csx1/Csm6-family effectors. For example, Molina et al. (2019) reported that SisCsx1 exhibits a strong preference for cleaving 5'-C-C-3′ dinucleotides. Other effectors like SthCsm6 and *Staphylococcus epidermidis* Csm6 showed a preference for cleaving after purines (Kazlauskiene et al., 2017; Foster et al., 2019) or are specific for adenosines (e.g., PfuCsx1 and TonCsm6; Sheppard et al., 2016; Jia et al., 2019b). Considering that SyCsx1 favors cytosine residues but cuts an ssRNA substrate that contains no long C-stretches, we can assume that SyCsx1 cuts before/after cytosine or in between CC dinucleotides. Favoring only one or two nucleotides makes SyCsx1 a mostly sequence-unspecific endoribonuclease that will target most cellular RNAs. We can only speculate that the observed nucleotide preference of SyCsx1 and other effectors is related to a difference in base composition of typically encountered invading genetic elements and essential host mRNAs. As the Cas10 homolog of CRISPR2 is missing the HD nuclease domain, which is cleaving single-stranded DNA during interference in canonical type III systems, it is tempting to speculate that the CRISPR2 system might depend on SyCsx1 activity for clearing invader sequences that are not complementary to the targeting crRNA. *S. solfataricus* Csx1 which binds cA4 with a dissociation constant (KD) of 130 ± 20 nM has a multiple-turnover kinetic constant (k_{cat}) for cA4-activated RNA cleavage of 0.44 ± 0.03 min^{-1} (Athukoralage et al., 2020b). As we did not aim at measuring kinetic parameters of SyCsx1 activity in detail, we are not able to compare the activities of both proteins directly. However, we do not have evidence that the cyanobacterial Csx1 behaves very different from the archaeal one.

Our results clearly demonstrate that SyCsm6 has ring-nuclease activity and can degrade cOAs, similar to other Csm6 family RNases that have a CARF domain and act as a dual cOA sensor and ring nuclease (Athukoralage et al., 2019; Jia et al., 2019b; Garcia-Doval et al., 2020; Smalakyte et al., 2020). While SyCsx1 is specifically activated by cA4, the CARF domain of SyCsm6 is apparently less specific as it binds and cleaves cOAs of various lengths. Such indiscriminate activity by the CARF domain was not observed in a previous study on Csm6 from *Streptococcus thermophilus* which showed specificity for cA6 (Smalakyte et al., 2020). The homology of the SyCsm6 CARF domain to Crn1-like ring-nucleases (Figure 4A) and the appearance of typical An>P cleavage products (Supplementary Figure S3) suggest that the CARF-domain catalyzes the cleavage of its cOA ligands. Nonetheless, we cannot definitely exclude a role of the RelE domain in cOA cleavage. As the CRISPR2 (III-D) system in *Synechocystis* does not encode any other obvious ring nuclease, SyCsm6 activity is likely the main "off-switch" that controls SyCsx1 activity by eliminating excess cOAs.

The absence of *in vitro* RNase activity in SyCsm6, should not be generalized. Considering the ribosome-dependent cleavage mechanism of *E. coli* RelE (Christensen and Gerdes, 2003; Pedersen et al., 2003; Neubauer et al., 2009), one could speculate that the SyCsm6 RelE domain can degrade actively translated mRNAs *in vivo* in a cOA-dependent manner. Nonetheless, this is purely speculative, as no CARF-RelE domain proteins have been characterized *in vivo* so far. Taken together, SyCsm6 is possibly a bifunctional, self-inactivating effector protein that minimizes self-toxicity.

Gradient profiling experiments suggest that SyCsx1 and SyCsm6 are part of the same complex (Riediger et al., 2021). Both proteins were shown to sediment together with crRNAs and ancillary proteins from the CRISPR2-system after separation of a whole cell extract in sucrose density gradient centrifugation. Hence, we suspect that in *Synechocystis*, the CARF-domain proteins are in close proximity to each other and to the Cas10 effector complex. Such a close association could facilitate invader clearance by ensuring timely activation and termination of cOA signaling and spatially limiting unspecific RNase activity.

The CRISPR2 (III-D) system of *Synechocystis* harbors required enzymatic functions for a functional cA4-mediated defense mechanism. Intriguingly, the CRISPR3 (III-B) system is a putative source of additional cOA synthesis and encompasses a gene (*slr7080*) that encodes a putative metal-dependent Csx3/Crn3 ring-nuclease domain (Slr7080) fused to an AAA+ ATPase domain with an uncharacterized cellular function (Shah et al., 2019; Athukoralage et al., 2020a). While both systems could rely on mutual exclusive cOAs, there is the potential for cross-talk between both systems to coordinate defense against invading genetic elements.

Materials and methods

Heterologous overexpression and purification of SyCsx1 and SyCsm6 in *Escherichia coli*

The gene sequences of *slr7061* (SyCsx1) and *sll7062* (SyCsm6) were amplified from *Synechocystis* genomic DNA, ligated into the pQE-80 vector by T4 DNA Ligase (NEB), and propagated in *E. coli* DH5α competent cells. Variants of SyCsx1 and SyCsm6 were generated by site-directed mutagenesis using fast cloning (Li et al., 2011) and verified by sequencing. Primers used in this study are shown in Supplementary Table S1. For overexpression of His-tagged proteins, BL21 (DE3) *E. coli* cells were transformed with the respective plasmids. Expression was induced with 1 mM isopropyl β-D-1-thiogalactopyranoside (IPTG) at an OD_{600nm} of ~0.6. Proteins were expressed overnight at 18°C in the case of SyCsx1 variants and 25°C for SyCsm6 variants. Cells were harvested by centrifugation at 4,000 × g at 4°C for 15 min, and pellets were resuspended in lysis buffer (50 mM Tris pH 8.0, 150 mM NaCl) supplemented with protease inhibitors (4 mM p-aminobenzamidine and 40 mM 6-aminohexaonic acid), and subsequently lysed by a French press. Cell lysates were centrifuged at 20,000 × g for 30 min at 4°C, and supernatants were filtered and loaded on Ni-NTA gravity columns (QIAGEN). After washing with lysis buffer supplemented with 10 mM imidazole, proteins were eluted with lysis buffer containing 200 mM imidazole. For further purification, the elution fractions were applied to size exclusion chromatography with a Superdex 200 10/300 column (GE Healthcare) in lysis buffer supplemented with 5% glycerol. Finally, all proteins were concentrated, aliquoted, flash-frozen with liquid nitrogen, and stored at −80°C.

Gel-based cleavage assays

Synthetic RNA and DNA oligos used in this study are listed in Supplementary Table S1. To hybridize dsRNA and dsDNA substrates, complementary oligos (RNA1/RNA2, DNA1/DNA2) were mixed in a 1:1 molar ratio in annealing buffer (10 mM HEPES pH 7.5, 50 mM NaCl, and 1 mM EDTA), heated for 5 min at 95°C, and cooled down (1°C per minute) to 25°C. Substrate specificity was determined by incubating 300 nM SyCsx1 with 5 μM substrate in reaction buffer (50 mM HEPES pH7.5, 50 mM KCl, 1 mM DTT, 300 nM cA4) at 30°C. The reaction was stopped at the indicated timepoints by adding 2 × RNA loading dye (New England Biolabs). To investigate sequence specificity, 25 nt RNA homoribopolymers (800 pmol with the exception of 25 pmol for poly(G)) were cleaved in the same way. 20 μl of the samples were heated for 10 min at 65°C and then separated by 12% PAA gel in 1× TBE (100 mM Tris borate pH 8.3, 20 mM EDTA,) at 120 V for 2 h. Nucleic acids were visualized using either SYBR Gold or ethidium bromide.

Fluorescence-based SyCsx1 activity assay

To measure SyCsx1 activity, 300 nM SyCsx1 or its mutant variants were mixed with 300 nM cA4 (Biolog Life Science Institute GmbH & Co. KG, Germany) in reaction buffer in a total volume of 100 μl. The mix was heated to 30°C and the reaction was started by adding 40 nM of RNaseAlert substrate (Integrated DNA Technologies). The fluorescence signal (excitation at 490 nm, emission at 520 nm) was continuously measured in a TECAN Infinite 200 plate reader.

The influence of SyCsm6 on SyCsx1 activity was determined by pre-incubating 20 nM cA4 or cFA4 (Biolog Life Science Institute GmbH & Co. KG, Germany) with 500 nM SyCsm6 or its mutant variant in reaction buffer at 30°C for 60 min. The reaction was stopped by heating the sample to 95°C for 5 min and denatured SyCsm6 was removed by centrifugation (20,000 × g for 5 min). Subsequently, the sample was used to activate the cleavage of 20 nM RNaseAlert substrate by 300 nM SyCsx1 in a total volume of 100 μl as before.

LC–MS analysis of cOA degradation products

The degradation of cA4 or cA6 (final concentration of 667 nM) was assayed by incubation of the substrates with 2 μM SyCsm6 or the K167A mutant at 30°C for 2 h in a total volume of 300 μl. The degradation products were extracted in 1.2 ml extraction solution (50:50 (v/v) acetonitrile and methanol, HPLC

grade). All samples were incubated for 15 min on ice, then heated to 95°C for 10 min, and immediately placed on ice. Precipitated proteins were removed by centrifugation (20,000 × g, 10 min at 4°C). The resulting final supernatants were dried in a speed-vac at 42°C. The residual pellet was resolved in 200 µl HPLC grade water (J.T. Baker, Deventer, The Netherlands). Then, 40 µl of the sample was mixed with 40 µl of water containing the internal standards (200 ng/ml $^{13}C_20^{15}N_{10}$-c-di-GMP, 200 ng/ml $^{13}C_20^{15}N_{10}$-c-di-AMP, and 100 ng/ml Tenofovir) and transferred to measuring vials.

For the identification of the cA4 and cA6 products, a LC–MS-IMS-qTOF experiment was performed on a ACQUITY UPLC I-Class/Vion IMS-QTOF high resolution LC–MS system (Waters Corporation, Milford, MA, USA). Therefore, a C18 column (Nucleodur Pyramid C18 3 µ 50 × 3 mm; Macherey Nagel, Düren, Germany) connected to a C18 security guard (Phenomenex, Aschaffenburg, Germany) and a 2 µm column saver was used. The column was kept at 50°C. A binary gradient of water containing 10 mM ammonium acetate (solvent A) and methanol (solvent B) was applied to achieve chromatographic separation of the analytes using a flow rate of 0.4 ml/min during the whole chromatographic run. The eluting program was as follows: 0 to 4 min: 0% B, 4 to 7.3 min: 0 to 10% B. This composition was hold for 1 min. Then the organic content was increased to 90% within 10.7 min followed by a 6 min re-equilibration step with 0% B. Total analysis run time was 25 min. High resolution mass spectrometry data were collected on a Vion IMS-QTOF mass spectrometer equipped with an electrospray ionization source (ESI). The ESI was operating in positive ionization mode using a capillary voltage of 2.5 kV and the cone voltage of 40 V. The source temperature and desolvation gas temperature was set at 150°C and 600°C, respectively. Analyte fragmentation was achieved using nitrogen as collision gas. Collision energy of 10 V was used to obtain a low collision energy spectrum. For high collision energy spectrum, the collision energy was ramped from 21 to 42 V. Mass to charge ratios between 50 and 2000 were collected. Data acquisition was controlled by the UNIFI 1.9.4.0 software (Waters). For metabolite identification, the retention times, drift times, CCS value and fragment spectra of a c-tri-AMP- and a A(3′,5′)pA(2′,3′)cp-standard were collected as a reference and compared to those of the suspected products in the samples.

Data availability statement

The original contributions presented in the study are included in the article/Supplementary materials, further inquiries can be directed to the corresponding author.

Author contributions

AW, NS, JD designed the study. JD and NS performed experiments, analyzed the data and wrote the first draft of the manuscript. HB conducted the LC–MS analysis. All authors contributed to the article and approved the submitted version.

Funding

This work was supported by the Deutsche Forschungsgemeinschaft (grant AW 2014/9-1 to AW) within the priority program "Much more than defense: The multiple functions and facets of CRISPR-Cas" (SPP2141). We acknowledge support by the Open Access Publication Fund of the University of Freiburg (Germany).

Acknowledgments

We would like to thank W.R. Hess and R. Bilger for fruitful discussions and preliminary data that was not included in the final manuscript.

Conflict of interest

The authors declare that the research was conducted in the absence of any commercial or financial relationships that could be construed as a potential conflict of interest.

Publisher's note

Supplementary material

The Supplementary material for this article can be found online at: https://www.frontiersin.org/articles/10.3389/fmicb.2022.1046388/full#supplementary-material

References

Anantharaman, V., Makarova, K. S., Burroughs, A. M., Koonin, E. V., and Aravind, L. (2013). Comprehensive analysis of the HEPN superfamily: identification of novel roles in intra-genomic conflicts, defense, pathogenesis and RNA processing. *Biol. Direct* 8:15. doi: 10.1186/1745-6150-8-15

Athukoralage, J. S., Graham, S., Grüschow, S., Rouillon, C., and White, M. F. (2019). A type III CRISPR ancillary ribonuclease degrades its cyclic Oligoadenylate activator. *J. Mol. Biol.* 431, 2894–2899. doi: 10.1016/j.jmb.2019.04.041

Athukoralage, J. S., Graham, S., Rouillon, C., Grüschow, S., Czekster, C. M., and White, M. F. (2020b). The dynamic interplay of host and viral enzymes in type III CRISPR-mediated cyclic nucleotide signalling. *eLife* 9:e55852. doi: 10.7554/eLife.55852

Athukoralage, J. S., McQuarrie, S., Grüschow, S., Graham, S., Gloster, T. M., and White, M. F. (2020a). Tetramerisation of the CRISPR ring nuclease Crn3/Csx3 facilitates cyclic oligoadenylate cleavage. *eLife* 9:e57627. doi: 10.7554/eLife.57627

Athukoralage, J. S., Rouillon, C., Graham, S., Grüschow, S., and White, M. F. (2018). Ring nucleases deactivate type III CRISPR ribonucleases by degrading cyclic oligoadenylate. *Nature* 562, 277–280. doi: 10.1038/s41586-018-0557-5

Athukoralage, J. S., and White, M. F. (2021). Cyclic oligoadenylate signaling and regulation by ring nucleases during type III CRISPR defense. *RNA* 27, 855–867. doi: 10.1261/rna.078739.121

Behler, J., Sharma, K., Reimann, V., Wilde, A., Urlaub, H., and Hess, W. R. (2018). The host-encoded RNase E endonuclease as the crRNA maturation enzyme in a CRISPR–Cas subtype III-Bv system. *Nat. Microbiol.* 3, 367–377. doi: 10.1038/s41564-017-0103-5

Christensen, S. K., and Gerdes, K. (2003). RelE toxins from bacteria and archaea cleave mRNAs on translating ribosomes, which are rescued by tmRNA. *Mol. Microbiol.* 48, 1389–1400. doi: 10.1046/j.1365-2958.2003.03512.x

Elmore, J. R., Sheppard, N. F., Ramia, N., Deighan, T., Li, H., Terns, R. M., et al. (2016). Bipartite recognition of target RNAs activates DNA cleavage by the type III-B CRISPR-Cas system. *Genes Dev.* 30, 447–459. doi: 10.1101/gad.272153.115

Foster, K., Kalter, J., Woodside, W., Terns, R. M., and Terns, M. P. (2019). The ribonuclease activity of Csm6 is required for anti-plasmid immunity by type III-A CRISPR-Cas systems. *RNA Biol.* 16, 449–460. doi: 10.1080/15476286.2018.1493334

Garcia-Doval, C., Schwede, F., Berk, C., Rostøl, J. T., Niewoehner, O., Tejero, O., et al. (2020). Activation and self-inactivation mechanisms of the cyclic oligoadenylate-dependent CRISPR ribonuclease Csm6. *Nat. Commun.* 11:1596. doi: 10.1038/s41467-020-15334-5

Griffin, M. A., Davis, J. H., and Strobel, S. A. (2013). Bacterial toxin RelE: a highly efficient ribonuclease with exquisite substrate specificity using atypical catalytic residues. *Biochemistry* 52, 8633–8642. doi: 10.1021/bi401325c

Hein, S., Scholz, I., Voss, B., and Hess, W. R. (2013). Adaptation and modification of three CRISPR loci in two closely related cyanobacteria. *RNA Biol.* 10, 852–864. doi: 10.4161/rna.24160

Jia, N., Jones, R., Sukenick, G., and Patel, D. J. (2019a). Second messenger cA4 formation within the composite Csm1 palm pocket of type III-A CRISPR-Cas Csm complex and its release path. *Mol. Cell* 75, 933–943.e6. doi: 10.1016/j.molcel.2019.06.013

Jia, N., Jones, R., Yang, G., Ouerfelli, O., and Patel, D. J. (2019b). CRISPR-Cas III-A Csm6 CARF domain is a ring nuclease triggering stepwise cA4 cleavage with ApA>p formation terminating RNase activity. *Mol. Cell* 75, 944–956.e6. doi: 10.1016/j.molcel.2019.06.014

Jiang, W., Samai, P., and Marraffini, L. A. (2016). Degradation of phage transcripts by CRISPR-associated RNases enables type III CRISPR-Cas immunity. *Cells* 164, 710–721. doi: 10.1016/j.cell.2015.12.053

Kazlauskiene, M., Kostiuk, G., Venclovas, Č., Tamulaitis, G., and Siksnys, V. (2017). A cyclic oligonucleotide signaling pathway in type III CRISPR-Cas systems. *Science* 357, 605–609. doi: 10.1126/science.aao0100

Kazlauskiene, M., Tamulaitis, G., Kostiuk, G., Venclovas, Č., and Siksnys, V. (2016). Spatiotemporal control of type III-A CRISPR-Cas immunity: coupling DNA degradation with the target RNA recognition. *Mol. Cell* 62, 295–306. doi: 10.1016/j.molcel.2016.03.024

Kim, Y. K., Kim, Y.-G., and Oh, B.-H. (2013). Crystal structure and nucleic acid-binding activity of the CRISPR-associated protein Csx1 of Pyrococcus furiosus. *Proteins* 81, 261–270. doi: 10.1002/prot.24183

Kopf, M., Klähn, S., Scholz, I., Matthiessen, J. K. F., Hess, W. R., and Voss, B. (2014). Comparative analysis of the primary transcriptome of *Synechocystis* sp. PCC 6803. *DNA Res.* 21, 527–539. doi: 10.1093/dnares/dsu018

Li, C., Wen, A., Shen, B., Lu, J., Huang, Y., and Chang, Y. (2011). FastCloning: a highly simplified, purification-free, sequence- and ligation-independent PCR cloning method. *BMC Biotechnol.* 11:92. doi: 10.1186/1472-6750-11-92

Makarova, K. S., Timinskas, A., Wolf, Y. I., Gussow, A. B., Siksnys, V., Venclovas, Č., et al. (2020b). Evolutionary and functional classification of the CARF domain superfamily, key sensors in prokaryotic antivirus defense. *Nucleic Acids Res.* 48, 8828–8847. doi: 10.1093/nar/gkaa635

Makarova, K. S., Wolf, Y. I., Alkhnbashi, O. S., Costa, F., Shah, S. A., Saunders, S. J., et al. (2015). An updated evolutionary classification of CRISPR–Cas systems. *Nat. Rev. Microbiol.* 13, 722–736. doi: 10.1038/nrmicro3569

Makarova, K. S., Wolf, Y. I., Iranzo, J., Shmakov, S. A., Alkhnbashi, O. S., Brouns, S. J. J., et al. (2020a). Evolutionary classification of CRISPR–Cas systems: a burst of class 2 and derived variants. *Nat. Rev. Microbiol.* 18, 67–83. doi: 10.1038/s41579-019-0299-x

Marraffini, L. A. (2015). CRISPR-Cas immunity in prokaryotes. *Nature* 526, 55–61. doi: 10.1038/nature15386

McMahon, S. A., Zhu, W., Graham, S., Rambo, R., White, M. F., and Gloster, T. M. (2020). Structure and mechanism of a type III CRISPR defence DNA nuclease activated by cyclic oligoadenylate. *Nat. Commun.* 11:500. doi: 10.1038/s41467-019-14222-x

Mohanraju, P., Makarova, K. S., Zetsche, B., Zhang, F., Koonin, E. V., and van der Oost, J. (2016). Diverse evolutionary roots and mechanistic variations of the CRISPR-Cas systems. *Science* 353:aad5147. doi: 10.1126/science.aad5147

Molina, R., Stella, S., Feng, M., Sofos, N., Jauniskis, V., Pozdnyakova, I., et al. (2019). Structure of Csx1-cOA(4) complex reveals the basis of RNA decay in type III-B CRISPR-Cas. *Nat. Commun.* 10:4302. doi: 10.1038/s41467-019-12244-z

Neubauer, C., Gao, Y.-G., Andersen, K. R., Dunham, C. M., Kelley, A. C., Hentschel, J., et al. (2009). The structural basis for mRNA recognition and cleavage by the ribosome-dependent endonuclease RelE. *Cells* 139, 1084–1095. doi: 10.1016/j.cell.2009.11.015

Niewoehner, O., Garcia-Doval, C., Rostøl, J. T., Berk, C., Schwede, F., Bigler, L., et al. (2017). Type III CRISPR–Cas systems produce cyclic oligoadenylate second messengers. *Nature* 548, 543–548. doi: 10.1038/nature23467

Pedersen, K., Zavialov, A. V., Pavlov, M. Y., Elf, J., Gerdes, K., and Ehrenberg, M. (2003). The bacterial toxin RelE displays codon-specific cleavage of mRNAs in the ribosomal a site. *Cells* 112, 131–140. doi: 10.1016/S0092-8674(02)01248-5

Reimann, V., Alkhnbashi, O. S., Saunders, S. J., Scholz, I., Hein, S., Backofen, R., et al. (2017). Structural constraints and enzymatic promiscuity in the Cas6-dependent generation of crRNAs. *Nucleic Acids Res.* 45, 915–925. doi: 10.1093/nar/gkw786

Riediger, M., Spät, P., Bilger, R., Voigt, K., Maček, B., and Hess, W. R. (2021). Analysis of a photosynthetic cyanobacterium rich in internal membrane systems via gradient profiling by sequencing (grad-seq). *Plant Cell* 33, 248–269. doi: 10.1093/plcell/koaa017

Rostøl, J. T., and Marraffini, L. A. (2019). Non-specific degradation of transcripts promotes plasmid clearance during type III-A CRISPR–Cas immunity. *Nat. Microbiol.* 4, 656–662. doi: 10.1038/s41564-018-0353-x

Rouillon, C., Athukoralage, J. S., Graham, S., Grüschow, S., and White, M. F. (2018). Control of cyclic oligoadenylate synthesis in a type III CRISPR system. *eLife* 7:e36734. doi: 10.7554/eLife.36734

Samai, P., Pyenson, N., Jiang, W., Goldberg, G. W., Hatoum-Aslan, A., and Marraffini, L. A. (2015). Co-transcriptional DNA and RNA cleavage during type III CRISPR-Cas immunity. *Cells* 161, 1164–1174. doi: 10.1016/j.cell.2015.04.027

Scholz, I., Lange, S. J., Hein, S., Hess, W. R., and Backofen, R. (2013). CRISPR-Cas Systems in the Cyanobacterium *Synechocystis* sp. PCC6803 exhibit distinct processing pathways involving at least two Cas6 and a Cmr2 protein. *PLoS One* 8, 8:e56470. doi: 10.1371/journal.pone.0056470

Shah, S. A., Alkhnbashi, O. S., Behler, J., Han, W., She, Q., Hess, W. R., et al. (2019). Comprehensive search for accessory proteins encoded with archaeal and bacterial type III CRISPR-cas gene cassettes reveals 39 new *cas* gene families. *RNA Biol.* 16, 530–542. doi: 10.1080/15476286.2018.1483685

Sheppard, N. F., Glover, C. V. C. 3rd, Terns, R. M., and Terns, M. P. (2016). The CRISPR-associated Csx1 protein of *Pyrococcus furiosus* is an adenosine-specific endoribonuclease. *RNA* 22, 216–224. doi: 10.1261/rna.039842.113

Smalakyte, D., Kazlauskiene, M. F., Havelund, J., Rukšėnaitė, A., Rimaite, A., Tamulaitiene, G., et al. (2020). Type III-A CRISPR-associated protein Csm6 degrades cyclic hexa-adenylate activator using both CARF and HEPN domains. *Nucleic Acids Res.* 48, 9204–9217. doi: 10.1093/nar/gkaa634

Sorek, R., Lawrence, C. M., and Wiedenheft, B. (2013). CRISPR-mediated adaptive immune systems in bacteria and archaea. *Annu. Rev. Biochem.* 82, 237–266. doi: 10.1146/annurev-biochem-072911-172315

You, L., Ma, J., Wang, J., Artamonova, D., Wang, M., Liu, L., et al. (2019). Structure studies of the CRISPR-Csm complex reveal mechanism of co-transcriptional interference. *Cells* 176, 239–253.e16. doi: 10.1016/j.cell.2018.10.052

frontiers | Frontiers in Microbiology

TYPE Review
PUBLISHED 18 November 2022
DOI 10.3389/fmicb.2022.1034471

OPEN ACCESS

EDITED BY
Srinivasan Ramanathan,
Prince of Songkla University, Thailand

REVIEWED BY
Sanjay Kumar Singh Patel,
Konkuk University, South Korea
Gausiya Bashri,
Aligarh Muslim University,
India

*CORRESPONDENCE
Prashant Kumar Singh
prashantbotbhu@gmail.com
Mukesh Kumar Yadav
mukiyadav@gmail.com
Suryakant Mehta
skmehta12@rediffmail.com

SPECIALITY SECTION:
This article was submitted to Microbiotechnology, a section of the journal Frontiers in Microbiology

RECEIVED 01 September 2022
ACCEPTED 18 October 2022
PUBLISHED 18 November 2022

CITATION
Kar J, Ramrao DP, Zomuansangi R, Lalbiaktluangi C, Singh SM, Joshi NC, Kumar A, Kaushalendra, Mehta S, Yadav MK and Singh PK (2022) Revisiting the role of cyanobacteria-derived metabolites as antimicrobial agent: A 21st century perspective.
Front. Microbiol. 13:1034471.
doi: 10.3389/fmicb.2022.1034471

Revisiting the role of cyanobacteria-derived metabolites as antimicrobial agent: A 21st century perspective

Joyeeta Kar[1], Devde Pandurang Ramrao[1], Ruth Zomuansangi[1], C. Lalbiaktluangi[1], Shiv Mohan Singh[2], Naveen Chandra Joshi[3], Ajay Kumar[4], Kaushalendra[5], Suryakant Mehta[6]*, Mukesh Kumar Yadav[1]* and Prashant Kumar Singh[1]*

[1]Department of Biotechnology, Mizoram University (A Central University), Pachhunga University College Campus, Aizawl, Mizoram, India, [2]Centre of Advanced Studies in Botany, Institute of Science, Banaras Hindu University, Varanasi, India, [3]Amity Institute of Microbial Technology (AIMT), Amity University, Noida, Uttar Pradesh, India, [4]Agriculture Research Organization (ARO) - The Volcani Center, Rishon LeZion, Israel, [5]Department of Zoology, Mizoram University (A Central University), Pachhunga University College Campus, Aizawl, Mizoram, India, [6]Department of Botany, Mizoram University, Aizawl, India

Cyanobacterial species are ancient photodiazotrophs prevalent in freshwater bodies and a natural reservoir of many metabolites (low to high molecular weight) such as non-ribosomal peptides, polyketides, ribosomal peptides, alkaloids, cyanotoxins, and isoprenoids with a well-established bioactivity potential. These metabolites enable cyanobacterial survival in extreme environments such as high salinity, heavy metals, cold, UV-B, etc. Recently, these metabolites are gaining the attention of researchers across the globe because of their tremendous applications as antimicrobial agents. Many reports claim the antimicrobial nature of these metabolites; unfortunately, the mode of action of such metabolites is not well understood and/or known limited. Henceforth, this review focuses on the properties and potential application, also critically highlighting the possible mechanism of action of these metabolites to offer further translational research. The review also aims to provide a comprehensive insight into current gaps in research on cyanobacterial biology as antimicrobials and hopes to shed light on the importance of continuing research on cyanobacteria metabolites in the search for novel antimicrobials.

KEYWORDS

antimicrobial, bioactivity, cyanobacteria, metabolites, signaling

Introduction

Cyanobacteria are the photodizaotrophic, oxygen-producing microbes on earth that have gained increasing attention in natural product research. Their ubiquity in the light-exposed biosphere is based on a considerable repertoire of survival strategies for withstanding challenging environments and protecting their niches against

competitors. To this end, cyanobacteria produce a wide range of secondary metabolites, often with a unique composition and specialized functions, which mediate various processes, such as chemical defence, preservation, and quorum sensing. Moreover, various metabolites with diverse bioactivities have been reported in cyanobacteria (Brilisauer et al., 2019). Some of the known cyanobacterial metabolites exhibit antiviral, antibacterial, antifungal, or herbicidal activities, promising possible applications in human health, agriculture, or industry.

The omnipresent nature of these organisms makes them excellent material for investigation by physiologists, biochemists, ecologists, molecular biologists, and pharmacists (Nagle and Paul, 1998). These metabolites' productivity is highly species-specific and even strain-dependent (Leflaive and Ten-Hage, 2007). Because of their wide range of uses can be exploited to improve human health and sustainable living practices.

Cyanobacteria metabolites can be a gold mine for the modern healthcare industry and clinical applications. With the onset of the global pandemic we are recently facing, we are also facing the silent pandemic of antibiotic resistance. It has been estimated that 1.27 million deaths in 2019 were directly due to antibiotic-resistant infection (Murray et al., 2022). This can be attributed to the excess use of antibiotics and insufficient access to certain geographical locations (Laxminarayan, 2022). Despite the presence of vaccines, overuse of antibiotics has led to an alarming increase in antibiotic resistance among the population in recent years. Humans are susceptible to microbial pathogens such as *Escherichia coli, Staphylococcus aureus, Klebsiella pneumoniae, Pseudomonas aeruginosa, candida albicans* etc.

Furthermore, secondary infections are common in patients hospitalized with viral infections both before and after hospitalizations (Singh et al., 2011). Cyanobacteria, one of the most primitive organisms with a rich array of bioactive compounds, have evolved to protect themselves against various pathogens. Exploiting cyanobacteria to find novel antivirals and antibiotics has become more evident than ever, especially since the onset of the pandemic of Covid-19, which showed our ill-preparedness and the extreme burden on healthcare facilities across the globe. Covid-19, like other viruses, can constantly mutate, resulting in the formation of new variants such as alpha (B.1.1.7), beta (B.1.351), gamma (P.1) variants, delta (B.1.617.2) variant, Theta (P.3) variant, Lambda (C.37) variant and omicron (B.1.1.529; Vasireddy et al., 2021). These new variants have critical mutations which increase their transmissibility, infectivity, contagiousness as well as their lethality, which further necessitates the need for novel antivirals (Thakur et al., 2021).

Antibiotic-resistant microbial infections can be managed by finding novel drug discoveries, and cyanobacteria metabolites could be potential candidates (Adamson et al., 2021). For example, diterpenoid noscomin, a terpene compound isolated from *Nostoc commune*, has potent activity against pathogenic microbes like *Staphylococcus epidermidis* and *Escherichia coli* (Jaki et al., 1999). Another example is calothrixin A, an alkaloid isolated from *Calothrix* sp., which inhibits different bacteria by inhibiting bacterial RNA polymerase (Doan et al., 2000).

Considering the usability of cyanobacteria across various industries, this review aims to focus on the findings on cyanobacteria as a source of novel antimicrobials and their mechanism of action against pathogens to mitigate to issue of dwindling novel antimicrobial discovery.

Cyanobacterial metabolites as novel antibacterial agents

The growing antibacterial resistance or bacterial antimicrobial resistance (AMR), which has been declared a silent pandemic, is one of the significant threats to public health. If left unchecked, they can prove to be far more lethal in coming years, so an urgent course of action needs to be taken to control their spread and discover newer drugs that can combat the growing resistance to the present (Murray et al., 2022). Cyanobacteria has emerged as a promising source for novel antibacterials with many antibacterial compounds. The antibacterial properties have been attributed to various combinations, namely alkaloids, terpenes, polyketides, lipids, peptides, etc. (Rojas et al., 2020). For example, Malyngolide, a polyketide isolated from *Lyngbya majuscule,* has been found to inhibit the growth of various pathogenic bacteria by inhibiting the quorum sensing system in the bacteria (Dobretsov et al., 2010; Kalia et al., 2019). Lipids like Lyngbyoic acid, pitinoic acid A, and doscadenamide A could also inhibit the quorum sensing system in *Pseudomonas aeruginosa* (Kwan et al., 2011; Montaser et al., 2011; Liang et al., 2019; Figure 1).

Alkaloids

Alkaloids are naturally occurring nitrogen-containing compounds having a large structural diversity. Cyanobacteria-derived alkaloids, mainly indole alkaloids, have been proven to be potent antimicrobials. A large number of alkaloid compounds were extracted from *Fischerella* sp. and are found to be effective against pathogens like *Staphylococcus aureus, Mycobacterium tuberculosis, Mycobacterium smegmatis, Bacillus anthracis, Bacillus subtilis, Staphylococcus aureus, Staphylococcus epidermis*, etc. (Ghasemi et al., 2004; Mo et al., 2010). The Hapalindole group of alkaloids were also obtained from cyanobacteria like *Hapalosiphon fontinalis* and *Fischerella sp.,* which are effective against *Staphylococcus* and *Streptococcus* species (Moore et al., 1987; Mo et al., 2009a). Another example of a potent antibacterial alkaloid is Calothrixin A obtained from *Calothrix sp.,* which can inhibit *Bacillus cereus, Bacillus subtilis and Staphylococcus aureus,* respectively (Rickards et al., 1999).

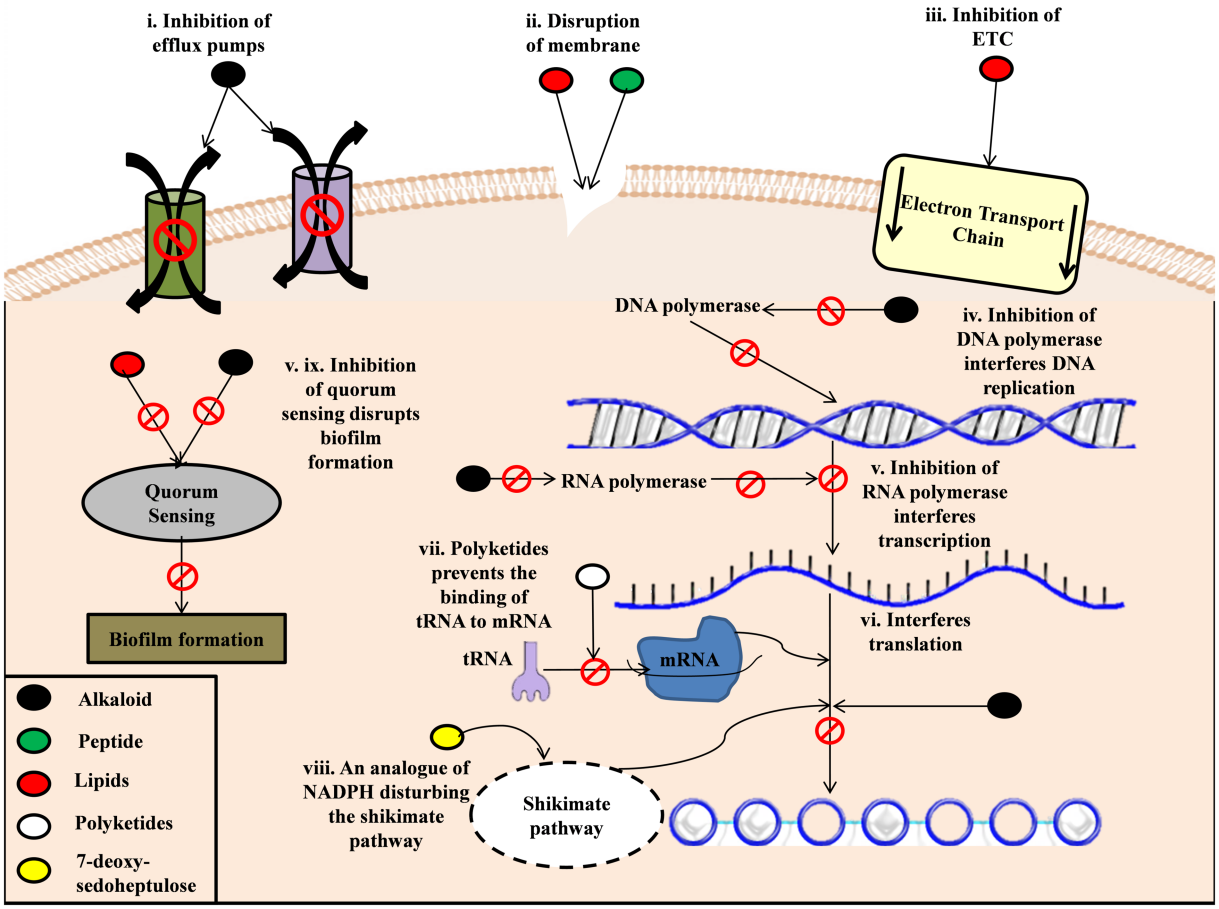

FIGURE 1
Mechanism of cyanobacterial metabolites action on bacteria. (i). Alkaloids derived from cyanobacteria inhibit the efflux pumps in bacteria (ii). Peptides and lipids of cyanobacteria disrupt the cell membrane and cause inner content leakage (iii). Lipids also inhibit the electron transport chain in bacteria disrupting the functioning of the cell (iv). Alkaloids inhibit DNA polymerase, which disrupts DNA replication (v). Alkaloids inhibit RNA polymerase, which interferes with the transcription process (vi). Alkaloids also interfere with the translation process (vii). Polyketides prevent tRNA binding to mRNA, which stops translation (iii). 7-deoxy-sedoheptulose, a sugar produced by cyanobacteria, acts as an analogue of NAPH in the Shikimate pathway, which disrupts the translation process.

Polyketides

Polyketides are one of the most abundant secondary metabolites distributed in plants, fungi, bacteria, insects, and some marine organisms. Polyketide synthases (PKS) enzymes produce them and have wide structural diversity due to various building blocks. They are also known to have significant bioactivity and the potential for novel natural product drug discovery (Ridley and Khosla, 2009; Ma et al., 2020; Yuzawa and Kuzuyama, 2020). Polyketides like anaephenes A-C and Cylindrofridins effectively against pathogens like Methicillin Resistant *Staphylococcus aureus, Bacillus cereus, Mycobacterium tuberculosis, Streptococcus pneumonia* (Preisitsch et al., 2015b; Brumley et al., 2018). Other examples of polyketides isolated from cyanobacteria are carbamidocyclophanes A – E isolated from *Nostoc* sp. CAVN 10 (Mundt et al., 2003), carbamidocyclophanes F and G isolated from *Nostoc sp.* (Luo et al., 2014), carbamidocyclophanes H–L from *Nostoc sp.* CAVN2 (Preisitsch et al., 2015a), Nostocyclyne A from *Nostoc sp.* (Ploutno and Carmeli, 2000), and Cylindrofridins A–C from *Cylindrospermum stagnale* (Preisitsch et al., 2015b). Polyketides like anaephenes A–C and Cylindrofridins effectively against pathogens like Methicillin Resistant *Staphylococcus aureus, Bacillus cereus, Mycobacterium tuberculosis, Streptococcus pneumonia* (Preisitsch et al., 2015b; Brumley et al., 2018).

Peptides

Peptides are abundantly extracted from cyanobacteria metabolites; many of them have been proven to be potent antimicrobials. AK-3, calophycin, hormothamnin A, lobocyclamide B, nostocyclamide, and tolybyssidin A and B are

some cyclic peptides isolated from cyanobacteria. Ishida et al. isolated three potent peptide compounds; Kawaguchipeptins A and B and Norharmane-HCl [9H-pyrido (3,4-b)indole-HCl] from *Nodularia harveyana* which have potent activity against *Escherichia coli, Pseudomonas aeruginosa, Staphylococcus aureus* and *Bacillus subtilis* (Ishida et al., 1997). Laxaphycin A, Tiahuramide A-C, Hormothamnin A, [D-Leu1] MC-LR are some of the compounds extracted from cyanobacteria (Gerwick et al., 1989; Ramos et al., 2015; Dussault et al., 2016; Levert et al., 2018). A previous review by Swain et al. reported an array of peptides isolated from various cyanobacteria (Swain et al., 2017).

Lipids

Various lipids have been isolated from cyanobacteria having antibacterial activities, such as Lyngbyoic acid, doscadenamide A, and pitinoic acid A as quorum sensing inhibitors in *Pseudomonas aeruginosa* (Carpine and Sieber, 2021) γ-linolenic acid (GLA), a potent antibacterial from Fischerella sp., was active against *Staphylococcus aureus* (Asthana et al., 2006). A lipid 2-Hydroxyethyl-11-hydroxyhexadec-9-enoate isolated from *Lyngbya sp.* is also effective against Methicillin-Resistant *Staphylococcus aureus* (MRSA). Another lipid (9Z,12Z)-9,12,15-hexadecatrienoic acid obtained from *Nostoc* sp. was effective against *Bacillus subtilis, Staphylococcus aureus* and *Micrococcus luteus* (Oku et al., 2014). Another example of cyanobacterial lipid is the Chlorosphaerolactylates family of fatty acids isolated from *Sphaerospermopsis sp.* were also found to have antibacterial activity against *Staphylococcus aureus* (Gutiérrez-del-Río et al., 2020).

Other classes of metabolites

Terpenes and polyphenols class of compounds has also been isolated from cyanobacteria having a potent antibacterial activity (Carpine and Sieber, 2021). For example, diterpenoid noscomin isolated from *Nostoc commune* EAWAG 122b is effective against three microbes: *Bacillus cereus, Staphylococcus epidermidis*, and *Escherichia coli* (Mo et al., 2010). Polyhalogenated compounds (PHCs) like Ambigols A, B, C, D, and E are also produced by cyanobacteria which are effective against MRSA (Choi et al., 2010). Recently 7-deoxy-sedoheptulose, an unusual sugar isolated from *Synechococcus elongatus,* showed potent activity against *Anabaena variabilis,* and its mode of action was *via* mimicking 3-deoxy-D-arabino-heptulosonate 7-phosphate (DAHP), an enzyme in the shikimate pathway and inhibits the reaction mechanism pathway that leads to a decreased level of aromatic amino acids triggered by the metabolic perturbation. Further studies on other pathogenic bacteria need to be conducted using this deoxy sugar to understand their medical importance better (Brilisauer et al., 2019).

Mechanism of action of cyanobacteria metabolites as antibacterial agents

The mechanism of action of most novel metabolites has not been explored and adequately established. However, they can be theorized using previously established studies on chemical classes and antibiotics similar to them. One of the metabolites' most common mechanisms of action is quorum sensing inhibition. Quorum sensing is an intercellular communication system in bacteria playing an important role in virulence and biofilm formation. Berberine, an alkaloid isolated from cyanobacteria, was found to inhibit the expression of biofilm genes (Sun et al., 2019). Various lipid compounds can also inhibit the bacterial quorum sensing system of bacteria like *Escherichia coli and Pseudomonas aeroginosa* (Carpine and Sieber, 2021). Another mechanism of action is disrupting the cell membrane of the target bacteria. It was found that most lipids and peptides show antibacterial activity by disrupting membrane integrity and the subsequent cell lysis, disrupting the electron transport chain, and inhibiting important bacterial cell enzymes (Yoon et al., 2018). Different bioactive compounds also interfere with the bacterial cell's important cellular pathways, such as the Shikimate pathway, Electron Transport chain and cell wall biosynthesis. Alkylphenols induce bacteriostasis by collapsing the proton motive force, thus inhibiting ATP synthesis and active transport (Denyer et al., 2011). A sugar isolated from *Synechococcus elongates* acts as an analogue of NADH enzyme in the Shikimate pathway, interfering with the Shikimate pathway (Brilisauer et al., 2019). In addition, the secondary metabolites of cyanobacteria are also able to the activity of various enzymes such as DNA polymerase and RNA polymerase, which affects the DNA, RNA and protein production. Alkaloids like 12-epi-hapalindole E isonitrile from *Fischerella* sp. and calothrixin A from *Calothrix sp.* showed their mode of action by inhibiting RNA polymerase independent of DNA concentration (Doan et al., 2000). Macrolides, a group of polyketides was found to interfere with aminoacyl tRNA-ribosome attachment and prevent the production of new proteins (Brumley et al., 2018).

Cyanobacterial metabolites as antiviral agents

Viral outbreaks like Ebola, Swine influenza, and SARS-CoV-2 are a huge burden on humanity, claiming millions of human life. The emergence of new strains with mutations making them resistant to standard antiviral drugs necessitates the need for novel antivirals. Metabolites isolated from cyanobacteria have proved to be significant antivirals. Deyab and colleagues found cyanobacteria isolates: *Arthrospira platensis*, *Leptolyngbya boryana*, *Nostoc punctiforme, Oscillatoria* sp., *Leptolyngbya sp.,* and *Arthrospira platensis* isolates showed high antiviral activity against Coxsackievirus B3 and Rotavirus

(Deyab et al., 2019). Cyanobacterial metabolites have also been tested as an antiviral agent against SARS-CoV2 with encouraging results (Pradhan et al., 2022). While some have been proven cytotoxic, many have shown their potential as less cytotoxic to mammalian cells, which can be used as antiviral therapeutics.

Proteins

Lectins, a carbohydrate-binding protein, is one of the most commonly isolated proteins of cyanobacteria showing promising antiviral activity (Carpine and Sieber, 2021). Cyanovirin, a lectin isolated from *Nostoc ellipsosporum,* has neutralising activity against various enveloped viruses such as HIV-1, feline immunodeficiency virus, and human herpesvirus 6 well as measles virus. A novel cyanobacterial protein, MVL, inhibited the HIV-1 Envelope-mediated cell fusion with an IC50 value of 30 nM (Bewley et al., 2004). *Oscillatoria agardhii* agglutinin (OAA), a lectin compound isolated from *Oscillatoria agardhii,* inhibited human immunodeficiency virus replication in MT-4 cells with an EC50 of 44.5 nM (Saad et al., 2022). Proteins griffithsin (GRFT) and scytovirin (SVN) isolated from cyanobacteria *Griffithsia sp.* inhibited HCV entry at nanomolar concentrations and showed significant *in vivo* efficacy in the mouse model system (Takebe et al., 2013). Cyanobacterial lectin scytovirin was demonstrated to have the ability to bind to the envelope glycoprotein of Zaire Ebola virus (ZEBOV), thus inhibiting its replication with a virus-inhibitory concentration (EC50) of 50 nM. Scytovirin is also effective against other viruses like HIV, Marburg virus and SARS-CoV2 (Garrison et al., 2014). Microvirin (MVN), isolated from *Microcystis aeruginosa,* exhibited anti-HIV activity in peripheral blood mononuclear cells with more minor cytotoxic effects than anti-human immunodeficiency virus protein cyanovirin-N, which is separated from *Nostoc ellipsosporum* (Huskens et al., 2010). *Galanthus nivalis* agglutinin (GNA) against cell culture Hepatitis C virus (HCV) was less toxic than its other lectin counterparts, *Microcystis viridis* lectin (MVL) and cyanovirin-N (CV-N), which were found to be potentially harmful due to their interaction with cellular proteins (Kachko et al. 2013a; Figure 2).

Carbohydrates

Cyanobacteria, especially marine cyanobacteria, contain abundant polysaccharides that are effective against various viruses (Pradhan et al., 2022). Nostoflam, a polysaccharide extract of *Nostoc flagelliforme,* showed potent and broad antiviral activity against herpes simplex virus type 1 (HSV-1), human cytomegalovirus, HSV-2, and influenza A virus (Kanekiyo et al., 2005). Galactosides isolated from *Agardhiella tenera* are effective against viruses such as HSV-1, HSV-2, HIV-1, HIV-2 and Hepatitis A, respectively. A polysaccharide, Carrageenan obtained from *Chondrus, Gigartina, Hypnea, and Eucheuma* was found to be capable of blocking the entry of Dengue virus (DENV) and HPV into the host cell (Grassauer et al., 2008). Other polysaccharides such as galactans obtained from species like *Callophyllis variegata, Agardhiella tenera, Schizymenia binderi, and Cryptonemia crenulat,* also have potent antiviral activity against HSV-1, HSV-2, HIV-1, HIV-2, and DENV (Rodríguez et al., 2005). The effect of the polysaccharide Calcium Spirulan isolated from *Arthrospira platensis* is also tested against Human cytomegalovirus virus, Influenza Virus, Mumps virus, Herpes Simplex Virus-1 (HSV-1) and Human Immuno Deficiency Virus-1 with promising results (Rechter et al., 2006). Another example is Phycobiliproteins isolated from *Arthrospira platens* which have antiviral activity against Influenza A and the H1N1 virus (Chen et al., 2020; Figure 3).

Other classes of compounds

Other compounds like alkaloids, lipids, polyphenols and polyketides have antiviral activity. Alkaloids, namely Bauerine A, B and C, effectively eradicate Herpes simplex virus-2 (Larsen et al., 1994). Other alkaloid compounds like Debromoaplysiatoxin, Anhydrodebromoaplysiatoxin, and 3-Methoxydebromoaplysiatoxin were also found to possess antiviral activity against Chikungunya virus (Gupta et al., 2014). Some lipid compounds were also found to have potent activity against Herpes Simplex Virus-1 (Chirasuwan et al., 2009). Polyketides isolated from *Trichodesmium erythraeum* were also found to be effective against the Chikungunya virus (Gupta et al., 2014).

Mechanism of action of cyanobacteria metabolites as antivirals

Clinical studies on many cyanobacterial antivirals have been conducted with promising broad-spectrum activity, lesser cytotoxicity, and a wide range of mechanisms of action. One of the most common modes of action is preventing infection by inhibiting the binding of viral proteins to the host cell. Antiviral metabolites like Scytovirin, Cyanovirin, and Microvirin bind to viral envelope proteins of HIV like gp120, gp160 and gp41, which prevents their binding from hosting cells like CD4, thus preventing the entry of the virus (Dey et al., 2000; Bokesch et al., 2003; Huskens et al., 2010). Scytovirin also block the entry of the hepatitis C virus to the host by binding to the viral envelope glycoprotein E1 and E2 (Takebe et al., 2013). A similar mode of action was seen in Griffithsin (GRFT), a cyanobacterial lectin isolated from Griffithsia sp., where it inhibited HIV-1 by blocking the coreceptor binding process and exposing the CD4 binding site of gp120 (Alexandre et al., 2011), preventing HIV-1 capture and transmission mediated by DC-SIGN receptor (Hoorelbeke et al., 2013) and improved antibody response against virus where communization with GRFT dramatically raised the anti-gp120

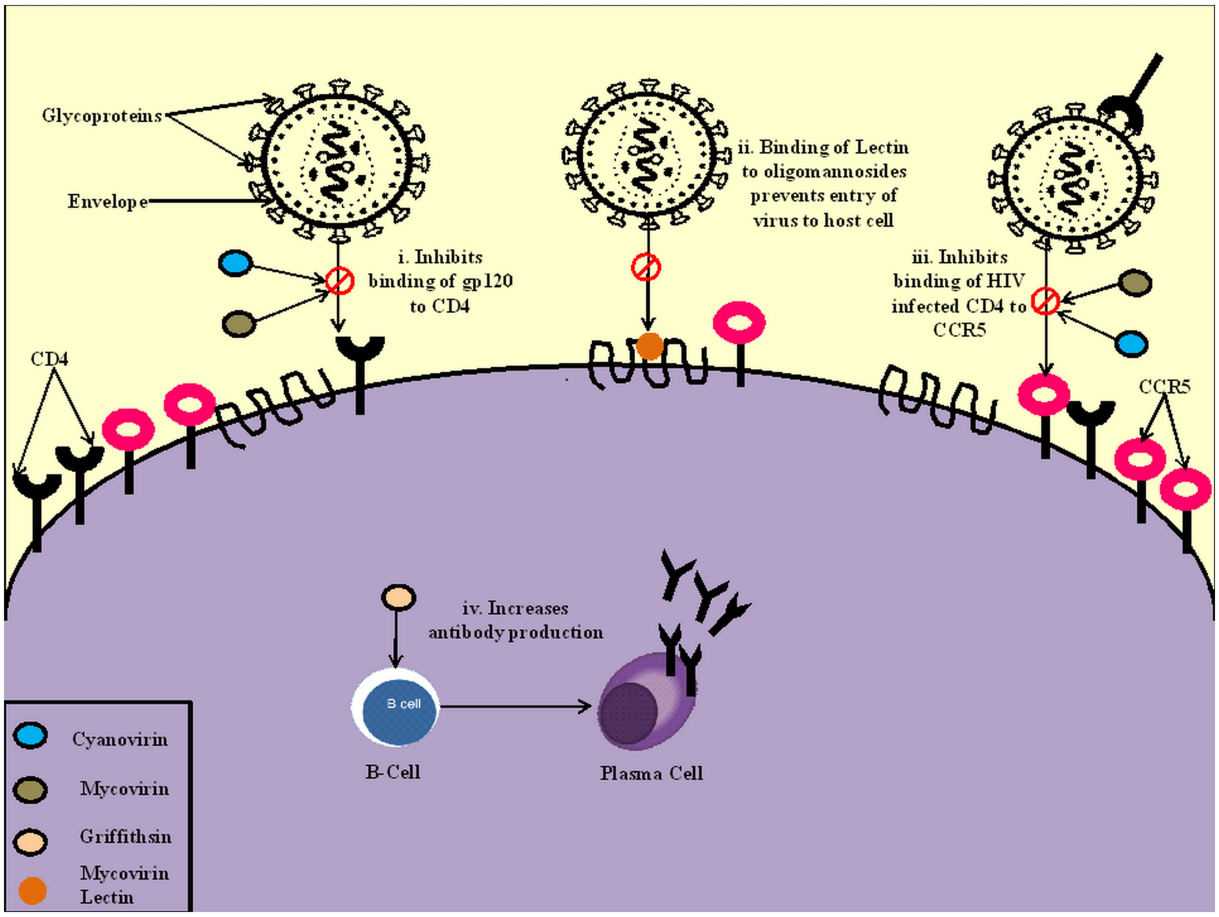

FIGURE 2
Mechanism of action of cyanobacteria on the virus. (i). Cyanovirin and Mycovirin inhibit the binding of a glycoprotein gp120 to CD4 cells, preventing the viral infection (ii). Mycovirin Lectin binds to oligomannosides on the cell wall, blocking the virus's entry to the host cell (iii). Cyanovirin and Mycovirin block the binding of CD4 infected cells to CCR5 receptors, which prevents the progression of infection (iv). Griffithsin increases the production of antibodies and increases the reactivity of IgG.

IgG reactivity (Banerjee et al., 2012; Lee, 2019). Griffithsin also binds to the spike glycoproteins of MERS-CoV and SARS-CoV, preventing host cell infection (O'Keefe et al., 2010). Another mode of action is the inhibition of viral replication. This mode of action is found to be exhibited by metabolites like Calcium Spirulan, sulfoglycolipids, *Oscillatoria agardhii* agglutinin (OAA) and Scytovirin against HIV-1 and HIV-2, HSV-1 and Zaire Ebola virus (ZEBOV; Loya et al., 1998; Férir et al., 2014; Garrison et al., 2014). Scytovirin inhibits viral replication by binding to the mucin domain of the glycoprotein of the Ebola virus (Garrison et al., 2014). Lipids like Sulfoquinovosyl diacylglycerol prevents DNA replication by inhibiting HIV–reverse transcriptase and DNA polymerases (Loya et al., 1998). The metabolites also prevent further infection by binding to the host cell's surface receptors and other host cells. An example is Mycovirin which prevents the binding of HIV-infected CD4 cells to host receptors CCR5 (Dey et al., 2000). One metabolite may have different modes of action, and the mode of action may differ in different species of viruses. For example, cyanovirin blocks the fusion pathway in HIV by blocking the binding of HIV envelope gp120 with CD4 disrupting the fusion between the host cell membrane and the virus. Not only that, but cyanovirin can also block the binding of CD4-activated gp120 to host membrane coreceptors such as CCR5. However, in the feline immunodeficiency virus, cyanovirin blocks the infection independent of CD4. They might also have other modes of action, such as interaction with another subunit of the virus envelope, such as gp41 or destabilization of the envelope (Dey et al., 2000). The potent broad-spectrum antiviral cyanobacterial-derived compounds can be explored to combat variously transmissible enveloped and non-enveloped viruses.

Arthrospira has shown potent antiviral activity in several clinical studies against HIV-1. A study showed that Arthrospira showed antiviral potential against SARS-CoV-2 using docking and *in silico* toxicity assessment. Four compounds, i.e., phycoerythrobilin, phycocyanobilin, phycourobilin, and folic acid,

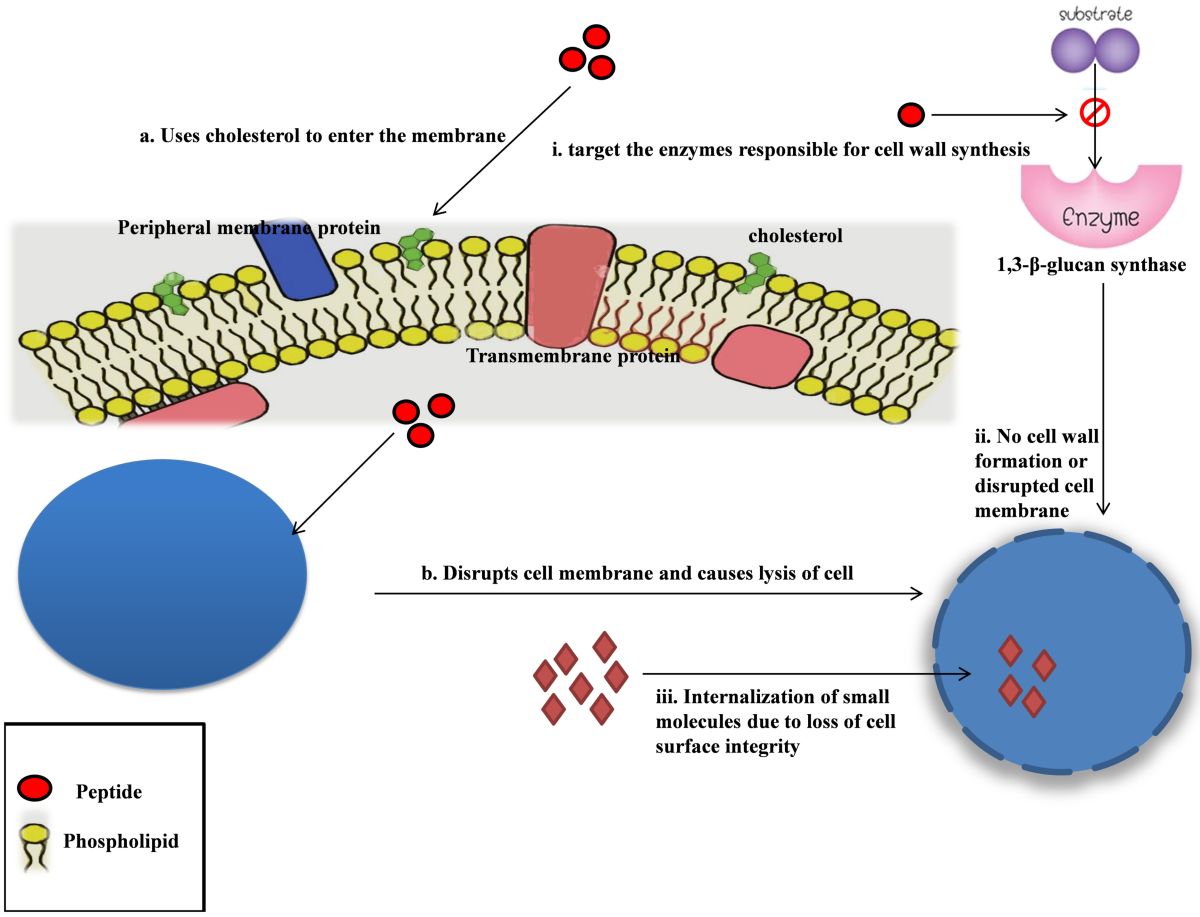

FIGURE 3
Mechanism of action of cyanobacteria as an antifungal agent. The peptides need cholesterol in the cell membrane to enter the cell, and from there on, they act by disrupting the cell membrane causing cell lysis. The peptides are hypothesized to target the enzyme responsible for cell wall synthesis. The increased internalization of molecules mainly implies a compromised cell membrane, confirming that these peptides majorly target the cell membrane.

displayed consistent binding energies from Autodock Vina and SwissDock with low toxicity risks. Very few *in vivo* and *in vitro* studies have been conducted on cyanobacteria metabolites as potent antivirals against SARS-CoV-2. These *in silico* studies provide a new way of research advancement towards clinical studies (Petit et al., 2021). A clinical trial studied the potential use of Spirulina platensis as a nutritional supplement in adults with HIV who are undernourished in Sub-Saharan Africa. The results were promising, where the nutritional status of malnourished HIV-infected patients was improved by spirulina (Azabji-Kenfack et al., 2011). Spirulina also blocked the entry of VSV-based pseudotyped viruses (PVs) of SARS-, MERS-, and SARS-2 CoVs when preincubated with their extracts. Understanding the core mechanism of how the compounds can block the entry of viruses inside the host cells in future studies will help expand this study toward significant novel compound discovery.

This shows that broad-spectrum antiviral cyanobacterial-derived compounds can be explored to combat various transmissible enveloped and non-enveloped viruses. Furthermore, more mechanisms of action-focused studies need to be conducted on cyanobacteria metabolites as there is an evident lack of them in the current research scenario. Also, even after substantial results in pre-clinical and clinical studies, the pharmaceutical community's antiviral properties of cyanobacterial extracts against the novel coronavirus and other human viruses seem to go unrecognized. Therefore, better approaches must be addressed to expand the research beyond academia to industry-level research.

Cyanobacterial metabolites as antifungal agents

Owing to major challenges faced by antifungal drug development, primarily that many of the toxic molecules to the fungal organism are toxic to the hosts, too, due to the cells' eukaryotic nature, novel antifungal discovery is slower than that of antibacterials (Seneviratne and Rosa, 2016). Nevertheless,

cyanobacteria metabolites have been regarded as one of the potential sources in the discovery of antifungals with a well-established mode of action that can translate into pharmaceutical products.

Nodularia harveyana and *Nostoc insulare* exometabolites (norharmane and 4′4′-dihydroxy biphenyl) were effective against *Candida albicans* with a MIC value of 40 μg/ml and 32 μg/ml, respectively (Volk and Furkert, 2006). Furthermore, 10 strains of cyanobacteria were found to have bioactive compounds inhibiting *Candida albicans,* and nine inhibiting *Aspergillus flavus* in a disc diffusion assay conducted with 194 cyanobacterial strains showing a wide range of strains is capable of producing antifungal compounds, which warrants further research. In addition, the nine cyanobacteria species inhibited the growth of seven phytopathogenic fungi, which cause disease in hot pepper (*Capsicum annuum* L). Of them, two species were of Oscillatoria, two were *Anabaena*, three were Nostoc, one was Nodularia, and one *Calothrix,* which were all retrieved from rice paddy field soil (Kim, 2018).

The fatty acids isolated from *Synechocystis* sp. successfully inhibited the growth of *Candida albicans* (Najdenski et al., 2013). Similarly, the *Microcystis aeruginosa* diethyl ether extract showed potent antifungal activity against a number of *Aspergillus species, Fusarium verticillioides, Fusarium proliferatum, Penicillium verrucosum* (Marrez and Sultan, 2016). Soltani et al. (2005) reported six cyanobacterial species and one cyanobacterium species inhibited the growth of *Candida kefyr* and *Candida albicans,* respectively (Soltani et al., 2005). A polyketide tolytoxin isolated from *Scytonema* sp. and *Tolypothrix sp*. showed strong antifungal activity against a wide range of fungi such Alternaria alternate, *Aspergillus oryzae.*

Bipolaris incurvata, Candida albicans, Saccharomyees cerevisiae, Penicillin notatum, etc. (Patterson and Carmeli, 1992). Glycosylated lipopeptide isolated from *Tolypothrix (basionym Hassallia) sp.* exhibited antifungal activity against *Aspergillus fumigatus* and *Candida albicans* (Neuhof et al., 2005). Prasanna et al. (2008) evaluated the 35 *Anabaena* strains and reported fungicidal potential against 74 phytopathogenic fungi (Prasanna et al., 2008). Similarly, the *Lyngbya aestuarii* and *Aphanothece bullosa* showed antifungal activity against *Candida albicans* (Kumar et al., 2013). In another study conducted with Brazilian cyanobacteria crude extracts, five isolated extracts showed potent antifungal activity against *Candida albicans*. Antifungal macrolide scytophycin was found in *Anabaena* sp. HAN21/1, Nostoc sp. HAN11/1, Anabaena *cf.* cylindrica PH133, and *Scytonema* sp. HAN3/2. In the same study, Anabaena species BIR JV1 and HAN7/1, Nostoc species 6sf Calc, and CENA 219 all produced the antifungal glycolipopeptide hassallidin. Hassallidins obtained from *Nostoc calcicula, Anabaena cylindrica, and Hassallia sp.* could also inhibit different *Candida* species and *Cryptococcus neoformans* (Neuhof et al., 2005, 2006). This shows the huge potential cyanobacteria has as a potential source of antifungals having future therapeutic applications.

Mechanism of action of antifungal activity

Most of the compounds extracted from cyanobacteria having antifungal activity are cyclic peptides in nature. Recent studies focused on their mode of action have shown that a majority of them target the cell membrane of eukaryotic cells.

Hassallidins, cyclic glycolipopeptides isolated from *Anabaena sp.,* were found to affect the function of cell membranes, resulting in lytic cell death with outer membrane disintegration and increased internalization of tiny molecules, which implies loss of cell surface integrity. It targets sterol-containing membranes, and cholesterol is necessary for them to enter the membrane (Humisto et al., 2019). Hassallidins production is not limited to *Anabaena* and *Cylindrospermopsis*; *Nostoc*, *Aphanizomenon*, and *Tolypothrix* are also known to produce them with great structural diversity and antifungal activity. They are also known to protect cyanobacteria from parasitic fungi (Vestola et al., 2014). Balticidins (A-D) are also a group of hassallidin-like lipopeptides isolated from *Anabaena cylindrica* which might have similar modes of action.

Laxaphycins A and B, first isolated from cyanobacteria *Anabaena laxa* (Patterson, 1992), have potent antifungal activity. The mode of action behind it is poorly understood, but as they are cyclic peptides in nature, it might be due to them targeting the enzymes responsible for cell wall synthesis, such as 1,3-β-glucan synthase (Zhang and Chen, 2022).

Tolytoxin, a diterpene lactone isolated from *Scytonema ocellatum* and *Scytonema mirabilei.* Has broad antifungal activity at nanomolar concentrations, and it was hypothesized that they inhibit a basic cell process exclusive to eukaryotes. Detailed modes of action on how they inhibit fungal growth are yet to be studied.

Another unrelated study showed that tolytoxin targets actin by preventing its polymerization and decreasing the number of Tunneling nanotubes (TNT), which contribute to the development of numerous diseases by facilitating the transfer of pathogens and protein aggregates (Senol et al., 2019). Furthermore, Puwainaphycins F and G, cyclic decapeptides isolated from *Cylindrospermum alatosporum,* result in necrotic cell death due to altered cell morphology and physiology, highlighting that not all antifungal peptides might be suitable for human use (Hrouzek et al., 2012). Understanding the mechanism of action behind their antifungal activity will help pinpoint which compounds can be further screened for clinical trials.

Other cyclic peptides which could be potent antifungal activity are Calophycin (Moon et al., 1992), Tolybyssidin (Jaki et al., 2001), and Schizotrin A (Pergament and Carmeli, 1994). In addition, other compounds such as alkaloid Ambiguine isonitrile (Smitka et al., 1992) and Carriebowlinol (Soares et al., 2015), terpene Scytoscalarol (Mo et al., 2009b) are also known to have potent antifungal activity. Indeed, further research on how they alter biological processes and investigations of the link between structure and activity is needed to find new application areas and potential therapeutic leads (Fewer et al., 2021).

Challenges of using cyanobacterial metabolites

Only a few compounds of cyanobacteria have entered clinical trials, and none of the compounds has not been approved by the Food and Drug Administration (Singh et al., 2011). One of the main reasons for this is the limited knowledge of the synthesis of metabolites by cyanobacteria. The functions and regulations of the enzymes involved in the cellular pathways and biosynthetic processes were only partially known, thus complicating the use of genetic engineering techniques to produce more metabolites (Jones et al., 2009). Further investigation is also required to understand the exact mechanism of the bioactive compounds to make them feasible for pharmaceutical use (Xu et al., 2016). Another problem is the stability and bioavailability of the bioactive compounds. For example, the cyanobacterial peptides are highly unstable and require different stabilising strategies like replacing amino acids with other amino acids more resistant to hydrolysis, structural restriction, cyclization or stapling (Skowron et al., 2019). Newer strategies will greatly improve the stability and bioavailability of these peptides. Although some cyanobacterial metabolites showed promising antimicrobial activities, the cytotoxicity of some bioactive compounds like microcystins, saxitoxins or anatoxins raised severe concerns about deterring their use in the pharmaceutical and food industry (Gademann and Portmann, 2008).

Conclusion

This review demonstrated the vast versatility of cyanobacteria and its metabolites in medical applications. They are rich in several bioactive compounds that can be explored to manage human health. Furthermore, with the advent of genetic engineering, it has been easier to manipulate a microorganism's genetic makeup to our benefit. In the same way, metagenomics can be used to screen and mass-produce anexic cultures of cyanobacteria to produce relevant metabolites that we need and modify metabolic pathways so that we can increase the quantity of bioactive compounds in the cyanobacteria. Cyanobacteria, as a primitive organism, have a huge potential for the benefit of human welfare in the 21st century as well as in the coming century with the scientific tools we have in hand. Even though they are a rich source of antifungals, antibacterials, and antioxidants, several roadblocks hinder their usage on a large scale. We need to find better ways to continue studying them to find strains with more usability and reproducibility so that their research can be forwarded to clinical trials and interdisciplinary research. It should not be labour and energy-intensive, and there should be enough co-products production along with the main compounds so that the capital and final product are cost-effective. With the right questions asked as well as small steps toward finding novel compounds and compiling new cyanobacterial strains from different habitats around the world and extracting their metabolites, we can take a bigger leap toward discovering compounds that will have a significant impact on the issues we are facing currently against antibiotic-resistant microbes and other pathogenic organisms.

Author contributions

PKS, MKY, CL, and JK formulated and wrote the manuscript. While drafting, SMS, NCJ, K, SKM, and AK are critical suggestions in the manuscript. DPR, RZ, and CL designed the tables and figures. All authors contributed to the article and approved the submitted version.

Funding

This study was supported by the Indian Council of Medical Research (ICMR), New Delhi (File No. 5/7/1770/Adhoc/NER/RBMCH-2021) to PS.

Conflict of interest

The authors declare that the research was conducted in the absence of any commercial or financial relationships that could be construed as a potential conflict of interest.

Publisher's note

Supplementary material

The Supplementary material for this article can be found online at: https://www.frontiersin.org/articles/10.3389/fmicb.2022.1034471/full#supplementary-material

References

Adamson, C. S., Chibale, K., Goss, R. J. M., Jaspars, M., Newman, D. J., and Dorrington, R. A. (2021). Antiviral drug discovery: preparing for the next pandemic. *Chem. Soc. Rev.* 50, 3647–3655. doi: 10.1039/d0cs01118e

Alexandre, K. B., Gray, E. S., Pantophlet, R., Moore, P. L., McMahon, J. B., Chakauya, E., et al. (2011). Binding of the mannose-specific lectin, Griffithsin, to HIV-1 Gp120 exposes the CD4-binding site. *J. Virol.* 85, 9039–9050. doi: 10.1128/JVI.02675-10

Asthana, R. K., Srivastava, A., Kayastha, A. M., Nath, G., and Singh, S. P. (2006). Antibacterial potential of c-linolenic acid from Fischerella Sp. colonizing neem tree bark. *World J Microbiol. Biotechnol.* 22, 443–448. doi: 10.1007/s11274-005-9054-8

Azabji-Kenfack, M., Edie Dikosso, S., Loni, E. G., Onana, E. A., Sobngwi, E., Gbaguidi, E., et al. (2011). Potential of Spirulina Platensis as a Nutritional Supplement in Malnourished HIV-Infected Adults in Sub-Saharan Africa: A Randomised, Single-Blind Study. *Nutrition and Metabolic Insights* 4, 29–37. doi: 10.4137/NMI.S5862

Banerjee, K., Michael, E., Eggink, D., van Montfort, T., Lasnik, A. B., Palmer, K. E., et al. (2012). Occluding the mannose moieties on human immunodeficiency virus type 1 Gp120 with Griffithsin improves the antibody responses to both proteins in mice. *AIDS Res. Hum. Retrovir.* 28, 206–214. doi: 10.1089/aid.2011.0101

Bewley, C. A., Cai, M., Ray, S., Ghirlando, R., Yamaguchi, M., and Muramoto, K. (2004). New carbohydrate specificity and HIV-1 fusion blocking activity of the cyanobacterial protein MVL: NMR, ITC and sedimentation equilibrium studies. *J. Mol. Biol.* 339, 901–914. doi: 10.1016/j.jmb.2004.04.019

Bokesch, H. R., O'Keefe, B. R., McKee, T. C., Pannell, L. K., Patterson, G. M. L., Gardella, R. S., et al. (2003). A potent novel anti-HIV protein from the cultured cyanobacterium Scytonema varium. *Biochemistry* 42, 2578–2584. doi: 10.1021/bi0205698

Brilisauer, K., Rapp, J., Rath, P., Schöllhorn, A., Bleul, L., Weiß, E., et al. (2019). Cyanobacterial antimetabolite 7-deoxy-Sedoheptulose blocks the shikimate pathway to inhibit the growth of prototrophic organisms. *Nat. Commun.* 10:476. doi: 10.1038/s41467-019-08476-8

Brumley, D., Spencer, K. A., Gunasekera, S. P., Sauvage, T., Biggs, J., Paul, V. J., et al. (2018). "*Isolation and characterization of Anaephenes a–C, Alkylphenols from a filamentous cyanobacterium (Hormoscilla Sp., Oscillatoriales)*."

Carpine, R., and Sieber, S. (2021). Antibacterial and antiviral metabolites from cyanobacteria: their application and their impact on human health. *Curr. Res. Biotechnol.* 3, 65–81. doi: 10.1016/j.crbiot.2021.03.001

Chen, X., Han, W., Wang, G., and Zhao, X. (2020). Application prospect of polysaccharides in the development of anti-novel coronavirus drugs and vaccines. *Int. J. Biol. Macromol.* 164, 331–343. doi: 10.1016/j.ijbiomac.2020.07.106

Chirasuwan, N., Chaiklahan, R., Kittakoop, P., Chanasattru, W., Ruengjitchatchawalya, M., Tanticharoen, M., et al. (2009). Anti HSV-1 activity of sulphoquinovosyl diacylglycerol isolated from Spirulina platensis. *Sci. Asia* 35, 137–141. doi: 10.2306/scienceasia1513-1874.2009.35.137

Choi, H., Engene, N., Smith, J. E., Preskitt, L. B., and Gerwick, W. H. (2010). Crossbyanols A–D, toxic brominated polyphenyl ethers from the Hawai'ian bloom-forming cyanobacterium Leptolyngbya crossbyana. *J. Nat. Prod.* 73, 517–522. doi: 10.1021/np900661g

Denyer, S. P., Hugo, W. B., and Witham, R. F. (2011). The antibacterial action of a series of 4-N-Alkylphenols. *J. Pharm. Pharmacol.* 32:27P. doi: 10.1111/j.2042-7158.1980.tb10830.x

Dey, B., Lerner, D. L., Lusso, P., Boyd, M. R., Elder, J. H., and Berger, E. A. (2000). Multiple antiviral activities of Cyanovirin-N: blocking of human immunodeficiency virus type 1 Gp120 interaction with CD4 and Coreceptor and inhibition of diverse enveloped viruses. *J. Virol.* 74, 4562–4569. doi: 10.1128/jvi.74.10.4562-4569.2000

Deyab, M., Mofeed, J., El, E., and Fatma, B. (2019). Antiviral activity of five filamentous cyanobacteria against Coxsackievirus B3 and rotavirus. *Arch. Microbiol.* 202, 213–223. doi: 10.1007/s00203-019-01734-9

Doan, N. T., Rickards, R. W., Rothschild, J. M., and Smith, G. D. (2000). Allelopathic actions of the alkaloid 12-epi-Hapalindole E Isonitrile and Calothrixin a from cyanobacteria of the genera Fischerella and Calothrix. *J. Appl. Phycol.* 12, 409–416. doi: 10.1023/A:1008170007044

Dobretsov, S., Teplitski, M., Alagely, A., Gunasekera, S. P., and Paul, V. J. (2010). Malyngolide from the cyanobacterium Lyngbya majuscula interferes with quorum sensing circuitry. *Environ. Microbiol. Rep.* 2, 739–744. doi: 10.1111/j.1758-2229.2010.00169.x

Dussault, D., Khanh, D. V., Vansach, T., Horgen, F. D., and Lacroix, M. (2016). Antimicrobial effects of marine algal extracts and cyanobacterial pure compounds against five foodborne pathogens. *Food Chem.* 199, 114–118. doi: 10.1016/j.foodchem.2015.11.119

Férir, G., Huskens, D., Noppen, S., Koharudin, L. M. I., Gronenborn, A. M., and Schols, D. (2014). Broad anti-HIV activity of the Oscillatoria agardhii agglutinin homologue lectin family. *J. Antimicrob. Chemother.* 69, 2746–2758. doi: 10.1093/jac/dku220

Fewer, D. P., Sivonen, K., Hrouzek, P., Aesoy, R., and Herfindal, L. (2021). Chemical diversity and cellular effects of antifungal cyclic Lipopeptides from cyanobacteria. *Physiol Plant* 173, 639–650. doi: 10.1111/ppl.13484

Gademann, K., and Portmann, C. (2008). Secondary metabolites from cyanobacteria: complex structures and powerful bioactivities. *Curr. Org. Chem.* 12, 326–341. doi: 10.2174/138527208783743750

Garrison, A. R., Giomarelli, B. G., Lear-rooney, C. M., Saucedo, C. J., Yellayi, S., Krumpe, L. R. H., et al. (2014). The cyanobacterial lectin Scytovirin displays potent in vitro and in vivo activity against Zaire Ebola virus. *Antivir. Res.* 112, 1–7. doi: 10.1016/j.antiviral.2014.09.012

Gerwick, W. H., Mrozek, C., Moghaddam, M. F., and Agarwal, S. K. (1989). Novel cytotoxic peptides from the tropical marine cyanobacteriumHormothamnion enteromorphoides 1. Discovery, isolation and initial chemical and biological characterization of the hormothamnins from wild and cultured material. *Experientia* 45, 115–121. doi: 10.1007/BF01954842

Ghasemi, Y., Yazdi, M. T., Shafiee, A., Amini, M., Shokravi, S., and Zarrini, G. (2004). Parsiguine, a novel antimicrobial substance from Fischerella ambigua. *Pharm. Biol.* 42, 318–322. doi: 10.1080/13880200490511918

Grassauer, A., Weinmuellner, R., Meier, C., Pretsch, A., Prieschl-Grassauer, E., and Unger, H. (2008). Iota-carrageenan is a potent inhibitor of rhinovirus infection. *Virol. J.* 5, 107–113. doi: 10.1186/1743-422X-5-107

Gupta, D. K., Kaur, P., Leong, S. T., Tan, L. T., Prinsep, M. R., and Chu, J. J. H. (2014). Anti-chikungunya viral activities of aplysiatoxin-related compounds from the marine cyanobacterium Trichodesmium erythraeum. *Mar. Drugs* 12, 115–127. doi: 10.3390/md12010115

Gutiérrez-del-Río, I., de Fraissinette, N. B., Castelo-Branco, R., Oliveira, F., Morais, J., Redondo-Blanco, S., et al. (2020). Chlorosphaerolactylates AD: the natural chlorinated lactylates isolated from the Portuguese 2 cyanobacterium Sphaerospermopsis sp. *LEGE* 3:00249. doi: 10.1021/acs.jnatprod.0c00072

Hoorelbeke, B., Xue, J., Li Wang, P. J., and Balzarini, J. (2013). Role of the carbohydrate-binding sites of Griffithsin in the prevention of DC-SIGN-mediated capture and transmission of HIV-1. *PLoS One* 8:e64132. doi: 10.1371/journal.pone.0064132

Hrouzek, P., Kuzma, M., Černý, J., Novák, P., Fišer, R., Simek, P., et al. (2012). The cyanobacterial cyclic Lipopeptides Puwainaphycins F/G are inducing necrosis via cell membrane Permeabilization and subsequent unusual actin Relocalization. *Chem. Res. Toxicol.* 25, 1203–1211. doi: 10.1021/tx300044t

Humisto, A., Jokela, J., Teigen, K., Wahlsten, M., Permi, P., Sivonen, K., et al. (2019). Characterization of the interaction of the antifungal and cytotoxic cyclic Glycolipopeptide Hassallidin with sterol-containing lipid membranes. *Biochim. Biophys. Acta Biomembr.* 1861, 1510–1521. doi: 10.1016/j.bbamem.2019.03.010

Huskens, D., Férir, G., Vermeire, K., Kehr, J. C., Balzarini, J., Dittmann, E., et al. (2010). Microvirin, a novel α(1,2)-mannose-specific lectin isolated from Microcystis Aeruginosa, has anti-HIV-1 activity comparable with that of Cyanovirin-N but a much higher safety profile. *J. Biol. Chem.* 285, 24845–24854. doi: 10.1074/jbc.M110.128546

Ishida, K., Matsuda, H., Murakami, M., and Yamaguchi, K. (1997). Kawaguchipeptin B, an antibacterial cyclic Undecapeptide from the cyanobacterium Microcystis Aeruginosa. *J. Nat. Prod.* 60, 724–726. doi: 10.1021/np970146k

Jaki, B., Orjala, J., and Sticher, O. (1999). A novel extracellular diterpenoid with antibacterial activity from the cyanobacterium Nostoc commune. *J. Nat. Prod.* 62, 502–503. doi: 10.1021/np980444x

Jaki, B., Zerbe, O., Heilmann, J., and Sticher, O. (2001). Two novel cyclic peptides with antifungal activity from the cyanobacterium Tolypothrix Byssoidea (EAWAG 195). *J. Nat. Prod.* 64, 154–158. doi: 10.1021/np000297e

Jones, A. C., Liangcai, G., Sorrels, C. M., Sherman, D. H., and Gerwick, W. H. (2009). New tricks from ancient algae: natural products biosynthesis in marine cyanobacteria. *Curr. Opin. Chem. Biol.* 13, 216–223. doi: 10.1016/j.cbpa.2009.02.019

Kachko, A., Loesgen, S., Shahzad-Ul-Hussan, S., Tan, W., Zubkova, I., Takeda, K., et al. (2013). Inhibition of hepatitis C virus by the cyanobacterial protein Microcystis Viridis lectin: mechanistic differences between the high-mannose specific lectins MVL, CV-N, and GNA. *Mol. Pharm.* 10, 4590–4602. doi: 10.1021/mp400399b

Kalia, V. C., Patel, S. K. S., Kang, Y. C., and Lee, J.-K. (2019). Quorum sensing inhibitors as antipathogens: biotechnological applications. *Biotechnol. Adv.* 37, 68–90. doi: 10.1016/j.biotechadv.2018.11.006

Kanekiyo, K., Lee, J.-B., Hayashi, K., Takenaka, H., Hayakawa, Y., Endo, S., et al. (2005). Isolation of an antiviral polysaccharide, Nostoflan, from a terrestrial cyanobacterium. *Nostoc Flagelliforme* 68, 1037–1041. doi: 10.1021/np050056c

Kim, J.-D. (2018). Screening of cyanobacteria (blue-green algae) from Rice Paddy soil for antifungal activity against plant pathogenic fungi 8093

Kumar, M., Tripathi, M. K., Srivastava, A., Gour, J. K., Singh, R. K., Tilak, R., et al. (2013). Cyanobacteria, Lyngbya Aestuarii and Aphanothece Bullosa as antifungal and Antileishmanial drug resources. *Asian Pac. J. Trop. Biomed.* 3, 458–463. doi: 10.1016/S2221-1691(13)60096-9

Kwan, J. C., Meickle, T., Ladwa, D., Teplitski, M., Paul, V., and Luesch, H. (2011). Lyngbyoic acid, a "tagged" fatty acid from a marine cyanobacterium, disrupts quorum sensing in Pseudomonas aeruginosa. *Mol. BioSyst.* 7, 1205–1216. doi: 10.1039/c0mb00180e

Larsen, L. K., Moore, R. E., and Patterson, G. M. L. (1994). β-Carbolines from the blue-green alga Dichothrix baueriana. *J. Nat. Prod.* 57, 419–421. doi: 10.1021/np50105a018

Laxminarayan, R. (2022). Comment the overlooked pandemic of antimicrobial resistance supporting bereaved family members: three steps in the right direction. *Lancet* 399, 606–607. doi: 10.1016/S0140-6736(22)00087-3

Lee, C. (2019). Griffithsin, a highly potent broad-Spectrum antiviral lectin from red algae: from discovery to clinical application. *Mar. Drugs* 17:567. doi: 10.3390/md17100567

Leflaive, J., and Ten-Hage, L. (2007). Algal and cyanobacterial secondary metabolites in freshwaters: a comparison of Allelopathic compounds and toxins. *Freshw. Biol.* 52, 199–214. doi: 10.1111/j.1365-2427.2006.01689.x

Levert, A., Alvariño, R., Bornancin, L., Mansour, E. A., Burja, A. M., Genevière, A.-M., et al. (2018). Structures and activities of tiahuramides A–C, cyclic depsipeptides from a Tahitian collection of the marine cyanobacterium Lyngbya majuscula. *J. Nat. Prod.* 81, 1301–1310. doi: 10.1021/acs.jnatprod.7b00751

Liang, X., Matthew, S., Chen, Q.-Y., Kwan, J. C., Paul, V. J., and Luesch, H. (2019). Discovery and total synthesis of doscadenamide a: a quorum sensing signaling molecule from a marine cyanobacterium. *Org. Lett.* 21, 7274–7278. doi: 10.1021/acs.orglett.9b02525

Loya, S., Reshef, V., Mizrachi, E., Silberstein, C., Rachamim, Y., Carmeli, S., et al. (1998). The inhibition of the reverse transcriptase of HIV-1 by the natural sulfoglycolipids from cyanobacteria: contribution of different moieties to their high potency. *J. Nat. Prod.* 61, 891–895. doi: 10.1021/np970585j

Luo, S., Kang, H.-S., Krunic, A., Chlipala, G. E., Cai, G., Chen, W.-L., et al. (2014). Carbamidocyclophanes F and G with anti-mycobacterium tuberculosis activity from the cultured freshwater cyanobacterium Nostoc Sp. *Tetrahedron Lett.* 55, 686–689. doi: 10.1016/j.tetlet.2013.11.112

Ma, L., Zhang, Q., Yang, C., Zhu, Y., Zhang, L., Wang, L., et al. (2020). "1.06-assembly line and post-PKS modifications in the biosynthesis of marine polyketide natural products," in *Comprehensive natural products III*. eds. LiuH.-W. (. B.). and T. P. Begley (Oxford: Elsevier), 139–197.

Marrez, D. A., and Sultan, Y. Y. (2016). Antifungal activity of the cyanobacterium Microcystis Aeruginosa against Mycotoxigenic fungi. *J. Appl. Pharmaceut. Sci.* 6, 191–198. doi: 10.7324/JAPS.2016.601130

Mo, S., Krunic, A., Chlipala, G., and Orjala, J. (2009a). Antimicrobial ambiguine isonitriles from the cyanobacterium Fischerella ambigua. *J. Nat. Prod.* 72, 894–899.

Mo, S., Aleksej, K., Bernard, D. S., Scott, G. F., and Jimmy, O. (2010). Hapalindole-Related Alkaloids from the Cultured Cyanobacterium Fischerella Ambigua. *Phytochemistry* 71, 2116–23. doi: 10.1016/j.phytochem.2010.09.004

Mo, S., Krunic, A., Pegan, S. D., Franzblau, S. G., and Orjala, J. (2009b). An antimicrobial guanidine-bearing Sesterterpene from the cultured cyanobacterium Scytonema Sp. *J. Nat. Prod.* 72, 2043–2045. doi: 10.1021/np900288x

Montaser, R., Abboud, K. A., Paul, V. J., and Luesch, H. (2011). Pitiprolamide, a proline-rich dolastatin 16 analogue from the marine cyanobacterium Lyngbya majuscula from Guam. *J. Nat. Prod.* 74, 109–112. doi: 10.1021/np1006839

Moon, S. S., Chen, J. L., Moore, R. E., and Patterson, G. M. L. (1992). Calophycin, a fungicidal cyclic Decapeptide from the terrestrial blue-green alga Calothrix Fusca. *J. Org. Chem.* 57, 1097–1103. doi: 10.1021/jo00030a013

Moore, R. E., Cheuk, C., Yang, X.-Q. G., Patterson, G. M. L., Bonjouklian, R., Smitka, T. A., et al. (1987). Hapalindoles, antibacterial and Antimycotic alkaloids from the Cyanophyte. *J. Org. Chem.* 52, 1036–1043.

Mundt, S., Kreitlow, S., and Jansen, R. (2003). Fatty acids with antibacterial activity from the cyanobacterium Oscillatoria Redekei HUB 051. *J. Appl. Phycol.* 15, 263–267. doi: 10.1023/A:1023889813697

Murray, C. J. L., Ikuta, K. S., Sharara, F., Swetschinski, L., Aguilar, G. R., Gray, A., et al. (2022). Global burden of bacterial antimicrobial resistance in 2019: a systematic analysis. *Lancet* 399, 629–655. doi: 10.1016/s0140-6736(21)02724-0

Nagle, D. G., and Paul, V. J. (1998). Chemical defense of a marine cyanobacterial bloom. *J. Exp. Mar. Biol. Ecol.* 225, 29–38. doi: 10.1016/S0022-0981(97)00205-0

Najdenski, H. M., Gigova, L. G., Iliev, I. I., Pilarski, P. S., Lukavský, J., Tsvetkova, I. V., et al. (2013). Antibacterial and antifungal activities of selected microalgae and cyanobacteria. *Int. J. Food Sci. Technol.* 48, 1533–1540. doi: 10.1111/ijfs.12122

Neuhof, T., Schmieder, P., Preussel, K., Dieckmann, R., Pham, H., Bartl, F., et al. (2005). Hassallidin a, a glycosylated Lipopeptide with antifungal activity from the cyanobacterium Hassallia Sp. *J. Nat. Prod.* 68, 695–700. doi: 10.1021/np049671r

Neuhof, T., Schmieder, P., Seibold, M., Preussel, K., and von Döhren, H. (2006). Hassallidin B—second antifungal member of the Hassallidin family. *Bioorg. Med. Chem. Lett.* 16, 4220–4222. doi: 10.1016/j.bmcl.2006.05.094

O'Keefe, B. R., Giomarelli, B., Barnard, D. L., Shenoy, S. R., Chan, P. K. S., McMahon, J. B., et al. (2010). Broad-spectrum in vitro activity and in vivo efficacy of the antiviral protein griffithsin against emerging viruses of the family Coronaviridae. *J. Virol.* 84, 2511–2521. doi: 10.1128/JVI.02322-09

Oku, N., Yonejima, K., Sugawa, T., and Igarashi, Y. (2014). Identification of the n-1 fatty acid as an antibacterial constituent from the edible freshwater cyanobacterium Nostoc verrucosum. *Biosci. Biotechnol. Biochem.* 78, 1147–1150. doi: 10.1080/09168451.2014.918484

Patterson, G. M. L. (1992). "*Blue-Green ALGAAnabaena Laxa*."

Patterson, G. M. L., and Carmeli, S. (1992). Biological effects of tolytoxin (6-hydroxy-7-O-methyl-scytophycin b), a potent bioactive metabolite from cyanobacteria. *Arch. Microbiol.* 157, 406–410. doi: 10.1007/BF00249096

Pergament, I., and Carmeli, S. (1994). Schizotrin a: A novel antimicrobial cyclic peptide from a cyanobacterium. *Tetrahedron Lett.* 35, 8473–8476. doi: 10.1016/S0040-4039(00)74436-4

Petit, A., Léa, V., and Jean, P. C. (2021). Docking and in Silico Toxicity Assessment of Arthrospira Compounds as Potential Antiviral Agents against SARS-CoV-2. *Journal of Applied Phycology* 33, 1579–1602. doi: 10.1007/s10811-021-02372-9

Ploutno, A., and Carmeli, S. (2000). Nostocyclyne a, a novel antimicrobial Cyclophane from the cyanobacterium Nostoc Sp. *J. Nat. Prod.* 63, 1524–1526. doi: 10.1021/np0002334

Pradhan, B., Nayak, R., Patra, S., Bhuyan, P. P., Dash, S. R., Ki, J.-S., et al. (2022). Cyanobacteria and algae-derived bioactive metabolites as antiviral agents: evidence, mode of action, and scope for further expansion; a comprehensive review in light of the SARS-CoV-2 outbreak. *Antioxidants* 11:354. doi: 10.3390/antiox11020354

Prasanna, R., Nain, L., Tripathi, R., Gupta, V., Chaudhary, V., and Middha, S. (2008). Evaluation of fungicidal activity of extracellular filtrates of cyanobacteria – possible role of hydrolytic enzymes. *J. Basic Microbiol.* 48, 186–194. doi: 10.1002/jobm.200700199

Preisitsch, M., Harmrolfs, K., Pham, H. T. L., Heiden, S. E., Füssel, A., Wiesner, C., et al. (2015a). Anti-MRSA-acting Carbamidocyclophanes H-L from the Vietnamese cyanobacterium Nostoc Sp. CAVN2. *J. Antibiot.* 68, 165–177. doi: 10.1038/ja.2014.118

Preisitsch, M., Niedermeyer, T. H. J., Heiden, S. E., Neidhardt, I., Kumpfmu, J., Wurster, M., et al. (2015b). Cylindrofridins A—C, linear cylindrocyclophane-related alkylresorcinols from the cyanobacterium cylindrospermum stagnale. *J. Nat. Prod.* 79, 106–115. doi: 10.1021/acs.jnatprod.5b00768

Ramos, D. F., Matthiensen, A., Colvara, W., de Votto, A. P. S., Trindade, G. S., da Silva, P. E. A., et al. (2015). Antimycobacterial and cytotoxicity activity of microcystins. *J. Venomous Animals Toxins Including Tropic. Dis.* 21, 1–7. doi: 10.1186/s40409-015-0009-8

Rechter, S., König, T., Auerochs, S., Thulke, S., Walter, H., Dörnenburg, H., et al. (2006). Antiviral activity of Arthrospira-derived spirulan-like substances. *Antivir. Res.* 72, 197–206. doi: 10.1016/j.antiviral.2006.06.004

Rickards, R. W., Rothschild, J. M., Willis, A. C., de Chazal, N. M., Kirk, J., Kirk, K., et al. (1999). Calothrixins A and B, novel pentacyclic metabolites from Calothrix cyanobacteria with potent activity against malaria parasites and human cancer cells. *Tetrahedron* 55, 13513–13520. doi: 10.1016/S0040-4020(99)00833-9

Ridley, C. P., and Khosla, C. (2009). "Polyketides," in *Encyclopedia of Microbiology*. ed. M. Schaechter. *3rd Edn.* (Oxford: Academic Press), 472–481.

Rodríguez, M. C., Merino, E. R., Pujol, C. A., Damonte, E. B., Cerezo, A. S., and Matulewicz, M. C. (2005). Galactans from cystocarpic plants of the red seaweed Callophyllis variegata (Kallymeniaceae, Gigartinales). *Carbohydr. Res.* 340, 2742–2751. doi: 10.1016/j.carres.2005.10.001

Rojas, V., Rivas, L., Cárdenas, C., and Guzmán, F. (2020). Cyanobacteria and eukaryotic microalgae as emerging sources of antibacterial peptides. *Molecules* 25:5804. doi: 10.3390/molecules25245804

Saad, M. H., El-Fakharany, E. M., Salem, M. S., and Sidkey, N. M. (2022). In vitro assessment of dual (antiviral and antitumor) activity of a novel lectin produced by the newly cyanobacterium isolate, Oscillatoria acuminate MHM-632 MK014210.1. *J. Biomol. Struct. Dyn.* 40, 3560–3580. doi: 10.1080/07391102.2020.1848632

Seneviratne, C. J., and Rosa, E. A. R. (2016). Editorial: antifungal drug discovery: new theories and new therapies. *Front. Microbiol.* 7:728. doi: 10.3389/fmicb.2016.00728

Senol, D., Aysegul, A. P., Grudina, C., Sassoon, N., Reiko, U., Bousset, L., et al. (2019). Effect of Tolytoxin on tunneling nanotube formation and function. *Sci. Rep.* 9:5741. doi: 10.1038/s41598-019-42161-6

Singh, R. K., Tiwari, S. P., Rai, A. K., and Mohapatra, T. M. (2011). Cyanobacteria: an emerging source for drug discovery. *J. Antibiot.* 64, 401–412. doi: 10.1038/ja.2011.21

Skowron, K. J., Speltz, T. E., and Moore, T. W. (2019). Recent structural advances in constrained helical peptides. *Med. Res. Rev.* 39, 749–770. doi: 10.1002/med.21540

Smitka, T. A., Bonjouklian, R., Doolin, L., Jones, N. D., Deeter, J. B., Yoshida, W. Y., et al. (1992). Ambiguine Isonitriles, fungicidal Hapalindole-type alkaloids from

three genera of blue-green algae belonging to the Stigonemataceae. *J. Org. Chem.* 57, 857–861. doi: 10.1021/jo00029a014

Soares, A. R., Engene, N., Gunasekera, S. P., Sneed, J. M., and Paul, V. J. (2015). Carriebowlinol, an antimicrobial Tetrahydroquinolinol from an assemblage of marine cyanobacteria containing a novel taxon. *J. Nat. Prod.* 78, 534–538. doi: 10.1021/np500598x

Soltani, N., Khavari-Nejad, R. A., Tabatabaei Yazdi, M., Shokravi, S., and Fernández-Valiente, E. (2005). Screening of soil cyanobacteria for antifungal and antibacterial activity. *Pharm. Biol.* 43, 455–459. doi: 10.1080/13880200590963871

Sun, T., Li, X. D., Hong, J., Liu, C., Zhang, X. L., Zheng, J. P., et al. (2019). Inhibitory effect of two traditional Chinese medicine monomers, Berberine and Matrine, on the quorum sensing system of antimicrobial-resistant Escherichia Coli. *Front. Microbiol.* 10, 1–11. doi: 10.3389/fmicb.2019.02584

Swain, S. S., Paidesetty, S. K., and Padhy, R. N. (2017). ScienceDirect antibacterial, antifungal and Antimycobacterial compounds from cyanobacteria. *Biomed. Pharmacother.* 90, 760–776. doi: 10.1016/j.biopha.2017.04.030

Takebe, Y., Saucedo, C. J., Lund, G., Uenishi, R., Hase, S., Tsuchiura, T., et al. (2013). Antiviral lectins from red and blue-green algae show potent in vitro and in vivo activity against hepatitis C virus. *PLoS One* 8:e64449. doi: 10.1371/journal.pone.0064449

Thakur, V., Bhola, S., Thakur, P., Patel, S. K. S., Kulshrestha, S., Ratho, R. K., et al. (2021). Waves and variants of SARS-CoV-2: understanding the causes and effect of the COVID-19 catastrophe. *Infection* 50, 309–325. doi: 10.1007/s15010-021-01734-2

Vasireddy, D., Vanaparthy, R., Mohan, G., Malayala, S. V., and Atluri, P. (2021). Review of COVID-19 variants and COVID-19 vaccine efficacy: what the clinician should know? *J. Clin. Med. Res.* 13, 317–325. doi: 10.14740/jocmr4518

Vestola, J., Shishido, T. K., Jokela, J., Fewer, D. P., Aitio, O., Permi, P., et al. (2014). Hassallidins, antifungal Glycolipopeptides, are widespread among cyanobacteria and are the end-product of a nonribosomal pathway. *Proc. Natl. Acad. Sci.* 111, E1909–E1917. doi: 10.1073/pnas.1320913111

Volk, R. B., and Furkert, F. H. (2006). Antialgal, antibacterial and antifungal activity of two metabolites produced and excreted by cyanobacteria during growth. *Microbiol. Res.* 161, 180–186. doi: 10.1016/j.micres.2005.08.005

Xu, S., Nijampatnam, B., Dutta, S., and Velu, S. E. (2016). Cyanobacterial metabolite calothrixins: recent advances in synthesis and biological evaluation. *Mar. Drugs* 14:17. doi: 10.3390/md14010017

Yoon, B. K., Jackman, J. A., Valle-González, E. R., and Cho, N.-J. (2018). Antibacterial free fatty acids and Monoglycerides: biological activities, experimental testing, and therapeutic applications. *Int. J. Mol. Sci.* 19:114. doi: 10.3390/ijms19041114

Yuzawa, S., and Kuzuyama, T. (2020). "1.05 – Engineering of acyltransferase domains in polyketide synthases" in *Comprehensive Natural Products III*. eds. Liu H.-W. B. and T. P. Begley (Oxford: Elsevier), 123–138.

Zhang, H., and Chen, S. (2022). Cyclic peptide drugs approved in the last two decades (2001–2021). *RSC Chem. Biol.* 3, 18–31. doi: 10.1039/d1cb00154j

frontiers | Frontiers in Microbiology

TYPE Original Research
PUBLISHED 16 February 2023
DOI 10.3389/fmicb.2023.1061927

OPEN ACCESS

EDITED BY
Prashant Kumar Singh,
Mizoram University, India

REVIEWED BY
Riti Thapar Kapoor,
Amity University Uttar Pradesh, India
Avinash Singh,
New York University, United States
Vijay Pratap Singh,
University of Allahabad, India

*CORRESPONDENCE
Neelam Atri
✉ neelam1409@bhu.ac.in

SPECIALTY SECTION
This article was submitted to Microbial Physiology and Metabolism, a section of the journal Frontiers in Microbiology

RECEIVED 05 October 2022
ACCEPTED 16 January 2023
PUBLISHED 16 February 2023

CITATION
Srivastava R, Kanda T, Yadav S, Singh N, Yadav S, Prajapati R, Kesari V and Atri N (2023) Salinity pretreatment synergies heat shock toxicity in cyanobacterium *Anabaena* PCC7120.
Front. Microbiol. 14:1061927.
doi: 10.3389/fmicb.2023.1061927

Salinity pretreatment synergies heat shock toxicity in cyanobacterium *Anabaena* PCC7120

Rupanshee Srivastava[1], Tripti Kanda[1], Sadhana Yadav[1], Nidhi Singh[1], Shivam Yadav[2], Rajesh Prajapati[1], Vigya Kesari[1] and Neelam Atri[3]*

[1]Department of Botany, Institute of Sciences, Banaras Hindu University, Varanasi, India, [2]Department of Botany, Thakur Prasad Singh (T.P.S.) College, Patna, Bihar, India, [3]Department of Botany, Mahila Mahavidyalaya (M.M.V.), Banaras Hindu University, Varanasi, India

This study was undertaken to bridge the knowledge gap pertaining to cyanobacteria's response to pretreatment. The result elucidates the synergistic effect of pretreatment toxicity in cyanobacterium *Anabaena* PCC7120 on morphological and biochemical attributes. Chemical (salt) and physical (heat) stress-pretreated cells exhibited significant and reproducible changes in terms of growth pattern, morphology, pigments, lipid peroxidation, and antioxidant activity. Salinity pretreatment showed more than a five-fold decrease in the phycocyanin content but a six-fold and five-fold increase in carotenoid, lipid peroxidation (MDA content), and antioxidant activity (SOD and CAT) at 1 h and on 3rd day of treatment, respectively, giving the impression of stress-induced free radicals that are scavenged by antioxidants when compared to heat shock pretreatment. Furthermore, quantitative analysis of transcript (qRT-PCR) for FeSOD and MnSOD displayed a 3.6- and 1.8-fold increase in salt-pretreated (S-H) samples. The upregulation of transcript corresponding to salt pretreatment suggests a toxic role of salinity in synergizing heat shock. However, heat pretreatment suggests a protective role in mitigating salt toxicity. It could be inferred that pretreatment enhances the deleterious effect. However, it further showed that salinity (chemical stress) augments the damaging effect of heat shock (physical stress) more profoundly than physical stress on chemical stress possibly by modulating redox balance *via* activation of antioxidant responses. Our study reveals that upon pretreatment of heat, the negative effect of salt can be mitigated in filamentous cyanobacteria, thus providing a foundation for improved cyanobacterial tolerance to salt stress.

KEYWORDS

cyanobacteria, *Anabaena* PCC7120, salinity, heat shock, pretreatments, stress

1. Introduction

Anthropogenic activities in agricultural fields such as overuse of chemical fertilizers and improper irrigation practices increase the salt and metal contents in the soil. Furthermore, an increase in greenhouse gas emissions leads to the accumulation of heat-trapping gases in the atmosphere and thus warms the climate, which eventually disturbs the soil ecosystem as well as soil microflora, particularly cyanobacteria. Thus, salinity and heat are considered agriculturally

relevant abiotic stresses and are of particular interest. Cyanobacteria are photosynthetic prokaryotes, present in extreme environments, and serve as a dominant producer in paddy fields. They tolerate unfavorable environmental conditions and thus have evolved various responses to acclimatize to stresses (Wannigama et al., 2012). *Anabaena*, a filamentous nitrogen-fixing cyanobacterium, is known to fix a significant amount of nitrogen in Indian paddy fields. However, in paddy fields, they are exposed to various abiotic stresses, including heat and salinity. Salt stress is an abiotic element that has a huge impact on cyanobacterial survival and growth. In cells of photosynthetic organisms, salt stress leads to a decrease in cell volume and an increase in osmotic stress (Yang et al., 2020). It also inhibits processes like photosynthesis, protein synthesis, energetics, and lipid metabolism. Changes in ion and water homeostasis due to salt cause damage at the molecular level, arrest growth, and can even cause death (Demiral and Türkan, 2006). The low concentration of Na^+ aids in the regulation of pH and nitrogen and carbon dioxide fixation in plants and cyanobacteria (Karandashova and Elanskaya, 2005; Han et al., 2012; Fan et al., 2019). Ion homeostasis is disrupted by excessive Na^+ and Cl^- fluxes into the cell, resulting in the build-up of ROS (Scarpeci et al., 2008; Feng et al., 2015; Song et al., 2020). ROS leads to the breakdown of the photosynthetic machinery and membrane lipid peroxidation, which has a negative impact on photosynthesis (Yang et al., 2020). Furthermore, high NaCl concentrations prevent the *de novo* synthesis of proteins, including several photosystem-related proteins like the D1 protein (Allakhverdiev et al., 2002).

However, heat damages the cellular membrane and leads to oxidative damage, thereby producing ROS such as superoxide anions, hydroxyl radicals, and peroxides (Liu and Huang, 2000). Furthermore, it is also known to inhibit growth, photosynthesis, metabolism, and RNA synthesis and induce protein denaturation and aggregation causing post-translational modifications leading to the loss of cell viability (Wen et al., 2005). Photosystem II (PSII) is regarded to be one of the most sensitive locations in photosynthetic machinery, and its activity is considerably reduced by high-temperature stress (Zhao et al., 2008).

However, most of the studies concerning stress are of single stress type (Rai et al., 2013). The pretreatment effect is distinctive and cannot be extrapolated from the responses to each of them when applied alone. It is reasonable to presume that the molecular signaling pathway and the complex network of interrelated genes may synergize and/or antagonize each other's effects (Rai et al., 2013). Even though the pretreatment phenomenon has not yet been reported to exist in the environment but it can be applied to various biotechnological approaches, as mentioned in the study of Ellison et al. (2019) in where they studied the effect of pretreatment for enhanced lipid extraction. Pretreatment studies of salt, temperature, and copper followed by UV stress in *Anabaena doliolum* (Srivastava et al., 2006), pretreatment of copper followed by UV stress in *Anabaena doliolum* (Bhargava et al., 2008), and heat pretreatment followed by UV stress in *Anabaena doliolum* (Mishra et al., 2009) are one of the very few reports on cyanobacteria pertaining to pretreatment.

A thorough review of the literature has revealed the availability of facts of cyanobacteria subjected to single stresses as well as in combination (Narayan et al., 2011; Pandey et al., 2012; Rai et al., 2013, 2014; Agrawal et al., 2014; Panda et al., 2014; Shrivastava et al., 2015; Singh et al., 2015; Teikari et al., 2015). However, studies pertaining to pretreatments are very limiting. Furthermore, heat treatment has been found to offer cross-tolerance to different abiotic stresses such as salt (Mishra et al., 2009) but studies pertaining to the effects of salt (chemical stress) on heat shock (physical stresses) is limiting. Therefore, this study was conducted to bridge the above-mentioned gap in the knowledge regarding the response of cyanobacteria subjected to pretreatment. In light of this and the physicochemical characteristics of the relevant stresses, we postulated that salinity pretreatment should enhance the heat effect while heat pretreatment should counteract the salinity effect even if applied after 7 days. To test the aforementioned hypotheses, experiments were conducted to investigate the effect of pretreatment with salt and temperature on the morphology, pigment content, lipid peroxidation (MDA content), enzymatic (superoxide dismutase and catalase) modifications, and expression pattern of antioxidative genes in *Anabaena* PCC7120.

Abbreviations: C, control; H, heat shock treatment; S, salinity; H + S, heat shock and salinity combined; H-S, heat shock pretreatment followed by salinity; S-H, salinity pretreatment followed by heat shock; SOD, superoxide dismutase; CAT, catalase.

2. Materials and methods

2.1. Organism and growth condition

Anabaena PCC7120 was grown axenically in BG-11 medium (Rippka et al., 1979) buffered with 4-(2-hydroxyethyl)-1-piperazine-ethanesulfonic acid (HEPES) buffer (1.2 g L^{-1}) at pH 7.5 in Erlenmeyer flask of capacity 250 ml containing 100 ml of culture at 24 ± 2^{o}C under a day light fluorescent tube emitting 72 μmol m^{-2} s^{-1} photosynthetically active radiation (PAR) light intensity and a photoperiod of 14:10 h. The flasks were plugged with non-absorbent cotton and were shaken 2–3 times daily for proper aeration. All experiments were performed under an exponentially growing culture.

2.2. Experimental design and treatments

Anabaena PCC7120 culture (OD_{750} = 0.5) never exposed to stress was taken as control strain. The single, combined, and pretreatment of heat and salt treatment were given to the strain at LC_{50} (lethal concentration). LC_{50} was determined through the colony count method (Rai and Raizada, 1985).

2.2.1. For LC_{50} NaCl determination

Exponentially growing *Anabaena* containing 10^4 cells mL^{-1} was aseptically spread on agar plates supplemented with various concentrations of NaCl (50–250 mM).

2.2.2. For LC_{50} heat shock determination

Exponentially growing *Anabaena* containing 10^4 cells mL^{-1} was aseptically spread on agar plates. The plates were shifted to the temperature-controlled incubator for heat treatment under continuous light of 72 μmol photon m^{-2} s^{-1} PAR provided by fluorescent lamps throughout the heat treatment. The plates were exposed to different temperatures (40–60^{o}C) for 1 h.

Cells were counted after 3 weeks. LC_{50} was obtained at 150 mM and 45^{o}C for NaCl and heat, respectively.

2.3. Experimental design

The experiments were performed in six sets: (1) cells never exposed to stress (C), (2) cells exposed to heat at 45^{o}C for 1 h (H), (3) cells exposed to salt at 150 mM (S), (4) cells pretreated with heat (45^{o}C for 1 h) followed by recovery for 7 days and application of salt at 150 mM (H-S), (5) cells pretreated with salt at 150 mM followed by recovery for 7 days and application of heat at 45^{o}C (S-H), and (6) cells exposed to combined heat and salt stress at respective LC_{50} (H + S) (**Figure 1**). All the parameters used in the present study were analyzed from the aforementioned cultures. Experiments were performed in triplicates and were repeated two times to confirm the reproducibility.

2.4. Growth measurements

Growth was estimated by observing the optical density of the culture at OD_{750} nm in a UV/visible spectrometer (Shimadzu, 2017) on alternate days up to the 15th day using the basal medium as blank (Küpper et al., 2000). It was also measured by cell count through a hemocytometer under a microscope (Olympus, 2019) at 40X on alternate days up to the 15th day (Lawton et al., 1999).

2.5. Morphological alterations

The morphological alteration was obtained by taking images of the control culture and culture exposed to stress on 0, 3, 7, and 15 days using a light microscope (Olympus, 2019 model no. CX21iLEDFS1) at 40X, and the image was processed through a computer with Magcam DC-10 camera model and MagVision software (Image calibration: 40X; X:50.000000/40 Micron/Pixel; Y: 50.000000/40 Micron/Pixel).

2.6. Pigments estimation

Pigment estimation was done by the protocol of Myers and Kratz (1955). A known volume of cyanobacterial culture was centrifuged and the pellet was incubated overnight at 4^{o}C in 80% acetone. The suspension was centrifuged and the supernatant was used to measure chlorophyll *a* and carotenoid at 663 and 480 nm, respectively. The pellet thus obtained was used for the estimation of phycocyanin. The pellet was resuspended in 30 mM *Tris–HCl* and sonicated. The suspension was centrifuged and the supernatant was used to measure the phycocyanin content at 610 nm.

2.7. Phycobiliproteins spectrum

The supernatant obtained in the pigment estimation for phycocyanin (Myers and Kratz, 1955) was used to study phycobiliproteins spectra by measuring the absorbance from the range of 400–700 nm (Adir and Lerner, 2003).

2.8. Malondialdehyde (MDA) estimation

The total content of 2-thiobarbituric acid (TBA) reactive substances expressed as MDA (malondialdehyde) was used to measure lipid peroxidation. These reactive substances were extracted by the protocol of Cakmak and Horst (1991). A known volume of culture was centrifuged and the pellet was suspended in 0.1% of TCA at 4^{o}C. The suspension was sonicated and centrifuged. A total of 0.5% TBA in 20% TCA was added to the supernatant and the solution was incubated at 90^{o}C, and then the reaction was terminated in ice-cold water. The suspension was again centrifuged. The absorbance of the supernatant was measured at 532 nm and corrected for non-specific turbidity by subtracting the absorbance at 600 nm. The concentration of MDA was calculated at its extinction coefficient (155 mM^{-1} cm^1).

2.9. Antioxidant assay

Cell pellets of *Anabaena* PCC7120 suspended in lysis buffer (pH 7.0) were sonicated in ice-cold condition. Cell lysis buffer for enzyme assay contained 1 mM EDTA and 1% PVP. The sonicated sample was centrifuged at 4^{o}C and the resulting supernatant containing crude extract or antioxidant enzymes was used for further assay. Total SOD activity was assayed by monitoring the inhibition of reduction of nitroblue tetrazolium (NBT) according to the method of Giannopolitis and Ries (1977). A 3 ml reaction mixture contained 50 mM potassium phosphate buffer (pH 7.8), 0.1 mM EDTA, 13 mM methionine, 75 μM NBT, enzyme extract, and 2 μM riboflavin. The reaction mixture was illuminated for 20 min at a light intensity of 5,000 μmol photon m^{-2} s^{-1}. One unit of SOD activity was defined as the amount of enzyme required to cause 50% inhibition of NBT reduction monitored at 560 nm. Catalase activity was estimated by measuring the consumption of H_2O_2 (extinction coefficient 39.4 mM^{-1} cm^{-1}) at 240 nm for 3 min (Aebi, 1984). A 3 ml reaction mixture contained 50 mM potassium phosphate buffer (pH 7), 10 mM H_2O_2, and enzyme extract. One unit of CAT activity was defined as the amount of enzyme utilized to decompose 1.0 μM of H_2O_2.

2.10. Transcript analysis

Total RNA extraction using the RNeasy Micro kit (Qiagen) was performed from 50 ml culture (OD_{750}nm = 0.6) of *Anabaena* PCC7120 grown in BG11 before and after stress treatment. Total RNA (1 μg) was reverse transcribed in a 20 μl reaction mixture using the iScript cDNA synthesis kit (BioRad). Transcript analysis was performed using gene-specific primer for antioxidative genes, FeSOD, MnSOD, and catalase (*all*0070, *alr*3090, and *alr*2938) as well as reference gene rnpB (**Table 1**). For qRT-PCR using a CFX-96 (BioRad), 15 ng of cDNA extracted from each sample was used in 20 μl including 10 pmol of each forward and reverse primers, and 1x Sso fast evagreen qPCR supermix (BioRad). Transcript levels were normalized to rnpB transcript and calculated using the $2^{-\Delta\Delta Ct}$ method to evaluate the relative quantities of each amplified product (Livak and Schmittgen, 2001). The threshold cycle (Ct) was automatically determined for each reaction by the system (default parameters). The specificity of the PCR was determined by melting curve analysis of the amplified products.

2.11. Statistical analysis

Values presented in the text indicate the mean ± S.E. of the three replicates. The experiments were done in triplicates and repeated

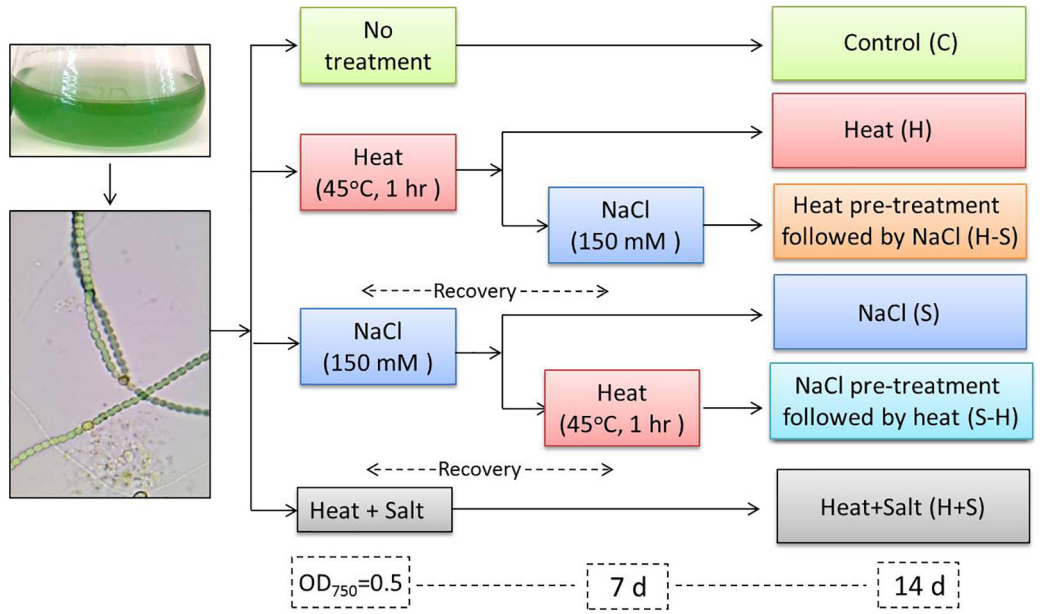

FIGURE 1
Experimental design.

TABLE 1 Oligonucleotide used for the analysis of the selected antioxidative gene for qRT-PCR.

Gene	Primers
all0070	F: TGGTAGTGGTTGGGTTTGGT R: AGCGTGTTCCCAGACATCAT
alr3090	F: AACGTGGATCAAACAGAGGC R: TCGCTCTCAAATCCCGAACT
alr2938	F: TGATGATGGCGGTACACTGA R: CTGGGCGAGCATTTCTGAAG
rnpB	F: AGGGAGAGAGTAGGCGTTGG R: GGTTTACCGAGCCAGTACCTCT

two times to confirm the reproducibility. Results were statistically analyzed using two-way ANOVA, followed by Dunnett's multiple comparisons test to compare changes within groups. A p-value of ≤ 0.05 was considered statistically significant. All the statistical analysis was performed using SPSS ver. 22.0 software.

3. Results

3.1. Growth measurements

The sharp decline in growth can be seen in cells subjected to S-H as shown in Figure 2A, and S-H density declined by 71.57, 56.90, and 50.06% on the 4, 6, and 10th days, respectively. The H-treated sample showed an appreciable decrease from the 6th day to the 10th day of treatment, thereafter there was an increase in its growth. S showed a decrease on the 10th day by 50.47%. However, H+S and pretreated sample, i.e., H-S did not show any stark difference in their growth and were always on par with the control sample. H, H+S, and H-S, did not show any significant change in their cell density. Control bears a sigmoid curve during its growth measurement.

Results pertaining to cell count (Figure 2B) portrayed that the sample treated with S-H was severely affected and showed a sharp decline in its number up to 15 days. H and H+S showed significant cell death by 67.54 and 57.14%, respectively, on the 15th day. S showed significant cell death from the 14th day onward. There was a decline of 71.31 and 69.09% on the 14th and 15 days, respectively. H-S showed a significant decrease on the 12th day by 53.35%, on the 14th day by 48.75%, and on the 15th day by 64.13%.

However, if a correlation has to be drawn between the optical density and cell count, it can be concluded that an increase in cell density does not correspond to an increase in live cell number. An increase in cell density and a decrease in live cell count in a sample can be attributed to the fact that optical density has included the density of live and dead cells together as can be observed in the case of samples treated with H, S, H-S, and H+S.

3.2. Morphological alterations

The morphological alterations of *Anabaena* PCC7120 were investigated through light microscopy under various stresses. There were significant differences in the morphological changes shown by the organism under study. Light microscopic studies on the interactions of the stress with *Anabaena* PCC7120 revealed extensive breakage of cyanobacterial filaments.

Significant variation was not observed in samples after 1 h of stress treatment sample and control. Slight yellowing of filaments could be observed in cells subjected to salt stress. Comparative shortening of filaments was observed in all samples on the 3rd day of stress treatment. The akinete formation could be observed in cultures exposed to H + S in order to survive stress conditions. Fragmentation of filaments was observed in the pretreated samples (H-S and S-H).

Abnormality in cell shape and size within the filaments was observed in treated cultures on the 7th day. The terminal akinete formation was observed in filaments exposed to stresses. Moreover,

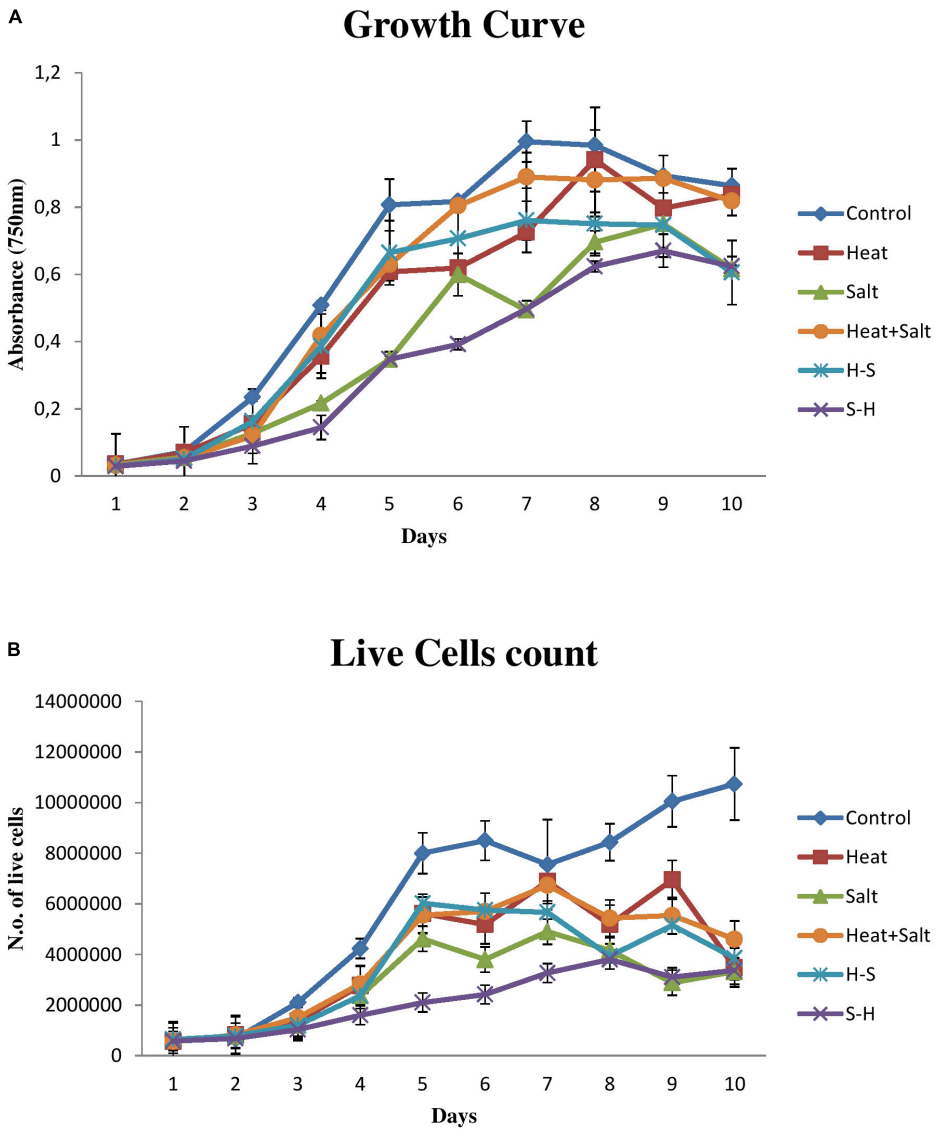

FIGURE 2
Growth behavior of *Anabaena* PCC 7120 exposed to stress. **(A)** Growth measurement *via* optical density. **(B)** Growth measurement *via* cell count.

prominent intercalary cell death was observed in the culture treated with H and in S-H. Abnormal bulging of cells in the filament of cyanobacterium was observed in H + S. Intercalary cell death appeared in H on the 15th day, whereas cell enlargement and the terminal akinete cell were observed under salt treatment. H + S treatment showed distinctive anomalous cell enlargement in filaments owing to osmotic and heat stress. Fragmentation of filaments was observed in H-S; 4–5 cells/filaments were observed. A peculiar phenomenon of contraction of the protoplast of a plant cell, which may be due to loss of water from the cells, was observed in S-H which resulted in plasmolysis of cells in the filaments due to salinity pretreatment (Figures 3A–D).

3.3. Pigment analysis

3.3.1. Chlorophyll *a*

No significant change was observed after 1 h of stress exposure. The chlorophyll content of the culture subjected to treatment declined throughout the observation. On the 3rd day, S showed a significant decline in its chlorophyll concentration by 2.60-fold. Moreover, on the 15th day, cultures subjected to S and H + S treatments showed a significant decrease of 2.73- and 3.02-fold, respectively, in the chlorophyll *a* content. Nonetheless, pretreatment samples showed a decline in the content (approximately 1–1.5-fold change) unlike the other stressed exposed culture but it was on par with the control. It may be that pretreatment had an antagonistic effect on the latter-induced stress (Figure 4).

3.3.2. Carotenoid

An increase in carotenoid content was observed throughout all cultures subjected to stress. However, H-S showed a significantly high amount of carotenoid from 1 h up to the 15th day. It showed an increase of 32.94, 33.98, 33.35, and 34.23% on 1 h and 3rd, 7th, and 15th day, respectively, in comparison to the control. Similarly, S-H also showed a significant increase in the amount of carotenoid on the 7 and 15th day (33.35 and 29.19%, respectively) after treatment

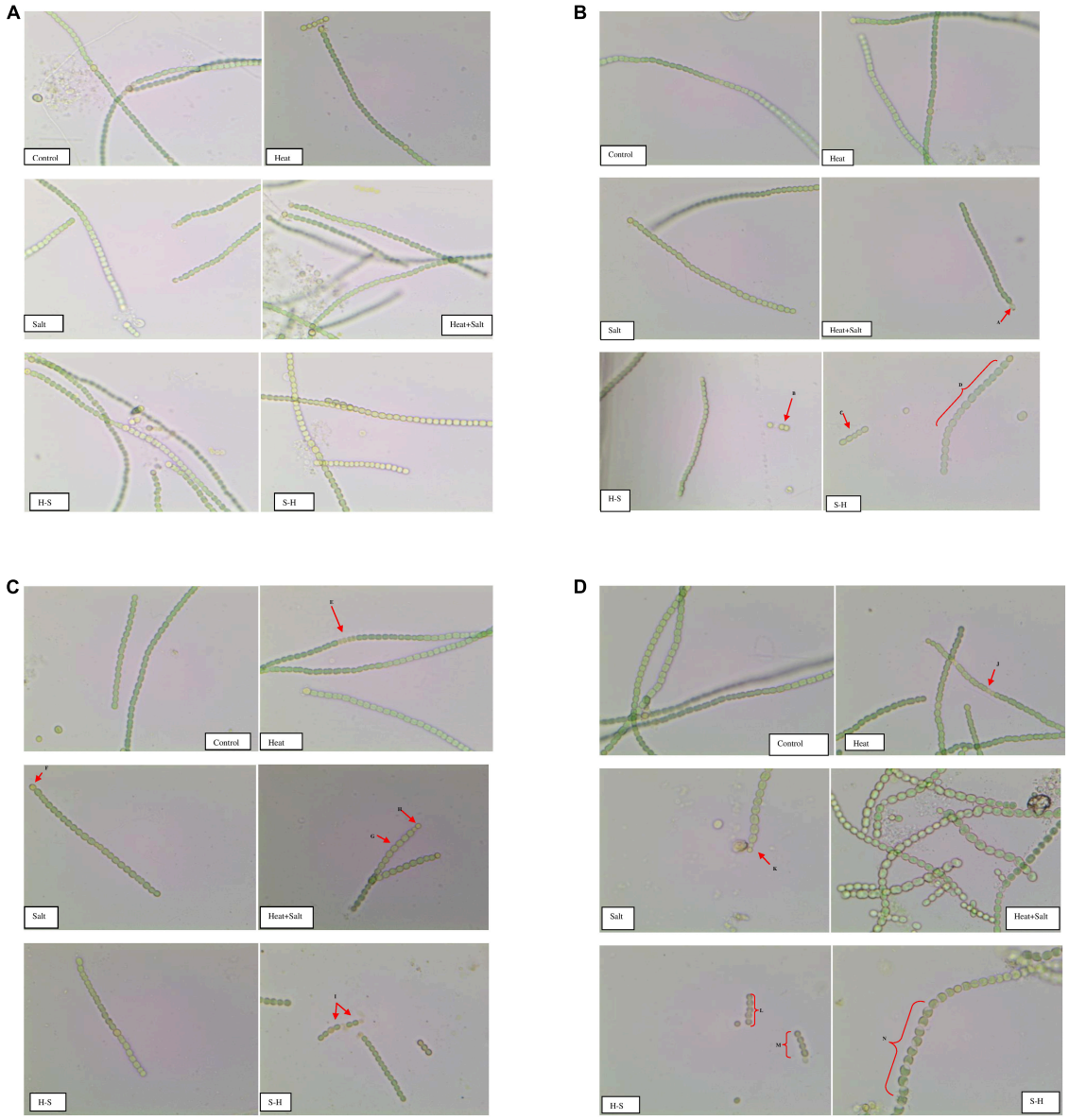

FIGURE 3
(A) Images of *Anabaena* PCC7120 subjected to selected stresses after 1 h (Image calibration: 40X; X:50.000000/40 Micron/Pixel; Y: 50.000000/40 Micron/Pixel). **(B)** Images of *Anabaena* PCC 7120 subjected to selected stresses on 3rd day. (Image calibration: 40X; X:50.000000/40 Micron/Pixel; Y: 50.000000/40 Micron/Pixel. Red arrows or braces indicate a morphological alteration in the filaments. A. Akinete formation; B. and C. Fragmentation of filaments; D. Bulging of cells in filaments). **(C)** Images of *Anabaena* PCC 7,120 subjected to selected stresses on the 7th day (Image calibration: 40X; X:50.000000/40 Micron/Pixel; Y: 50.000000/40 Micron/Pixel. E. & I. Intercalary cell death; F. and H. Akinetes formation; G. Cell bulging). **(D)** Images of *Anabaena* PCC7120 subjected to selected stresses on the 15th day (Image calibration: 40X; X:50.000000/40 Micron/Pixel; Y: 50.000000/40 Micron/Pixel. J. Intercalary cell death; K. Akinete formation; L. and M. Fragmentation of filaments; N. Plasmolysis of cells in filament).

(Figure 5). The increase of carotenoids in pretreated samples can be attributed as a positive strategy as it protects light-harvesting pigments against photochemical damage.

3.3.3. Phycocyanin

Phycocyanin content was always low for the treated sample up to the 15th day of observation in comparison to the control. There was no significant decline in the phycocyanin content in the H-treated sample. Significant changes were observed in all cultures subjected to stress on 1 h and 15th day except in H, whereas the pretreated sample also showed a significant decrease in the content on the 3rd and 7th day. There was a decrease of 2. 45-, 2. 22-, 2. 29-, and 5.21-fold in S, H + S, H-S, and S-H, respectively, on 1 h after treatment, and 1. 13-, 3. 15-, 5. 52-, and 3.74-fold in S, H + S, H-S, and S-H, respectively, on day 15. S-H showed a decrease in content by 2.49- and 4.426-fold on the 3rd and 7th day, respectively, and H-S showed a decrease of 3.15-fold on day 7 (Figure 6). Pretreatment enhanced the degradation of phycocyanin.

3.4. Phycobiliprotein spectrum

A study was conducted to assess the effect of stress on phycobiliproteins of *Anabaena* PCC7120. It resulted in a large peak

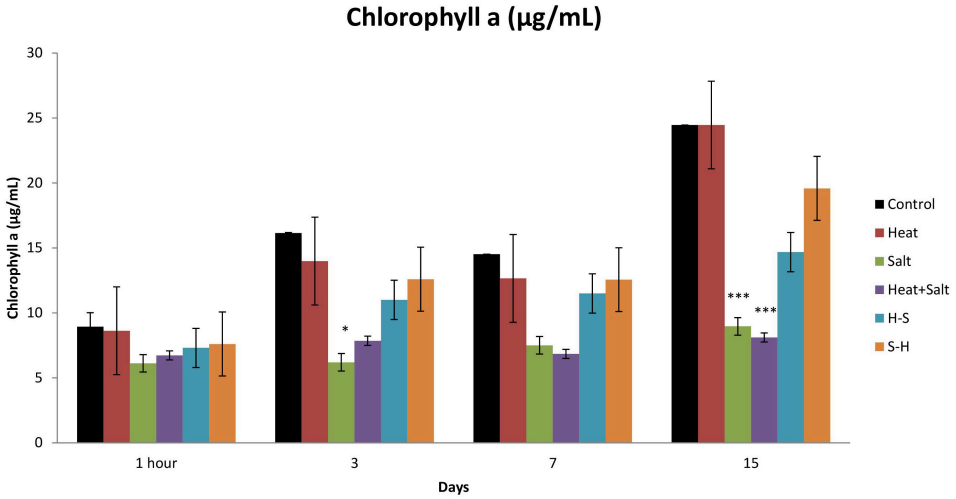

FIGURE 4
Effect of selected stresses on chlorophyll *a* content of *Anabaena* PCC 7120 up to the 15th day. Asterisk (*) indicates $p < 0.05$ and triple asterisk (***) indicates $p < 0.001$. (H-S indicates heat pretreatment; S-H indicates salt pretreatment).

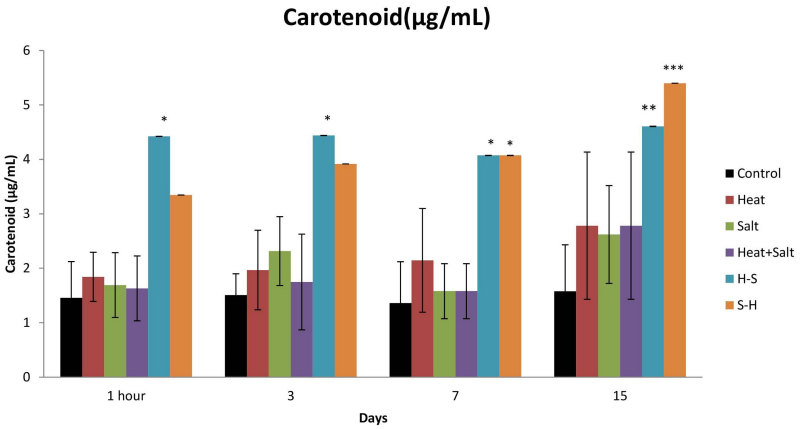

FIGURE 5
Effect of selected stresses on carotenoid content of *Anabaena* PCC 7120 up to 15th day. Asterisk (*) indicates $p < 0.05$, a double asterisk (**) indicates $p < 0.01$, and the triple asterisk (***) indicates $p < 0.001$. (H-S indicates heat pretreatment; S-H indicates salt pretreatment).

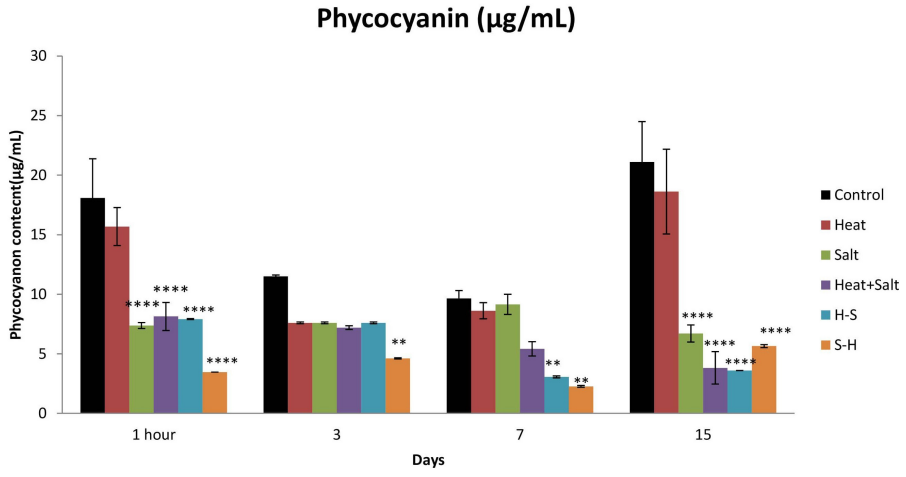

FIGURE 6
Effect of selected stresses on phycocyanin content of *Anabaena* PCC 7120 up to 15th day. A double asterisk (**) indicates $p < 0.01$, the triple asterisk (***) indicates $p < 0.001$, and the four asterisk (****) indicates $p < 0.0001$. (H-S indicates heat pretreatment; S-H indicates salt pretreatment).

of allophycocyanin (620–660 nm) and phycocyanin (600–640 nm) in control. Phycoeyrthrocyanin peak was also higher in control than in stresses throughout the observation period. The peak area was least affected in H, whereas S-H was severely affected in terms of peak area except on the 15th day. Rest were showing intermediate results. H and H + S showed similar absorption for phycoerythrin and S and H-S also bear close resemblance in peak. A similar result was obtained on the 3rd day with the exception that H + S showed a further decrease in peak. On the 7th day, H was on par with control for the phycoerythrin peak but there was a significant decrease in peak in terms of allophycocyanin and phycocyanin. S and H-S samples were on par with each other in terms of the peak for phycocyanin, whereas the absorption of others remains almost the same as that of the 3rd day. H + S and H-S showed a decrease in their phycocyanin, allophycocyanin, and phycoerythrin peak but S-H showed a large peak on the 15th day (Figure 7). The change in absorption spectra of phycocyanin was similar to the change in the concentration of phycocyanin.

3.5. Malondialdehyde (MDA)

The untreated sample showed a low level of MDA formation throughout the observation, whereas the treated one showed a comparatively high MDA level. MDA formation was significantly increased after 1 h of stress (4.25-fold increase) for H. The MDA content for S gradually increased up to the 7th day (5. 25-, 2. 66-, and 2.18-fold increase on 1 h and 3rd and 7th day, respectively). H + S showed significant production after 1 h of treatment (5.88-fold increases). H-S and S-H showed a significantly high content of MDA throughout the observation period. In pretreatment, the salt-pretreated sample showed the highest induction of MDA (Figure 8). The high amount of MDA marks high oxidative lipid injury under stress.

3.6. Antioxidant assay

3.6.1. Superoxide dismutase

S-H showed the highest increase in SOD activity throughout the observation with 6. 04-, 5. 49-, 7. 53-, and 2.18-fold increase on 1 h, and 3rd, 7th, and 15th day, respectively, in comparison with control which was followed by H-S. SOD activity was the highest on the 0th day (1-fold), followed by the 3rd day (3.58-fold), the 7th day (3.28-fold), and the 15th day (1.05-fold) for H-S. The least SOD activity among all the treatments shown by H. S showed an increase in activity up to the 7th day (4. 45-, 1. 67-, and 3.12-fold, respectively). H + S displayed an increase in its SOD activity on 1 h and 3rd day by 2.52- and 2.43-fold, respectively (Figure 9).

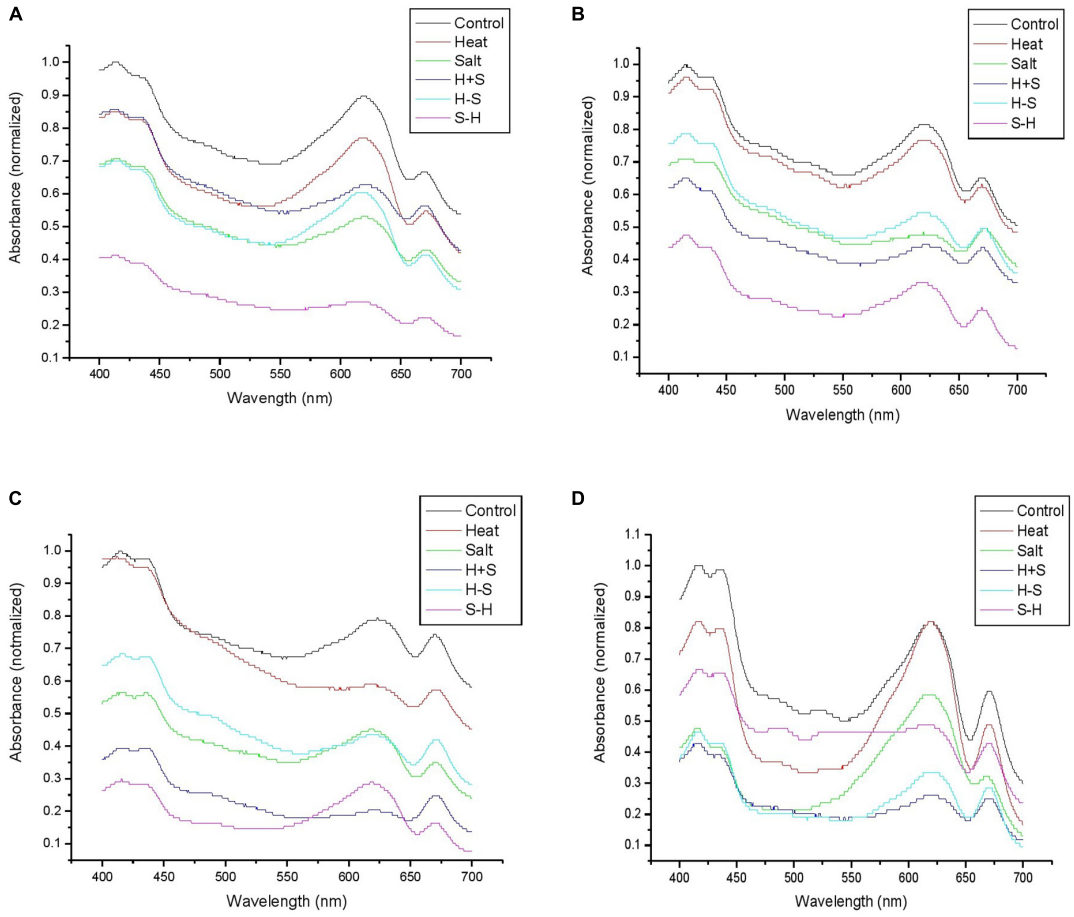

FIGURE 7
Graph representing the phycobiliprotein spectrum (460–670 nm) of *Anabaena* PCC 7120 exposed to stress on 1 h **(A)**, 3rd **(B)**, 7th **(C)**, and 15th **(D)** day. (H-S indicates heat pretreatment; S-H indicates salt pretreatment).

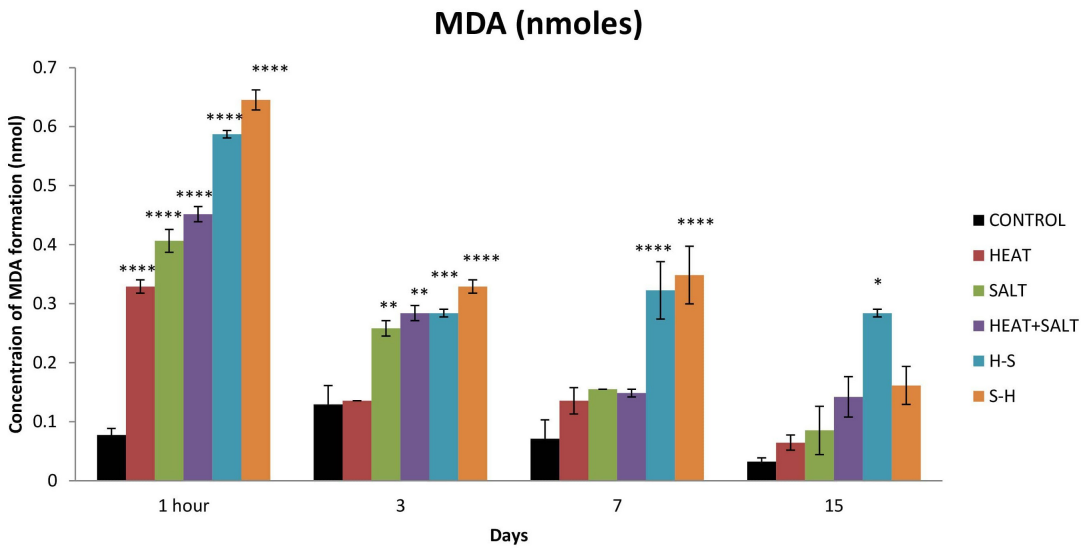

FIGURE 8
Effect of selected stresses on MDA production in *Anabaena* PCC 7120 up to the 15th day. Asterisk (*) indicates $p < 0.05$, a double asterisk (**) indicates $p < 0.01$, the triple asterisk (***) indicates $p < 0.001$, and the four asterisk (****) indicate $p < 0.0001$. (H-S indicates heat pretreatment; S-H indicates salt pretreatment).

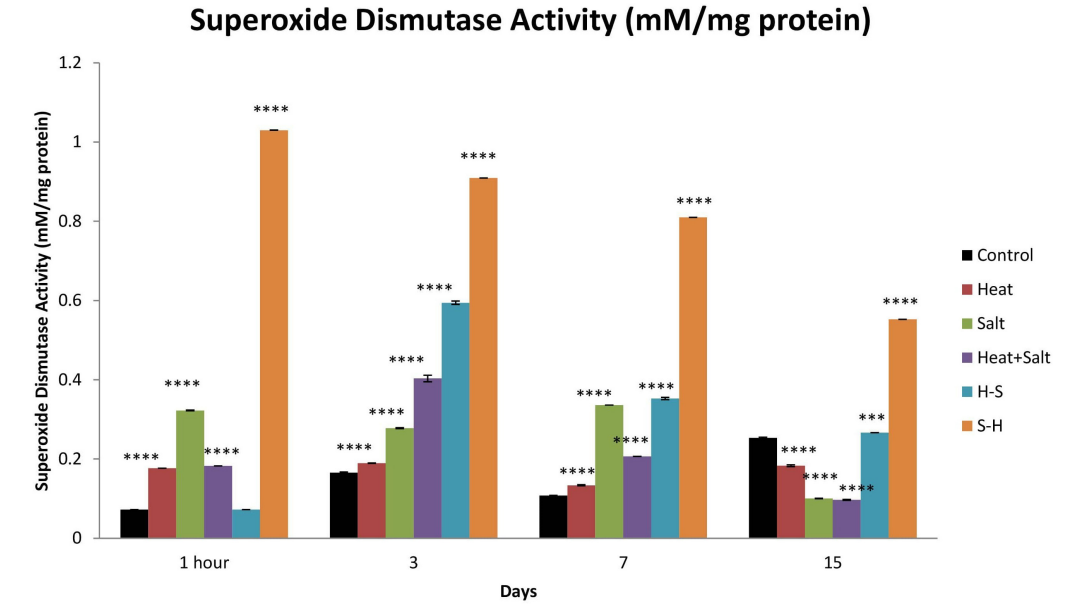

FIGURE 9
Effect of selected stresses on superoxide dismutase activity in *Anabaena* PCC 7120 up to the 15th day. Four asterisks (****) indicate $p < 0.0001$. (H-S indicates heat pretreatment; S-H indicates salt pretreatment).

3.6.2. Catalase

No significant changes were observed in catalase activity after 1 h of treatment. Catalase activity showed maximum induction throughout the observation in S-H. There were 5. 96-, 1. 79-, and 1.61-fold increase on 3rd, 7th, and 15th day, respectively. H-S showed an increase in its activity up to the 7th day with a significant increase on the 3rd day (3.97-fold). S and H + S showed similar activity to that of heat pretreatment. However, no significant increase in catalase activity was shown by H (**Figure 10**).

3.7. Transcript analysis

Expression of three genes of the antioxidative defense system (FeSOD, MnSOD, and catalase) was observed in response to selected stresses, which displayed differential accumulation as compared to control. The expression of the genes *alr*2938 and *all*0070, which, respectively, code for FeSOD and MnSOD, increased by 3.6- and 1.8-fold in salt-pretreated (S-H) samples, indicating activation of stress defense pathways in response to ROS generation, supporting

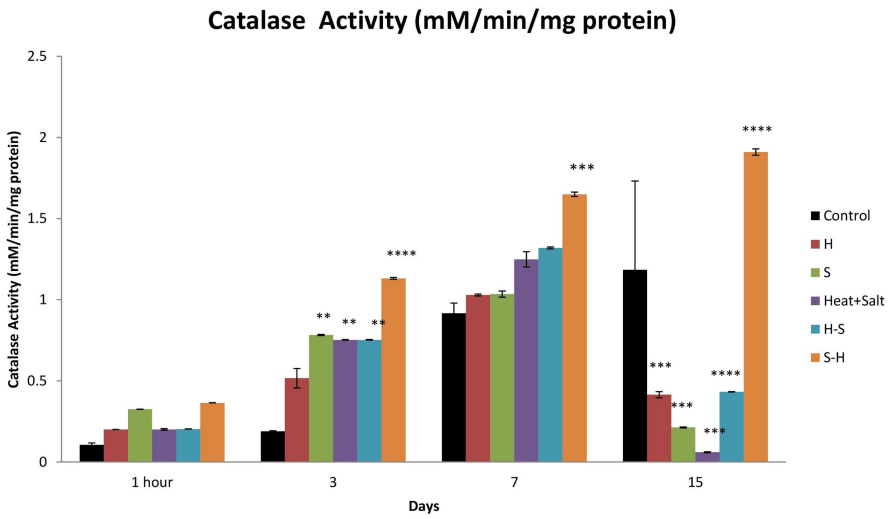

FIGURE 10
Effect of selected stresses on catalase activity in *Anabaena* PCC 7,120 up to the 15th day. A double asterisk (**) indicates $p < 0.01$, the triple asterisk (***) indicates $p < 0.001$, and the four asterisk (****) indicates $p < 0.0001$. (H-S indicates heat pretreatment; S-H indicates salt pretreatment).

our biochemical findings. Likewise, cells exposed to H and S also displayed accumulation of *alr*2938 and *all*0070. Transcript levels of *all*0070 were downregulated under H-S and H + S samples. Similarly, catalase (*alr*3090) expression was also downregulated in H and H + S samples, whereas increased in S, S-H, and H-S samples (**Figure 11**).

4. Discussion

The present study deals with the effect of heat shock, salinity, their combination, and pretreatment stresses on growth, morphological alteration, pigments, lipid peroxidation, and antioxidant enzymes of *Anabaena* PCC 7120.

Morphological alterations through light microscopy demonstrated extensive shrinkage of cyanobacterial filament, cell degeneration, and terminal akinetes formation. It further revealed that the heat initially had no impact on the cellular structure, however, significant cell degeneration was observed in later phases. A similar result was observed under salinity stress, but anomalous swelling of cells was a unique feature observed on the 15th day, which could be due to osmotic stress leading to the accumulation of osmoprotectant (Singh and Montgomery, 2013). Heat pretreatment showed fragmentation of the filaments. H + S showed abnormal bulging of the cells in the filaments, which could be attributed to the fact that in addition to the cellular toxicity brought on by high ion concentrations, high salt concentrations in the growth media are known to reduce the water potential (Singh and Montgomery, 2013). Osmotic stress is thus caused by salt stress, and under these circumstances, many organisms, including cyanobacteria, store or synthesis suitable solutes or osmoprotectants to maintain reduced water potential inside the cell (Singh and Montgomery, 2013). In S-H, plasmolysis of cells in the filaments due to salinity pretreatment followed by heat was observed, which may be due to the hypertonic environment of the cyanobacterium. Similar to past observations on the response of cyanobacteria to abiotic stress conditions, particularly nitrogen constraint, akinete formations were observed. These findings require in-depth analysis because they are intriguing (Mahawar et al., 2018).

The decline in the chlorophyll *a* content in stressed samples could be attributed to the production of ROS that caused bleaching due to active oxygen-mediated peroxidation (Rai et al., 2021). Moreover, the comparative increase in the content of pretreated samples reflects the occurrence of cross-tolerance of heat-pretreated and salt-pretreated *Anabaena* to salt and heat stress, respectively. This result was concordant with the study of Mishra et al. (2009), which reported heat-mediated alleviation of UV-B toxicity in *Anabaena doliolum*.

The result of the pretreatment effect on carotenoid content can be further supported by the study of Mishra et al. (2009), where they reported an increase in carotenoid content on heat shock pretreatment followed by UV-B treatment. An increase in carotenoids in *Anabaena* PCC7120 under stress can be attributed to a positive strategy (Nonnengiesser et al., 1996). It is due to its role of protecting light harvesting pigments in the antenna complex against photochemical damage by allowing triplet energy transfer from chlorophyll *a* to carotenoid (Kim et al., 2005). They exert photoprotective and antioxidative functions by dissipating excess energy as heat by non-photochemical quenching (NPQ) or by scavenging excess ROS (El Bissati et al., 2000). Moreover, carotenoids are potent non-enzymatic antioxidants, which scavenge a variety of reactive oxygen species when cyanobacteria are exposed to stress. They play a role of a modulator of membrane homeostasis and photosynthetic apparatus against abiotic stress (Kirilovsky and Kerfeld, 2016).

Phycocyanin content significantly decreased under all treatments except heat up to the 15th day of observation compared to the control. The decrease in phycocyanin under S, H + S, H-S, and S-H may be due to the rapid entry of sodium ions leading to the dismantling of phycobilisomes from the thylakoid membranes causing photosynthesis inhibition and reduced energy transfers from phycobiliproteins to the reaction center (Lu and Vonshak, 2002;

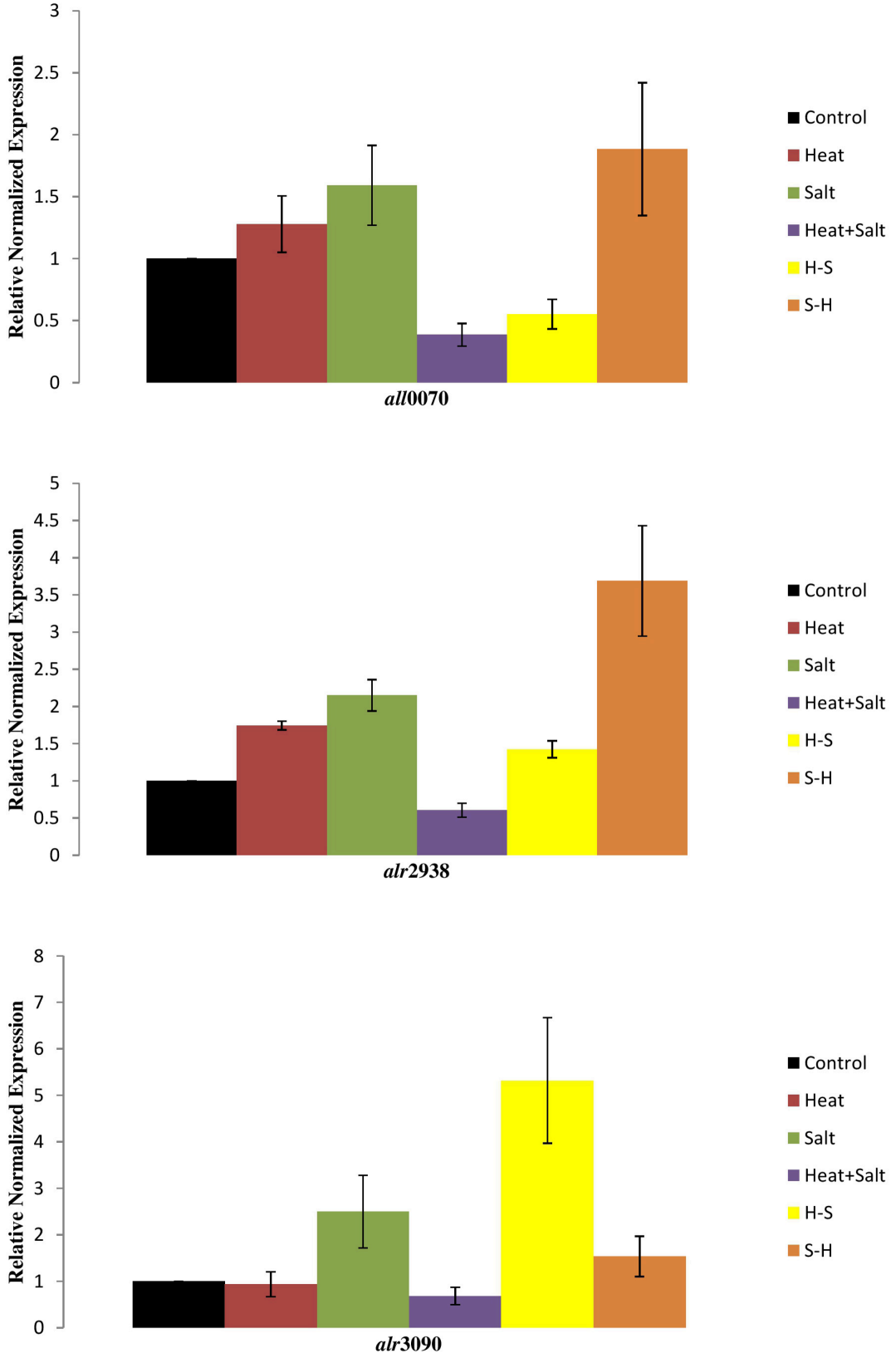

FIGURE 11
Transcript level of cyanobacterial genes under stresses.

Rafiqul et al., 2003). Similar results have been earlier reported by Hemlata and Fatima (2009) on *Anabaena* NCCU-9, Singh et al. (2012) on *Anabaena* sp. PCC 7120, and Verma and Mohanty (2000) on *Spirulina platensis*, thus supporting present findings. Samples exposed to salt pretreatment were the most affected followed by heat pretreatment. Moreover, an increase in the intracellular

concentration of NaCl inactivates ATP synthase and decreases the intracellular level of ATP (Murata et al., 2007). Moreover, ROS-induced protein peroxidation may also cause a damaging effect on phycocyanin.

Phycobiliproteins are water-soluble proteins that are covalently bonded with phycobilins (Hu, 2019). Due to phycobilins, phycobiliprotein have distinct absorption spectra from 460 to 670 nm (Adir and Lerner, 2003). Phycobiliproteins are divided into three different classes based on phycobilin energy or absorption spectra. Phycoerythrin (PEs) or phycoerythrocyanin (PECs) are of higher energy with main absorption at 480–580 nm, phycocyanin (PCs) of intermediate level with absorption at 600–640 nm, and allophycocyanins (APCs) with absorption at 620–660 nm. The change in the spectrum can be attributed to the fact that stresses led to photosynthetic inhibition. Inside the photosynthetic apparatus, the phycobilisome, which is involved in light capture, may be a target of photodamage and oxidative toxicity. These results find support from the studies of Wen et al. (2005) and Zhang et al. (2010) on *Spirulina platensis* under salt and heat stress, respectively.

Lipids play an important role in the tolerance to several physiological stressors in a variety of organisms including cyanobacteria (Parida and Das, 2005). An increase in the level of lipid peroxidation under various stresses can be attributed to the increased production of reactive oxygen species indicating oxidative stress in cyanobacteria, which can lead to cellular damage (Rai et al., 2021). In cyanobacteria, the membrane contains a high amount of polyunsaturated fatty acid (PUFA) (Halliwell, 1999), and increased MDA content is due to oxidative degradation of PUFA (Girotti, 1990). Increased lipid peroxidation in salt pretreatment (S-H) could be due to salinity-induced membrane damage, which was followed by heat treatment and enhanced lipid peroxidation. This finds support from the work of Srivastava et al. (2006), where a similar increase was reported in salt-pretreated samples followed by UV-B in *Anabaena doliolum*.

In order to scavenge stress-induced ROS, cyanobacteria activate their antioxidative defense system. SOD activity followed a general trend of S-H > H-S > S > H > C except on the 15th day of treatment suggesting recovery and suppression of the antioxidative defense system on the 15th day. Cyanobacteria induce a complex antioxidant defense system to combat the increasing level of ROS. SODs are the first line of defense against ROS. Superoxide dismutase is induced by a variety of cyanobacteria under stress and dismutates the superoxide radical (Zutshi et al., 2008). Superoxide dismutase is a major oxygen-free radical scavenger and it functions by disproportionating free radicals into hydrogen peroxide which is further scavenged by catalase (Macháèková, 1995).

A similar result was obtained for catalase, where pretreatment enhanced the activity. Peroxide radical produced by SOD during the scavenging of free radicals is further scavenged by catalase (Halliwell and Gutteridge, 2015). Catalases belong to the category of well-characterized antioxidant enzymes for hydroperoxide detoxification that cleaves the peroxide bond in hydrogen peroxide (H–O–O–H) to form molecular oxygen and water (Srivastava, 2010). Hence, it appears that peroxide can be detoxified by CAT.

Biochemical findings were further strengthened after analyzing the transcript levels of respective genes. Our findings imply that salinity pretreatment has an impact on the transcriptional control of genes involved in antioxidant production. Surprisingly, at heat pretreatment, the transcript levels of FeSOD and MnSOD were significantly downregulated. This may imply that the production of FeSOD and MnSOD is not alarm-driven by ROS or other cellular signals of temperature stress. Nevertheless, catalase gene expression

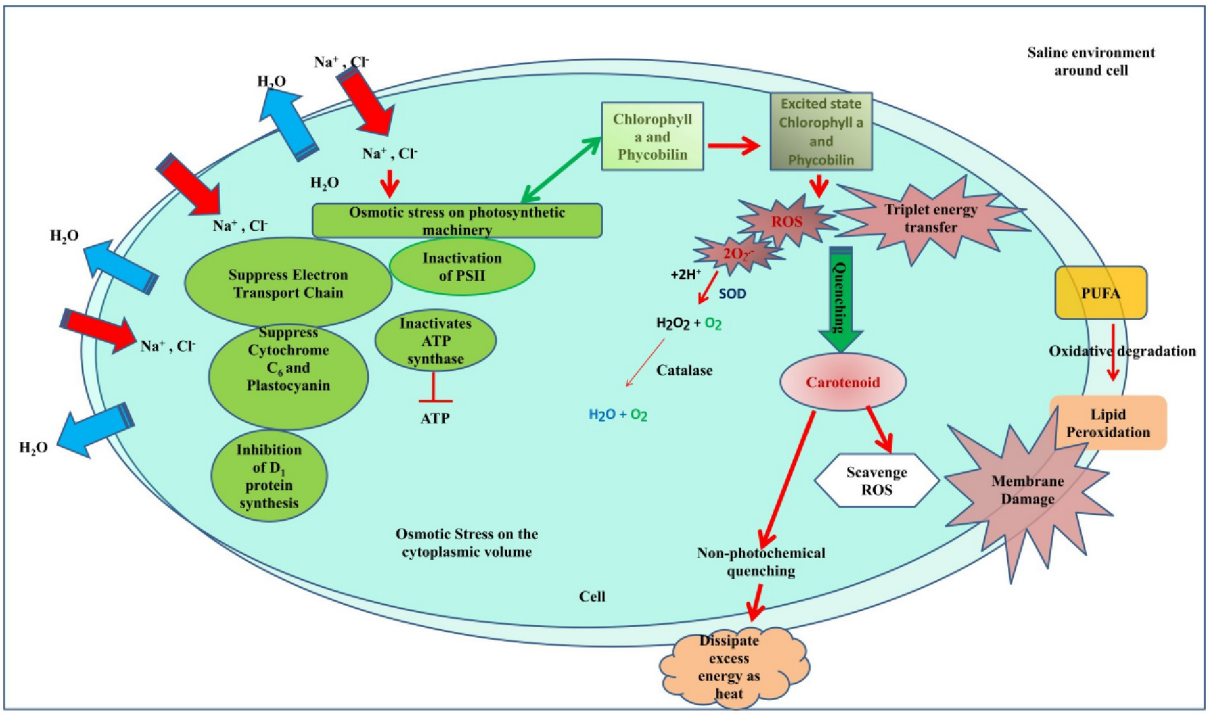

FIGURE 12
Hypothetical model showing how salinity pretreatment impairs the cell equilibrium and metabolism which when exposed to heat shock makes the cell more fragile.

was elevated. However, enhanced FeSOD and MnSOD under salt pretreatment (S-H), as compared with salinity, indicate an adaptive strategy of *Anabaena* for scavenging excessive ROS produced by the cyanobacteria.

5. Conclusion

The study was conducted to analyze the effect of stresses on cyanobacteria with the main aim to examine the effect of pretreatments on growth, development, pigment, lipid peroxidation, and antioxidant activity. Cyanobacteria were chosen due to their cosmopolitan nature, and particularly, *Anabaena* PCC7120 was chosen as a model organism as it bears a close resemblance to higher plant and easy maintenance of the culture in the laboratory. The cyanobacterium was able to effectively detoxify the surplus reactive oxygen species formed inside the cells of stressed *Anabaena* PCC7120 due to the enhanced expression of SOD in salt pretreatment. It can be concluded that the salinity pretreatments enhanced the deleterious effect. Salt was found to synergize the effect of heat on cyanobacteria as it caused osmotic stress in the cells that affect the cellular equilibrium whereas heat has been found to offer some cross tolerance to abiotic stresses due to the production of heat shock proteins. Heat shock proteins may be responsible for the protective effect of heat against salt. Pretreatment at sublethal temperatures increases the thermotolerance of cyanobacterial species, both unicellular and filamentous, and suggests that heat shock genes and proteins are involved in thermotolerance. Due to the constant synthesis of the two Hsp60 proteins throughout the heat stress and their great stability even after returning to normal growth circumstances, *Anabaena* demonstrates exceptional recovery from heat stress. On the other hand, salinity increased heat toxicity. The cellular equilibrium of the cell is disturbed by salt. Pretreatment with salinity impairs membrane permeability. In addition, it interferes with the cell's ideal environment, which hinders enzyme activity, and is further hampered by heat shock (**Figure 12**). When exposed to heat, such pretreated cells become more fragile. Hence, it can be inferred that when physical and chemical stresses are superimposed 7 days apart, pretreatment chemical stress synergizes the deleterious effect of physical stress but pretreatment physical stress offers some tolerance to chemical stress. Therefore, this study is the first to provide how cyanobacteria respond in the presence of physical and chemical stresses and that chemical stress enhances the damaging effect of physical stress.

Data availability statement

The original contributions presented in this study are included in the article/supplementary material, further inquiries can be directed to the corresponding author.

Author contributions

RS and NA conceived the idea and designed the experiments. RS conducted the experiments. VK performed the transcript analysis. RS, TK, SaY, NS, ShY, RP, VK, and NA analyzed the data. RS and ShY wrote the manuscript with input from other co-authors. All authors contributed to the article and approved the submitted version.

Acknowledgments

RS would like to thank the University Grant Commission (UGC), New Delhi for financial support in form of a research fellowship.

Conflict of interest

The authors declare that the research was conducted in the absence of any commercial or financial relationships that could be construed as a potential conflict of interest.

Publisher's note

References

Adir, N., and Lerner, N. (2003). The crystal structure of a novel unmethylated form of C-phycocyanin, a possible connector between cores and rods in phycobilisomes. *J. Biol. Chem.* 278, 25926–25932. doi: 10.1074/jbc.M302838200

Aebi, H. (1984). Catalase in vitro. *Methods Enzymol.* 105, 121–126. doi: 10.1016/S0076-6879(84)05016-3

Agrawal, C., Sen, S., Singh, S., Rai, S., Singh, P. K., Singh, V. K., et al. (2014). Comparative proteomics reveals association of early accumulated proteins in conferring butachlor tolerance in three N(2)-fixing *Anabaena* spp. *J. Proteome* 96, 271–290. doi: 10.1016/j.jprot.2013.11.015

Allakhverdiev, S. I., Nishiyama, Y., Miyairi, S., Yamamoto, H., Inagaki, N., Kanesaki, Y., et al. (2002). Salt stress inhibits the repair of photodamaged photosystem II by suppressing the transcription and translation of psbA genes in *Synechocystis*. *Plant Physiol.* 130, 1443–1453. doi: 10.1104/pp.011114

Bhargava, P., Kumar, A., Mishra, Y., and Rai, L. C. (2008). Copper pretreatment augments ultraviolet B toxicity in the cyanobacterium *Anabaena* doliolum: A proteomic analysis of cell death. *Funct. Plant Biol.* 35, 360–372. doi: 10.1071/FP07267

Cakmak, I., and Horst, W. J. (1991). Effect of aluminium on lipid peroxidation, superoxide dismutase, catalase, and peroxidase activities in root tips of soybean (Glycine max). *Physiol. Plant.* 83, 463–468.

Demiral, T., and Türkan, I. (2006). Exogenous glycinebetaine affects growth and proline accumulation and retards senescence in two rice cultivars under NaCl stress. *Environ. Exp. Bot.* 56, 72–79.

El Bissati, K., Delphin, E., Murata, N., Etienne, A.-L., and Kirilovsky, D. (2000). Photosystem II fluorescence quenching in the cyanobacterium *Synechocystis* PCC 6803: Involvement of two different mechanisms. *Biochim. Biophys. Acta (BBA) Bioenergetics* 1457, 229–242. doi: 10.1016/s0005-2728(00)00104-3

Ellison, C. R., Overa, S., and Boldor, D. (2019). Central composite design parameterization of microalgae/cyanobacteria co-culture pretreatment for enhanced lipid extraction using an external clamp-on ultrasonic transducer. *Ultrason. Sonochem.* 51, 496–503. doi: 10.1016/j.ultsonch.2018.05.006

Fan, Y., Yin, X., Xie, Q., Xia, Y., Wang, Z., Song, J., et al. (2019). Co-expression of SpSOS1 and SpAHA1 in transgenic *Arabidopsis* plants improves salinity tolerance. *BMC Plant Biol.* 19:74. doi: 10.1186/s12870-019-1680-7

Feng, Z. T., Deng, Y. Q., Zhang, S. C., Liang, X., Yuan, F., Hao, J. L., et al. (2015). K+ accumulation in the cytoplasm and nucleus of the salt gland cells of *Limonium bicolor* accompanies increased rates of salt secretion under NaCl treatment using NanoSIMS. *Plant Sci.* 238, 286–296. doi: 10.1016/j.plantsci.2015.06.021

Giannopolitis, C. N., and Ries, S. K. (1977). Superoxide dismutases: I. Occurrence in higher plants. *Plant Physiol.* 59, 309–314.

Girotti, A. W. (1990). Photodynamic lipid peroxidation in biological systems. *Photochem. Photobiol.* 51, 497–509.

Halliwell, B. (1999). Chemistry of free radical and related'reactive species'; Transition metal, Hydroxyl radical. *Free Radic. Biol. Med.* 53–55.

Halliwell, B., and Gutteridge, J. M. (2015). *Free radicals in biology and medicine*. Oxford: Oxford University Press.

Han, N., Lan, W., He, X., Shao, Q., Wang, B., and Zhao, X. (2012). Expression of a *Suaeda salsa* vacuolar H+/Ca2+ transporter gene in *Arabidopsis* contributes to physiological changes in salinity. *Plant Molecular Biology Reporter* 30, 470–477.

Hemlata, and Fatima, T. (2009). Screening of cyanobacteria for phycobiliproteins and effect of different environmental stress on its yield. *Bull. Env. Contam. Toxicol.* 83, 509–515.

Hu, I. (2019). *Production of potential coproducts from microalgae, Biofuels from Algae*. Amsterdam: Elsevier.

Karandashova, I., and Elanskaya, I. (2005). Genetic control and mechanisms of salt and hyperosmotic stress resistance in cyanobacteria. *Russian J. Genet.* 41, 1311–1321.

Kim, H., Dashdorj, N., Zhang, H., Yan, J., Cramer, W. A., and Savikhin, S. (2005). An anomalous distance dependence of intraprotein chlorophyll-carotenoid triplet energy transfer. *Biophys. J.* 89, L28–L30. doi: 10.1529/biophysj.105.069609

Kirilovsky, D., and Kerfeld, C. A. (2016). Cyanobacterial photoprotection by the orange carotenoid protein. *Nat. Plants* 2, 1–7.

Küpper, H., Spiller, M., and Kupper, F. C. (2000). Photometric method for the quantification of chlorophylls and their derivatives in complex mixtures: Fitting with Gauss-peak spectra. *Anal. Biochem.* 286, 247–256. doi: 10.1006/abio.2000.4794

Lawton, L., Marsalek, B., Padisak, J., and Chorus, I. (1999). "Determination in the laboratory," in *Toxic cyanobacteria in water: A guide to public health consequences*, ed. F. Spon (New York, NY: Monitoring and Management), 347–367.

Liu, X., and Huang, B. (2000). Heat stress injury in relation to membrane lipid peroxidation in creeping bentgrass. *Crop Sci.* 40, 503–510.

Livak, K. J., and Schmittgen, T. D. (2001). Analysis of relative gene expression data using real-time quantitative PCR and the $2-\Delta\Delta CT$ method. *Methods* 25, 402–408.

Lu, C., and Vonshak, A. (2002). Effects of salinity stress on photosystem II function in cyanobacterial *Spirulina platensis* cells. *Physiol. Plant.* 114, 405–413.

Macháèková, I. (1995). McKersie, BD, Leshem, YY: Stress and stress coping in cultivated plants. *Biol. Plant.* 37, 380–380.

Mahawar, H., Prasanna, R., Singh, S. B., and Nain, L. (2018). Influence of silver, zinc oxide and copper oxide nanoparticles on the cyanobacterium Calothrixelenkinii. *BioNanoScience* 8, 802–810.

Mishra, Y., Chaurasia, N., and Rai, L. C. (2009). Heat pretreatment alleviates UV-B Toxicity in the Cyanobacterium *Anabaena* doliolum: A proteomic analysis of cross tolerance. *Photochem. Photobiol.* 85, 824–833. doi: 10.1111/j.1751-1097.2008.00469.x

Murata, N., Takahashi, S., Nishiyama, Y., and Allakhverdiev, S. I. (2007). Photoinhibition of photosystem II under environmental stress. *Biochim. Biophys. Acta (BBA) Bioenergetics* 1767, 414–421.

Myers, J., and Kratz, W. (1955). Relations between pigment content and photosynthetic characteristics in a blue-green alga. *J. General Physiol.* 39, 11–22. doi: 10.1085/jgp.39.1.11

Narayan, O. P., Kumari, N., and Rai, L. (2011). Iron starvation-induced proteomic changes in *Anabaena* (Nostoc) sp. PCC 7120: Exploring Survival Strategy. *J. Microbiol. Biotechnol.* 21, 136–146. doi: 10.4014/jmb.1009.09021

Nonnengiesser, K., Schuster, A., and Koenig, F. (1996). Carotenoids and reaction center II-D1 Protein in light regulation of the photosynthetic Apparatus in *Aphanocapsa*. *Botanica Acta* 109, 115–124.

Panda, B., Basu, B., Rajaram, H., and Apte, S. K. (2014). Methyl viologen responsive proteomedynamics of *Anabaena* sp. strain PCC7120. *Proteomics* 14, 1895–1904.

Pandey, S., Rai, R., and Rai, L. (2012). Proteomics combines morphological, physiological and biochemical attributes to unravel the survival strategy of Anabaena sp. PCC7120 under arsenic stress. *J. Proteome* 75, 921–937. doi: 10.1016/j.jprot.2011.10.011

Parida, A. K., and Das, A. B. (2005). Salt tolerance and salinity effects on plants: A review. *Ecotoxicol. Environ. Safety* 60, 324–349.

Rafiqul, I. M., Hassan, A., Sulebele, G., Orosco, C. A., Roustaian, P., and Jalal, K. C. A. (2003). Salt stress culture of blue-green algae *Spirulina fusiformis*. *Pak. J. Biol. Sci. (Pakistan)* 6, 648–650.

Rai, L., and Raizada, M. (1985). Effect of nickel and silver ions on survival, growth, carbon fixation and nitrogenase activity in Nostoc muscorum: Regulation of toxicity by EDTA and calcium. *J. General Appl. Microbiol.* 31, 329–337.

Rai, R., Singh, S., Rai, K. K., Raj, A., Sriwastaw, S., and Rai, L. (2021). Regulation of antioxidant defense and glyoxalase systems in cyanobacteria. *Plant Physiol. Biochem.* 168, 353–372. doi: 10.1016/j.plaphy.2021.09.037

Rai, S., Agrawal, C., Shrivastava, A. K., Singh, P. K., and Rai, L. (2014). Comparative proteomics unveils cross species variations in Anabaena under salt stress. *J. Proteome* 98, 254–270. doi: 10.1016/j.jprot.2013.12.020

Rai, S., Sibgh, S., Shrivastava, A. K., and Rai, L. (2013). Salt and UV-B induced changes in *Anabaena* PCC 7120: Physiological, proteomic and bioinformatic perspectives. *Photosynth. Res.* 118, 105–114. doi: 10.1007/s11120-013-9931-1

Rippka, R., Deruelles, J., Waterbury, J. B., Herdman, M., and Stanier, R. Y. (1979). Generic assignments, strain histories and properties of pure cultures of cyanobacteria. *Microbiology* 111, 1–61.

Scarpeci, T. E., Zanor, M. I., Carrillo, N., Mueller-Roeber, B., and Valle, E. M. (2008). Generation of superoxide anion in chloroplasts of *Arabidopsis thaliana* during active photosynthesis: A focus on rapidly induced genes. *Plant Mol. Biol.* 66, 361–378. doi: 10.1007/s11103-007-9274-4

Shrivastava, A. K., Chatterjee, A., Yadav, S., Singh, P. K., Singh, S., and Rai, L. (2015). UV-B stress induced metabolic rearrangements explored with comparative proteomics in three *Anabaena* species. *J. Proteome* 127, 122–133. doi: 10.1016/j.jprot.2015.05.014

Singh, P. K., Shrivastava, A. K., Chatterjee, A., Pandey, S., Rai, S., Singh, S., et al. (2015). Cadmium toxicity in diazotrophic *Anabaena* spp. adjudged by hasty up-accumulation of transporter and signaling and severe down-accumulation of nitrogen metabolism proteins. *J. Proteome* 127, 134–146. doi: 10.1016/j.jprot.2015.05.019

Singh, S. P., and Montgomery, B. L. (2013). Salinity impacts photosynthetic pigmentation and cellular morphology changes by distinct mechanisms in Fremyelladiplosiphon. *Biochem. Biophys. Res. Commun.* 433, 84–89. doi: 10.1016/j.bbrc.2013.02.060

Singh, V. P., Srivastava, P. K., and Prasad, S. M. (2012). Differential effect of UV-B radiation on growth, oxidative stress and ascorbate–glutathione cycle in two cyanobacteria under copper toxicity. *Plant Physiol. Biochem.* 61, 61–70. doi: 10.1016/j.plaphy.2012.09.005

Song, Y., Li, J., Sui, Y., Han, G., Zhang, Y., Guo, S., et al. (2020). The sweet sorghum SbWRKY50 is negatively involved in salt response by regulating ion homeostasis. *Plant Mol. Biol.* 102, 603–614. doi: 10.1007/s11103-020-00966-4

Srivastava, A. K. (2010). Assessment of salinity-induced antioxidative defense system of diazotrophic cyanobacterium *Nostoc* muscorum. *J. Microbiol. Biotechnol.* 20, 1506–1512. doi: 10.4014/jmb.1005.05037

Srivastava, A. K., Bhargava, P., Mishra, Y., Shukla, B., and And Rai, L. C. (2006). Effect of pretreatment of salt, copper and temperature on ultraviolet-B-induced antioxidants in diazotrophic cyanobacterium *Anabaena* doliolium. *J. Basic Microbiol.* 46, 135–144. doi: 10.1002/jobm.200510059

Teikari, J., Österholm, J., Kopf, M., Battchikova, N., Wahlsten, M., Aro, E. M., et al. (2015). Transcriptomic and proteomic profiling of Anabaena sp. strain 90 under inorganic phosphorus stress. *Appl. Environ. Microbiol.* 81, 5212–5222. doi: 10.1128/AEM.01062-15

Verma, K., and Mohanty, P. (2000). Alterations in the structure of phycobilisomes of the cyanobacterium, *Spirulina platensis* in response to enhanced Na^+ level. *World J. Microbiol. Biotechnol.* 16, 795–798.

Wannigama, D. L., Agrawal, C., and Rai, L. (2012). *A comparative study on proteomic and biochemical alterations in the cyanobacterium Anabaena sp. PCC 7120 under short term exposure of abiotic stresses: Pesticide, salinity, heavy metal and UV-B 3rd world congress on biotechnology*. Hyderabad, TG: International Convention Centre.

Wen, X., Gong, H., and Lu, C. (2005). Heat stress induces an inhibition of excitation energy transfer from phycobilisomes to photosystem II but not to photosystem I in a cyanobacterium *Spirulina* platensis. *Plant Physiol. Biochem.* 43, 389–395. doi: 10.1016/j.plaphy.2005.03.001

Yang, Z., Li, J. L., Liu, L. N., Xie, Q., and Sui, N. (2020). Photosynthetic regulation under salt stress and salt-tolerance mechanism of sweet sorghum. *Front. Plant Sci.* 10:1722. doi: 10.3389/fpls.2019.01722

Zhang, T., Gong, H., Wen, X., and Lu, C. (2010). Salt stress induces a decrease in excitation energy transfer from phycobilisomes to photosystem II but an increase to photosystem I in the cyanobacterium Spirulina platensis. *J. Plant Physiol.* 167, 951–958. doi: 10.1016/j.jplph.2009.12.020

Zhao, B., Wang, J., Gong, H., Wen, X., Ren, H., and Lu, C. (2008). Effects of heat stress on PSII photochemistry in a cyanobacterium Spirulina platensis. *Plant Sci.* 175, 556–564.

Zutshi, S., Choudhary, M., Bharat, N., Abdin, M. Z., and Fatma, T. (2008). Evaluationofantioxidant defense responses tp lead stress in Hapalosiphon fontainalis-339 1. *J. Phycol.* 44, 889–896.

frontiers | Frontiers in Microbiology

TYPE Original Research
PUBLISHED 17 February 2023
DOI 10.3389/fmicb.2023.1057264

OPEN ACCESS

EDITED BY
Prashant Kumar Singh,
Mizoram University,
India

REVIEWED BY
Da Huo,
Institute of Hydrobiology (CAS),
China
Krishna Kumar Rai,
Banaras Hindu University,
India

*CORRESPONDENCE
Wei Ding
✉ dingwei@iphy.ac.cn
Lingling Feng
✉ fll708@mail.ccnu.edu.cn

†These authors have contributed equally to this work

SPECIALTY SECTION
This article was submitted to Microbiotechnology, a section of the journal Frontiers in Microbiology

RECEIVED 29 September 2022
ACCEPTED 24 January 2023
PUBLISHED 17 February 2023

CITATION
Guo X, Li Z, Jiang Q, Cheng C, Feng Y, He Y, Zuo L, Rao L, Ding W and Feng L (2023) Structural insight into the substrate-binding mode and catalytic mechanism for MlrC enzyme of *Sphingomonas* sp. ACM-3962 in linearized microcystin biodegradation. *Front. Microbiol.* 14:1057264. doi: 10.3389/fmicb.2023.1057264

Structural insight into the substrate-binding mode and catalytic mechanism for MlrC enzyme of *Sphingomonas* sp. ACM-3962 in linearized microcystin biodegradation

Xiaoliang Guo[1†], Zengru Li[2†], Qinqin Jiang[1†], Cai Cheng[1], Yu Feng[1], Yanlin He[1], Lingzi Zuo[1], Li Rao[1], Wei Ding[2*] and Lingling Feng[1*]

[1]Key Laboratory of Pesticide and Chemical Biology (CCNU), Ministry of Education, College of Chemistry, Central China Normal University, Wuhan, China, [2]The Institute of Physics, Chinese Academy of Sciences, Beijing, China

Removing microcystins (MCs) safely and effectively has become an urgent global problem because of their extremely hazardous to the environment and public health. Microcystinases derived from indigenous microorganisms have received widespread attention due to their specific MC biodegradation function. However, linearized MCs are also very toxic and need to be removed from the water environment. How MlrC binds to linearized MCs and how it catalyzes the degradation process based on the actual three-dimensional structure have not been determined. In this study, the binding mode of MlrC with linearized MCs was explored using a combination of molecular docking and site-directed mutagenesis methods. A series of key substrate binding residues, including E70, W59, F67, F96, S392 and so on, were identified. Sodium dodecane sulfate-polyacrylamide gel electrophoresis (SDS-PAGE) was used to analyze samples of these variants. The activity of MlrC variants were measured using high performance liquid chromatography (HPLC). We used fluorescence spectroscopy experiments to research the relationship between MlrC enzyme (E), zinc ion (M), and substrate (S). The results showed that MlrC enzyme, zinc ion and substrate formed E-M-S intermediates during the catalytic process. The substrate-binding cavity was made up of N and C-terminal domains and the substrate-binding site mainly included N41, E70, D341, S392, Q468, S485, R492, W59, F67, and F96. The E70 residue involved in both substrate catalysis and substrate binding. In conclusion, a possible catalytic mechanism of the MlrC enzyme was further proposed based on the experimental results and a literature survey. These findings provided new insights into the molecular mechanisms of the MlrC enzyme to degrade linearized MCs, and laid a theoretical foundation for further biodegradation studies of MCs.

KEYWORDS

MlrC enzyme, microcystins biodegradation, substrate-binding mode, catalytic mechanism, active center, molecular docking

1. Introduction

Due to water eutrophication and global warming, the ecological crisis and public health problems caused by harmful cyanobacterial blooms (HCBs) have become a global environmental issue (Paerl et al., 2011; Paerl and Otten, 2013; Xu et al., 2015; Bullerjahn et al., 2016; Visser et al., 2016; Huisman et al., 2018; Sadhasivam et al., 2019; Sehnal et al., 2019; Ji et al., 2020; Li et al., 2020; Du et al., 2021). During the overgrowth of HCBs, toxin-producing cyanobacteria release

various microcystins (MCs) into the water body, with MC-LR, MC-RR, and MC-YR being the most toxic and widely distributed MC variants (Hoeger et al., 2007; Atencio et al., 2008; Zeller et al., 2012; Okogwu et al., 2014; He et al., 2018; Tao et al., 2018; Zhang et al., 2021). MCs are potent liver toxins and tumor promoters (Fujiki and Suganuma, 1994; Zhang et al., 2012; Tian et al., 2013; Wang et al., 2014, 2022; Hernandez et al., 2021). These cyanotoxins are extremely stable and are not effectively removed by conventional methods. They accumulate in aquatic animals and threaten human health and safety through the food chain (Zurawell et al., 2005; Zhang et al., 2009; Lance et al., 2010; Sotton et al., 2014; Pham and Utsumi, 2018; Kim et al., 2019; Zamora-Barrios et al., 2019). Human health risks caused by MCs may continue to increase in the future without effective intervening measures (Chen et al., 2005; Tian et al., 2013; Zhao et al., 2016, 2020; Janssen, 2019; Xiang et al., 2019; Weir et al., 2021; He et al., 2022). Consequently, it is essential to find a safe and effective MC treatment strategy.

Biodegradation is an especially promising means of MC removal (Wu et al., 2015; Li et al., 2017, 2021). Previous studies have reported many indigenous microorganisms in cyanobacterial bloom water. These microorganisms, which carry functional genes for specifically degrading cyanotoxins (Tsuji et al., 2006), include *Sphingomonas* sp. ACM-3962 (Bourne et al., 1996), *Sphingopyxis* sp. USTB-05 (Dexter et al., 2018), *Sphingopyxis* sp. IM-1 (Lezcano et al., 2016), *Sphingopyxis* sp. X20 (Qin et al., 2019), *Sphingopyxis* sp. YF1 (Yang et al., 2020), *Novosphingobium* sp. THN1 (Jiang et al., 2011), and *Novosphingobium* sp. ERW19 (Zeng et al., 2021). The genes involved in the MC degradation pathway, *mlr*A, *mlr*B, *mlr*C, and *mlr*D, together form the *mlr* gene cluster, which encodes the corresponding enzymes (Moron-Lopez et al., 2017; Zeng et al., 2020; Zhang et al., 2020). Unfortunately, not all genes of the *mlr* cluster can be successfully transcribed and expressed (Jiang et al., 2011). Therefore, it is necessary to separately study the heterogeneous expression and detailed catalytic mechanisms of these genes for furthering MC biodegradation. Among these enzymes, MlrA is responsible for the linearizing process of converting MCs to linearized MCs (Dexter et al., 2021). However, linearized MCs are still extremely toxic and must be further degraded (Wei et al., 2021). MlrB can degrade linearized MCs into tetrapeptides, but some reports show transcriptional silencing of the *mlr*B gene. This phenomenon is extremely unfavorable for the further detoxification of linearized MCs (Dziga et al., 2016; Li et al., 2022). Fortunately, the MlrC enzyme has dual degradation functions. MlrC can not only utilize the tetrapeptides obtained from the degradation of MCs by MlrB as substrate but also directly degrade the linearized MCs into the almost non-toxic Adda (Dziga et al., 2012). Therefore, it is essential to study the MlrC enzyme from different angles including the structural characteristics, degradation activity, biodegradation mechanism, and enzymatic improvements and modifications.

Knowledge of the molecular biodegradation processes of linearized MCs by the MlrC enzyme is limited. In previous studies on the molecular mechanism of MlrC, the MlrC structure had to be predicted first by homology modeling (Wei et al., 2021). The predicted structure may cause uncertainty in the mechanism studies. We obtained the actual three-dimensional structure of the MlrC enzyme derived from *Sphingomonas* sp. ACM-3962 in a previous study (PDB: 7YLQ), which laid the theoretical foundation for the further study of the catalytic mechanism. The MlrC enzyme is a type of metallopeptidase, and there is a zinc ion and four coordinated residues to form the catalytic center. The zinc ion plays a critical role in the catalytic activity of linearized MCs. There is also an empty position in the catalytic center next to the four residues and one water molecule. The empty position may be used for substrate binding in the subsequent degradation process. In addition, the two large domains of MlrC form a large central cavity for better accommodation of linearized heptapeptide substrates. Based on the actual three-dimensional structure of MlrC and its structural characteristics, we further explored the biodegradation molecular mechanism of the MlrC enzyme.

This study aimed to investigate the catalytic mechanism of the MlrC enzyme. The binding mode of MlrC and linearized MCs was obtained by the molecular docking method, and a series of key substrate-binding residues were found. They were further verified by site-directed mutagenesis. At the same time, the relationship between the MlrC enzyme (E), zinc ion (M), and substrates (S) was also studied in detail, and the components of the MlrC active center were explained. Finally, based on experimental studies and a literature survey, a possible catalytic mechanism was proposed. This study provided a better understanding of the catalytic mechanism of MlrC.

2. Materials and methods

2.1. Materials

Restriction enzymes Nde I and Xho I (Takara Biotech. Co. Ltd., Japan) were used to construct plasmids of wild-type MlrC and its variants. Standard MC-LR with purity ≥ 95% was purchased from Taiwan Algal Science Inc. (Taiwan, China) and stored at −20°C. Phosphoric acid and acetonitrile were purchased from TEDIA (HPLC/Spectro, United States) and used for high-performance liquid chromatography (HPLC) analysis. The expression vector pET21b and *E. coli* strain DH5α and BL21 (DE3) were purchased from Vazyme (Nanjing, China). Invitrogen Platinum SuperFi II DNA Polymerase, T4 DNA ligase, and restriction enzymes Nde I and Xho I were obtained from Thermo Fisher Scientific (United States).

2.2. Plasmid construction of MlrC and variants

MlrC and variant plasmids were constructed in *E. coli* strain BL21 (DE3) for protein overexpression and activity testing. The *mlr*C gene was PCR-amplified from genomic DNA derived from *Sphingomonas* sp. ACM-3962 and constructed into the pET21b vector (Invitrogen) with a C-terminal 6×His tag. All primers used in this study are shown in Supplementary Table S2. Plasmid extraction was performed using the Tiangen Plasmid Mini Kit, and all clones were verified by DNA sequencing.

Site-directed mutagenesis was achieved by bridge PCR, and primers are listed in Supplementary Table S2, which generated the restriction enzyme sites NdeI and Xho1. pET21b-*mlr*C was used as the template for all mutants. The PCR program started at 95°C for 30 s, followed by 35 cycles of 58°C for 30 s and 72°C for 1.5 min. The plasmids containing the genes with a site-directed mutation were transferred into the *E. coli* strain BL21 (DE3). All mutants of pET21b-*mlr*C were verified by DNA sequencing.

2.3. Expression and purification of MlrC and variants

Transformed *E. coli* BL21 (DE3) containing pET21b-*mlr*C and the mutant vectors were cultured in liquid LB medium with 100 μg mL^{-1} ampicillin and shaken at constant conditions of 37°C and 220 rpm. When the optical density at 600 nm was approximately 0.6, isopropyl-β-D-thiogalactoside (IPTG) was added at a final concentration of 0.2 mM to induce protein expression. The induction conditions were 16°C, 210 rpm for 12–16 h. The *E. coli* cells were harvested by centrifugation (8,000 ×*g*, 10 min, 4°C), and the cells were resuspended in lysis buffer (Tris–HCl, pH 7.0, 150 mM NaCl). Cells were lysed by high-pressure cell disruption and then subjected to high-speed centrifugation (14,000 ×*g*, 60 min, 4°C). The crude enzyme solution was purified by Ni-NTA (Qiagen), washed with buffer B (25 mM Tris–HCl, pH 8.0, 150 mM NaCl, 15 mM imidazole), and eluted with buffer C (25 mM Tris–HCl, pH 8.0, 250 mM imidazole). The MlrC enzyme was characterized by sodium dodecyl sulfate–polyacrylamide gel electrophoresis (SDS-PAGE) on a 12% polyacrylamide gel. The concentration of purified MlrC protein was determined at 280 nm using an ultra-micro spectrophotometer (Nanodrop OneC, Thermo Fisher Scientific, United States).

2.4. Molecular docking calculations

Molecular docking of the linearized MC-LR to the MlrC structure was carried out with flexible zinc metalloprotein docking using AutoDock Vina. The crystal structure of MlrC was used as the receptor structure. The crystallized water molecules present in the structure and the metal ions (except the zinc ion in the active site) were removed. The ligand molecules of MlrC were prepared using Coot software, and before docking, the nonpolar H atoms were merged into both the ligands and the target by AutoDock Tools. Basic docking was performed by AutoDock Vina 1.1.2. The grid box was centered at x: 9.683, y: −36.275, and z: −27.867 with grid sizes of 80, 80, and 80 Å, respectively. Nine conformations were generated, and the best docking model of the linearized MC-LR with the lowest binding energy (−9.2 kcal mol^{-1}) was selected and used as an evaluation standard for the subsequent calculations. Furthermore, the flexible zinc metalloprotein docking was also performed by AutoDock Vina 1.2.3. One zinc pseudo atom was added to the receptor. The grid box was centered at x: 7, y: −33, and z: −30 with grid sizes of 26.25, 31.5, and 24 Å, respectively. A total of 126 conformations were evaluated based on the proper distances of the hydrolysis site to the zinc ion, and the best conformation corresponded to the interactions between MlrC and the linearized MC-LR with a binding energy of −15.78 kcal mol^{-1} (from the AutoDock4 force field of AutoDock Vina 1.2.3). The docking method and processing of the linearized MC-RR and MC-YR were consistent with the linearized MC-LR. All figures representing the structures were generated by PyMOL (PyMOL Molecular Graphics System, Schrödinger, Inc.).

2.5. Enzyme activity assay

HPLC was used to determine the concentration of linearized MCs and their degradation products in samples. Linearized MCs were prepared by using MlrA to degrade standard MCs. The HPLC instrument was a DIONEX UltiMate 3000 (Thermo Fisher Scientific, United States) with a diode array detector equipped with an Acclaim™ 120 C18 column (4.6 mm × 250 mm, 5 μm particles, Thermo Fisher Scientific, Sunnyvale, United States). Linearized MCs and their degradation products were detected at a 238 nm wavelength and 1.0 mL min^{-1} flow rate. The injected volume was 50 μL, and the column temperature was 30°C. The mobile phase consisted of a gradient of a phosphoric acid solution (pH 3.84) containing 0.05% (V/V) of phosphoric acid (solvent A) and acetonitrile (solvent B). The gradient program was as follows: First, the column was balanced with 10% B for 3 min; then from 0 to 5 min, B was increased from 10 to 40%; from 5 to 12 min, B was increased from 40 to 70%; and from 12 to 12.5 min, B was decreased from 70 to 10%, and 10% B was used for 0.5 min. The linearized MC concentration was calculated using a linearized MC calibration curve method. The HPLC system had a detection limit of 0.1 μg L^{-1}.

2.6. Analysis of circular dichroism spectra

Far-UV (190–260 nm) circular dichroism (CD) experiments for MlrC and variants of the zinc ion coordinated residues were carried out using a Chirascan CD Spectrometer (Applied Photophysics Ltd., Leatherhead, United Kingdom). Experiments were performed using solutions of protein at a concentration of 0.5 mg mL^{-1} in a 1 mm cell (Hellma UK Ltd., Southend, United Kingdom). Each CD spectrum represented the accumulation of three scans at 1 nm intervals with a 1.0 nm bandwidth and a time constant of 1 s. Protein secondary structure content was determined using CDNN version 2.1 (Institut für Biotechnologie, Martin-Luther Universität Halle-Wittenberg, Halle, Germany).

2.7. Fluorescence measurements

All fluorescence measurements were performed on a fluorescence spectrophotometer (Agilent Cary Eclipse, Malaysia) equipped with a xenon lamp source and a 1.0 cm quartz cell. Fluorescence emission spectra were recorded in the wavelength range of 285–420 nm upon an excitation wavelength of 280 nm. The excitation and emission bandwidth were 5 nm. The fluorescence quenching experiments of MlrC (1 μM) were performed at different concentrations of linearized MC-LR using a 1 cm path length fluorescence cuvette.

3. Results and discussion

3.1. The substrate-binding mode of MlrC

To elucidate the substrate-binding mode of MlrC, we first attempted crystallography to obtain its complex structure with linearized MC-LR. However, neither co-crystallization nor soaking was successful on the complex, probably because its low solubility prevented us from using high concentrations of linearized MC-LR. Alternatively, we analyzed the substrate-binding mode by the molecular docking method using the crystal structure of MlrC (PDB: 7YLQ). The two large domains together formed a long and shallow cleft with dimensions of about 29 and 10 Å, which were used to accommodate the linearized substrates. The surface of the

substrate-binding cleft was hydrophobic (Figures 1A,B). The amide bond of the linearized MC-LR cleavage site was close to the zinc ion, which was responsible for catalyzing the degradation of the substrate (Figure 1C).

The binding mode between the substrate and MlrC was mainly formed by the polar group of the linearized substrates. First, it was observed that E70 formed a hydrogen bond with an amine group of the linearized MC-LR (Figure 1E). Q468 formed a hydrogen bond with one of the carboxyl groups, and S485 and N41 formed a hydrogen bond with the other two carboxyl groups. R492 formed a hydrogen bond with a carbonyl, and D341 and S392 interacted with the terminal guanidine group of the linearized MC-LR. The hydrophobic regions formed by W59, F67, and F96 were used to accommodate the phenyl ring of the substrates and formed π–π interactions (Figure 1D). For the substrate-binding mode of MlrC and the linearized MC-RR and MC-YR, the key binding residues were similar to the linearized MC-LR. The only inconsistency was caused by the different characteristic groups between the three substrates (Supplementary Figures 2, 7). The residue R261 of MlrC was the binding site of the characteristic structure of linearized MC-RR. For the characteristic structure of linearized MC-YR, the binding site of MlrC was residue Y189 (Supplementary Figures 9, 10). The MlrC sequences

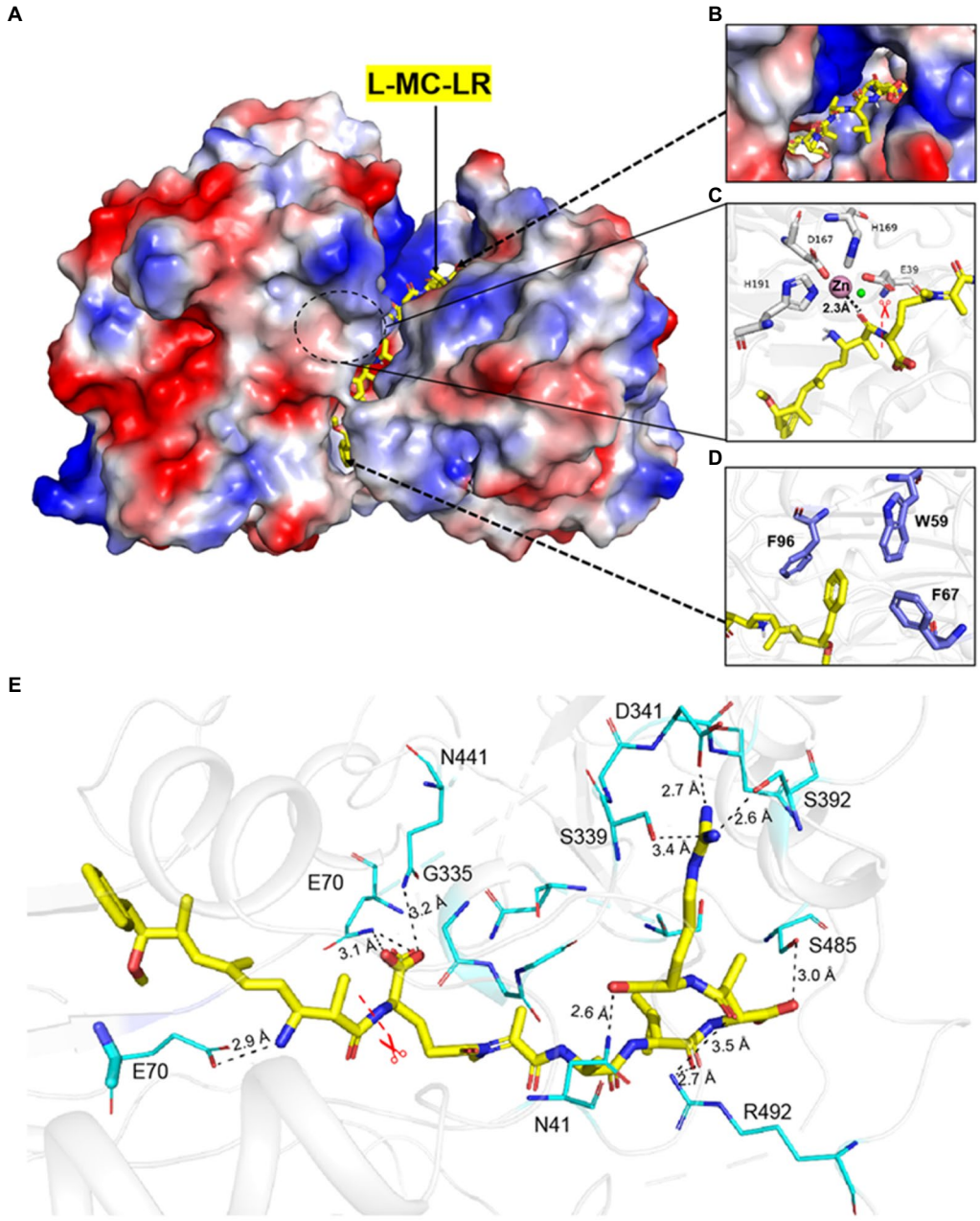

FIGURE 1
Interaction between MlrC and substrates. **(A–D)** The catalytic triad and the docking model of the reaction intermediate of linearized MC-LR in MlrC. **(E)** Residues involved in the binding site of MlrC. The MlrC structure is presented as a cartoon diagram in gray. Residues involved in binding linearized MC-LR are shown as a line model, and the amide bond that was cleaved by the enzyme is indicated with a star mark. The linearized MC-LR docking model is shown as a yellow stick figure. The hydrogen bonds formed between the residues and the substrate are shown as black lines.

of other microorganism species had high conservation according to sequence alignment, and this high conservation indicated excellent representativeness of the MlrC crystal structure from *Sphingomonas* sp. ACM-3962 (Supplementary Figure 3).

3.2. Enzyme activity of wild-type MlrC and variants

Based on the analysis of the binding mode results by molecular docking, mutants were constructed, and their hydrolysis activities were measured. The activity of MlrC variants was reduced by different degrees (Figures 2A,B). It is worth noting that the *K*m and *K*cat values of E70 were both reduced. We suspected that E70 was not only responsible for binding with the linearized substrates but also involved in the catalytic process (Figure 2B; Table 1). F260, K464, H133, and D332 residues were mentioned by Wang et al. (2020), but no data were reported. We also tested the activity of the mutants, and the results showed that F260A and K464A did not significantly affect the activity of MlrC. However, H133A and D332A directly led to the unavailability of the MlrC enzyme, so we suspected that the two residues were critical for proper protein folding and stabilizing the structure of MlrC (Figure 2B; Supplementary Figure 11). All mutants were identified by circular dichroism experiments, except for the non-expressing mutants H133A and D332A. The results showed that the secondary structure of these mutants did not change, and the change in activity was caused by the destruction of the substrate-binding site (Supplementary Figure 6).

3.3. Analysis of the relationship between the MlrC enzyme, zinc ion and substrate

Based on the analysis of the actual three-dimensional structure and substrate-binding mode of MlrC, we knew that the active center comprised the catalytic site and substrate-binding site. However, the relationship between the MlrC enzyme (E), zinc ion (M), and substrate (S) were not clear. Hence, their relationship was analyzed in detail in this study.

The activity of MlrC was closely related to the zinc ion, which is located within the internal flexible region of the N-terminal catalytic domain to form the catalytic center. The crucial role of the zinc ion had been verified in our previous study. For the catalytic center of MlrC, the zinc ion coordinated with four residues, E39, D167, H169, and H196, to form a catalytic quadruplet, with a water molecule next to the zinc ion (Figure 3A). The zinc ion coordination condition of the homologous structure (PDB: 3IUU) was similar to that of MlrC, but the difference was that the zinc ion in 3IUU was coordinated by three residues and an exogenous imidazole group to form saturated coordination (Figure 3B). In contrast, the zinc ion in MlrC had four residues and one water molecule around it and left an unoccupied location for substrate binding. In conclusion, the zinc ion of MlrC was unsaturated coordination and left a redundant location that could be used to bind the substrates. Hence, the zinc ion of the catalytic center might bring MlrC and the substrate close to each other to guide the reactive group to the correct position (Figures 3A,B).

Although the zinc ion was essential for the MlrC activity, we questioned whether the absence of the zinc ion would affect MlrC and substrate binding. That is to say, the compositional relationship between the MlrC enzyme (E), zinc ion (M), and substrate (S) needed to be further explored. In this study, we used fluorescence spectroscopy experiments to research the relationship. Proteins have endogenous fluorescent properties. When the MlrC enzyme interacted with its specific substrates, the microenvironment around the fluorescent group in the MlrC enzyme changed, resulting in a decrease in the fluorescence intensity of the fluorescent molecule. If the MlrC enzyme could not interact with its substrates, the MlrC enzyme would not produce a significant fluorescence change. Therefore, mutants of residues D167 and H169, which made up the zinc ion catalytic center, were constructed. The wild-type MlrC was used as the control group, which could bind

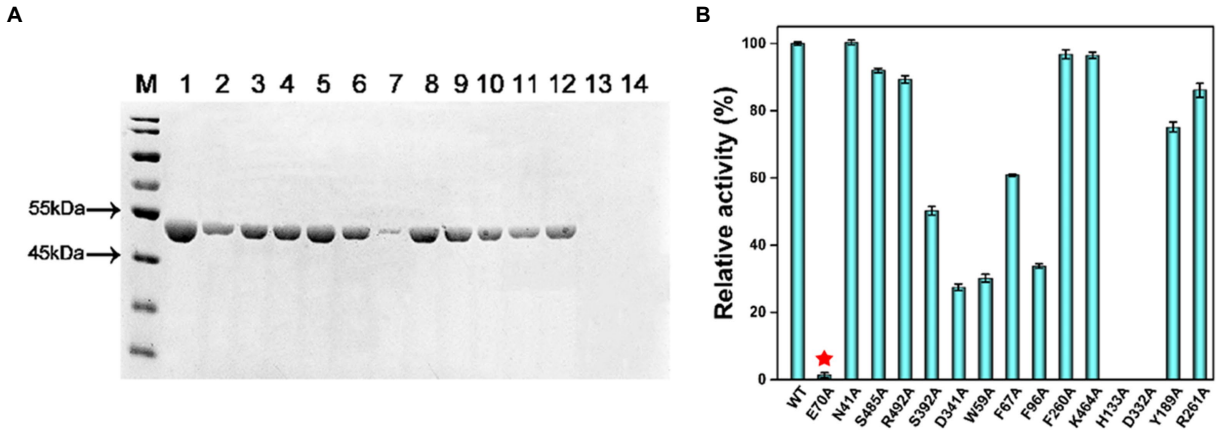

FIGURE 2
(A) Sodium dodecane sulfate–polyacrylamide gel electrophoresis (SDS-PAGE) was used to analyze samples of the variants for their substrate-binding residues. M, protein marker; Lane 1, wild-type MlrC; Lane 2, E70A; Lane 3, N41A; Lane 4, S485A; Lane 5, R492A; Lane 6, S392A; Lane 7, D341A; Lane 8, W59A; Lane 9, F67A; Lane 10, F96A; Lane 11, F260A; Lane 12, K464A; Lane 13, H133A; and Lane 14, D332A. **(B)** Hydrolytic activities of MlrC and its variants using linearized MC-LR as a substrate. Activities of MlrC and its variants were measured using a linearized MC-LR concentration of 0.25mgL^{-1} and an enzyme concentration of 0.12mgL^{-1}. The amount of Adda produced was monitored by HPLC analysis. The activities of the variants were compared with wild-type MlrC.

with substrates normally. The results showed that the two mutants D167A and H169A did not display an obvious change in fluorescence intensity, and only the wild-type MlrC did. We suspected that MlrC could bind the substrates normally, as it showed a change in fluorescence intensity. However, the D167A and H169A mutants directly prevented the formation of the zinc ion catalytic center, so the substrate and MlrC were not able to bind correctly, resulting in no significant change in fluorescence intensity (Figures 3D–F). Combined with the above analysis, we speculated that the MlrC enzyme (E), substrate (S), and zinc ion (M) formed E-M-S intermediates during the catalytic process of MlrC. The zinc ion acted as a metal bridge, which brought MlrC and the substrates closer to each other and guided the reactive group of the substrates into the correct position (Figure 3C). Therefore, MlrC and the substrates could not bind once the zinc ion was absent.

TABLE 1 Kinetic parameters of wild-type MlrC and variants.

Protein	K_m (μM)	K_{cat} (s − 1)	K_{cat}/ K_m (s^{-1}·μM^{-1})
MlrC ^{WT}	0.24 ± 0.12	2409.98 ± 345.10	10041.48 ± 345.10
E70A	0.88 ± 0.55	1162.97 ± 397.00	1321.56 ± 397.00
N41A	0.65 ± 0.35	2276.20 ± 696.78	3501.85 ± 696.78
S392A	0.59 ± 0.10	2258.16 ± 203.15	3827.39 ± 203.15
S485A	0.47 ± 0.08	2072.21 ± 222.69	4406.83 ± 222.69
R492A	0.84 ± 0.24	2614.28 ± 420.62	3112.24 ± 420.62
D341A	0.81 ± 0.32	2730.61 ± 664.75	3371.12 ± 664.75
W59A	0.70 ± 0.22	2505.85 ± 460.63	3579.79 ± 460.63
F67A	0.70 ± 0.29	2549.51 ± 627.57	3642.16 ± 627.57
F96A	0.56 ± 0.10	2167.43 ± 216.98	3870.41 ± 216.98
F260A	0.25 ± 0.13	2464.32 ± 393.97	9857.28 ± 393.97
K464A	0.25 ± 0.14	2503.41 ± 485.77	10013.64 ± 485.77
D332A	-	-	-
H133A	-	-	-

3.4. Linearized MC degradation mechanism by MlrC

Based on the results of the molecular docking and biochemical experiments, a possible catalytic mechanism of MlrC was proposed (Figure 4). The MlrC active center was mainly composed of two parts, the catalytic site and the substrate-binding site. The catalytic site was composed of the zinc ion and the four coordinated residues E39, D167, H169, and H191, with one water molecule involved in catalysis. The coordination layer of the zinc ion was not saturated, leaving an extra position that combined with the substrate to form a saturated coordination layer. The enzyme (E), substrate (S), and metal ion (M) formed E-M-S intermediates during the catalytic process. The zinc ion acted as a metal ion bridge, making the distance between MlrC and the substrates closer, which is conducive to MlrC acting on the reactive group of the substrates. This meant that the MlrC enzyme and its substrate could not be combined once the metal ion was absent. This was verified by fluorescence spectroscopy experiments (Figures 3D–F). The substrate-binding cavity was made up of N-and C-terminal domains (Figure 3A), and the substrate-binding site mainly included N41, E70,

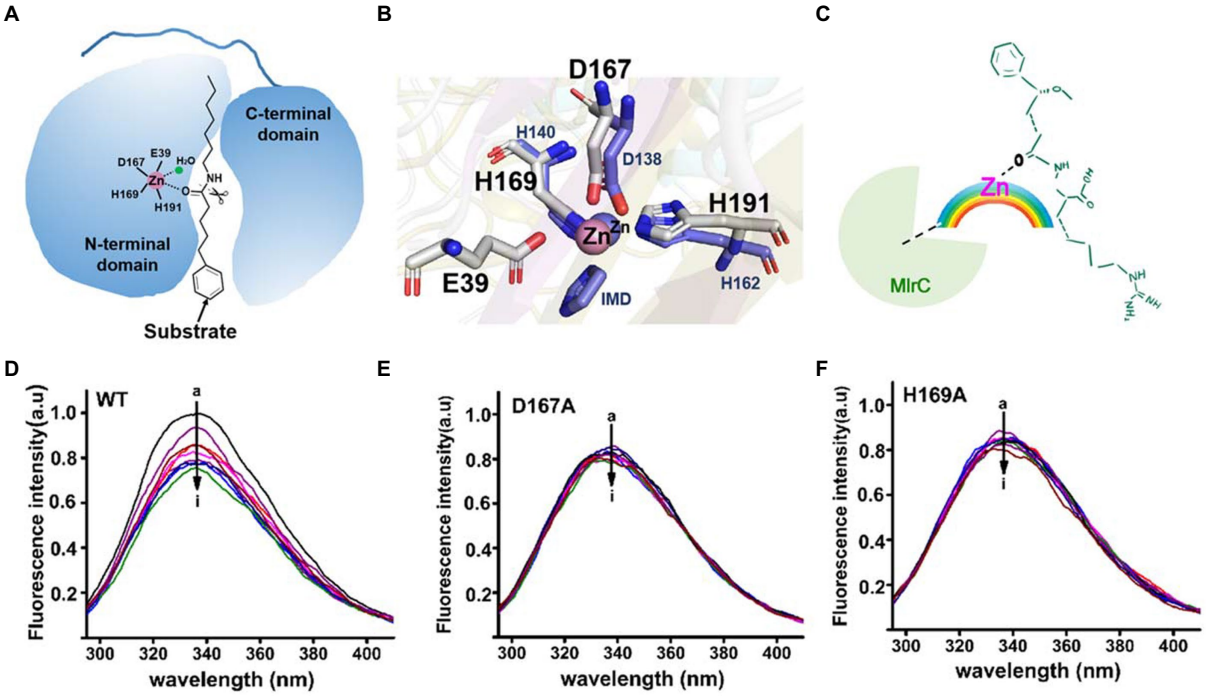

FIGURE 3
Analysis of the relationship between the MlrC enzyme, zinc ion, and linearized MC-LR. **(A)** Schematic model of the MlrC monomer structure and substrate. The two domains, the zinc ion with coordinated residues and the substrate model, are indicated. **(B)** Alignment of the zinc ion and coordinated residues between MlrC and 3IUU. **(C)** Schematic of the E-M-S model of the relationship between the MlrC enzyme, zinc ion, and linearized MC-LR, with the zinc ion acting as a metal bridge connecting the MlrC enzyme and substrate. **(D–F)** Synchronous fluorescence spectra of MlrC and variants: **(D)** wild-type MlrC; **(E)** D167A; and **(F)** H169A. The concentration of MlrC: 1μM, and the concentration of linearized MC-LR a–i: 0, 1, 2, 3, 4, 5, 6, 7, and 8μM, respectively.

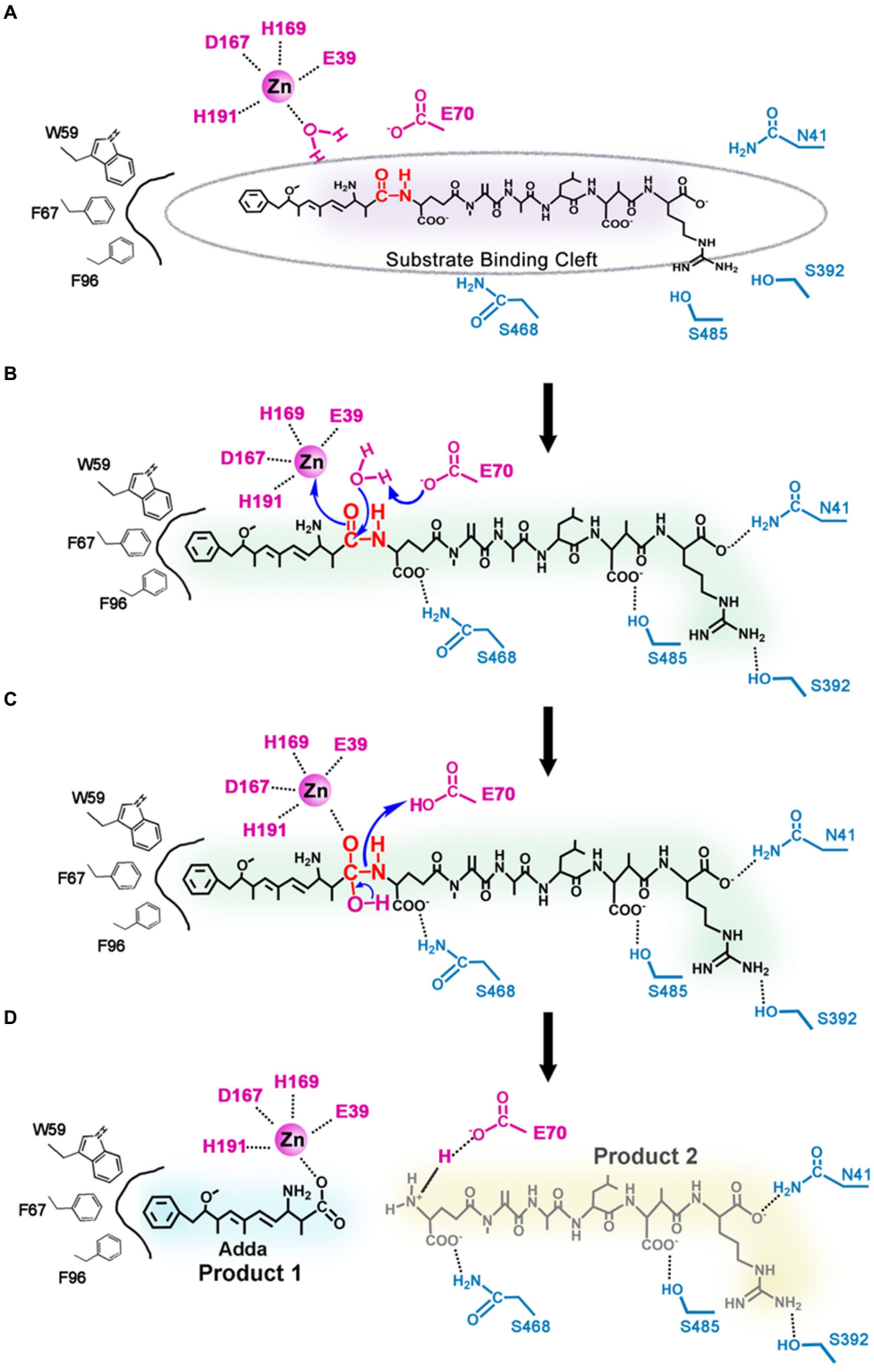

FIGURE 4
Proposed catalytic mechanism of linearized MC-LR biodegradation by MlrC. **(A)** The MlrC active center is composed of the catalytic site (the zinc ion, one water molecule, and the residues E39, D167, H169, and H191) and the substrate-binding site (the residues E70, W59, F67, F96, N41, S392, S485, and S468); **(B)** Residue E70 as a general base catalyst removing a proton of the metal-bound water to form zinc-OH-nucleophile for attacking the amide bond of the substrate. **(C)** E70 as a general acid catalyst donating a proton to the amine. **(D)** Two products of linearized MC-LR biodegradation by MlrC.

D341, S392, Q468, S485, R492, W59, F67, and F96. These residues were verified by site-directed mutagenesis and activity test experiments. Among them, the E70 residue was very critical. On the one hand, this residue was responsible for forming hydrogen bonds with one amine group of the substrate. On the other hand, it was responsible for activating the H_2O molecule, which was next to the zinc ion to form

zinc-OH-nucleophile to attack the substrate cleavage site. Activity experiments also showed that the activity of residue E70A was significantly reduced (Figure 3C; Table 1).

During the entire catalytic process, residue E70 acted as a general base catalyst by removing a proton from the metal-bound water in the first step, allowing the metal-bound hydroxide to attack the carbonyl group of the substrate peptide, while the negative charge of E39 stabilized the transition state (Figure 4A). The other substrate-binding residues, N41, D341, S392, Q468, S485, R492, W59, F67, and F96, played a role in binding substrates and helped locate the substrate to be catalyzed. In the next step, E70 acted as a general acid catalyst by donating a proton to the leaving amine (Figure 4B), which eventually led to the collapse of the metal-bound tetrahedral intermediate (Figure 4C). The N-terminal product left and water returned to the metal ion, while the C-terminal product was still bound to E70 through a salt bridge. Through a series of reactions, the substrate peptide bond was finally hydrolyzed (Figure 4D). In conclusion, the nucleophilic attack on the substrate cleavage site was mediated by the water molecule, and the water molecule cooperated with the metal ion-zinc ion coordinated by multiple residues to complete the catalytic process of MlrC.

4. Conclusion

Through molecular docking and site-directed mutagenesis methods, the binding mode of MlrC with linearized MC-LR was studied. A series of key substrate-binding residues were identified. Among them, residue E70 was very specific and crucial for the substrate degradation process by the MlrC enzyme. E70 formed a hydrogen bond with one amine group of the substrates. More importantly, E70 was responsible for activating the water molecule near the zinc ion to attack the cleavage site of the substrates. The importance of residue E70 was verified by biochemical experiments. Other substrate-binding residues were also evaluated by site-directed mutagenesis. Based on the analysis of the active center formed by the catalytic site and substrate-binding site, the relationship between the MlrC enzyme (E), zinc ion (M), and substrate (S) was analyzed in detail. They formed an E-M-S intermediate during the catalytic process. The zinc ion acted as a metal ion bridge, making the distance between MlrC and the substrates closer, which is conducive to MlrC acting on the reactive group of the substrates. Eventually, the catalytic degradation mechanism of MlrC was proposed. The nucleophilic attack on the substrate cleavage site was mediated by the water molecule, and the zinc ion assisted in the catalytic process, which is coordinated with multiple residues.

In conclusion, MlrC effectively promoted the degradation of linearized MCs, which play a unique role in detoxifying MCs. This study lays a foundation for the biodegradation mechanism of linearized MCs. MlrC may be useful for the complete elimination of cyanotoxins. This is of great significance for the research and application of MCs decontamination. Finally, how to apply the MC-specific enzymes to cyanotoxins degradation in polluted water is worthy of further study.

Data availability statement

The original contributions presented in the study are included in the article/Supplementary material, further inquiries can be directed to the corresponding authors.

Author contributions

XG, LF, and WD conceived and designed all experiments. XG performed protein purification and crystallization. XG, ZL, and QJ analyzed the data. XG, QJ, CC, YF, YH, and LZ performed the biochemical assays. XG and LF wrote and revised the paper. All authors contributed to the article and approved the submitted version.

Funding

This study was supported by the National Natural Science Foundation of China (grant numbers 22277037, 21877046, 21472061, and 21272089), the Fundamental Research Funds for the Central Universities (grant numbers CCNU18ZDPY02, CCNU18TS010, CCNU16A02041, and CCNU14A05006), and the Program of Introducing Talents of Discipline to Universities of China (111 Program, B17019).

Conflict of interest

The authors declare that the research was conducted in the absence of any commercial or financial relationships that could be construed as a potential conflict of interest.

Publisher's note

Supplementary material

The Supplementary material for this article can be found online at: https://www.frontiersin.org/articles/10.3389/fmicb.2023.1057264/full#supplementary-material

References

Atencio, L., Moreno, I., Prieto, A. I., Moyano, R., Molina, A. M., and Camean, A. M. (2008). Acute effects of microcystins MC-LR and MC-RR on acid and alkaline phosphatase activities and pathological changes in intraperitoneally exposed tilapia fish (Oreochromis sp.). *Toxicol. Pathol.* 36, 449–458. doi: 10.1177/0192623308315356

Bourne, D. G., Jones, G. J., Blakeley, R. L., Jones, A., Negri, A. P., and Riddles, P. (1996). Enzymatic pathway for the bacterial degradation of the cyanobacterial cyclic peptide toxin microcystin LR. *Appl. Environ. Microbiol.* 62, 4086–4094. doi: 10.1128/aem.62.11.4086-4094.1996

Bullerjahn, G. S., McKay, R. M., Davis, T. W., Baker, D. B., Boyer, G. L., D'Anglada, L. V., et al. (2016). Global solutions to regional problems: collecting global expertise to address the problem of harmful cyanobacterial blooms. A Lake Erie case study. *Harmful Algae* 54, 223–238. doi: 10.1016/j.hal.2016.01.003

Chen, J., Xie, P., Guo, L., Zheng, L., and Ni, L. (2005). Tissue distributions and seasonal dynamics of the hepatotoxic microcystins-LR and-RR in a freshwater snail (Bellamya aeruginosa) from a large shallow, eutrophic lake of the subtropical China. *Environ. Pollut.* 134, 423–430. doi: 10.1016/j.envpol.2004.09.014

Dexter, J., Dziga, D., Lv, J., Zhu, J., Strzalka, W., Maksylewicz, A., et al. (2018). Heterologous expression of mlrA in a photoautotrophic host-engineering cyanobacteria to degrade microcystins. *Environ. Pollut.* 237, 926–935. doi: 10.1016/j.envpol.2018.01.071

Dexter, J., McCormick, A. J., Fu, P., and Dziga, D. (2021). Microcystinase—a review of the natural occurrence, heterologous expression, and biotechnological application of MlrA. *Water Res.* 189:116646. doi: 10.1016/j.watres.2020.116646

Du, W., Li, G., Ho, N., Jenkins, L., Hockaday, D., Tan, J., et al. (2021). CyanoPATH: a knowledgebase of genome-scale functional repertoire for toxic cyanobacterial blooms. *Brief. Bioinform.* 22:bbaa375. doi: 10.1093/bib/bbaa375

Dziga, D., Wasylewski, M., Szetela, A., Bochenska, O., and Wladyka, B. (2012). Verification of the role of MlrC in microcystin biodegradation by studies using a heterologously expressed enzyme. *Chem. Res. Toxicol.* 25, 1192–1194. doi: 10.1021/tx300174e

Dziga, D., Zielinska, G., Wladyka, B., Bochenska, O., Maksylewicz, A., Strzalka, W., et al. (2016). Characterization of enzymatic activity of MlrB and MlrC proteins involved in bacterial degradation of cyanotoxins microcystins. *Toxins* 8:76. doi: 10.3390/toxins8030076

Fujiki, H., and Suganuma, M. (1994). Tumor necrosis factor-alpha, a new tumor promoter, engendered by biochemical studies of okadaic acid. *J. Biochem.* 115, 1–5. doi: 10.1093/oxfordjournals.jbchem.a124282

He, J., Chen, J., Chen, F., Chen, L., Giesy, J. P., Guo, Y., et al. (2022). Health risks of chronic exposure to small doses of microcystins: an integrative metabolomic and biochemical study of human serum. *Environ. Sci. Technol.* 56, 6548–6559. doi: 10.1021/acs.est.2c00973

He, Q., Kang, L., Sun, X., Jia, R., Zhang, Y., Ma, J., et al. (2018). Spatiotemporal distribution and potential risk assessment of microcystins in the Yulin River, a tributary of the three gorges reservoir, China. *J. Hazard. Mater.* 347, 184–195. doi: 10.1016/j.jhazmat.2018.01.001

Hernandez, B. Y., Zhu, X., Sotto, P., and Paulino, Y. (2021). Oral exposure to environmental cyanobacteria toxins: implications for cancer risk. *Environ. Int.* 148:106381. doi: 10.1016/j.envint.2021.106381

Hoeger, S. J., Schmid, D., Blom, J. F., Ernst, B., and Dietrich, D. R. (2007). Analytical and functional characterization of microcystins [Asp3]MC-RR and [Asp3, Dhb7]MC-RR: consequences for risk assessment? *Environ. Sci. Technol.* 41, 2609–2616. doi: 10.1021/es062681p

Huisman, J., Codd, G. A., Paerl, H. W., Ibelings, B. W., Verspagen, J., and Visser, P. M. (2018). Cyanobacterial blooms. *Nat. Rev. Microbiol.* 16, 471–483. doi: 10.1038/s41579-018-0040-1

Janssen, E. M. (2019). Cyanobacterial peptides beyond microcystins—a review on co-occurrence, toxicity, and challenges for risk assessment. *Water Res.* 151, 488–499. doi: 10.1016/j.watres.2018.12.048

Ji, X., Verspagen, J., Van de Waal, D. B., Rost, B., and Huisman, J. (2020). Phenotypic plasticity of carbon fixation stimulates cyanobacterial blooms at elevated CO2. *Sci. Adv.* 6:x2926:eaax2926. doi: 10.1126/sciadv.aax2926

Jiang, Y., Shao, J., Wu, X., Xu, Y., and Li, R. (2011). Active and silent members in the mlr gene cluster of a microcystin-degrading bacterium isolated from Lake Taihu, China. *FEMS Microbiol. Lett.* 322, 108–114. doi: 10.1111/j.1574-6968.2011.02337.x

Kim, D., Hong, S., Choi, H., Choi, B., Kim, J., Khim, J. S., et al. (2019). Multimedia distributions, bioaccumulation, and trophic transfer of microcystins in the Geum River estuary, Korea: application of compound-specific isotope analysis of amino acids. *Environ. Int.* 133:105194. doi: 10.1016/j.envint.2019.105194

Lance, E., Neffling, M. R., Gerard, C., Meriluoto, J., and Bormans, M. (2010). Accumulation of free and covalently bound microcystins in tissues of Lymnaea stagnalis (Gastropoda) following toxic cyanobacteria or dissolved microcystin-LR exposure. *Environ. Pollut.* 158, 674–680. doi: 10.1016/j.envpol.2009.10.025

Lezcano, M. A., Moron-Lopez, J., Agha, R., Lopez-Heras, I., Nozal, L., Quesada, A., et al. (2016). Presence or absence of mlr genes and nutrient concentrations co-determine the microcystin biodegradation efficiency of a natural bacterial community. *Toxins* 8:318. doi: 10.3390/toxins8110318

Li, H., Barber, M., Lu, J., and Goel, R. (2020). Microbial community successions and their dynamic functions during harmful cyanobacterial blooms in a freshwater lake. *Water Res.* 185:116292. doi: 10.1016/j.watres.2020.116292

Li, J., Li, R., and Li, J. (2017). Current research scenario for microcystins biodegradation—a review on fundamental knowledge, application prospects and challenges. *Sci. Total Environ.* 595, 615–632. doi: 10.1016/j.scitotenv.2017.03.285

Li, R., Ren, W., Teng, Y., Sun, Y., Xu, Y., Zhao, L., et al. (2021). The inhibitory mechanism of natural soil colloids on the biodegradation of polychlorinated biphenyls by a degrading bacterium. *J. Hazard. Mater.* 415:125687. doi: 10.1016/j.jhazmat.2021.125687

Li, Y., Si, S., Huang, F., Wei, J., Dong, S., Yang, F., et al. (2022). Ultrasensitive label-free electrochemical biosensor for detecting linear microcystin-LR using degrading enzyme MlrB as recognition element. *Bioelectrochemistry* 144:108000. doi: 10.1016/j.bioelechem.2021.108000

Moron-Lopez, J., Nieto-Reyes, L., and El-Shehawy, R. (2017). Assessment of the influence of key abiotic factors on the alternative microcystin degradation pathway(s) (mlr(−)): a detailed comparison with the mlr route (mlr(+)). *Sci. Total Environ.* 599-600, 1945–1953. doi: 10.1016/j.scitotenv.2017.04.042

Okogwu, O. I., Xie, P., Zhao, Y., and Fan, H. (2014). Organ-dependent response in antioxidants, myoglobin and neuroglobin in goldfish (Carassius auratus) exposed to MC-RR under varying oxygen level. *Chemosphere* 112, 427–434. doi: 10.1016/j.chemosphere.2014.05.011

Paerl, H. W., and Otten, T. G. (2013). Harmful cyanobacterial blooms: causes, consequences, and controls. *Microb. Ecol.* 65, 995–1010. doi: 10.1007/s00248-012-0159-y

Paerl, H. W., Xu, H., McCarthy, M. J., Zhu, G., Qin, B., Li, Y., et al. (2011). Controlling harmful cyanobacterial blooms in a hyper-eutrophic Lake (lake Taihu, China): the need for a dual nutrient (N & P) management strategy. *Water Res.* 45, 1973–1983. doi: 10.1016/j.watres.2010.09.018

Pham, T. L., and Utsumi, M. (2018). An overview of the accumulation of microcystins in aquatic ecosystems. *J. Environ. Manage.* 213, 520–529. doi: 10.1016/j.jenvman.2018.01.077

Qin, L., Zhang, X., Chen, X., Wang, K., Shen, Y., and Li, D. (2019). Isolation of a novel microcystin-degrading bacterium and the evolutionary origin of mlr gene cluster. *Toxins* 11:269. doi: 10.3390/toxins11050269

Sadhasivam, G., Gelber, C., Zakin, V., Margel, S., and Shapiro, O. H. (2019). N-Halamine derivatized nanoparticles with selective cyanocidal activity: potential for targeted elimination of harmful cyanobacterial blooms. *Environ. Sci. Technol.* 53, 9160–9170. doi: 10.1021/acs.est.9b01368

Sehnal, L., Prochazkova, T., Smutna, M., Kohoutek, J., Lepsova-Skacelova, O., and Hilscherova, K. (2019). Widespread occurrence of retinoids in water bodies associated with cyanobacterial blooms dominated by diverse species. *Water Res.* 156, 136–147. doi: 10.1016/j.watres.2019.03.009

Sotton, B., Guillard, J., Anneville, O., Marechal, M., Savichtcheva, O., and Domaizon, I. (2014). Trophic transfer of microcystins through the lake pelagic food web: evidence for the role of zooplankton as a vector in fish contamination. *Sci. Total Environ.* 466-467, 152–163. doi: 10.1016/j.scitotenv.2013.07.020

Tao, Y., Hou, D., Zhou, T., Cao, H., Zhang, W., and Wang, X. (2018). UV-C suppression on hazardous metabolites in Microcystis aeruginosa: unsynchronized production of microcystins and odorous compounds at population and single-cell level. *J. Hazard. Mater.* 359, 281–289. doi: 10.1016/j.jhazmat.2018.07.052

Tian, D., Zheng, W., Wei, X., Sun, X., Liu, L., Chen, X., et al. (2013). Dissolved microcystins in surface and ground waters in regions with high cancer incidence in the Huai River basin of China. *Chemosphere* 91, 1064–1071. doi: 10.1016/j.chemosphere.2013.01.051

Tsuji, K., Asakawa, M., Anzai, Y., Sumino, T., and Harada, K. (2006). Degradation of microcystins using immobilized microorganism isolated in a eutrophic lake. *Chemosphere* 65, 117–124. doi: 10.1016/j.chemosphere.2006.02.018

Visser, P. M., Verspagen, J., Sandrini, G., Stal, L. J., Matthijs, H., Davis, T. W., et al. (2016). How rising CO2 and global warming may stimulate harmful cyanobacterial blooms. *Harmful Algae* 54, 145–159. doi: 10.1016/j.hal.2015.12.006

Wang, L., Jin, H., Zeng, Y., Tan, Y., Wang, J., Fu, W., et al. (2022). HOXB4 Mis-regulation induced by microcystin-LR and correlated with immune infiltration is unfavorable to colorectal cancer prognosis. *Front. Oncol.* 12:803493. doi: 10.3389/fonc.2022.803493

Wang, R., Li, J., and Li, J. (2020). Functional and structural analyses for MlrC enzyme of Novosphingobium sp. THN1 in microcystin-biodegradation: involving optimized heterologous expression, bioinformatics and site-directed mutagenesis. *Chemosphere* 255:126906. doi: 10.1016/j.chemosphere.2020.126906

Wang, H., Liu, J., Lin, S., Wang, B., Xing, M., Guo, Z., et al. (2014). MCLR-induced PP2A inhibition and subsequent Rac1 inactivation and hyperphosphorylation of cytoskeleton-associated proteins are involved in cytoskeleton rearrangement in SMMC-7721 human liver cancer cell line. *Chemosphere* 112, 141–153. doi: 10.1016/j.chemosphere.2014.03.130

Wei, J., Huang, F., Feng, H., Massey, I. Y., Clara, T., Long, D., et al. (2021). Characterization and mechanism of linearized-Microcystinase involved in bacterial degradation of microcystins. *Front. Microbiol.* 12:646084. doi: 10.3389/fmicb.2021.646084

Weir, M. H., Wood, T. A., and Zimmer-Faust, A. (2021). Development of methods to estimate microcystins removal and water treatment resiliency using mechanistic risk modelling. *Water Res.* 190:116763. doi: 10.1016/j.watres.2020.116763

Wu, X., Wang, C., Tian, C., Xiao, B., and Song, L. (2015). Evaluation of the potential of anoxic biodegradation of intracellular and dissolved microcystins in lake sediments. *J. Hazard. Mater.* 286, 395–401. doi: 10.1016/j.jhazmat.2015.01.015

Xiang, L., Li, Y. W., Liu, B. L., Zhao, H. M., Li, H., Cai, Q. Y., et al. (2019). High ecological and human health risks from microcystins in vegetable fields in southern China. *Environ. Int.* 133:105142. doi: 10.1016/j.envint.2019.105142

Xu, H., Paerl, H. W., Qin, B., Zhu, G., Hall, N. S., and Wu, Y. (2015). Determining critical nutrient thresholds needed to control harmful cyanobacterial blooms in eutrophic Lake Taihu, China. *Environ. Sci. Technol.* 49, 1051–1059. doi: 10.1021/es503744q

Yang, F., Huang, F., Feng, H., Wei, J., Massey, I. Y., Liang, G., et al. (2020). A complete route for biodegradation of potentially carcinogenic cyanotoxin microcystin-LR in a novel indigenous bacterium. *Water Res.* 174:115638. doi: 10.1016/j.watres.2020.115638

Zamora-Barrios, C. A., Nandini, S., and Sarma, S. (2019). Bioaccumulation of microcystins in seston, zooplankton and fish: a case study in Lake Zumpango, Mexico. *Environ. Pollut.* 249, 267–276. doi: 10.1016/j.envpol.2019.03.029

Zeller, P., Quenault, H., Huguet, A., Blanchard, Y., and Fessard, V. (2012). Transcriptomic comparison of cyanotoxin variants in a human intestinal model revealed major differences in oxidative stress response: effects of MC-RR and MC-LR on Caco-2 cells. *Ecotoxicol. Environ. Saf.* 82, 13–21. doi: 10.1016/j.ecoenv.2012.05.001

Zeng, Y. H., Cai, Z. H., Zhu, J. M., Du, X. P., and Zhou, J. (2020). Two hierarchical LuxR-LuxI type quorum sensing systems in Novosphingobium activate microcystin degradation through transcriptional regulation of the mlr pathway. *Water Res.* 183:116092. doi: 10.1016/j.watres.2020.116092

Zeng, Y. H., Cheng, K. K., Cai, Z. H., Zhu, J. M., Du, X. P., Wang, Y., et al. (2021). Transcriptome analysis expands the potential roles of quorum sensing in biodegradation and physiological responses to microcystin. *Sci. Total Environ.* 771:145437. doi: 10.1016/j.scitotenv.2021.145437

Zhang, D., Xie, P., Liu, Y., and Qiu, T. (2009). Transfer, distribution and bioaccumulation of microcystins in the aquatic food web in Lake Taihu, China, with potential risks to human health. *Sci. Total Environ.* 407, 2191–2199. doi: 10.1016/j.scitotenv.2008.12.039

Zhang, X., Yang, F., Chen, L., Feng, H., Yin, S., and Chen, M. (2020). Insights into ecological roles and potential evolution of Mlr-dependent microcystin-degrading bacteria. *Sci. Total Environ.* 710:136401. doi: 10.1016/j.scitotenv.2019.136401

Zhang, L., Yang, J., Liu, L., Wang, N., Sun, Y., Huang, Y., et al. (2021). Simultaneous removal of colonial Microcystis and microcystins by protozoa grazing coupled with ultrasound treatment. *J. Hazard. Mater.* 420:126616. doi: 10.1016/j.jhazmat.2021.126616

Zhang, Z., Zhang, X. X., Qin, W., Xu, L., Wang, T., Cheng, S., et al. (2012). Effects of microcystin-LR exposure on matrix metalloproteinase-2/−9 expression and cancer cell migration. *Ecotoxicol. Environ. Saf.* 77, 88–93. doi: 10.1016/j.ecoenv.2011.10.022

Zhao, Y., Xue, Q., Su, X., Xie, L., Yan, Y., Wang, L., et al. (2016). First identification of the toxicity of microcystins on pancreatic islet function in humans and the involved potential biomarkers. *Environ. Sci. Technol.* 50, 3137–3144. doi: 10.1021/acs.est.5b03369

Zhao, Y., Yan, Y., Xie, L., Wang, L., He, Y., Wan, X., et al. (2020). Long-term environmental exposure to microcystins increases the risk of nonalcoholic fatty liver disease in humans: a combined fisher-based investigation and murine model study. *Environ. Int.* 138:105648. doi: 10.1016/j.envint.2020.105648

Zurawell, R. W., Chen, H., Burke, J. M., and Prepas, E. E. (2005). Hepatotoxic cyanobacteria: a review of the biological importance of microcystins in freshwater environments. *J. Toxicol. Environ. Health B Crit. Rev.* 8, 1–37. doi: 10.1080/10937400590889412

Frontiers in Microbiology

Explores the habitable world and the potential of microbial life

The largest and most cited microbiology journal which advances our understanding of the role microbes play in addressing global challenges such as healthcare, food security, and climate change.

Discover the latest Research Topics

See more →

Frontiers

Avenue du Tribunal-Fédéral 34
1005 Lausanne, Switzerland
frontiersin.org

Contact us

+41 (0)21 510 17 00
frontiersin.org/about/contact